

**PREPARATION CHARACTERIZATION AND
TRIBOLOGICAL BEHAVIOR OF LUBE OIL WITH
NANOPARTICLES ADDITIVES**

WALEED ALGHANI

**FACULTY OF ENGINEERING
UNIVERSITY OF MALAYA
KUALA LUMPUR**

2020

**PREPARATION CHARACTERIZATION AND
TRIBOLOGICAL BEHAVIOR OF LUBE OIL WITH
NANOPARTICLES ADDITIVES**

WALEED ALGHANI

**THESIS SUBMITTED IN FULFILMENT OF THE
REQUIREMENTS FOR THE DEGREE OF DOCTOR OF
PHILOSOPHY**

**FACULTY OF ENGINEERING
UNIVERSITY OF MALAYA
KUALA LUMPUR**

2020

UNIVERSITY OF MALAYA
ORIGINAL LITERARY WORK DECLARATION

Name of Candidate: Waleed Alghani

Matric No: KHA140087

Name of Degree: Doctor of Philosophy

Title of Thesis: "Preparation Characterization and Tribological Behavior of Lube Oil with Nanoparticles Additives"

Field of Study: Engineering Design

I do solemnly and sincerely declare that:

- (1) I am the sole author/writer of this Work;
- (2) This Work is original;
- (3) Any use of any work in which copyright exists was done by way of fair dealing and for permitted purposes and any excerpt or extract from, or reference to or reproduction of any copyright work has been disclosed expressly and sufficiently and the title of the Work and its authorship have been acknowledged in this Work;
- (4) I do not have any actual knowledge, nor do I ought reasonably to know that the making of this work constitutes an infringement of any copyright work;
- (5) I hereby assign all and every right in the copyright to this Work to the University of Malaya ("UM"), who henceforth shall be owner of the copyright in this Work and that any reproduction or use in any form or by any means whatsoever is prohibited without the written consent of UM having been first had and obtained;
- (6) I am fully aware that if in the course of making this Work, I have infringed any copyright whether intentionally or otherwise, I may be subject to legal action or any other action as may be determined by UM.

Candidate's Signature

Date: August 30, 2020

Subscribed and solemnly declared before,

Witness's Signature

Date:

Name:

Designation:

ABSTRACT

There are many companies worldwide that would like to improve and upgrade the lube oil and enhance its performance. There is a big concern for the enhancement of lube oil by using nanotechnology and more precisely with using nanomaterial additives. Much work has made to explore and develop new sorts of lubricating oil nano-additives to diminish wear and friction in tribological configurations and to enhance surface morphology. It has noted that the use of dual nano-additives should examine the lubricating capacity and durability of lubricant.

(TiO₂ Anatase + Graphene) and (ZnO + Graphene) nanoparticles have selected to formulate nano-additives that can add to API Group II base oil (PBO-GII). Nanoparticles have characterized by employing a transmission electron microscope (TEM) to examine the morphology of these three nanostructures. Sonication treatment and dispersion stability investigation carried out for the mixtures. A range of concentrations (0.0 wt%, 0.2 wt%, 0.4 wt%, and 0.6 wt% mg/ml) of two groups of dual nanoparticles which include (TiO₂ (A) + Graphene) and (ZnO + Graphene) were blended with PBO-GII individually to recognize the lowest friction and wear losses that took place throughout the sliding motion. Oil formulations tested by using a four-ball machine to find out the coefficient of friction (COF), wear scar diameter (WSD), and specific wear rate (SWR) for each sample. Additionally, balls scars have characterized by using field emission-scanning electron microscopy (FE-SEM), energy-dispersive x-ray spectroscopy (EDX/EDS), elements mapping, Raman spectroscopy, and surface roughness measurements for distinguishing the morphology structure, presence of tribofilm, surface finish, friction, and wear effect on all employed balls. It is also noteworthy a 3-dimensional optical (contact-free) surface texture analysis apparatus used to study the scarred region on each ball surface. For the (TiO₂ (A) + Graphene) group/samples, the average reduction in COF, WSD, and SWR

for an hour was 38.83%, 36.78%, and 15.78% respectively, for (0.4 wt% TiO₂ (A) + 0.2 wt% Graphene) nanolubricant compared to PBO-GII. The formation of the tribofilm and the deposition of nanoparticles on contacted areas protected the surfaces of balls from acute friction and adhesion wear. For the (ZnO + Graphene) group/samples, the average reduction in COF, WSD, and SWR was 43.81%, 36.78%, and 39.47% respectively for (0.4 wt% ZnO + 0.2 wt% Graphene) nanolubricant compared to PBO-GII. The superb lubrication performance was due to the tribofilm of the nanoparticle mixture deposition on the mating metal surfaces during sliding motion. The driving force for nano-sized particles (TiO₂ (A) + Graphene) and (ZnO + Graphene) in pure base oil entering the sliding surfaces throughout three mechanisms micro rolling bearing technique, depositing film technique, and mending technique. These phenomena confirmed the significance of uniform nanoparticles dispersion for improved wear protection.

The tribological analyses and the surface characterization tools TEM, FE-SEM, EDX/EDS, elements mapping, Raman spectra, and surface roughness measurements have clearly explained the nanoparticles' role and lubrication mechanisms. This research proved the essential role of blending two mixtures of nanoparticles to enhance the tribological performance and surface morphology via the surface activity of the additives.

Keywords: Nanoparticle, Lubrication, Tribology, Morphology, Characterization, and Surface Roughness.

ABSTRAK

Terdapat banyak syarikat di seluruh dunia yang ingin memperbaiki dan meningkatkan minyak pelumas dan meningkatkan prestasinya. Terdapat keprihatinan besar untuk peningkatan minyak pelumas dengan menggunakan nanoteknologi dan lebih tepatnya dengan menggunakan bahan tambahan bahan nano. Banyak kerja telah dilakukan untuk meneroka dan mengembangkan jenis baru nano-minyak pelincir untuk mengurangkan keausan dan geseran dalam konfigurasi tribologi dan untuk meningkatkan morfologi permukaan. Telah diperhatikan bahawa penggunaan bahan tambahan nano ganda harus mengkaji keupayaan pelinciran dan ketahanan pelincir.

(TiO₂ Anatase + Graphene) dan (ZnO + Graphene) nanopartikel telah dipilih untuk merumuskan bahan tambahan nano yang dapat menambah minyak asas API Kumpulan II (PBO-GII). Nanopartikel telah dicirikan dengan menggunakan mikroskop elektron transmisi (TEM) untuk memeriksa morfologi ketiga struktur nano ini. Penyiasatan rawatan sonikasi dan kestabilan penyebaran dilakukan untuk campuran tersebut. Julat kepekatan (0.0 wt%, 0.2 wt%, 0.4 wt%, dan 0.6 wt% mg / ml) dua kumpulan berganda nanopartikel yang merangkumi (TiO₂ (A) + Graphene) dan (ZnO + Graphene) dicampur dengan PBO-GII secara individu untuk mengenali geseran dan kerugian keausan terendah yang berlaku sepanjang gerakan gelongsor. Formulasi minyak diuji dengan menggunakan mesin empat bola untuk mengetahui pekali geseran (COF), diameter parut pakai (WSD), dan kadar haus tertentu (SWR) untuk setiap sampel. Selain itu, parut bola dicirikan dengan menggunakan mikroskopi elektron pemindaian pelepasan medan (FE-SEM), spektroskopi sinar-x penyebaran tenaga (EDX / EDS), pemetaan elemen, spektroskopi Raman, dan pengukuran kekasaran permukaan untuk membezakan struktur morfologi, kehadiran tribo-selaput, kemas permukaan, geseran, dan kesan keausan pada semua bola yang digunakan. Perlu diperhatikan juga alat analisis tekstur permukaan optik 3

dimensi (bebas sentuhan) yang digunakan untuk mengkaji kawasan berparut pada setiap permukaan bola. Untuk kumpulan / sampel (TiO_2 (A) + Graphene), penurunan purata COF, WSD, dan SWR selama satu jam masing-masing adalah 38.83%, 36.78%, dan 15.78%, untuk (0.4 wt% TiO_2 (A) + 0.2 wt% Graphene) pelincir nano berbanding PBO-GII. Pembentukan tribo-selaput dan pemendapan nanopartikel di kawasan yang dihubungi melindungi permukaan bola dari geseran akut dan keausan lekatan. Bagi kumpulan / sampel (ZnO + Graphene), penurunan purata COF, WSD, dan SWR masing-masing adalah 43.81%, 36.78%, dan 39.47% untuk pelincir nano (0.4 wt% ZnO + 0.2 wt% Graphene) berbanding PBO-GII. Prestasi pelinciran yang luar biasa disebabkan oleh tribo-selaput pengendapan campuran nanopartikel pada permukaan logam kawin semasa gerakan gelongsor. Daya penggerak untuk zarah bersaiz nano (TiO_2 (A) + Graphene) dan (ZnO + Graphene) dalam minyak asas tulen memasuki permukaan gelongsor di sepanjang tiga mekanisme teknik gelas rolling mikro, teknik filem simpanan, dan teknik memperbaiki. Fenomena ini mengesahkan betapa pentingnya penyebaran nanopartikel yang seragam untuk perlindungan memakai yang lebih baik.

Analisis tribologi dan alat pencirian permukaan TEM, FE-SEM, EDX / EDS, pemetaan elemen, spektrum Raman, dan pengukuran kekasaran permukaan telah menjelaskan mekanisme peranan dan pelinciran nanopartikel dengan jelas. Penyelidikan ini membuktikan peranan penting untuk mencampurkan dua campuran nanopartikel untuk meningkatkan prestasi tribologi dan morfologi permukaan melalui aktiviti permukaan bahan tambahan.

Kata kunci: Nanopartikel, Pelinciran, Tribologi, Morfologi, Pencirian, dan Permukaan Permukaan.

ACKNOWLEDGMENTS

First of all, I am thankful to Almighty Allah, the creator of the whole world, the Merciful, for bestowing His favor upon me, because without His will we cannot do anything and so I complete this research study, which would otherwise have not been possible at all.

I would like to provide my sincerest thanks to my supervisors Dr. Mohd Sayuti Bin Ab Karim, and Dr. Samira Bagheri who's have been a source of guidance, inspiration, and friendliness for me during this candidature-ship. Without their encouragement, it would have been a stage with a lot of difficulties.

I am thankful to all the honorable associates and postgraduate students of the Centre of Advanced Manufacturing and Material Processing (AMMP Centre), Faculty of Engineering, University of Malaya. I cannot overlook my research companionship Miss Nor Amirah Mohd Amran, Miss Wan Nur Izzati, and Mrs. Aqilah Derahman for their support by logistics and procurement. I sincerely admire the kind assistance of the technical staff of the General Tribology Lab, FE-SEM Lab, and Surface Roughness Lab.

I ought to admit my mother who sacrificed a lot and continuously prayed for my success. I am tremendously thankful to my kind wife and lovely son, Moamel Alghani who experienced difficult periods owing to my research obligations and commitment in lengthy periods of lab work. I am truly thankful to my colleagues Dr. Arman Amani and Dr. Mubashir Gulzar for their valuable advice.

In the end, I would like to acknowledge that I am extremely indebted to the University of Malaya for the sponsorship through the UMRG Program, Grant number: RP039A-15AET and Grand Challenge Program, Grant number: GC001D-14AET.

TABLE OF CONTENTS

ABSTRACT	iii
ABSTRAK	v
Acknowledgments	vii
Table of Contents	viii
List of Figures	xii
List of Tables	xvii
List of Symbols and Abbreviations	xviii
List of Appendices	xxii
CHAPTER 1: INTRODUCTION.....	2
1.1 Introduction.....	2
1.2 Background of the Study	2
1.3 Research Problem	6
1.4 Research Objectives.....	7
1.5 Research Importance	8
1.6 Scope of Research.....	8
1.7 Conclusion	9
CHAPTER 2: LITERATURE REVIEW.....	11
2.1 Introduction.....	11
2.2 Base Oil Types and Variations	12
2.3 API Base Oil Groups	13
2.4 Oil Additives.....	15
2.4.1 Friction Modifiers and Wear Protection Additives	16
2.4.1.1 Nanoscale Particles as Additives.....	17

2.4.1.2	Stability of Nanoparticles and Dispersion Technique.....	26
2.4.1.3	Dispersion Stability Analysis for Nanolubricants.....	31
2.4.1.4	Techniques to Improve the Nano-oils Dispersion Stability	33
2.4.1.5	Importance of Nanoscale Particles Concentration	36
2.4.1.6	Role of Nanoparticle Size.....	39
2.4.1.7	Role of Nanoscale Particle Shape and Structure	40
2.4.1.8	Optimize the Concentration for Tribology Boosting	46
2.4.1.9	The Function of Tribo-Testers Standard and Configurations ...	56
2.4.1.10	Lubrication Mechanisms	61
2.4.1.11	The Tribological Performance	66
2.5	Conclusion	67
CHAPTER 3: MATERIALS AND METHODS		69
3.1	Introduction.....	69
3.2	Source of Materials.....	72
3.3	Characterization of Nanoparticles	72
3.4	Formulation of Nanoparticles	74
3.5	Experimental Set-up:	77
3.5.1	Sonication Treatment	77
3.5.2	Dispersion Stability Analysis	78
3.5.3	Tribology Tribo-testers.....	80
3.6	Surface Characterization.....	83
3.6.1	Field Emission-Scanning Electron Microscope (FE-SEM)	84
3.6.2	Energy-Dispersive X-ray Spectroscopy and Elements Mapping	85
3.6.3	Raman Spectroscopy	87
3.6.4	Surface Roughness Measurements	88
3.7	Conclusion	89

CHAPTER 4: RESULTS AND DISCUSSION	91
4.1 Introduction.....	91
4.2 TEM Characterization for Nanoparticles.....	92
4.3 Coefficient of Friction (COF) Behavior	94
4.3.1 TiO ₂ (A) + Graphene COF	94
4.3.2 ZnO + Graphene COF	95
4.4 Wear Scar Diameter (WSD) Behavior	97
4.4.1 TiO ₂ (A) + Graphene WSD.....	97
4.4.2 ZnO + Graphene WSD	99
4.5 Specific Wear Rate (SWR) Behavior	101
4.5.1 TiO ₂ (A) + Graphene SWR	101
4.5.2 ZnO + Graphene SWR	104
4.6 Lubrication Mechanism.....	106
4.7 Metallographic Characterization	109
4.7.1 FE-SEM Characterization for TiO ₂ (A) + Graphene.....	109
4.7.2 EDX/EDS and Elements Mapping for TiO ₂ (A) + Graphene	113
4.7.3 FE-SEM Characterization for ZnO + Graphene.....	118
4.7.4 EDX/EDS and Elements Mapping for ZnO + Graphene	123
4.8 Raman Spectra.....	127
4.8.1 Raman Spectroscopy for TiO ₂ (A) + Graphene	127
4.8.2 Raman Spectroscopy for ZnO + Graphene	129
4.9 Surface Characterization.....	132
4.9.1 Surface Roughness Characterization for TiO ₂ (A) + Graphene	132
4.9.2 Surface Roughness Characterization for ZnO + Graphene	139
4.10 Conclusion	149
CHAPTER 5: CONCLUSIONS AND RECOMMENDATIONS.....	152

5.1	Introduction.....	152
5.2	Conclusions	152
5.3	Recommendations for Future Work	155
	References	158
	List of Publications and Papers Presented	175
	Appendix	177

University of Malaya

LIST OF FIGURES

Figure 1.1: Introduction to tribology field and parameters of a tribosystem	3
Figure 1.2: Schematic representation of the tribological optimization configuration	4
Figure 1.3: Nanoparticles overview with respect to material type, size/volume, surface, and shape type	5
Figure 1.4: Schematic illustration of tribofilm formation by nanoparticles.....	6
Figure 2.1: Timeline for the advancement of oil additives	17
Figure 2.2: The primary categories of nanoscale particles with subgroups of engineered nanoscale particles associated with tribological researches.....	20
Figure 2.3: Coefficient of friction performance of stirred and unstirred oils exhibiting the efficiency of well-dispersed of nano-MoS ₂ enhanced lubricant	27
Figure 2.4: Sedimentation technique of aluminum nanoscale particles dispersed in paraffin oil.....	32
Figure 2.5: The influence of nanoparticle's shape on contacting area during loading ...	41
Figure 2.6: Planar graphene structure has no difficulty to slide between mating surfaces in the lubricant.....	42
Figure 2.7: Schematic diagram of the multilayered crystal molecular structure of TiO ₂ (A)	43
Figure 2.8: The spherical structure of TiO ₂ nanoparticles in the lubricating film can play as bearing balls between the working roll and the substrate exhibiting a rolling effect .	43
Figure 2.9: (a) A TEM micro image of FIB foil cut from the rolling steel surface, (b) TEM micro image of a magnified region in (a), representing the role of Nano-TiO ₂ -particles	44
Figure 2.10: ZnO nanoparticles morphology	44
Figure 2.11: Illustration of nano-ZnO structure as a solid lubricating film.....	45
Figure 2.12: FE-SEM micro-image of cross-sectional wear scars of ZnO tribo-layer film at 800 °C.....	45
Figure 2.13: Frequently employed tribo-testers structure setups (a) four-ball, (b) ball-on-plane, (c) pin-on-disk (d) piston ring-on-cylinder (e) pin-on-plane.....	57

Figure 2.14: Graphical representation of the lubrication technique of silica nanoscale particle blended in PAO	63
Figure 2.15: Protecting film structure on metal-to-metal contact by Bio-lubricant.....	67
Figure 2.16: Potential research gap/ research problem of adding nanoscale particles to formulate effective nanolubricant	68
Figure 3.1: Research path of the study.....	70
Figure 3.2: Nanolubricants research areas and methodologies.....	71
Figure 3.3: Transmission electron microscopy (TEM) device by Carl Zeiss microscopy	72
Figure 3.4: Nanoparticles (A) TiO ₂ (Anatase), (B) ZnO and (C) Graphene samples.....	73
Figure 3.5: Desiccator cabinet for drying the samples.....	74
Figure 3.6: Addition stages of nanolubricant formulation.....	75
Figure 3.7: Stability and constancy of nanoparticles for two types of lubricant samples using a sonication device	78
Figure 3.8: Dispersion stability analysis after 1-month of sedimentation for (A) (TiO ₂ (A) + Graphene) samples and (B) (ZnO + Graphene) samples.....	79
Figure 3.9: Lubricants tribo-examining utilizing DUCOM Four-Ball tribometer TR-30H	81
Figure 3.10: (A) Photograph of pot and spindle of the Four-ball machine. (B) 2D drawing of spindle fastened to one ball and pot clamped the three other balls. (C) Schematic diagram of the Four-ball tribotester arrangement	81
Figure 3.11: Scar wear acquisition microscope	83
Figure 3.12: Field Emission-Scanning Electron Microscope (FE-SEM) apparatus equipped with multi units' specimen holder	85
Figure 3.13: Energy-Dispersive X-ray Spectroscopy EDX/EDS and elemental mapping device with sample holder.....	86
Figure 3.14: Raman microscope employed to investigate worn of scar balls.....	88
Figure 3.15: Alicona Infinite Focus 3-Dimensional surface, contact-free, surface finish analysis device	89

Figure 4.1: The morphology of nanoparticles by TEM (A) TiO ₂ (Anatase), (B) ZnO, and (C) graphene.....	93
Figure 4.2: Differences in coefficient of friction among six different types of lubricants	95
Figure 4.3: Coefficient of friction measurement (dimensionless) for six lubricants	96
Figure 4.4: Differences in wear scar diameter mean (mm) for six sorts of lubricants....	99
Figure 4.5: Wear scar diameter mean measurement (mm) for six different lubricants	100
Figure 4.6: Differences in specific wear rate (*10 ⁻¹⁶) m ³ /Nm for 1-hour duration for six sorts of lubricants	103
Figure 4.7: Specific wear rate (*10 ⁻¹⁶) m ³ /Nm measurement for six lubricants	104
Figure 4.8: Mechanism and role of dual nanoparticles during nano-lubrication	107
Figure 4.9: Schematic diagram of lubrication mechanisms for synergetic nanoparticles	107
Figure 4.10: Nanoparticles entered the interacting surfaces and formed well-distributed tribofilm overcomes friction and wear	108
Figure 4.11: FE-SEM micrographs of the surface morphology of AISI balls treated with six sorts of lubricants	113
Figure 4.12: EDX/EDS, elements mappings, and spectrums of steel balls treated with (A) plain lubricant and (B) dual nanoparticles lubricant.....	115
Figure 4.13: FE-SEM and EDX demonstrate the formation of a protective film on the scar region of ball treated with (0.4 wt% TiO ₂ (A) + 0.2 wt% Graphene) nanolubricant....	116
Figure 4.14: EDX of the surface morphology of AISI balls treated with (A) pure base oil Group II and (B) dual nanoparticles lubricant	117
Figure 4.15: Elements mapping confirm the deposition of titanium and graphene on the sliding surface of synergetic lubricant (0.4 wt% TiO ₂ (A) + 0.2 wt% Graphene).....	118
Figure 4.16: Field Emission Scanning Electron Microscopy (FE-SEM) of surface topography of AISI balls employed with six types of oils (A) PBO-GII, (B) 0.2 wt% ZnO, (C) 0.2 wt% Graphene, (D) 0.2 wt% ZnO + 0.2 wt% Graphene, (E) 0.2 wt% ZnO + 0.4 wt% Graphene, and (F) 0.4 wt% ZnO + 0.2 wt% Graphene	122
Figure 4.17: Energy Dispersive X-Ray Spectroscopy (EDX/EDS) for PBO-GII oil presenting the ball combinations without nanoscale particles detection	125

Figure 4.18: EDX/EDS and elements mapping identifying Zinc and Carbon (Graphene) elements on the steel ball's scar employed with (0.4 wt% ZnO + 0.2 wt% Graphene) nano-oil	126
Figure 4.19: Raman spectra of five nano-oils: Oil (A) 0.2 wt% TiO ₂ anatase, Oil (B) 0.2 wt% Graphene, Oil (C) 0.2 wt% TiO ₂ anatase + 0.2 wt% Graphene, Oil (D) 0.2 wt% TiO ₂ anatase + 0.4 wt% Graphene, Oil (E) 0.4 wt% TiO ₂ anatase + 0.2 wt% Graphene.....	128
Figure 4.20: Raman spectra of five nanolubricants Oil (a) 0.2 wt% ZnO, Oil (b) 0.2 wt% Graphene, Oil (c) 0.2 wt% ZnO + 0.2 wt% Graphene, Oil (d) 0.2 wt% ZnO + 0.4 wt% Graphene, Oil (e) 0.4 wt% ZnO + 0.2 wt% Graphene.....	130
Figure 4.21: (A) Worn surface of a ball when applying PBO-GII lubricant and (B) sliding region of a ball when applying (0.4 wt% TiO ₂ (A) + 0.2 wt% Graphene) nanolubricant	132
Figure 4.22: Profile roughness measurement (Ra), (RMS) or (Rq), and (Rz) for (A) PBO-GII oil and (B) (0.4 wt% TiO ₂ (A) + 0.2 wt% Graphene) nano-oil	133
Figure 4.23: Profile roughness investigation of surface morphology of AISI balls employed with six various sorts of lubricants.....	134
Figure 4.24: Surface texture measurement (Sa), (Sq), (Sp), (Sv), (Sz), (Ssk), and (Sku) for (A) additive-free oil, and (B) effective nano-oil	135
Figure 4.25: Surface texture investigation (μm) of the surface morphology of AISI balls used with six various sorts of lubricants	136
Figure 4.26: Surface skewness and surface kurtosis measurement (dimensionless) of the surface morphology of AISI balls employed with six various sorts of lubricants.....	138
Figure 4.27: Profile form investigation (μm) of the surface morphology of AISI balls employed with six various sorts of lubricants.....	139
Figure 4.28: (A) Worn ball region after using PBO-GII lubricant and (B) Scar ball surface after using (0.4 wt% ZnO + 0.2 wt% Graphene) nanolubricant	140
Figure 4.29: Profile roughness measurement (Ra), (RMS) or (Rq), and (Rz) for (A) Additive-free oil and (B) (0.4 wt% ZnO + 0.2 wt% Graphene) nano-oil	141
Figure 4.30: Profile roughness investigation of the surface morphology of AISI balls employed with six various sorts of lubricants.....	142
Figure 4.31: Surface texture measurement (Sa), (Sq), (Sp), (Sv), (Sz), (Ssk), and (Sku) for (A) PBO-GII oil, and (B) (0.4 wt% ZnO + 0.2 wt% Graphene) nanolubricant.....	143

Figure 4.32: Surface texture investigation (μm) for the surface morphology of AISI balls employed with six various sorts of lubricants..... 144

Figure 4.33: Surface skewness and kurtosis measurement (dimensionless parameters) of the surface morphology of AISI balls employed with six various sorts of lubricants.. 146

Figure 4.34: Profile form measurement for (A) additive-free lubricant and (B) formulated dual nanoparticles lubricant 148

Figure 4.35: Profile form measurement (μm) of the surface morphology of AISI balls employed with six various sorts of lubricants..... 148

University of Malaya

LIST OF TABLES

Table 2.1: Saturated level, sulfur level, and viscosity index of five API groups.....	15
Table 2.2: Review of origins and common characteristics of nanoscale particles employed as oil additives.....	21
Table 2.3: A literature review of generally employed dispersion methods to boost dispersion constancy	28
Table 2.4: Standard surfactants/agents, their chemical composition, and functionality .	35
Table 2.5: Literature survey of the performance/function/role of nanoscale particles and ideal concentrations for various lubricants	37
Table 2.6: Literature survey of four-ball tribotester employed parameters	57
Table 2.7: Literature review of tribo-testings' parameters influencing sliding contact ..	60
Table 2.8: Survey of summarized outcomes of nanoscale particles on tribological characteristics, lubrication mechanisms, and surfaces characterization	64
Table 3.1: Formulation of nanoparticles (TiO ₂ (A) + Graphene), base stock, and surfactant for six types of samples.....	75
Table 3.2: Formulation of nanoparticles (ZnO + Graphene), base stock, and surface-agent for six types of samples.....	76
Table 3.3: Specifications of pure Group II base oil	76
Table 3.4: Steel ball mechanical properties of the Four-ball tester.....	80
Table 3.5: ASTM Standard D4172 of the four-ball method	82
Table 4.1: Observed element weight percentages via EDX/EDS analysis for six different lubricants	115
Table 4.2: Element weight percentages deducted via EDX analysis for six different lubricants.....	124
Table 4.3: Raman shifts of the TiO ₂ Anatase groups associated with Raman modes ..	127

LIST OF SYMBOLS AND ABBREVIATIONS

Al	:	Aluminum
A. L.	:	Applied load
Al/Sn	:	Aluminum-tin
Al ₂ O ₃	:	Aluminum oxide
Al ₂ O ₃ /SiO ₂	:	Alumina-Silica
AW	:	Antiwear
APS	:	Average particle size
BN	:	Boron nitride
C	:	Carbon
Co	:	Cobalt
Cu	:	Copper
COF	:	Coefficient of friction
CuO	:	Copper (II) oxide
CaCO ₃	:	Calcium carbonate
CATO302	:	Cationic starch
CMRO	:	Chemically modified rapeseed oil
EP	:	Extreme pressure
EDS	:	Energy dispersive spectrometer
EDX	:	Energy-dispersive X-ray spectroscopy
Fe	:	Iron
FM	:	Friction modifier
Fe ₃ O ₄	:	Iron (II, III) oxide
FE-SEM	:	Field emission scanning electron microscopy
g	:	Gravity

Gpa	:	Gigapascal
hBN	:	Hexagonal boron nitride
Lc	:	Sample Length
ISL	:	Initial seizure load
LNSL	:	Last non-seizure load
MoS ₂	:	Molybdenum disulfide
MoS ₂ /TiO ₂	:	Molybdenum disulphide-titanium dioxide
N	:	Newton unit
Ni	:	Nickel
nm	:	Nanometer
NP	:	Nanoparticle
NPs	:	Nanoparticles
O	:	Oxygen
OA	:	Oleic acid
P.	:	Pressure
Pb	:	Lead
PAO	:	Polyalphaolefin
PBO-GII	:	Pure base oil group two
PbS	:	Lead sulfide
PTFE	:	Polytetrafluoroethylen
r	:	Radius of nanoparticle
Ra	:	Arithmetic average roughness
Rq	:	Root mean square
Rz	:	Mean roughness depth
RMS	:	Root mean square
S	:	Sulfur

Sa	:	Average surface height
Si	:	Silicon
Sp	:	Maximum peak height
Sp.	:	Speed
Sq	:	Root-mean-square height
Sv	:	Maximum valley depth
Sz	:	Maximum height
SEM	:	Scanning electron microscope
SiO ₂	:	Silicon dioxide, Silica
Sku	:	Surface kurtosis
Ssk	:	Surface skewness
SWR	:	Specific wear rate
TAN	:	Total acid number
Ti	:	Titanium
TiO ₂	:	Titanium dioxide
TiO ₂ (A)	:	Titanium dioxide (anatase)
TMP	:	Trimethylolpropane
UV-vis	:	Ultraviolet-visible
v _z	:	settling velocity
WL	:	Weld load
WS ₂	:	Tungsten disulfide
WSD	:	Wear scar diameter
XPS	:	X-ray photoelectron spectroscopy
Z1	:	Surface Depth One
Z2	:	Surface Depth Two
ZnO	:	Zinc oxide

ZrO_2	:	Zirconium dioxide
$ZnAl_2O_4$:	Zinc aluminate
ZrO_2/SiO_2	:	Zirconia-Silica
ZDDP	:	Zinc dialkyl dithiophosphate
ρ_{NP}	:	Density of nanoparticles
ρ_F	:	Density of fluid
μ	:	Coefficient of friction
μm	:	Micrometer

University of Malaya

LIST OF APPENDICES

Appendix A: Comparison of poor-results of anti-friction and anti-wear	177
.....	

University of Malaya

CHAPTER 1: INTRODUCTION

1.1 Introduction

This chapter will discuss the background of study and from where the term tribology originates. The tribology branch will be defined, and its applications will be discussed thoroughly and how the tribology optimizes the moving operating system. The nanomaterials, its categories, and its main benefits will be explained too. The research problem will be revealed the missing research contributions for various mixtures of nanoparticles and API base stock lubricants. Moreover, the objectives of research will be listed in this section. The importance of research and how the nanomaterials become a skeleton bone in advance technology will be discussed thoroughly. Furthermore, in the scope of research work will explain formulation and morphological characterization of nanomaterials titanium dioxide anatase TiO_2 (A), zinc oxide (ZnO) and graphene. A range of nano-concentrations with PBO-GII to distinguish the smallest friction and wear damages that happen while sliding movement will be discussed too. This study will demonstrate the crucial role of dual nanoparticles (TiO_2 (A) + Graphene) and (ZnO + Graphene) in improving the tribological properties via surface activity of the additives confirmed by the COF, WSD, SWR, FE-SEM, EDX/EDS, elements mapping, Raman spectra, and surface roughness measurements.

1.2 Background of the Study

The term tribology originates from Greek root τριβ- of verb tribo, "To rub" in ancient Greek and suffix -logy from -λογία, -logia "study of" or "knowledge of". Tribology is a branch of mechanical engineering and materials science. It incorporates the interdisciplinary science and technology of contacting components in relative movement and linked topics and systems. It encompasses sections of physics, solid mechanics, fluid

mechanics, lubricant theology, heat transfer, materials science, chemistry, reliability, and performance (Jost et al., 1966).

Tribology is a fundamental facilitating technology in practically all mechanical operations, involving biomedical purposes as illustrated in Figure 1.1.

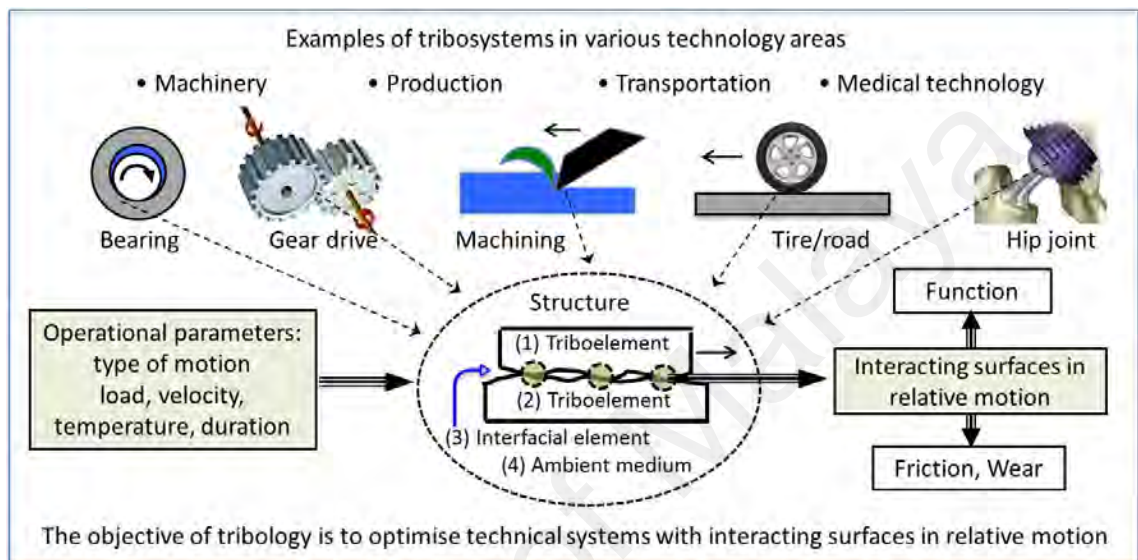


Figure 1.1: Introduction to tribology field and parameters of a tribosystem

Source: (Horst Czichos, 2017)

Tribology is a science and engineering of rubbing materials in relative movement. It involves the study and interaction of the principle of friction and wear and lubrication and the associated interfacial reactions between metals/solids, between metals/solids and liquids, or between metals/solids and gases. (This explanation is in accordance with the previous standard, DIN 50323). Consequently, an essential purpose of tribology is to enhance movable systems functionally, economically, in addition to ecologically (Tribology, 2019), as presented in Figure 1.2.

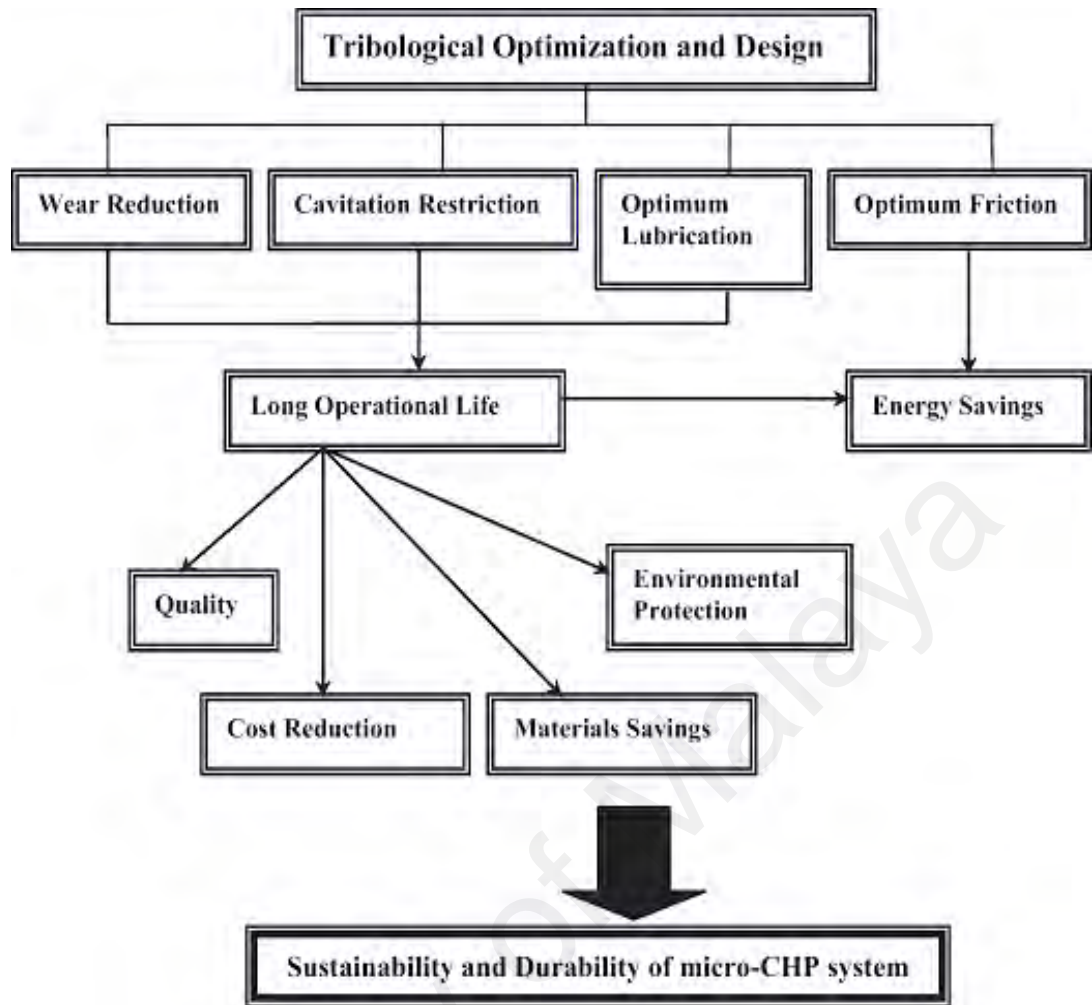


Figure 1.2: Schematic representation of the tribological optimization configuration

Source: (I. Tzanakis, 2012)

Nanomaterials define as nanoparticles range from 1 to 100 nanometers (nm) in size, as illustrated in Figure 1.3. In nanotechnology, a particle is described as a tiny body that performs as a full part in reference to its transporter and characteristics. Particles are further categorized based on diameter (Batista, 2015), as follows:

1. Extremely tiny particles are identical to nanoscale particles and range from 1 to 100 nanometers (nm) in size.
2. Tiny particulates are range from 100 to 2,500 nm.
3. Small particles comprise a scale between 2,500 and 10,000 nm (Granqvist, Buhrman, Wyns, & Sievers, 1976).

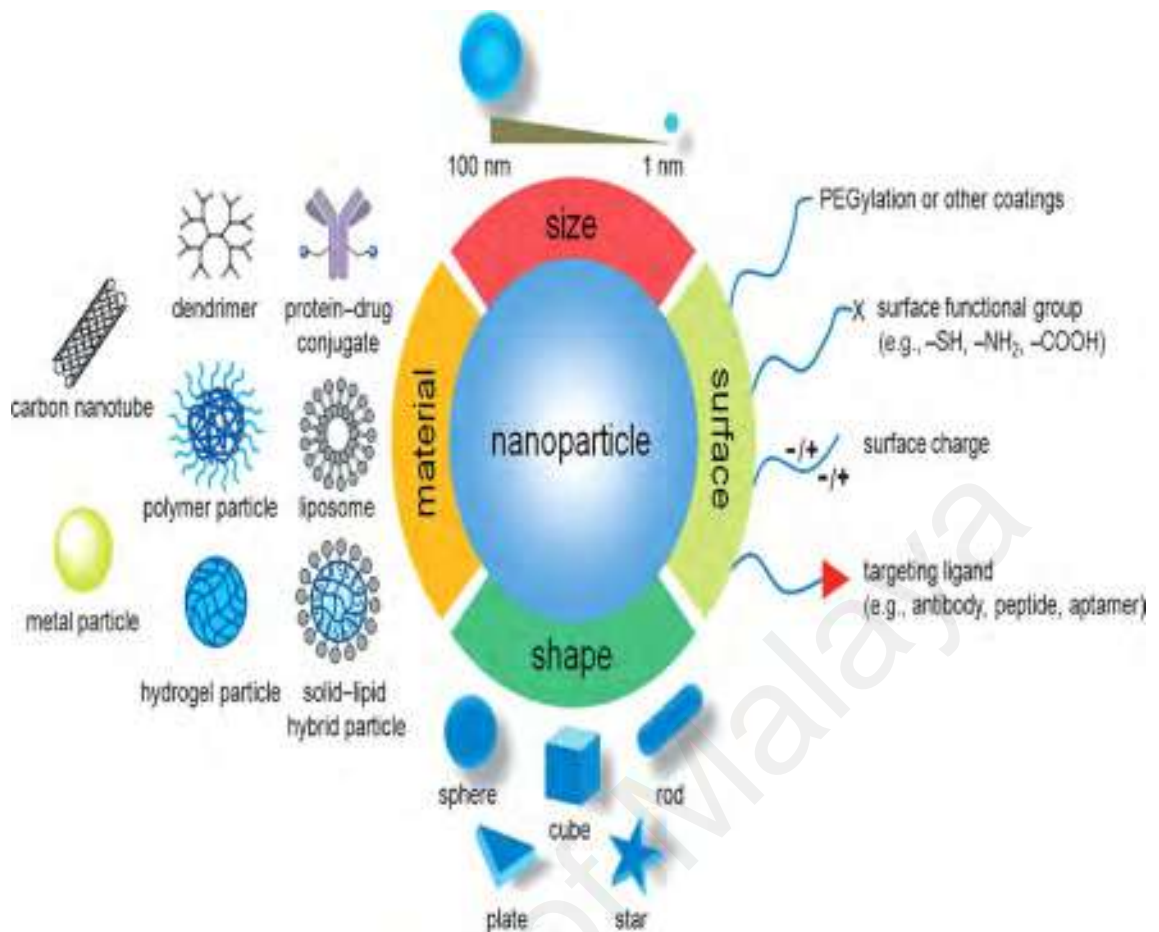


Figure 1.3: Nanoparticles overview with respect to material type, size/volume, surface, and shape type

Source: (Hendrik Heinz, 2017)

In this context, modern advancements in nanoparticle engineering have revealed distinct possibilities for oil additives, with this technology take advantage of the engaging friction and wear-reduction attributes of nanoscale particles. A number of purposes urge the chosen of nanoscale particles as oil additives, the most crucial of which is their nano-size, which facilitates nanoscale particles to step inside the contacting region and perform a wear protection layer leading to deliver a favorable lubrication result as illustrated in Figure 1.4 (N. G. Demas, Timofeeva, Routbort, & Fenske, 2012; Ghaednia, 2014). Besides, their tiny-sized enables them to move freely throughout the filters utilized in some oil equipment (Ghaednia, 2014; Hugh Spikes, 2015). Five main benefits of

employing nanoscale particles as oil additives have been stated by Hugh Spikes (2015), as follows:

- 1) Non soluble in nonpolar lubricating stock oil;
- 2) Poor reactivities characteristics with different oil additives;
- 3) High occurrence of layer formation on different surfaces;
- 4) More endurance; and
- 5) High ability to resist high temperatures due to high non-volatility.

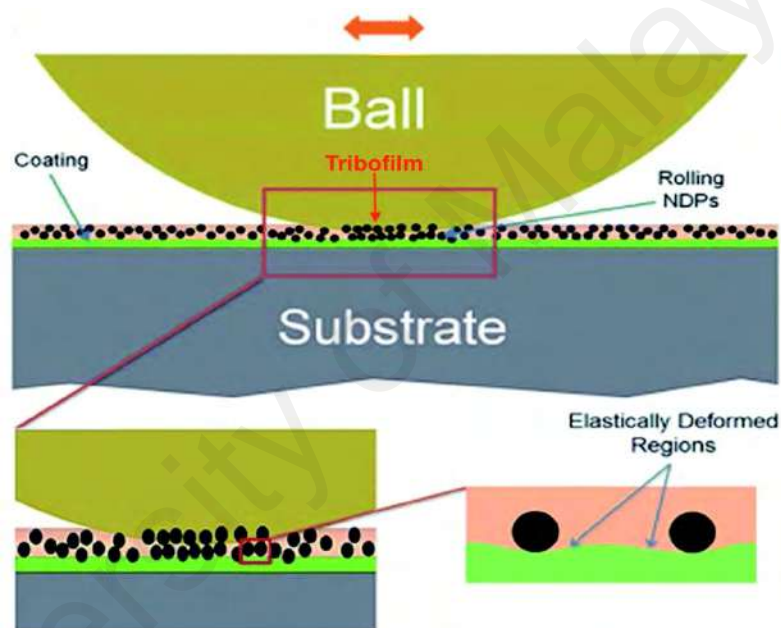


Figure 1.4: Schematic illustration of tribofilm formation by nanoparticles

Source: (Kong, Sun, & Bao, 2017)

1.3 Research Problem

Over the past decade, nanoscale particles have appeared as versatile additives owing to their capability to serve multiple purposes, for example, antiwear additives and friction modifiers. There are many findings that exhibited the lubrication potential of nanoparticles as lubricant additives through tribological interactions. However, many of the investigations have used synthetic base oils and bio-lubricants.

Despite potential tribological benefits, research contributions are missing for various mixtures of nanoparticles and API base stock lubricants. Thus, research contributions are necessary to examine the lubrication potential of nanoparticle combinations as additives to API base stock group II through four-ball interaction.

After conducting a desk-research about a range of nanoparticles to be a suitable candidate as an additive to API base stock lubricant group II to achieve excellent lubricity: (reduced equipment wear through improving lubricant film, longer equipment life, less downtime, low maintenance costs, energy savings through friction reduction, and surface roughness decrement), therefore, nanographene particulates have been selected to blend it with two types of nano-metal oxides (TiO_2 anatase and ZnO) to formulate novel nano-additives can be added to industrial base oil.

To the best of my knowledge, studies on the tribological behavior of nano combined (TiO_2 Anatase + Graphene) and (ZnO + Graphene) are not entirely understood. Besides, no study has been presented the surface roughness measurements of these nanoparticles' mixtures. Therefore, the present study investigates this research gap and highlights the key findings.

1.4 Research Objectives

The objectives of the research are as follows:

1. To select novel nano-additive can be appropriate for lubrication industry from the tribological perspective.
2. To formulate a variety of nanoparticles (single and dual combination) with different concentrations with API base oil group II as a lubricating oil additive.
3. To investigate the tribological performance of the formulated lubricants.
4. To characterize the morphology of balls scars for all tested lubricants.

5. To determine surface roughness measurements for defective balls regions after applying various types of lubricants.

1.5 Research Importance

Nowadays, nanomaterials become a skeleton bone in advance technology. These nano-smart materials have broad applications in several industries. Moreover, there are many companies worldwide that would like to improve and upgrade the lube oil and enhance its performance. There is a big concern for improving the lube oil by using nanotechnology and more precisely with using nanomaterials. Therefore, this research was implemented to find out a distinct nanolubricant feasible as an antifriction, antiwear, surface morphology improvement, more extended machining cycle, shorter downtime, lowering maintenance expenses, energy savings, and surface roughness reduction. For these purposes, formulation of metal oxides (TiO_2 anatase and ZnO) with graphene through various concentrations in pure base oil group II (PBO-GII) as lubricating oil additives have been carried out. Furthermore, investigations of the tribological performance were done for the prepared friction modifier lubricants. Moreover, characterizing the surface morphology of each ball with particularly treated lubricant. Consequently, optimization in the tribological properties of PBO-GII in virtue of combined nanoparticle additives. The synergetic combination of two nanoparticles was presenting a reduction in friction, wear loss and surface protection enhancement.

1.6 Scope of Research

This work revolves around formulation of nanomaterials titanium dioxide anatase TiO_2 (A), zinc oxide (ZnO) and graphene with one type of surfactant and API base oil group II (PBO-GII). The morphology of these three nanostructures of TiO_2 (A), ZnO , and graphene was characterized by transmission electron microscopy (TEM). Sonication treatment, and dispersion stability analysis were conducted after the formulation of nanoparticles with surfactant and pure base oil for certain concentrations. A range of

concentrations (0.0 wt%, 0.2 wt%, 0.4 wt%, and 0.6 wt% mg/ml) of two groups of dual nanoparticles which include (TiO₂ (A) + Graphene) and (ZnO + Graphene) were blended with PBO-GII individually to distinguish the smallest friction and wear damages that happen while sliding movement.

A Four-ball tester utilized to measure the tribological performance of nanolubricants and base lube oil. The evaluations were based mainly on average friction coefficient (COF), average wear scar diameter (WSD) and average specific wear rate (SWR). This tribological analysis was further aided by surface characterization tools (FE-SEM, EDX/EDS, and elements mapping microanalyses). Moreover, Raman analysis was used to further examine the presence of nanoparticles TiO₂ (A), ZnO, and graphene over the steel balls after tribological tests. Additionally, a 3-dimensional optical (non-contact) surface texture analysis apparatus was employed to examine the worn area on each ball. Besides, to conduct profile roughness measurement, surface texture measurement, surface skewness and surface kurtosis measurement, and profile form measurement for identifying surface texture, friction, and wear losses of all tested steel balls.

The synergistic lubrication effect of (TiO₂ (A) + graphene) and (ZnO + graphene) nanoparticles, as well as the morphology structure of scar balls, have been explained. Thus, it has been discovered to be efficient lubricant additives that perform better than base stock oil.

1.7 Conclusion

Much work has been made to explore and develop new sorts of lubricating oil nano-additive to diminish wear and friction in tribological systems and to enhance surface morphology. The use of dual nano-additives have examined for the lubricating capacity and durability of lubricant. This study demonstrated the crucial role of dual nanoparticles (TiO₂ (A) + Graphene) and (ZnO + Graphene) in improving the tribological properties

via surface activity of the additives confirmed by the COF, WSD, SWR, FE-SEM, EDX/EDS, elements mapping, Raman spectra, and surface roughness measurements. To this end, based on experiment results and surface analyses, the conclusions and recommendations were made.

University of Malaya

CHAPTER 2: LITERATURE REVIEW

2.1 Introduction

This chapter will discuss about reviewing several topics such as base oil types and variations, API base oil groups, general oil additives, friction modifiers and wear protection additives, and nanoscale particle additives. Moreover, two groups of nanoparticles will be studied (TiO₂ and graphene) and (ZnO and graphene) in this research. The stability of nanoparticles, dispersion Technique, dispersion stability analysis for nanolubricants, and techniques to improve the nano-oils dispersion stability will be reviewed as well. The importance of nanoscale particles concentration, role of nanoparticle size, role of nanoscale particle shape and structure will be considered. The optimization of the concentration for tribology boosts and comparison of poor-results of anti-friction and anti-wear will be discussed as well. The function of tribo-testers standard and configurations and the tribological performance also studied thoroughly.

The high amount of frictional energy losses between tribo-pairs has urged the tribologists and researchers to examine different additives as the potential constituent of conventional lubricating oil. It has been well-known that using additives to improve the lubrication capacity and durability of oil plays a main part in the wear and friction process of materials (Juozas Padgurskas, 2013), (Hayrettin Düzcükoğlua, 2015), (Tianyi Sui, 2016), and (Adli Bahari, 2017). Many research works have been carried out to decrease friction and wear to save energy and metal surface using water and mud till oil with lubrication additives (Diana Berman, 2014) and (Xin Quan, 2016). Globally one car uses an average of 340 liters of fuel per year as frictional energy losses (Holmberg K, 2012). Overall in transportation sector, 1 million barrels/day (48 million USD/day) is lost due to friction (Fenske G, 2009).

2.2 Base Oil Types and Variations

Oil function relies mainly on the condition and characteristics of the base oil. Oils can be classified into three categories, as follows:

1. Mineral crude oil derived: characteristics rely on the quality of the crude oil and refining method. A mineral lubricant is the most fundamental sort of engine lubricant. It is produced in the refinery after having been distilled from crude oil. As a complete stock, mineral oil is 80-85% base oil with 15-20% additives to determine viscosity and emissions agreement. The more popular viscosity would be 15W-40 or 20W-50.
2. Synthetic or man-made lubricants: integrated from various chemical mixtures. It is not entirely man-made, but it is very imminent. To make a polymerized lubricant the refinery still begins with crude oil, however, after the crude is refined and petroleum is distilled, this is later employed to begin the synthetic lubricant method. The upright oil stock is chemically separated or “cracked”, and the molecules are reconstructed in particular techniques to generate a synthetic base lubricant. The complete stock is later a blend of synthetic base petrol and also multiple additive combinations to create the needed engine lubricant. Owing to these additional methods a synthetic lubricant can be customized to nearly any viscosity series comprising 0W-30, 0W-40 and 10W-60. According to engine configuration and application, a synthetic stock can be much greater resistance to wear when compared with mineral or semi-synthetic base stocks. These parameters also lead to a much higher cost to manufacture and this can be restrictive for vehicle producers when taking into account engine, maintenance, disposal methods of oil, and availability of oil. Besides, synthetic oil is not supported for rotary model engines.

3. Vegetable obtained from vegetable oils: unique refining processes according to sort of seed. Vegetable lubricants, or vegetable fats, are oils derived from seeds, or less commonly, from other pieces of fruits. Furthermore, animal fats, vegetable fats are composed of triglycerides. Soybean oil, rapeseed oil, and cocoa butter are instances of fats from seeds. Olive oil, palm oil, and rice bran oil are instances of fats from other pieces of fruits. In general use, vegetable oil could indicate particularly to vegetable fats which are liquid at room temperature. Vegetable oils are regularly edible; non-edible oils extracted principally from petroleum base stocks are termed mineral oils. One of the limiting factors in industrial applications of vegetable lubricants is that all such lubricants are exposed to converting rancid. Oils that are steadier, for example, ben oil or mineral oil, are therefore favored for industrial purposes. Castor oil has various industrial applications, due to the behavior of hydroxyl group on the fatty acid. Castor lubricant is a precursor to Nylon 11. Despite, vegetable lubricants are less steady chemically, so they are commonly utilized in systems where they are not presented to oxygen, and they are also high-priced than crude oil distillation. This parameter further results in an expensive cost to synthesize and this can be limiting for industry producers when taking into consideration servicing and affordability (Lubrication, 2019; Moly, 2019; Thomas, 2002).

2.3 API Base Oil Groups

Practically every oil employed in factories now began off as only a base oil. The American Petroleum Institute (API) has classified base oils into five classes (API 1509, Appendix E). The first three groups are derived from petroleum crude oil. Group IV base lubricants are complete synthetic (polyalphaolefins) oils. Group V is for all other base petroleums not mentioned in Groups I through IV. Before all the additives are blended with the oil, lubricating oils start as one or more of these five API groups.

1. Group I oils are solvent processed, which is a more simplistic refining method, giving them the least processed and thus also the most economical base oils possible. Solvent-refined lubricants compose generally of a blend of diverse hydrocarbon molecules which cannot be recognized in the refining process. These irregular molecules in oil resulted in high friction consequent. Group I lubricants are hence applied most often in limited particular purposes.
2. Group II base oils undergo hydrocracking which is a more complex method than the method of Group I lubricants. Hydrocracking is a process that separates down long hydrocarbon molecules into shorter ones. The hydrocarbon molecules of these lubricants are saturated, making them excellent antioxidation characteristics. Group II lubricants are priced closely to Group I lubricants.
3. Group III oils undergo an even more extended process than Group II petroleums. The process, called severe hydrocracking, is also more concentrated. More pressure and heat are implemented throughout the refinery process, so it can increase the cost of the oil. This process provides a purer base stock with higher quality. Even though Group III petroleums are obtained from crude oil, they are sometimes described as synthesized hydrocarbons.
4. Group IV base oils are polyalphaolefins. These are not derived but proceeded from tiny uniform molecules. This is also the most significant benefit of PAOs because they can be fully customized to have a composition with predictable characteristics. They are perfectly suited for application in extreme cold or extreme hot circumstances.
5. Group V oils included any sort of base oils other than specified in the earlier described groups. If it is a synthetic lubricant and it is not PAO it is a group V base oil. They comprise, amongst others, of naphthenic oils and esters.

Commonly, Group V oils are not applied as a base oil but as an additive to other base stocks, as tabulated in Table 2.1.

Table 2.1: Saturated level, sulfur level, and viscosity index of five API groups

Group Type	Manufacturing Process	Saturated Level	Sulfur Level	Viscosity Index
Group I	Solvent Refining	< 90%	> 0.03%	80 – 120
Group II	Hydro-processing (Hydrocracking)	≥ 90%	≤ 0.03%	80 – 120
Group III	Severe Hydrocracking (Catalytic De-waxing)	≥ 90%	≤ 0.03%	≥ 120
Group IV	Chemical Reaction (Synthesizing)	100% PAOs (Poly-Alpha-Olefins)		
Group V	As Indicated	All others not indicated in Groups I, II, III, or IV Naphthenic oils and esters		

Source: (Lubrication, 2019)

2.4 Oil Additives

While engine works, oil is supposed to deliver efficient lubricating for extensive term before it is emptied. To fulfill these requirements, the base oil is mixed with many additives, which need to be meticulously chosen to form the oil with the wanted behavior. The additive groupings have developed to perform a progressively essential role in

lubricant preparation. The base oils include normally 75 – 83 wt% of marketing engine oil. For various engine purposes, viscosity enhancers (5 – 8 wt%) and limited numbers of other additives (12 –18 wt%) are applied to improve additional oil characteristics (Watson, 2010). Standard additives are artificial chemical compounds blended with plain lubricants to enhance many properties of oils. Hence oils can minimize the higher demand and meet the required specifications. Additives usually develop actual features, overcome unwanted characteristics, and add distinct attributes to the plain lubricants. One of the major characteristics that additives improve is an oil's capability to create protecting layers, which is particularly significant in boundary lubricating conditions. During mixing additives with plain lubricants, it is essential to have a consistent and suitable structure to develop the behavior of the oil. This normally needs the formation of high-efficiency plain lubricants that are obtained from remarkably distilled oils and then blended with additives for additional improvement in lubricant's features. Numerous of the most popular additive packages employed in oil preparation is wear protection additives, extreme pressure resistance additives, viscosity enhancers, oxidation suppressants, corrosion suppressants, detergents, dispersants, and foam suppressants.

2.4.1 Friction Modifiers and Wear Protection Additives

In tribo-pairs, when couple bodies involve in metal-to-metal interaction and start moving related to one another, antiwear (AW) additives and friction modifiers (FMs) have a crucial role of engine lubricant to resist seizure, wear damage, and friction defects. Wear and friction enhancers composed of chemical additives that could be categorized into three sets: adsorption or boundary additives; antiwear additives; and extreme pressure (EP) additives. Boundary additives are friction and wear protectors such as fatty acids that are blended to the plain lubricant to reduce the asperity interaction. All of these additives assist in supporting the lubrication behavior of the lubricant which makes their usage useful. In the result of inefficient lubricating, deep friction and severe wear will

happen, creating defects to the contacting bodies with commonly an increment in energy loss. Comprehensive research on the appropriateness and concentration of FMs and AW additives have been accomplished for standard oils. A lot of research workers (Lukas Bogunovic, 2015), (F.A. Essa, 2017), and (Siti Safiyah Nor Azman, 2016) confirmed that nanoscale particles addition is more efficient for oils' tribological properties improvement.

2.4.1.1 Nanoscale Particles as Additives

The inquisition for energy proficiency has directed the study towards distinct substances, rather than conventional substances, for the usage of oil additives. Presently, different sorts of nanoscale particles are under research as oil additives (V.N. Bakunin, 2004), (Wei Dai, 2016), and (Kwangho Lee, 2009). In the expansion history of oil additives, nanoscale particles are a comparatively latest range of oil additives as specified in Figure 2.1.

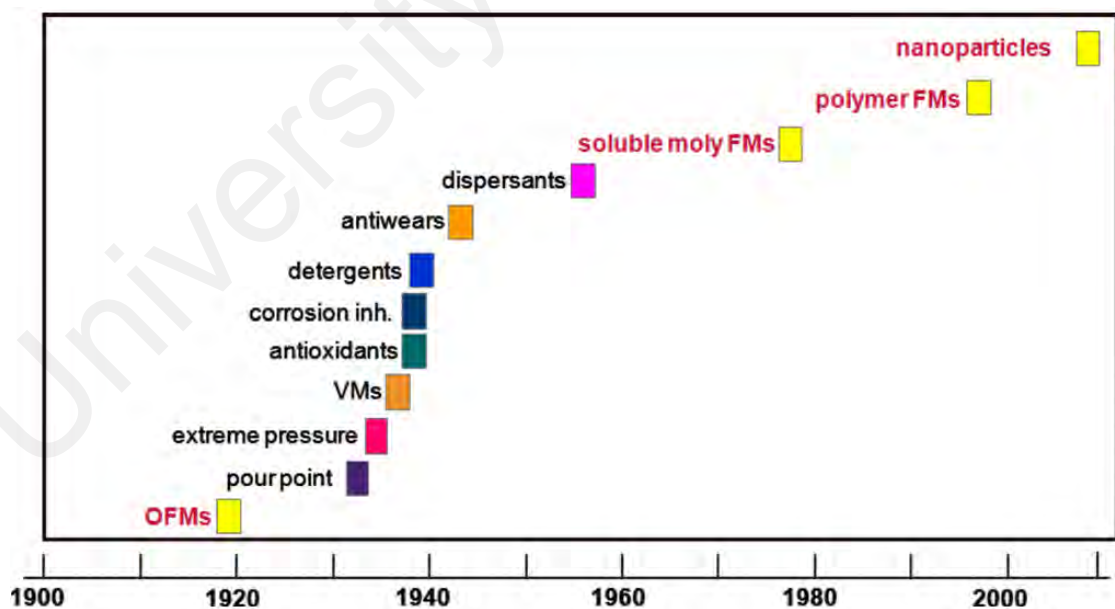


Figure 2.1: Timeline for the advancement of oil additives

Source: (H. Spikes, 2015)

Nano-oils usually composed of plain lubricants or completely prepared oils with colloidal solid particulates dissolved within the mixture (L. Joly-Pottuz, Vacher, B., Ohmae, N., Martin, J. M., & Epicier, T., 2008) and (Emad Sadeghinezhad, 2016). There are typically three basics in a nano-lubricant; the lubricant/base oil fluid, the nanoscale particulates that perform as antiwear (AW)/extreme pressure (EP) additive or friction modifier (FM), and the precursor that resides the interfacial between the lubrication oil and the nanoscale particles (L. Joly-Pottuz, Vacher, B., Ohmae, N., Martin, J. M., & Epicier, T., 2008).

Nano-lubricating contributes an answer to various obstacles related to common oils that include Sulfur and Phosphorus (L. Joly-Pottuz, Vacher, B., Ohmae, N., Martin, J. M., & Epicier, T., 2008). Despite, some nanoscale particles bear toxic characteristics, for similar nano-oils, the removal of nano-oils after draining period is required to be handled in agreement with local administrations by authorized waste disposal department, considering the stock properties at the event of disposal. Nanoscale particles are multipurpose, and many research workers have mentioned that a particular sort of nanoscale particle delivered versatile as AW/EP additives in addition to FMs (J. E. F. R. A. Hernandez Battez, A. Navas Arias, J.L. Viesca Rodriguez, R. Chou Rodriguez, J.M. Diaz Fernandez, 2006; Cho, 2012; P. Nallasamy, Saravanakumar, N., Nagendran, S., Suriya, E., & Yashwant, D., 2014; V. Srinivas, 2016). Owing to the different sorts, sizes, and morphologies of nanoscale particulates, the mixtures of nanoscale particulates and oils may lead to various nanofluids/nano-oils.

Figure 2.2 and Table 2.2 present the distinction in sorts, origins, volume and geometry for generally applied nanoscale particles in many subjects. Even though several types of research have revealed excellent tribological advancement in oils dispersed with various sorts of nanoscale particles, it is quite hard to choose the suitable nanoscale particle

additive. The efficiency of nano particulates relies on multiple parameters, involving their adaptability with lubricant/base oil, concentrations, sizes, along with their morphologies (L. Peña-Parás, Taha-Tijerina, J., Garza, L., Maldonado-Cortés, D., Michalczewski, R., & Lapray, C., 2015). In order to specify a convenient nanoscale particle and oil mixture, it is expected to review all these factors while concentrating on their tribological testing circumstances and associated lubricating techniques.

University of Malaya

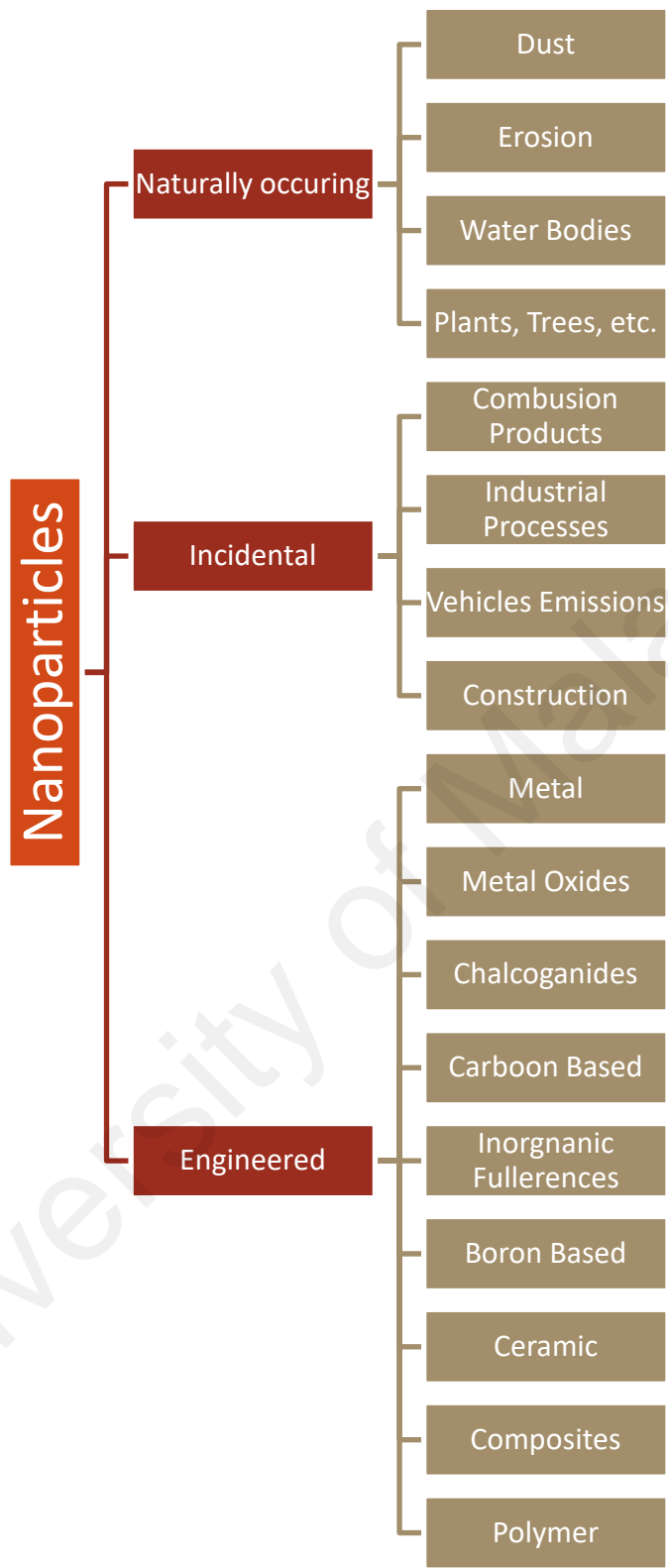


Figure 2.2: The primary categories of nanoscale particles with subgroups of engineered nanoscale particles associated with tribological researches

Table 2.2: Review of origins and common characteristics of nanoscale particles employed as oil additives

Sort	NPs	Source	APS (nm)	Geometry	Authors
Metal	Cu	Saleable	25	Nearly spherical	(J. L. Viesca, Battez, González, Chou, & Cabello, 2011)
	Ni		20	Nearly spherical	(R. Chou et al., 2010)
	Al		65	Spherical	(Peng, Kang, Chen, Shu, & Chang, 2010)
	Pb	Formulated	2.2	Spherical	(L. Kolodziejczyk, Martinez-Martinez, Rojas, Fernandez, & Sanchez-Lopez, 2007)
			40	Spherical	(Zhao, Zhang, & Dang, 2004)
Metal Oxides	CuO	Formulated	5	Sphere-like	(Y. Y. Wu, Tsui, & Liu, 2007)
			4.35	Nearly spherical	(Alves, Barros, Trajano, Ribeiro, & Moura, 2013)
	ZnO	Formulated	11.71	Nearly spherical	(Alves et al., 2013)
		Saleable	20	Nearly spherical	(Battez et al., 2007)
	TiO ₂	Formulated	80	Sphere-like	(Y. Y. Wu et al., 2007)
TiO ₂ Anatase	Saleable	25	Semi-Spheres	(Waleed Alghani, 2019)	
Chalcogenides	MoS ₂	Saleable	90	Layered lamellar flaky	(C. P. Koshy, Rajendrakumar, & Thottackkad, 2015)
		Formulated	350, 150	Layered	(P. Rabaso, 2014)
	100		Rectangular, oblate	(Yadgarov et al., 2013)	
	WS ₂	Formulated	100	Spherical	(L. Rapoport et al., 2003)
120			Polyhedral, faceted	(Yadgarov et al., 2013)	

‘Table 2.2: continued’

Sort	Nanoscale particles	Source	APS (nm)	Geometry	Authors
Carbon based	Diamond	Saleable	10	Sphere-like	(Y. Y. Wu et al., 2007)
	Graphite		55	Spherical	(Lee et al., 2009)
	Carbon nano horns		80	Dahlia like	(V. Zin, Agresti, F., Barison, S., Colla, L., & Fabrizio, M., 2015)
	Graphene	Formulated	10	Spheroidal	(L. Joly-Pottuz, Vacher, B., Ohmae, N., Martin, J. M., & Epicier, T., 2008)
Saleable		5	Planar	(Waleed Alghani, 2019)	
Nitrides	BN	Saleable	70	Spherical	(M. I. H. C. Abdullah et al., 2016)
			114	Non-spherical	(Çelik, Ay, & Göncü, 2013)
Ceramic	Al ₂ O ₃	Formulated	78	Spherical	(T. Luo, Wei, Huang, Huang, & Yang, 2014)
	SiO ₂	Saleable	30	Spherical	(H. Xie, Jiang, He, Xia, & Pan, 2015)
		Formulated	362, 215, 140, 58	Spherical	(Peng, Chen, Kang, Chang, & Chang, 2010)
Composites	Al ₂ O ₃ /SiO ₂	Formulated	70	Elliptical	(D. Jiao, Zheng, S., Wang, Y., Guan, R., & Cao, B., 2011)
	ZrO ₂ /SiO ₂		50-80	Nearly spherical	(W. Li, Zheng, Cao, & Ma, 2011)
Polymer	PTFE	Saleable	30-50	Spherical	(K. D. Mukesh, Jayashree, & SSV, 2013)

Most works focused on developing high-performance lubricating oil additives to decrease wear, friction, wear scar diameter, and friction coefficient while enhancing the load carrying capacity and extreme pressure in tribological systems. Nanomaterials

possess very different properties compared to its macroscale counterparts' due to surface effects, where there are more atoms on its surface, which translate into higher surface energy and increased rates of chemical reactions. Volume effects also play a role in the effectiveness of the nanoparticles, where lower wavelengths translate into higher frequency and energy (D. P. Macwan, 2011). Advances in nanotechnology have helped introduce the use of nanoparticles in lubricating oil, which, in the majority of previous research works, has indicated improved lubrication properties (Wang, 2008), (J. E. F. R. A. Hernandez Battez, A. Navas Arias, J.L. Viesca Rodriguez, R. Chou Rodriguez, J.M. Diaz Fernandez, 2006), (S.A. Angayarkanni, 2015), (Debrupa Lahiri, 2014), (Wei Dai, 2016), and (Wei Li, 2017). Metal oxide nanoparticles possess exclusive chemical and physical features as lubricant additives, for instance, ZnO, CuO, TiO₂, ZrO₂, Fe₃O₄, and Al₂O₃ (Wei Dai, 2016).

These paragraphs below covered the selection of ideal dual nanoparticles mixtures, an overview of the tribological importance of nanoscale particles, source, geometry and volume in addition to the role of oil/nanoparticulate adaptability, weight/excellent nanoscale particles concentrations, and laboratory analyses circumstances (topography, applied load, interaction, temperature, rotating speed, duration, etc.).

A. TiO₂ and Graphene Nanoparticles

Titanium dioxide (TiO₂), or titania, is a very well-known and well-researched material due to the stability of its chemical structure, biocompatibility, and favorable physical, properties. It exists in three mineral forms: anatase, rutile, and brookite. Anatase has a tetragonal crystalline structure (dipyramidal habit). TiO₂ anatase preferred as a metal oxide additive due to its high specific area, non-toxic, relatively inexpensive, better dispersion of the formulation, barrier properties in the coatings, and self-healing effect improving its anti-corrosion behavior (D. P. Macwan, 2011). TiO₂ nanoparticles reported

superior anti-friction and anti-wear characteristics as well (S. K. H. M. Vijayaraj, A. K. Harinarain & S. S. V. Ramakumar, 2016). Besides, when applied to discs, they adequately cover the tribochemical layers created during the experimental run, which resulted in reduced wear (Lukas Bogunovic, 2015).

Nano graphene is the material of the century due to its superb physiochemical properties in tribology applications. Graphene is two-dimensional material that exhibits exclusive friction and wear properties that are uncommon in conventional materials. Moreover, its well-established thermal, and mechanical properties allow it to function as a solid or colloidal liquid lubricant. Its high chemical inertness, extreme strength, and simple shear capability on a thickly packed and atomically smooth surface are key positive attributes that made its unusual tribological behavior possible. It is also ultra-thin, even if multi-layered, and can be applied to nano-scale or micro-scale systems, such as microelectromechanical systems (MEMS) and nanoelectromechanical systems (NEMS) with oscillating, rotating, and sliding contacts to reduce adhesion, friction, and wear (Diana Berman, 2014) and (S. K. H. M. Vijayaraj, A. K. Harinarain & S. S. V. Ramakumar, 2016).

B. ZnO and Graphene Nanoparticles

ZnO nanoparticles have a polycrystalline structure that resembles a seed-like or nearly spherical morphology (J. E. F. R. A. Hernandez Battez, A. Navas Arias, J.L. Viesca Rodriguez, R. Chou Rodriguez, J.M. Diaz Fernandez, 2006; Manjula G. Nair, 2011; B. S. B. S.M. Alves, M.F. Trajano, K.S.B. Ribeiro, E. Moura., 2013). ZnO is comparatively cheaper than various other nanoparticles (Shailesh K. Dhoke, 2009). 60SN base oil with ZnO nanoscale particles could notably decrease friction and wear. When the quantity of oleic acid blended was 8 wt% and ZnO nanoscale particles were 0.5 wt%, the coefficient of friction and mean diameter of the wear marks were smallest and the nanofluid

presented more favorable friction-reduction and wear protection characteristics (Xu Ran, 2016). ZnO exhibits outstanding behavior in friction reduction, wear protection ($WSD = 256.0 \pm 4.2 \mu\text{m}$) and a better film formation when blended with mineral oil (B. S. B. S.M. Alves, M.F. Trajano, K.S.B. Ribeiro, E. Moura., 2013). Likewise, ZnO nanoscale particles can reduce the coefficient of friction and improve the wear lifecycle to different degrees (Hao-Jie Song, 2010). ZnO nanoparticles as a lubricant additive exhibit superior EP characteristics in PAO6 mixtures (J. E. F. R. A. Hernandez Battez, A. Navas Arias, J.L. Viesca Rodriguez, R. Chou Rodriguez, J.M. Diaz Fernandez, 2006).

Recently, ample studies have been conducted on the usage of carbon-based nanostructures to formulate nanolubricants (S.A. Angayarkanni, 2015) and (Monireh B. Moghaddam, 2013). Relatedly, numerous researchers seem to prefer Graphene due to its unique thermal, electrical, optical, mechanical and other relevant characteristics (Vikas Kumar, 2015). The study of Graphene-based nanofluids and nanolubricants has also been prominent in recent years (A.K. Rasheed, 2016). Graphene is among the best materials deliberated in this decade (S. T. L. Mohammad Mehrali, Mehdi Mehrali, Teuku Meurah Indra Mahlia, Hendrik Simon Cornelis Metselaar, 2013) and (S. T. L. Mohammad Mehrali, Mehdi Mehrali, Teuku Meurah Indra Mahlia, Hendrik Simon Cornelis Metselaar, Mohammad Sajad Naghavi, Emad Sadeghinezhad, Amir Reza Akhiani, 2013). It is a single-atom-thick film of hexagonally arrayed sp^2 -bonded carbon atoms, which has gained momentous consideration since Novoselov et al. discovered it (K. S. Novoselov, 2004). Graphene nanoparticles are significant for they possess the following advantages: simple to synthesize, long suspension time (extra steady), great surface area/volume ratio (1000 times superior to other nanoparticles), high thermal conductivity, minor erosion, corrosion and clogging, low demand for pumping power, lower inventory fluid heat transfer and substantial energy saving potential (Emad Sadeghinezhad, 2016). Graphene is also a lamellar structured material, can shear directly at contact interfaces and presents

unusual mechanical strength and conductivity, which assure its potential for tribological purposes (Wei Li, 2017). Graphene particles and carbon nanotubes (CNT) exhibit remarkable anti-wear, and extreme pressure, anti-friction and physicochemical properties (Shanhong Wan, 2016).

2.4.1.2 Stability of Nanoparticles and Dispersion Technique

When nanoparticles (NPs) added to an oil medium, the size of the NPs is tiny to continue scattered in fluids by Brownian movement. This is owing to the irregular movement of NPs that was initially recognized by Robert Brown and confirmed by Albert Einstein in 1905 (Einstein, 1905). The NPs in lubricant might adhere unitedly and produce further accumulation, perhaps will be sedimented because of gravity. The agglomeration of NPs effects not just in settling down but also in wear loss and friction damage. Hence, the dispersion technique is very useful for good lubrication behavior. In the act of inadequate dispersion balance, sedimentation, and agglomeration might occur (K. Lee, Hwang, Y., Cheong, S., Choi, Y., Kwon, L., Lee, J., & Kim, S. H., 2009). The constancy of NPs indicates that the particles do not agglomerate at a notable rate. For constant dispersion stability of nano-oils, the chosen technique for dispersion is one of the controlling factors after the selection of lubricant and NPs. As reported by Rabaso (P. Rabaso, 2014), stirring the oil blend before examining will assist in decreasing agglomerates percentage and lead to a reduction in COF, as shown in Figure 2.3.

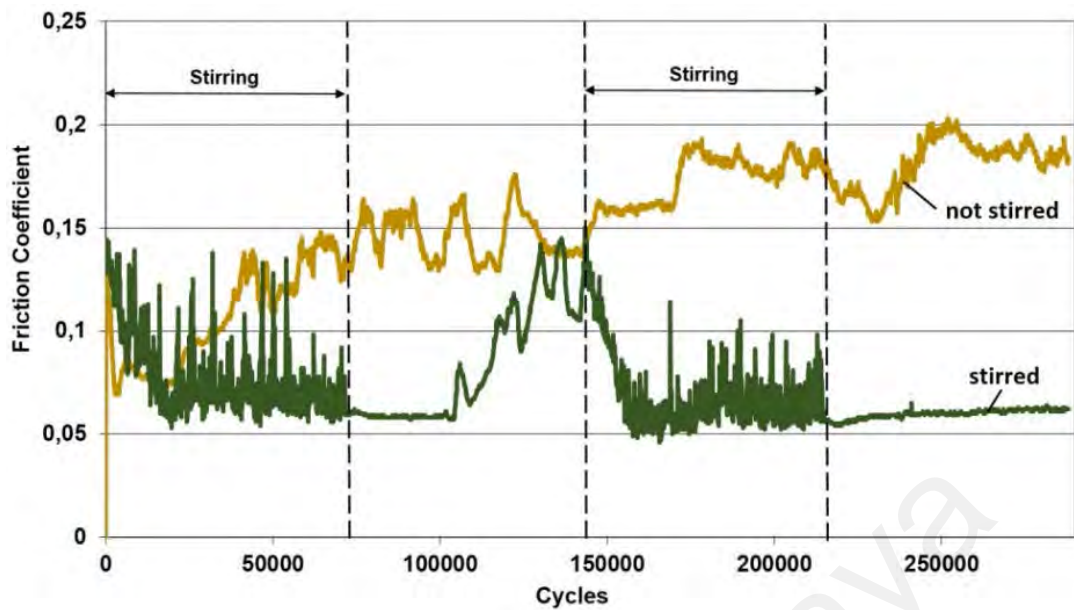


Figure 2.3: Coefficient of friction performance of stirred and unstirred oils exhibiting the efficiency of well-dispersed of nano-MoS₂ enhanced lubricant

Source: Rabaso (P. Rabaso, 2014)

Different techniques have been employed comprising magnetic stirring (P. Rabaso, 2014), chemical stir (M. Laad, & Jatti, V. K. S., 2016), stirring utilizing ultrasonic shaker (M. V. Thottackkad, Perikinalil, R. K., & Kumarapillai, P. N., 2012), stirring utilizing mechanical ball milling agitation, ultrasonic probe (B. S. B. S.M. Alves, M.F. Trajano, K.S.B. Ribeiro, E. Moura., 2013), (J. E. F. R. A. Hernandez Battez, A. Navas Arias, J.L. Viesca Rodriguez, R. Chou Rodriguez, J.M. Diaz Fernandez, 2006), and (R. G. A. Hernandez Battez, D. Felgueroso, J.E. Fernandez, Ma. del Rocío Fernandez, M.A. Garcia, I. Penuelas, 2007) and ultrasonication bath (H. M. M. Gulzar, M Varman, MA Kalam, R.A. Mufti, NWM Zulkifli, R. Yunus, Rehan Zahid, 2015), (Siti Safiyah Nor Azman, 2016), and (L. Joly-Pottuz, Vacher, B., Ohmae, N., Martin, J. M., & Epicier, T., 2008), as stated in Table 2.3.

Following the choice of the dispersion technique, the period of distribution is another an essential factor in governing the trend of accumulations. It has been noted that an

addition in the stirring duration drives to a reduction in the size of total NPs when ultrasonication bath employing (L. Joly-Pottuz, Vacher, B., Ohmae, N., Martin, J. M., & Epicier, T., 2008). Rabaso (P. Rabaso, 2014), has summarized that the friction decreased substantially as the stirring duration elevated for nano-oils. Therefore, the stirring time performs a crucial role in distribution balance and as a result, influences the lubrication behavior. Agitation time as low as 2 minutes (J. E. F. R. A. Hernandez Battez, A. Navas Arias, J.L. Viesca Rodriguez, R. Chou Rodriguez, J.M. Diaz Fernandez, 2006), and (R. G. A. Hernandez Battez, D. Felgueroso, J.E. Fernandez, Ma. del Rocio Fernandez, M.A. Garcia, I. Penuelas, 2007) and as high as 24 hours have been described (Cho, 2012), as detailed in Table 2.3.

Table 2.3: A literature review of generally employed dispersion methods to boost dispersion constancy

NPs	Oil	Dispersion Technique and Time	Surface Reform	Surface Modifying Agent/ Surfactant	Dispersion stability Analysis	Authors
ZrO ₂ / SiO ₂	20# Machine oil	Ultrasonic dispersion, 30 mins.	Yes	Aluminum zirconium coupling agent	Zeta Potential, UV-Vis Absorbance	(W. Li, Zheng, S., Cao, B., & Ma, S., 2011)
Al ₂ O ₃ / SiO ₂		Ultrasonic dispersion, 30 mins.	Yes	Silane coupling agent KH-560	Sedimentation	(D. Jiao, Zheng, S., Wang, Y., Guan, R., & Cao, B., 2011)
Al ₂ O ₃		Ultrasonic dispersion, 30 mins.	Yes	Silane coupling agent KH-560	Sedimentation, Zeta potential UV-Vis Absorbance	(T. Luo, Wei, X., Huang, X., Huang, L., & Yang, F., 2014)
TiO ₂	Servo 4T synth 10W-30	Chemical shaker for agitation, 30 mins.	No	-	UV-Vis Absorbance	(M. Laad, & Jatti, V. K. S., 2016)

‘Table 2.3: continued’

NPs	Lubricant	Dispersion Technique and Time	Surface Reform	Surface Modifying Agent/ Surfactant	Dispersion stability Analysis	Authors
ZnAl ₂ O ₄	Lubricating oil	-	Yes	OA	UV-Vis Absorbance	(X. Song, Zheng, S., Zhang, J., Li, W., Chen, Q., & Cao, B., 2012)
CuO	Multi-grade engine oil	Ultrasonic agitation, 30 mins.	No	-	UV-Vis Absorbance	(V. S. Jatti, & Singh, T. P., 2015)
	SAE-40, Coconut oil	Ultrasonic shaker, 40 mins.	No	-	UV-Vis Absorbance	(M. V. Thottakkad, Perikinalil, R. K., & Kumarpillai, P. N., 2012)
ZrO ₂	20# machine oil	-	Yes	Silane coupling agent KH-560	No	(Ma, 2010)
ZnO	60SN base oil	Ultrasonic bath 30 mins, stirrer 20 mins.	Yes	OA	Sedimentation	(Xu Ran, 2016)
CuO, MoS ₂	Palm TMP ester	Ultrasonic bath, 60 mins.	Yes	OA	UV-Vis Absorbance	(H. M. M. Gulzar, M Varman, MA Kalam, R.A. Mufti, NWM

						Zulkifli, R. Yunus, Rehan Zahid, (2015)
--	--	--	--	--	--	---

‘Table 2.3: continued’

NPs	Oil	Dispersion Technique and Time	Surface Reform	Surface Modifying Agent/ Surfactant	Dispersion stability Analysis	Authors
SiO ₂	Liquid paraffin	Ultrasonic stirrer, 60 mins.	Yes	OA	Sedimentation	(D. X. Peng, Chen, C. H., Kang, Y., Chang, Y. P., & Chang, S. Y., 2010)
hairy silica	PAO100	Stirrer	Yes	Amino Functionalized	Sedimentation	(T. Sui, Song, B., Zhang, F., & Yang, Q., 2015)
Cu	PAO6	Ultrasonic probe, 30 mins.	No	-	Sedimentation	(J. L. Viesca, Battez, A. H., González, R., Chou, R., & Cabello, J. J., 2011)
Ni		Ultrasonic probe, 30 mins.	No	-	Sedimentation	(R. Chou, Battez, A. H., Cabello, J. J., Viesca, J. L., Osorio, A., & Sagastume, A., 2010)

‘Table 2.3: continued’

NPs	Oil	Dispersion Technique and Time	Surface Reform	Surface Modifying Agent/ Surfactant	Dispersion stability Analysis	Authors
Carbon onion, Graphite	PAO	Ultrasonic bath, 300 mins.	No	-	No	(L. Joly-Pottuz, Vacher, B., Ohmae, N., Martin, J. M., & Epicier, T., 2008)
Carbon nano-onions		Ultrasonic bath, 300 mins.	No	-	Sedimentation	(L. Joly-Pottuz, Vacher, B., Ohmae, N., Martin, J. M., & Epicier, T., 2008)
SiO ₂ , MoS ₂	EOT5#	Ultrasonic shaker, 120 mins.	No	-	No	(H. Xie, Jiang, B., He, J., Xia, X., & Pan, F., 2015)

2.4.1.3 Dispersion Stability Analysis for Nanolubricants

For a study of dispersion balance, various techniques utilized. These analyses involve sedimentation, spectral absorbency, zeta potential, and metallographic characterization constancy test. Table 2.3 presents generally applied methods in different research works.

Sedimentation is the most manageable way to assess nanolubricants stability. This approach has also named as “observation stability test” (Siti Safiyah Nor Azman, 2016). For the stability measurement, sedimentation image of specimens in testing tubes are normally used (Amiruddin, 2015; C. P. Koshy, Rajendrakumar, P. K., & Thottackkad, M.

V., 2015; K. D. Mukesh, Jayashree, B., & SSV, R., 2013; D. X. Peng, Chen, C. H., Kang, Y., Chang, Y. P., & Chang, S. Y., 2010; T. Sui, Song, B., Zhang, F., & Yang, Q., 2015; Tianyi Sui, 2016). The common limitation of this process is a long time to collect the results. Furthermore, some cares must be taken such as preservation of equal volume, temperatures, and ambient circumstances for all the studied specimens. This stability study is normally conducted directly after the dispersing of nano particulates in the oil. Agitation or movements are also necessary to eliminate and to ensure accuracy. Figure 2.4 presents the sedimentation of paraffin oil blended with surface modified and unmodified aluminum nanoscale particles that were reported after one month of preparation.



Figure 2.4: Sedimentation technique of aluminum nanoscale particles dispersed in paraffin oil

Source: (D. X. Peng, Chen, C. H., Kang, Y., Chang, Y. P., & Chang, S. Y., 2010)

The period of this method differs from days to months. Peng et al. (D. X. Peng, Chen, C. H., Kang, Y., Chang, Y. P., & Chang, S. Y., 2010) stated the sedimentation performance after one month for silica and alumina nanoscale particles dispersed in

paraffin oil (D. X. Peng, Chen, C. H., Kang, Y., Chang, Y. P., & Chang, S. Y., 2010; D. X. Peng, Kang, Y., Chen, S., Shu, F., & Chang, Y., 2010). Another research by Sui et al. (T. Sui, Song, B., Zhang, F., & Yang, Q., 2015), the constancy of the nano-silica enhanced polyalphaolefin (PAO) oils were analyzed by preserving the oils for 2-month. Amiruddin et al. (Amiruddin, 2015), analyzed the dispersion constancy of SAE 15W40 enhanced with nano-hBN for two months as well. Koshy et al. (C. P. Koshy, Rajendrakumar, P. K., & Thottackkad, M. V., 2015) have summarized a testing time of 100 days for coconut oil and paraffin oil enhanced with nano-MoS₂. Mukesh et al. (K. D. Mukesh, Jayashree, B., & SSV, R., 2013) conducted this test for 7 days for PTFE based nano-oils. Therefore, various test durations have been considered by authors for diverse nanoscale particles and oils blends.

In conclusion, the sedimentation method is the most accurate and reliable techniques compared with spectral absorbency, zeta potential, and metallographic characterization constancy tests owing to the sedimentation method duration can remain to months while for the spectral absorbency method can remain for certain hours (72, 120, 125, and 140) (T. Luo, Wei, X., Huang, X., Huang, L., & Yang, F., 2014), (C. P. Koshy, Rajendrakumar, P. K., & Thottackkad, M. V., 2015), (V. S. Jatti, & Singh, T. P., 2015), and (X. Song, Zheng, S., Zhang, J., Li, W., Chen, Q., & Cao, B., 2012), and the rest methods can collect the results after a short while (Yu, 2012), and (T. Luo, Wei, X., Huang, X., Huang, L., & Yang, F., 2014).

2.4.1.4 Techniques to Improve the Nano-oils Dispersion Stability

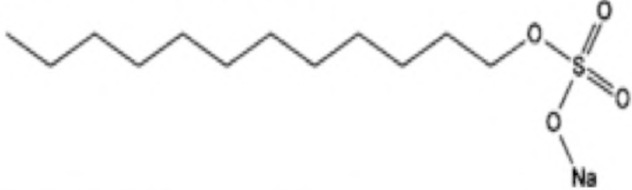
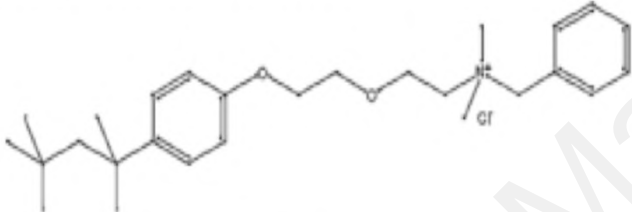

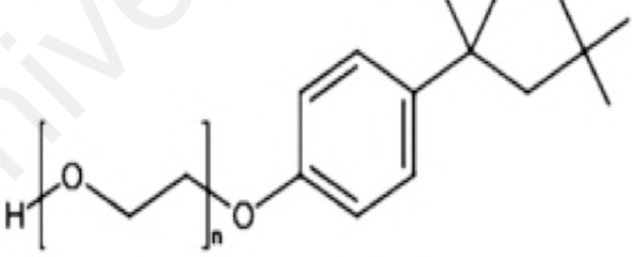
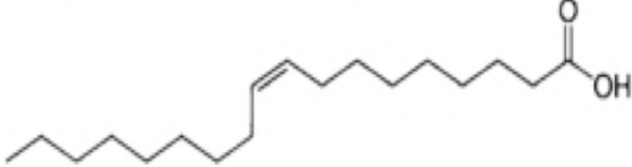
To discuss the effect of dispersion stability of nanoscale particles in lubrication oils, nanoscale particles surface functionalization is deemed as a fundamental stage (Akbulut, 2012). For constant dispersions within surface functionalization, the scientists have invented two techniques: a) Electrostatic stabilization, and b) Steric stabilization.

Electrostatic stabilization is commonly combined via the adsorption of ionic surfactants on the nanoscale particle surface. This synergy is relying on the hypothesis that like-charged dismiss one another in accordance with Coulomb's law. Whereas, the steric repulsion is accomplished by functionalizing the nanoscale particle surface with a polymer or an agent single-layer (Min, 2008). Generally employed surface functionalization procedures and related researches have been explained subsequently.

A. Impact of Surfactants/Agents

Surfactants/agents employed in nano-oils are also named as dispersants. Blending surfactants in the nano-oils are a simple and budgetary technique to improve the dispersion stability. Usually, utilizing surfactant comprises OA (M. I. H. C. Abdullah, Abdollah, M. F. B., Tamaldin, N., Amiruddin, H., Mat Nuri, N. R., Gachot, C., & Kaleli, H., 2016; N. G. Demas, Timofeeva, E. V., Routbort, J. L., & Fenske, G. R., 2012) and sodium dodecyl sulfate (SDS) (N. G. Demas, Timofeeva, E. V., Routbort, J. L., & Fenske, G. R., 2012; C. P. Koshy, Rajendrakumar, P. K., & Thottackkad, M. V., 2015). Demas et al. (N. G. Demas, Timofeeva, E. V., Routbort, J. L., & Fenske, G. R., 2012) have analyzed five distinct surfactants to measure the dispersion of nano-MoS₂ and nano-BN in PAO, as tabulated in Table 2.4. Also, stated that the usage of surfactant was not only useful in suspending the nanoscale particles, but also decreased the friction and wear by itself.

Table 2.4: Standard surfactants/agents, their chemical composition, and functionality

Surfactant	Functionality
<p>#1 Sodium dodecyl sulfate</p> 	Anionic
<p>#2 Benzethonium chloride</p> 	Cationic
<p>#3 Benzalkonium chloride</p> 	Cationic
<p>#4 Triton™ X 102</p> 	Non-ionic
<p>#5 Oleic acid</p> 	Anionic

Source: (H. H. M. M. Gulzar, M. A. Kalam, M. Varman, N. W. M. Zulkifli, R. A. Mufti, Rehan Zahid, 2016)

B. *Nanoscale Particles Surface Modification*

In this technique, the surface characteristics of the nanoscale particles are customized by the organic modification precursors. Usually applied modification dispersants such as oleic acid (OA) is adsorbed by the nanoscale particle, decreasing their surface energy efficiently to avoid the agglomeration (D. X. Peng, Chen, C. H., Kang, Y., Chang, Y. P., & Chang, S. Y., 2010). The behavior of organic chains improves their dispersion stability in an organic solution. Researches have revealed the efficiency of surface modification as mentioned in Table 2.5. Besides organic acids (S. Chen, & Liu, W., 2006; X. Song, Zheng, S., Zhang, J., Li, W., Chen, Q., & Cao, B., 2012; Ye, 2003) silane coupling surfactants (D. Jiao, Zheng, S., Wang, Y., Guan, R., & Cao, B., 2011; T. Luo, Wei, X., Huang, X., Huang, L., & Yang, F., 2014; T. Sui, Song, B., Zhang, F., & Yang, Q., 2015) are further observed to be effective in stabilized nano-oil suspensions.

2.4.1.5 **Importance of Nanoscale Particles Concentration**

Proper concentration is another major parameter that changes the lubrication properties of nano-oils (C. P. Koshy, Rajendrakumar, P. K., & Thottackkad, M. V., 2015; T. Luo, Wei, X., Huang, X., Huang, L., & Yang, F., 2014; T. Sui, Song, B., Zhang, F., & Yang, Q., 2015; M. V. Thottackkad, Perikinalil, R. K., & Kumarapillai, P. N., 2012). The addition of nanoscale particles, either tiny or immense amount, can result in a negative impact on several instances whether by rising friction or wear or both (Siti Safiyah Nor Azman, 2016). The way to ideal nanoscale particles concentration for oil lubrication relies on three essential conditions which involve dispersion technique/duration, the purpose of nanoscale particles (FM, AW or EP additives) and tribological test parameters. Table 2.5 reviews reported findings, presenting a series of concentrations and excellent concentrations as well as the function of nano additives for various oils and nanoscale particles mixtures. It is interesting to recognize that the identical MoS₂ nanoscale particles exhibit various optimum concentrations for two various base oils viz. 0.53 wt% for

coconut oil and 0.58 wt% for mineral oil utilizing a pin on disk contact rig (C. P. Koshy, Rajendrakumar, P. K., & Thottackkad, M. V., 2015). Contrastingly, a set optimum concentration of 0.5 wt% nano CuO and nano ZnO has been applied for mineral, synthetic and vegetable lubricants for a ball on disk contact rig (B. S. B. S.M. Alves, M.F. Trajano, K.S.B. Ribeiro, E. Moura., 2013). It shows that the optimum concentration is completely system-specific which means it will alter for each experiment circumstances.

Table 2.5: Literature survey of the performance/function/role of nanoscale particles and ideal concentrations for various lubricants

NPs Sort	Lubrication Oil	NPs Function	Concentration (wt%)	Ideal Concentration (wt%)	Authors
ZnO	Mineral, PAO, Sunflower, Soybean	FM, AW	0.5	0.5	(Alves et al., 2013)
	60SN base oil	FM, AW	0.5	0.5	(Ran, Yu, & Zou, 2016)
CuO	Coconut oil	FM, AW	0.1-0.6	0.34	(M. V. Thottackkad, Perikinalil, & Kumarapillai, 2012)
	CMRO	FM, AW	0.1,0.5,1	0.5	(Arumugam & Sriram, 2014)
	Mineral based engine oil	FM, AW	0.5, 1, 1.5	1.5	(V. S. Jatti & Singh, 2015)
	SAE 75W-85	FM, AW, EP	0.5, 1.0, and 2.0	2	(L. Peña-Parás et al., 2015)
	PAO8	FM, AW, EP	0.5, 1.0, and 2.0	2	(L. Peña-Parás et al., 2015)
	Mineral, PAO, Sunflower, Soybean	FM, AW	0.5	0.5	(Alves et al., 2013)

‘Table 2.5: continued’

NPs Sort	Lubrication Oil	NPs Function	Concentration (wt%)	Ideal Concentration (wt%)	Authors
MoS ₂	Coconut oil	FM, AW	0.25,0.5,0.75,1	0.53%	(C. P. Koshy et al., 2015)
	Mineral oil	FM, AW	0.25,0.5,0.75,1	0.58%	(C. P. Koshy et al., 2015)
	EOT5#	FM, AW, EP	0.2, 0.5, 0.7 and 1.0	1	(H. Xie et al., 2015)
	SE 15W-40	FM, AW, EP	0.1, 0.5, 1.0, 2.0 and 5.0	~ 1	(Wan, Jin, Sun, & Ding, 2014)
SiO ₂	Liquid paraffin	FM, AW	0.0125, 0.025, 0.05,0.1,0.2,0.5, 1, 2, 4	0.05-0.5wt%	(Peng, Chen, et al., 2010)
	EOT5#	FM, AW, EP	0.2, 0.5, 0.7 and 1.0	0.7	(H. Xie et al., 2015)
PbS	Liquid paraffin	FM, AW	0.05-0.2	0.2	(S. Chen & Liu, 2006)
Fe ₃ O ₄	#40 engine oil	FM, AW	0.5, 1.0, 1.5, 2.0	1.5	(Gao, Wang, Hu, Pan, & Xiang, 2013)
Hairy Silica	PAO100	FM, AW	0.5,1,2,4	1	(T. Sui, Song, Zhang, & Yang, 2015)
Cu	PAO6	AW, EP	0.5,2	0.5	(J. L. Viesca et al., 2011)
Carbon Coated Cu		AW, EP	0.5,2	0.5	(J. L. Viesca et al., 2011)
Ni		FM, AW, EP	0.5, 1 and 2	0.5	(R. Chou et al., 2010)
ZrO ₂ , ZnO, CuO		AW, EP	0.5%, 1.0% and 2.0%	0.5	(Ma, 2010) and (Alves et al., 2013)
Carbon nano-onions	PAO	FM, AW	0.1	0.1	(L. Joly-Pottuz, Vacher, Ohmae, Martin, & Epicier, 2008)

‘Table 2.5: continued’

NPs Sort	Lubrication Oil	NPs Function	Concentration (wt%)	Ideal Concentration (wt%)	Authors
ZrO ₂ /SiO ₂	20 [#] machine oil	FM, AW	0.05, 0.1, 0.3, 0.5, 0.75, 1	0.1	(W. Li et al., 2011)
Al ₂ O ₃ /SiO ₂		FM, AW	0.05, 0.1, 0.5, 1	0.5	(D. Jiao, Zheng, Wang, Guan, & Cao, 2011)
Al ₂ O ₃		FM, AW	0.05, 0.1, 0.5, 1	0.1	(T. Luo et al., 2014)
TiO ₂	Servo 4T Synth 10W30	FM, AW	0.3, 0.4, 0.5	0.3	(M. Laad & Jatti, 2016)
ZnAl ₂ O ₄	Lubricating Oil	FM, AW	0.05, 0.1, 0.5, 1	0.1	(X. Song et al., 2012)

2.4.1.6 Role of Nanoparticle Size

The tribological behavior of nano-oils has a direct relationship with the nanoscale particle size in several techniques. Primarily, the dispersion balance/stability is a function of nanoscale particle size which is a principal condition for precise nano-oil formulation. In this respect, the sedimentation amount is a critical factor to conclude the dispersion balance/constancy which can be determined by applying Stokes’ law as per Equation 2.1.

$$v_z = \frac{2(\rho_{NP} - \rho_F)gr^2}{9\mu} \dots\dots\dots \text{Equation 2.1}$$

While V_z is settling velocity, ρ_{NP} is a density of nanoscale particles, ρ_F is a density of the fluid, g is gravity, r is the radius of the nanoscale particle, and μ is the viscosity of the fluid. This easy equation reveals that for a 10-fold increment in nanoparticulate size (i.e., 100 nm in lieu of 10 nm), sedimentation time will reduce 100-fold. It explains the function of nanoscale particle size in delivering stable nano-oil.

Further, the tiny size of nanoscale particles benefits them to enter the mating surfaces and their reaction with the environment based on their surface-to-volume rate. The essential mechanical characteristics of nanoscale particles for instance hardness are represented by its size which leads to affect the tribological performance. For nanoparticles in the size range of 100 nm or higher, the hardness rises with shrinking particle size (Schiøtz, 2003; Weertman, 1993). In the case the hardness of nanoscale particles is higher than the hardness of the substrate/body of the tribo-pair, the consequence is indenture and scratching. The similar phenomenon has been notified by (L. Peña-Parás, Taha-Tijerina, J., Garza, L., Maldonado-Cortés, D., Michalczewski, R., & Lapray, C., 2015). In accordance with their research, high hardness (8–9 Mohs) of nano Al₂O₃ than the metal body produced abrasive wear and nanoscale particles re-agglomerated. Consequently, the relation between size and hardness of nanoscale particles need to be studied during nano-oil formulation.

Finally, during analyzing the suitable nanoscale particle size choice, the ratio of root mean square roughness of the oiled substrate to the radius of the nanoscale particle is a major condition. If the size of the nanoscale particles is too large as compared to the hole among asperities, particles will not accumulate on the mating position which will direct to inadequate lubrication.

2.4.1.7 Role of Nanoscale Particle Shape and Structure

For several kinds of tribological applications, the role of nanoscale particle shape and structure performs a crucial role. The shape of nanoscale particle associates with pressure encountered by nanoparticles while loading. Spherical shape nanoscale particles present great load carrying capacity and EP properties owing to their ball-bearing consequence (T. Luo, Wei, X., Huang, X., Huang, L., & Yang, F., 2014). The cause for this action is based upon the contact between the nanoscale particle and the lubricated surface. The

spherical shape of nanoscale particles leads to in point touch with the counterpart surface. The line contact is linked with the nanosheets when the planar touch is the characteristic of nanoplatelets as shown in Figure 2.5.

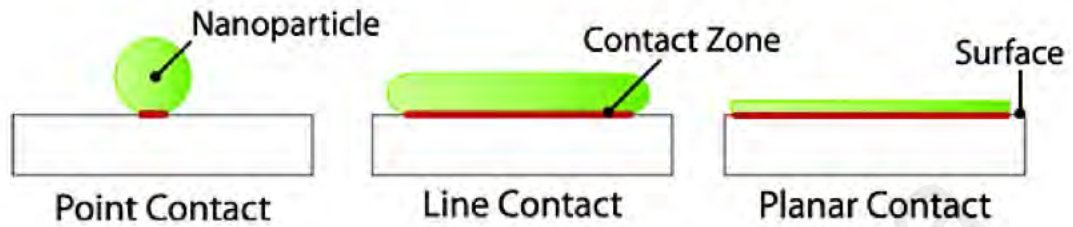


Figure 2.5: The influence of nanoparticle's shape on contacting area during loading

Source: (Akbulut, 2012)

In most of the investigations related to the application of nano-oils, spherical shape nanoscale particles have been employed (L. Joly-Pottuz, Vacher, B., Ohmae, N., Martin, J. M., & Epicier, T., 2008; L. Kolodziejczyk, Martinez-Martinez, D., Rojas, T., Fernandez, A., & Sanchez-Lopez, J., 2007; L. Rapoport, 2003; C.-G. Lee, Hwang, Y.-J., Choi, Y.-M., Lee, J.-K., Choi, C., & Oh, J.-M., 2009; T. Luo, Wei, X., Huang, X., Huang, L., & Yang, F., 2014; D. X. Peng, Chen, C. H., Kang, Y., Chang, Y. P., & Chang, S. Y., 2010; D. X. Peng, Kang, Y., Chen, S., Shu, F., & Chang, Y., 2010). During identifying the morphology of nanoscale particles, their internal nanostructure can affect their tribological characteristics. Usually applied nanoscale particles, such as graphene and metal oxides owing to their excellent lubrication behavior because of structure (Varrla Eswaraiah, 2011), (B. S. B. S.M. Alves, M.F. Trajano, K.S.B. Ribeiro, E. Moura., 2013), (R. G. A. Hernandez Battez, D. Felgueroso, J.E. Fernandez, Ma. del Rocio Fernandez, M.A. Garcia, I. Penuelas, 2007), and (Y.Y. Wu, 2007). It can be seen that the graphene's geometry is planar as shown in Figure 2.6 and Figure 3.3 (C), so it simply slips during sliding of surfaces in the lubricant (Varrla Eswaraiah, 2011).

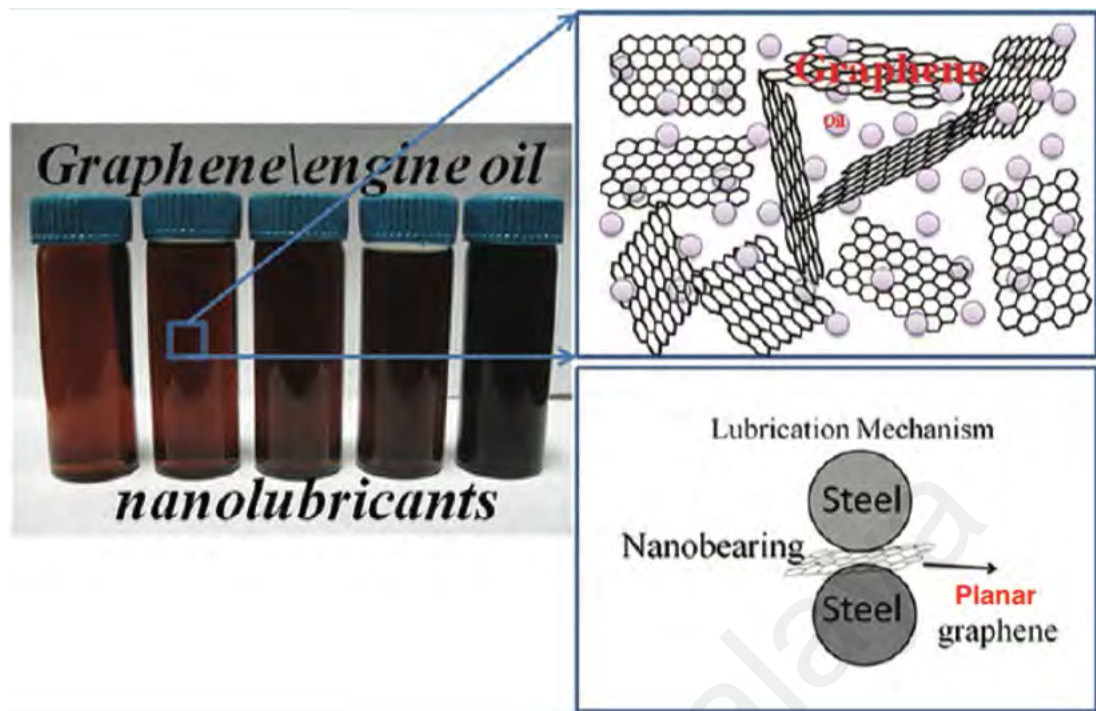


Figure 2.6: Planar graphene structure has no difficulty to slide between mating surfaces in the lubricant

Source: (Varrla Eswaraiah, 2011)

TiO₂ anatase has a tetragonal crystalline structure (dipyramidal habit) (S. K. H. M. Vijayaraj, A. K. Harinarain, and S. S. V. Ramakumar, 2016) resembles a semi-spheres geometry as shown in Figure 2.7 and Figure 3.3 (A) that roller bearing impact could be one of the principal lubricating mechanism led to a reduction in friction and wear, as per Figure 2.8 and Figure 2.9.

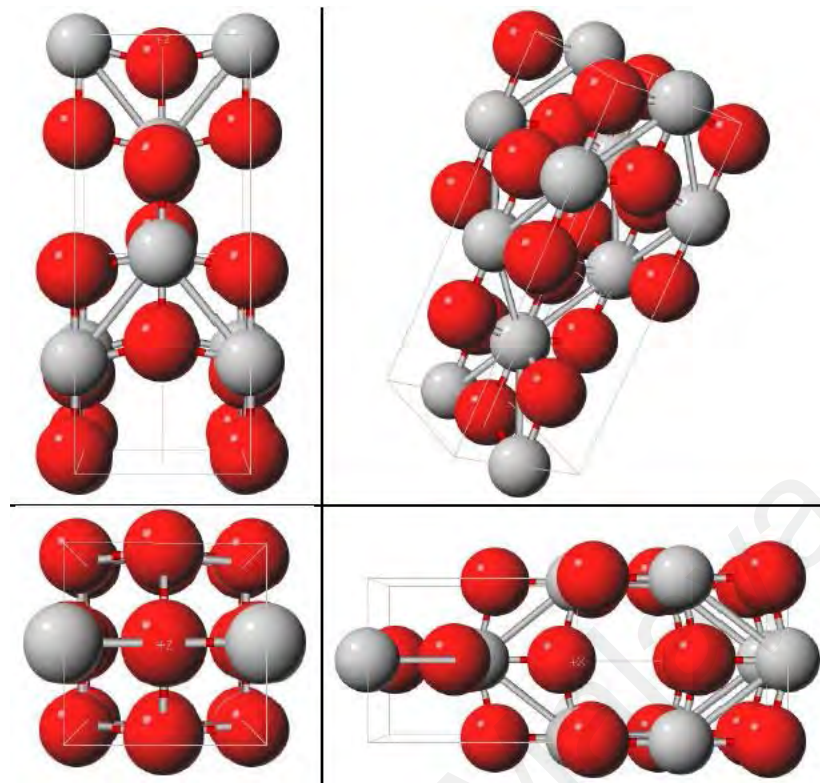


Figure 2.7: Schematic diagram of the multilayered crystal molecular structure of TiO_2 (A)

Source: (U.S. Naval Research Lab, 2019)

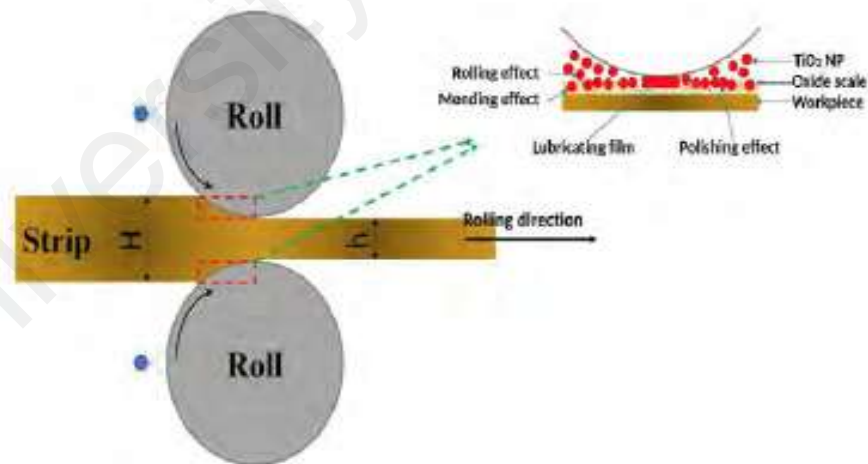


Figure 2.8: The spherical structure of TiO_2 nanoparticles in the lubricating film can play as bearing balls between the working roll and the substrate exhibiting a rolling effect

Source: (Hui Wu, 2018)

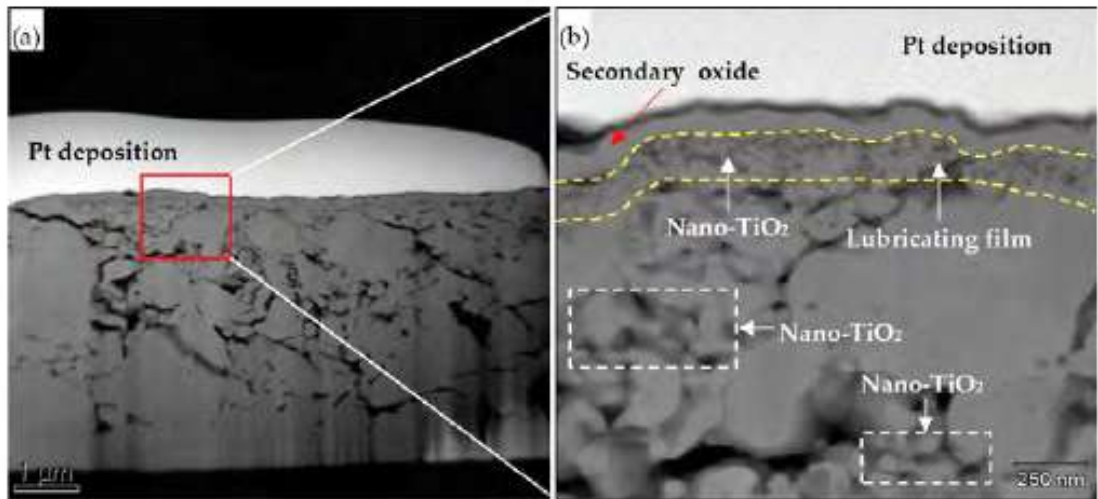


Figure 2.9: (a) A TEM micro image of FIB foil cut from the rolling steel surface, (b) TEM micro image of a magnified region in (a), representing the role of Nano-TiO₂-particles

Source: (Hui Wu, 2018)

ZnO nanoparticles have a polycrystalline geometry that similar to a seed-like structure (Manjula G. Nair, 2011), as per Figure 2.10 and Figure 3.3 (B). It packs up the micro- and nanoholes of the sliding balls thus it prevents immediate rubbing of the steel balls and reduces the friction and wear, as per Figure 2.11 and 2.12.

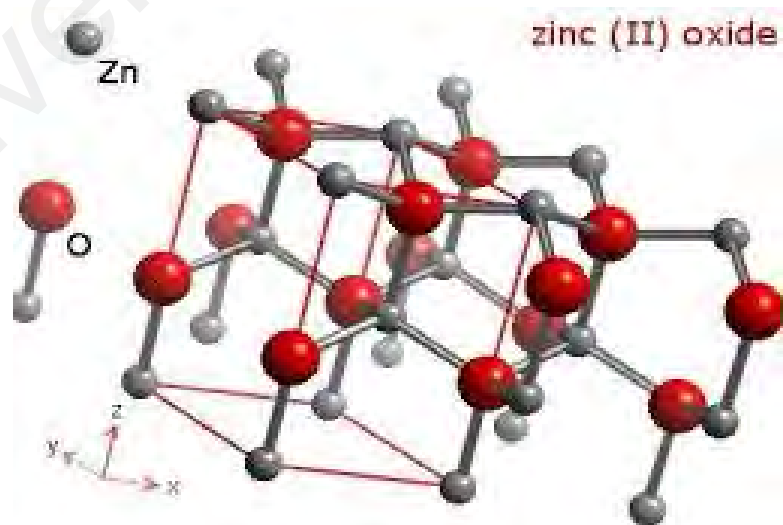


Figure 2.10: ZnO nanoparticles morphology

Source: (Mark Winter, 2019)

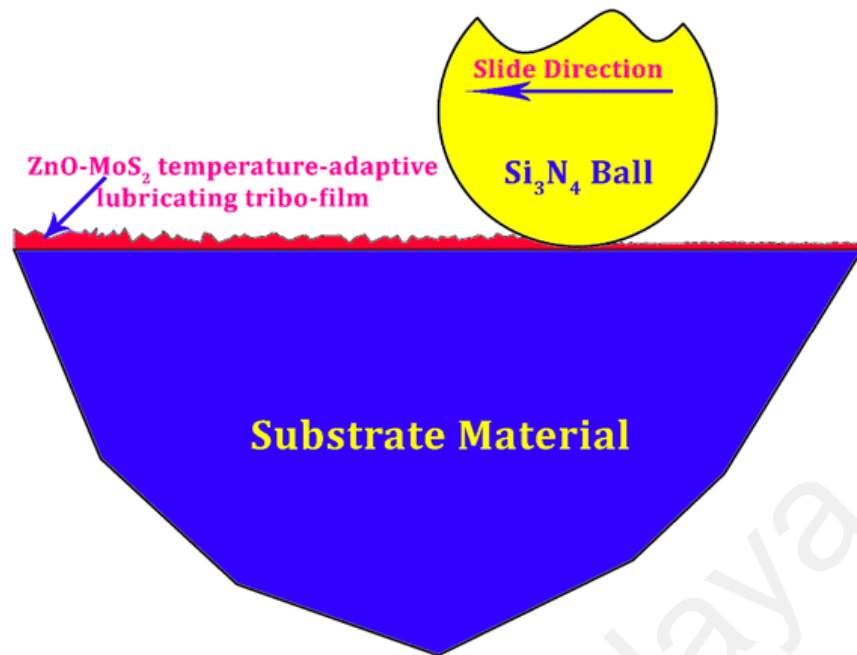


Figure 2.11: Illustration of nano-ZnO structure as a solid lubricating film

Source: (F. A. Essa, 2017)

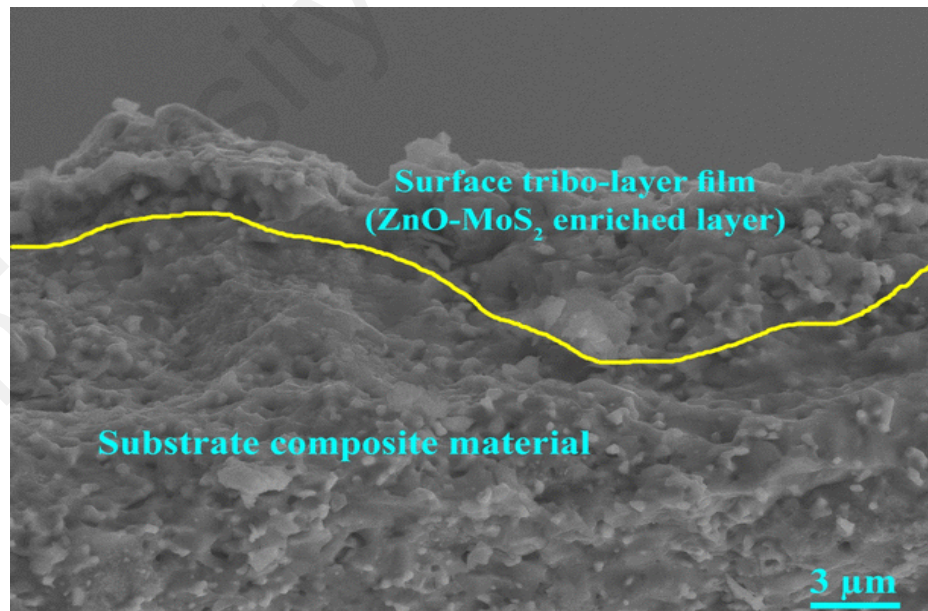


Figure 2.12: FE-SEM micro-image of cross-sectional wear scars of ZnO tribo-layer film at 800 °C

Source: (F. A. Essa, 2017)

2.4.1.8 Optimize the Concentration for Tribology Boosting

1. Bogunovic et al (Lukas Bogunovic, 2015) demonstrated the optimal particle concentration for highest lubrication performance with minimum expenses. The concentration of 0.2 wt% T 805 particles was just sufficient to reduce friction while a minimum number of particles and more additives are required. Furthermore, an increase in the particle concentration does not lead to further improved anti-friction performance of the lubricant.
2. According to Ingole et al (Sudeep Ingole, 2013), 0.25 wt% addition of TiO₂ anatase to mineral oil reduced the variability and stabilized the frictional behavior. While 1 wt% and 2 wt% addition of TiO₂ anatase to the mineral oil was increased coefficient of friction slightly. Further, commercially available TiO₂ P25 which comprises a compound of rutile and anatase phase. When employed as lubrication additives, it revealed abrasive effects on the wear surface. The severity of this abrasion was raised with wt% of P25 in the base oil. Higher content of P25 presented indication of severe damages on the wear track.
3. Ali et al (H. X. Mohamed Kamal Ahmed Ali, Liqiang Mai, Cai Qingping, Richard Fiifi Turksonad, Chen Bicheng, 2016) demonstrated that all concentrations of TiO₂ anatase nanolubricants exhibited a reduction in the friction coefficient. TiO₂ anatase nanolubricants had a reduced friction coefficient by around 50% with a 0.25 wt% concentration of nanoparticles. Based on the collected results, it was evident that the nanolubricant with 0.25 wt% concentration of nanoparticles was the best sample of the nanolubricants considered, as this sample decreased the friction coefficient by half, as corresponded with engine oil 5W-30 without nanoparticles. So, the optimum concentration 0.25 wt% of TiO₂ anatase nanoparticles, for the current study, was consistent with literature reports as well (Hakimizad, 2015).

4. Vijayaraj et al (S. K. H. M. Vijayaraj, A. K. Harinarain, and S. S. V. Ramakumar, 2016) confirmed the Ti concentration of 500 ppm was observed to be excellent because an additional increment in the amount in the base oil to 1,000 or 2,000 ppm did not reveal any further antiwear enhancement; neither low Ti concentration (100, 250 ppm) was adequate to decrease wear.
5. Sarma et al (Pullela K Sarma, 2011) studied the copper <50 nm and titanium dioxide TiO₂ <25 nm nanoparticles in different mass fractions (0.05, 0.1, and 0.2%) then blended into the base lubricant SAE 20W-40 to formulate the needed sample. The required amount is made in batches of 400 c.c at a time with the nanomaterials. Formulation of nanoparticles into the lubricant efficiently decreases the overall frictional power. The reduction in frictional power may be due to a significant decrease in the coefficient of friction between reciprocating and rotating components.
6. Wang et al (Shibo Wang, 2009) indicated that both ZnO nanoparticles and ZnO whiskers can enhance the mechanical and tribological characteristics of nylon suspensions. Composites packed with either ZnO nanoparticles or ZnO whiskers 5, 10, 15, and 20 wt% have almost similar friction coefficients which place within 0.4 and 0.45. It points out that the shape of zinc oxides fillers has a small impact on friction coefficients, as recognized with the previous experimental findings. When a polymer dries moving toward a steel counterface, the transfer layer is made, which happened from polymer to steel. A removal layer of suspensions loaded with inorganic nanoscale particles relies on the filler's degradation technique. The similar removal layer will be created on the counterface owing to the similar structure of ZnO nanoparticles and ZnO whisker. This took part in similar friction coefficients. The coefficients of friction of each packed suspension were greater than that of blank nylon. This was possibly ascribed to partial rubbing

within the exhibited packs and the metal counterface. Wear values of suspensions are greatly affected by the shape of nano-ZnO fillers. The wear protection capabilities of whisker-suffused nylon composites are more powerful than that of particle-suffused nylon composites. It may be observed that the wear values of the composites have an inverted proportion related to their scratch coefficients. Normally, bigger scratch coefficients for composites indicate the possible raise in the protection toward abrasive wear to the firm counterparts. Furthermore, the best-preferred load-supporting of ZnO whiskers was an additional cause for wear reduction corresponding to ZnO nanoparticles. The combined impact of needles of whiskers occurred in the more prominent actions of the whisker-loaded composites than ZnO nanoparticles. The exhibited ZnO nanoparticles with ball shape were more simply cleaned off from wearing zone of suspensions than the tetrapod ZnO whiskers. This can be another reason participated in the large wear value of the particle-packed composites.

7. Essa et al (F.A. Essa, 2017) investigated the possible tribological advantages of a mixture M50 steel-based composites (M, M50 + 0.0% additive) were formulated employing zinc oxide ZnO (MZ, M50 + 0.0% WS₂ + 10.0% ZnO), tungsten disulfide WS₂ (MW, M50 + 10.0% WS₂ + 0.0% ZnO) and a blend of ZnO and WS₂ (MZW, M50 + 10.0% WS₂ + 10.0% ZnO). Temperature-adaptable firm lubricating composites were applied across a series of temperatures RT, 200, 400, 600, and 800 °C. Utilizing just single solid oil may not deliver the wanted questionable lubrication properties for M50 steel which is employed in most of the advanced technological operations for example aerospace and biomedical fields. While 10.0% of WS₂ offers supreme lubricating properties during the low temperatures from room temperature to 400 °C excluded at 200 °C, but it has a poor lubricating result within 400 °C and above. Moreover, 10.0% of ZnO

produces superior lubricating properties within raised temperatures from 600 to 800 °C, but it has a worse lubricating influence over the average and small temperatures below 400 °C. Consequently, adopting a single nanoparticle additive, either ZnO or WS₂, may not yield constant lubrication characteristics to achieve the desired tribological properties across a broad spectrum of temperatures. 10.0% ZnO + 10.0% WS₂ have the advantage of temperature-adapting behavior to implement low friction coefficient, and therefore, great tribological actions of MZW are collected along with the whole broad series of temperatures from room temperature to 800 °C in respect of individual M, MZ, or MW. The friction coefficients of MZW, MZ, and MW are reduced by 43.64%, 22.17%, and 13.51%, consecutively in respect of M at 800 °C owing to the presence of lubricating tribo-layers on the scarred areas. The tribological characteristics of MZW achieved the most favorable findings at 800 °C, where the friction noted its smallest amount of 0.19. In general, this current investigation exhibits that the hybrid temperature-adapting oils of ZnO-WS₂ are suitable candidates for M50 matrix to acquire demanded tribological performances along with a broad scope of temperatures. Additionally, the outcomes of this research contribute some recommendations to address the issues when using M50 matrix suspensions as an MZW in mechanical systems under extreme circumstances.

8. Gara et al (Zou, 2013) studied the friction and wear properties of water-based nano-liquids. A market exists water-based nano-liquids with 50% ZnO and 50% Al₂O₃ nanoscale particles concentration were employed as lubricating oil. The 50% volume nano-liquids were diluted utilizing deionized H₂O fluid and an ultrasonic immersion with various mass concentrations. ZnO and Al₂O₃ nanoscale particles help in friction decrease. The friction-reducing result is clear for smooth surfaces. Despite, for rough surfaces, the friction-reducing result is insignificant.

Wear investigations for a polished surface reveal that the nanoscale particles perform similar to coarse wear fragments and create wear on the surfaces. More solid fragments create more wear. Friction loss could be owing to two reasons. Firstly, spherical nanoscale particles perform similar to nanoscale bearings and rough fragments between the moving areas. However, friction will be reduced because of granular wear on the interface area. Secondly, is a film deposit mechanism that generates on the sliding zones, which is useful for friction-reducing purpose.

9. Alves et al (B. S. B. S.M. Alves, M.F. Trajano, K.S.B. Ribeiro, E. Moura, 2013) investigated the improvement of vegetable-based oils and the increment of oxides nanoscale particles ZnO and CuO as properties enhancer for extreme pressure EP, examining the EP and lubricant impact on tribological performance. The findings revealed that with the increment of nanoscale particles to plain oil, the tribological characteristics can be considerably enhanced. A softer and compacting tribo-layer has generated on the scar area, which is efficient for additional friction and wear reduction. Moreover, oils produced from transformed vegetable lubricant can substitute mineral oil, developing the tribological and ecological features. While the increment of nanoscale particles in vegetable base oils is not effective for anti-wear. The wear protection performance of the oxide nanoscale particles relies on the lubrication oil. Where, oxides do not demonstrate satisfactory wear protection when blended with epoxidized vegetable oil like sunflower and soybean lubricants, due to the effect of chemical type of vegetable lubricant on layer creation owing to polar groups that adhere to texture zone. In such a case, the nanoscale particles have a third body action raising the friction. ZnO exhibits remarkable behavior in friction and wear reducing when mixed with mineral oil. The wear protection technique is assigned to the deposit of nanoscale particles in

surface and physical layer generation, which may result in friction and wear reduction.

10. Battez et al (R. G. A. Hernandez Battez, D. Felgueroso, J.E. Fernandez, Ma. del Rocío Fernandez, M.A. Garcia, I. Penuelas, 2007) performed and explained the extreme pressure performance of nanoscale particle mixtures in a poly-alpha-olefin PAO6. CuO, ZnO and ZrO₂ nanoscale particles were disseminated at 0.5, 1.0 and 2.0 wt.% in PAO6. Each value of nanoscale particles enhanced the EP characteristics of PAO6. CuO nanoscale particles presented the superior EP performance and ZrO₂ the poorest; CuO and ZnO blends exhibited more favorable findings at 0.5% and 2.0 wt.% of nanoscale particles, sequentially, whereas ZrO₂ performed equivalently despite nanoparticulate value. Each outcome was analyzed based on the nanoscale particles' size and hardness, and their depositing on wear defect area. All nanoparticulate values in PAO6 decreased the wear scar diameter from initial seizure load and so on. Consequently, the load-wear index elevated with the increment of each nanoparticulate to PAO6. Though, each concentration of nanoparticulate blends presented various extreme pressure EP impacts. The PAO6 + ZnO mixture enhanced their LWI while the ZnO value raised. However, the LWI was promoted in whole conditions in comparison with PAO6, the initial seizure load ISL and weld load WL managed the same rates as for PAO6. The mentioned findings indicate to nanoparticulate performance at the sliding spot. Wear action of mixtures are equal to pure PAO6 and no nanoparticulate accumulation was observed on the wear region. These outcomes apparently associated with the quick test period and that experiments were conducted in the AW region. However, several findings can be observed at ISL. WSD at ISL were equal to 0.5 and 2% of ZnO for PAO6 + ZnO mixtures, but elements spectroscopy and mapping analysis revealed extra zinc accumulation on

the wear area for the 2% ZnO blend 2.38% than for its 0.5% equivalent 0.49%. The rate of nanoscale particles accumulation for these couple blends (PAO6 + ZnO and PAO6 + CuO) correlated exactly with nanoparticulate volume in PAO6 while oxide group was at 0.5%. In contrast, when the nanoparticulate volume in PAO6 was 2%, the accumulation concentration was larger. The AW procedure of nanoparticle additive can be described as the oil layer between tribo-pairs turned more delicate and blended lubrication or boundary lubrication happens from LNSL and so on. The nanoscale particles may take a part of the load and distribute the two contacts to avoid metal's sticking, consequently, serve the AW characteristics. In contrast, three various methods can occur: the nanoscale particles could be melted and welded on the shearing zone (this possibility is unlikely for the nanoscale particles here investigated due to their melting points are between 1326 and 2700 °C), functioned with the substrate to create a protective film (this possibility is impossible because the electropositive constitution of metal oxide nanoscale particles and ball's element), or tribo-sintering on the sliding zone. This last possibility was also confirmed by other researchers Kato et al (H. Kato, 2007) employing nanoscale-sized oxide particles as solid lubrication additive. It is necessary to take into account that ZnO and CuO have equivalent bulk hardness (around 4 on the Mohs size, equal to HRC 32) so their tribological performance at ISL could be associated to the larger-scaled CuO particles compared to the ZnO nanoparticles and their superior capability to depart sliding metals. In contrast, the scar defect is the same as for ZnO and CuO mixtures. The EP effects of examined blends were in regard to the size and hardness of the nanoscale particles. CuO has smaller bulk hardness than the balls' body and biggest nanosized-particles, presented superior EP performance, ZnO has similar bulk hardness as CuO but smaller nanosized-particle exhibited

reasonable EP properties while ZrO_2 with an average volume and biggest bulk hardness showed the poorest EP properties among all samples.

11. Berman et al (Diana Berman, 2014) described the significant friction and wear characteristics of some graphene layers on steel contacts. Particularly, a small amount of solution-processed graphene SPG was deposited from low concentration ethanol solution 1 mg/L with only partial coverage of the steel surface around 25% of the total surface area, which was sufficient to decrease both friction and wear in the dry nitrogen and humid air conditions.
12. Berman et al (Diana Berman, 2014) also indicated that even the smallest amount of graphene platelets added to oil is capable of a noticeable reduction in friction and wear of steel. For chemically modified graphene platelets that were dispersed in base oil by sonication and stirring with a magnet, tribological tests were conducted on a four-ball rig with a 1200 rpm speed under a constant load of 147 N at the elevated temperature of 75 C. The optimal 0.075 wt% weight amount of modified graphene platelets was able to produce a better load-carrying capacity than a base oil or oil with graphite flake additive. Both the coefficient of friction and wear diminished with the added graphene platelets.
13. Azman et al (Siti Safiyah Nor Azman, 2016) confirmed the addition of 0.05 wt% graphene nanoparticles GNP in blended lubricant resulted in the lowest coefficient of friction and wear scar diameter, therefore chosen as the most proper concentration of GNP in the blended lubricant. Friction and wear were diminished by 5 and 15% respectively, with the presence of 0.05 wt% GNP in the formulated lubricant.
14. Lahiri et al (Debrupa Lahiri, 2014) reported that nano-scratch performance of ultrahigh molecular weight polyethylene UHMWPE strengthened with graphene nanoplatelets GNP in a differing proportion of 0, 0.1, 0.5 and 1 wt%. Hot

compressed composite arrangements are described for their tribological conduct in scratch method applying a normal load of 100 – 300 μN . Rising GNP rate from 0.1 to 1 wt% reflects in reducing of the COF owing to simple shear of graphene nanoplatelets. Graphene reinforcement further improves the wear protection by over four times, which is a consolidated outcome of lubricating and hardening are given by graphene nanoplatelets.

15. Eswaraiah et al (Varrla Eswaraiah, 2011) explained that the ultrathin graphene made by solar exfoliation method. Various weight percentages of graphene were separated evenly in plain lubricant with help of probe sonication. With fewer rates of solar graphene, the tribological characteristics of graphene-engine oil enhanced tremendously. For 0.025 mg/mL of graphene in engine oil, frictional coefficient FC and wear scar diameter WSD were diminished by 80 and 33%, consecutively. This case has been approved for reducing FC when graphene mixed engine oil involved with no need to modify the surface area. Another issue has been noticed which is when weight percentage of graphene raised the FC and WSD rose as well owing to coalesce and segregation of nanoparticles. Nano bearing generation among the balls performs a significant role in decreasing friction and wear. The superior behavior of graphene in enhancing the tribological characteristics of the base oil is assigned to the supreme mechanical durability and morphological geometry of graphene. Dispersion of solar graphene is simply with no addition of any precursor to the employed lubricant and nanoplatelets can be stable in the base oil for a month with not much sedimentation. Moreover, the steel ball surface seems smooth during micro-and nanoscale image acquisition. While the surface was involved with hills and grooves when metal surfaces in action. From the microscopical view, the sliding of these damaged balls occurs friction among surfaces. However, when ultrathin nanographene blended with the base oil micro-

and nanogaps of the mating surfaces will be filled up. Therefore, it prevents the direct interface of moving steel balls and thereby, reducing friction. The FC levels reduced significantly when the ideal amount used, and it remains stable during 1 hour of friction time. A constant lubrication graphene layer generated in the lubricant over the sliding surfaces. Authors proposed that sliding is the principal mechanism behind decreasing friction in the event of graphene mixed with engine oil. Owing to the morphology of the graphene is planar, so it can swiftly slide among the balls in the base oil. Additionally, an increment in concentration will occur in aggregation and coagulation of nanographene, which will raise the wear and friction among surfaces. The obvious reduction in WSD of balls resulting from the penetration of 12 nm nanographene sheets inside the surfaces simply and enhances the wear resistance ability. Another case of carbon nano particulate such as carbon nanotubes, it is distinguished that roller bearing influence is the chief lubricating mechanism behind friction reduction and additionally, there are speculations of atomistic simulations of carbon nanotubes when shear forces applied on tribological features. Investigation of the defected areas after friction verified that the excellent lubricating behavior of modified graphene platelets MGP might be ascribed to their tiny size and very thin laminated morphology, which enable the MGP to simply penetrate through mating surfaces, by avoiding the coarse surfaces from getting into close each other. While friction, the nanoscale particles viz. carbon nanotubes CNTs and carbon nanofibers CNFs will initially load the micro-holes of the moving surfaces through developing auto-organized thin lubricating film. The aspects of roller bearing impact in carbon nanotubes and carbon nanofibers could enhance the lubrication behavior of the oils.

See Appendix A: Comparison of poor-results of anti-friction and anti-wear.

2.4.1.9 The Function of Tribo-Testers Standard and Configurations

The tribological efficiency of nano-oils apparently quite system-specific and consequently, a distinct behavior probably to be seen in various investigation conditions. M.R. Falvo and R. Superfine (Falvo, 2000) have remarked that the corresponding orientation of the mating surfaces influences the frictional performance of the nanoscale lubricating regime. Table 2.6 presents a review of merely four-ball tester and applying parameters by several scholars. For friction performance and AW properties, most scientists have assumed the interacting contact between various counter materials. Table 2.7 explains the test parameters for different types of geometric arrangements, in addition, the four-ball tester rig.

To review the tribological behavior of nanoscale particles as additives in lubrication oils, multiple experimental investigations has conducted employing various geometric shapes, which involve four-ball, ball-on-flat, pin-on-disk, cylinder-on-flat, piston ring-on-cylinder liner and block-on-ring as per Figure 2.13. Many of tests have been carried out at a typical running temperature of an engine (e.g., 70–100 °C) as stated in Table 2.7 and Table 2.8. Likewise, the amounts of various testing parameters, for example, test duration, sliding velocity, sliding distance, and normal load also changed.

Moreover, for EP properties and load-carrying capability of nano-oils, most of the nano-oils have analyzed by four-ball tribotester applying ASTM D2783 standard method (M. I. H. C. Abdullah, Abdollah, M. F. B., Tamaldin, N., Amiruddin, H., Mat Nuri, N. R., Gachot, C., & Kaleli, H., 2016; R. Chou, Battez, A. H., Cabello, J. J., Viesca, J. L., Osorio, A., & Sagastume, A., 2010; J. L. Viesca, Battez, A. H., González, R., Chou, R., & Cabello, J. J., 2011).

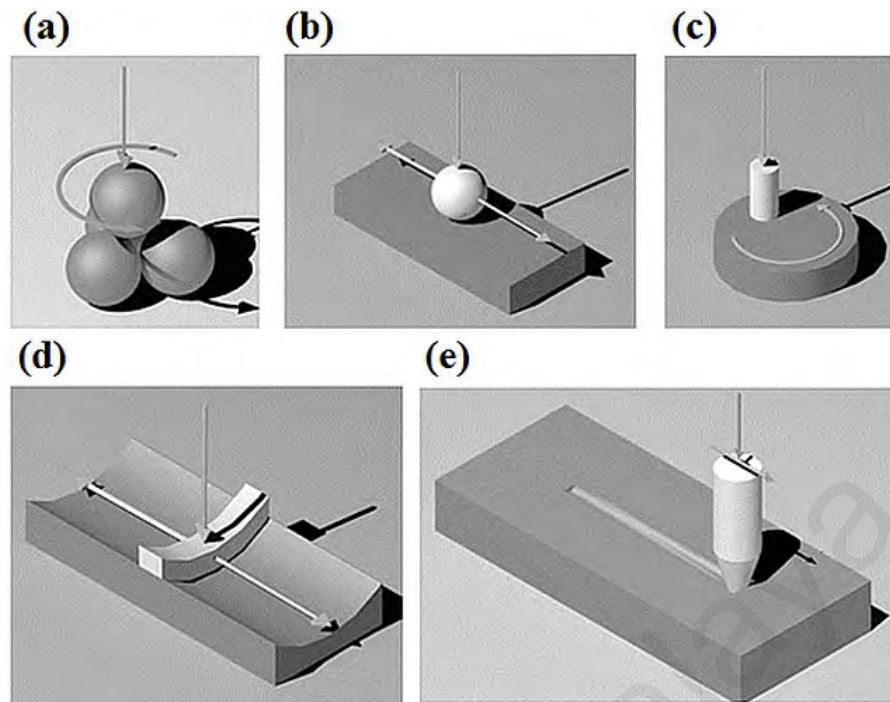


Figure 2.13: Frequently employed tribo-testers structure setups (a) four-ball, (b) ball-on-plane, (c) pin-on-disk (d) piston ring-on-cylinder (e) pin-on-plane

Table 2.6: Literature survey of four-ball tribotester employed parameters

NPs	Oil	Testing Time (sec)	Temp (°C)	Applied Load (N)	Speed (rpm)	Findings	Author
TiO ₂	palm TMP ester	300	25	392,78 4,1176, 1568	1200	WSD, Friction	(N. W. M. Zulkifli, Kalam, Masjuki, & Yunus, 2013)
MoS ₂ / TiO ₂	Liquid paraffin	1800	25	300	1450	WSD, Friction	(K. H. Hu, Huang, Hu,

							Xu, & Zhou, 2011)
--	--	--	--	--	--	--	----------------------

‘Table 2.6: continued’

NPs	Oil	Testing Time (sec)	Temp (°C)	Applied Load (N)	Speed (rpm)	Findings	Author
ZnO	PAO6	3600	75	392	1200	WSD	(Battez et al., 2006)
		10/ stage till weld	25	Varies/ stage till weld	1470	ISL, LNSL, WL, LWI, WSD	(Battez et al., 2006)
	60SN base oil	1800	75	500	1000	WSD, Friction	(Ran et al., 2016)
TiO ₂ (A)/ Graphene	Base oil Group II	3600	75	392	1200	COF, WSD, SWR	(Waleed Alghani, 2019)
Graphene	Engine oil	3600	75	392	600	COF, WSD	(Varrla Eswaraiah, 2011)
CuO	Liquid paraffin	900	60-70	392	1200	WSD, Friction	(Asrul, Zulkifli, Masjuki, & Kalam, 2013)
	PAO6	10 /stage till weld	25	Varies/ stage till weld	1470	Friction, ISL, LNSL, WL, LWI, WSD	(Fernandez, Viesca, & Battez, 2008)
Cu	Liquid paraffin	1800	-	300	1450	WSD, Friction	(Zhang et al., 2015)
	PAO6	10 /stage till weld	25	Varies/ stage till weld	1470	ISL, WL, LWI, WSD	(J. L. Viesca et al., 2011)
MoS ₂	SAE 20W-40	3600	75	392	600, 1200	WL, WSD	(Thakur, Srinivas, & Jain, 2016)
		10 /stage till weld	25	Varies/ stage till weld	1470	ISL, WL, LWI, WSD	(Thakur et al., 2016)

Al ₂ O ₃ / SiO ₂	20 [#] machine oil	1800	75	147	1,450	Friction, WSD	(D. Jiao et al., 2011)
--	-----------------------------------	------	----	-----	-------	------------------	---------------------------

‘Table 2.6: continued’

NPs	Oil	Testing Time (sec)	Temp (°C)	Applied Load (N)	Speed (rpm)	Findings	Author
CuO, ZnO, ZrO ₂	PAO6	10 /stage till weld	25	Varies/ stage till weld	1470	ISL, LNSL, WL, LWI, WSD	(Battez et al., 2008)
PTFE	150N group II base oil	3600	75	392	1200	WL, WSD	(K. D. Mukesh et al., 2013)
ZrO ₂ / SiO ₂	20 [#] machine oil	1800	75	147	1,450	Friction, WSD	(W. Li et al., 2011)
Ni	PAO6	10 /stage till weld	25	Varies/ stage till weld	1470	ISL, LNSL, WL, LWI, WSD	(R. Chou et al., 2010)
hBN	SAE 15W40	10 /stage till weld	25	Varies/stage till weld	1760	WSD	(M. I. H. C. Abdullah et al., 2016)
Fe, Cu, Co	SAE10	3600	25	150	1420	WSD, Friction	(Padgurskas, Rukuiza, Prosyčėvas, & Kreivaitis, 2013)
CaCO ₃	PAO+5% palm TMP ester	3600	25	392	1200	WSD, Friction	(Zainal, Zulkifli, Yusoff, Masjuki, & Yunus, 2015)

Table 2.7: Literature review of tribo-testings' parameters influencing sliding contact

NPs	Oil	Tribo-Rig	Test Time (sec)	Temp. (°C)	A. L. (N)	P. (Gpa)	Sp.	Author
Cu	PAO6	Block-on-ring	3066	-	165	0.1	1 (m/s)	(J. L. Viesca et al., 2011)
MoS ₂ , BN	PAO10	Piston skirt-liner	10800	20,40, 100	250	-	120 (rpm)	(N. G. Demas et al., 2012)
CuO	CMRO	Piston ring-liner	7200	60	80	0.005	600 (rpm)	(Arumugam & Sriram, 2014)
	Mineral oil	Pin-on-disk	400, 600, 1200	-	40,60	-	0.5, 1.0, 1.5 (m/s)	(V. S. Jatti & Singh, 2015)
	Coconut Oil	Pin-on-disc	178 to 714	-	49 to 98	0.001 to 0.002	1.4 to 5.6 (m/s)	(M. V. Thottakkad et al., 2012)
	Mineral, PAO, Sunflower, Soybean	Ball-on-disk	3600	50	10	-	1200 (rpm)	(Alves et al., 2013)
WS ₂	SAE 30	Piston ring-liner	27000	70	160	0.01	2.29 (m/s)	(Gullac & Akalin, 2010)
	Paraffin oil	Pin-on-disk	24000	-	100–500	-	0.6 (m/s)	(L. Rapoport et al., 2003)
Pb	Paraffin oil	Pin-on-disk	5000	-	7	1.26	1 (m/s)	(L. Kolodziejczyk et al., 2007)
Cu, TiO ₂ , carbon horns	SAE40	Ball-on-flat	120 /step for 13 steps	25	-	0.6	0.001 –1.8 (m/s)	(V. Zin, Agresti, Barison, Colla, & Fabrizio, 2015)

CuO, ZnO, ZrO ₂	PAO6	Block -on- ring	1533	-	165	0.1	2 (m/s)	(Battez et al., 2008)
----------------------------------	------	-----------------------	------	---	-----	-----	------------	-----------------------------

‘Table 2.7: continued’

NPs	Oil	Tribo- Rig	Test Time (sec)	Temp. (°C)	A. L. (N)	P. (Gpa)	Sp.	Author
Ni	PAO6	Block -on- ring	1533	-	165	0.1	2 (m/s)	(R. Chou et al., 2010)
BN	SAE10W	Ball on disk	160	20	10	2.93	0.25 (m/s)	(Çelik et al., 2013)
Graphite	Vegetable based oil	Pin- on- disk	3600	24	2,10	-	100 (rpm)	(Su, Gong, & Chen, 2015)
Carbon Nano- onions, Graphite	PAO	Pin- on- flat	1000, 20000	25	2,5,1 0	0.83, 1.12, 1.42	0.25 (m/s)	(L. Joly- Pottuz et al., 2008)
MoS ₂ , SiO ₂	EOT5# engine oil	Ball- on- flat	1800, 4500	25	1,3, 5, 8	0.223, 0.312, 0.381, 0.446	0.08, 0.03 (m/s)	(H. Xie et al., 2015)
MoS ₂	PAO4 + PAO 40	Ball- on- flat	144000 cycles	80	10	1.4	600 (rpm)	(Pierre Rabaso et al., 2014)
CuO, Al ₂ O ₃	PAO8, SAE 75W- 85)	Ball on disk	7200	50	200	-	3000 (rpm)	(L. Peña- Parás et al., 2015)

2.4.1.10 Lubrication Mechanisms

The study of lubrication mechanisms is deemed as a fundamental aspect to thoroughly explain the tribology of nanoscale particles. Nevertheless, describing the existing mechanisms remains a matter of investigation for numerous research considerations

concerned nanoscale particles using lubrication methods. Several mechanisms have been introduced by scientists employing the surface interpretation methods to describe the lubrication improvement by the nanoscale particle mixed with lubrication oil. These mechanisms involve:

- The ball bearing impact (Chiñas-Castillo, 2003; L. Rapoport, Leshchinsky, V., Lvovsky, M., Nepomnyashchy, O., Volovik, Y., & Tenne, R., 2002; Y. Y. Wu, Tsui, W. C., & Liu, T. C., 2007),
- The protecting film composition (Ginzburg, 2002; Z. S. Hu, Lai, R., Lou, F., Wang, L. G., Chen, Z. L., Chen, G. X., & Dong, J. X., 2002; Xiaodong, 2007),
- The mending influence (G. Liu, Li, X., Qin, B., Xing, D., Guo, Y., & Fan, R., 2004), and
- The polishing influence (T. Sui, Song, B., Zhang, F., & Yang, Q., 2015; Tao, 1996)

All these lubrication mechanisms stated for PAO blended with amino-functionalized hairy silica nanoscale particles as represented in Figure 2.14.

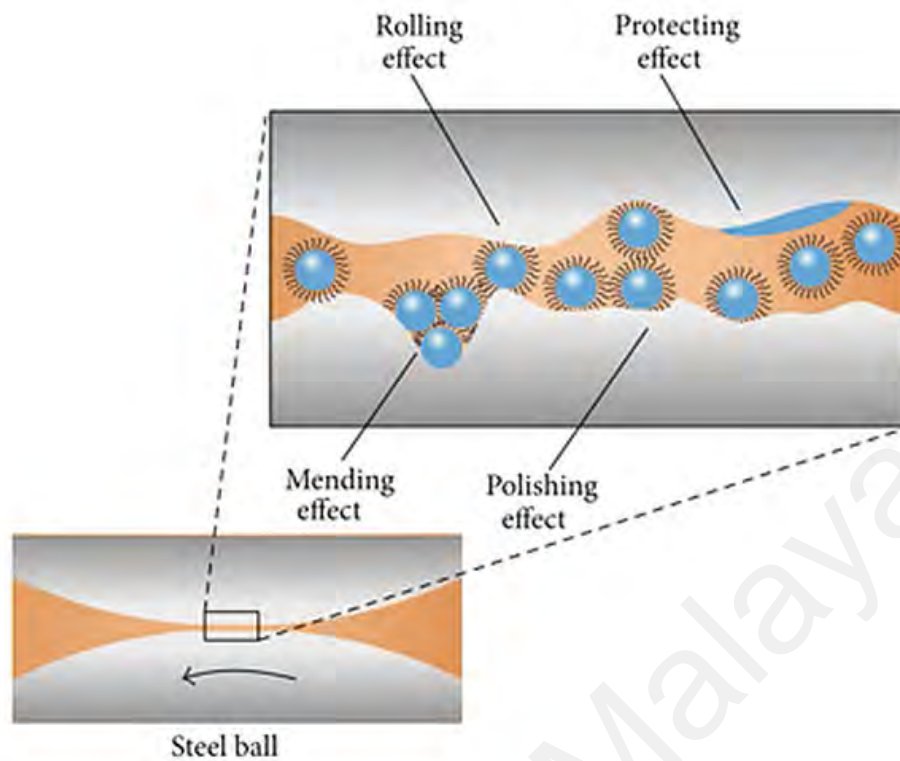


Figure 2.14: Graphical representation of the lubrication technique of silica nanoscale particle blended in PAO

Source: (T. Sui, Song, B., Zhang, F., & Yang, Q., 2015)

These mechanisms can be classified as two major groups:

- The first is the immediate impact of the nanoscale particles that involves ball bearings influence and protecting/tribofilm disposition.
- The other is the subsequent impact which provides surface improvement by mending/repairing outcome and polishing/smoothing result.

Table 2.8 shows the literature survey of mainly summarized lubrication mechanisms for various nanoscale particles/lubricating oil mixtures. For better comprehension, the elaboration of possible lubrication mechanisms by the behavior of nanoscale particles, are additionally reviewed subsequently.

Table 2.8: Survey of summarized outcomes of nanoscale particles on tribological characteristics, lubrication mechanisms, and surfaces characterization

NPs	Oil	Additives Function	Mechanism	Surface Tool	Author
Cu	PAO6	AW, EP	Tribosinterization	SEM, EDS	(J. L. Viesca et al., 2011)
Ni		FM, AW, EP	Tribosinterization	SEM, EDS	(R. Chou et al., 2010)
ZnO, ZrO ₂ , CuO		AW, EP	Deposition	SEM, EDS	(Battez et al., 2008)
Graphite	Super-gear EP220	FM, AW	Polishing	SEM, AFM	(Lee et al., 2009)
Fullerene, Carbon nanoballs	SAE-20W50	AW	Mending	SEM	(Ettefaghi, Ahmadi, Rashidi, & Mohtasebi, 2013)
Al/Sn	SE15W/40	AW, EP	Mending	SEM, EDS	(G. Liu, Li, Lu, & Fan, 2005)
Pb	Liquid paraffin	FM, AW	Ball bearing tribofilm	SEM, EDS	(L. Kolodziejczyk et al., 2007)
Fe, Cu, Co	SAE10	FM, AW	Tribofilm	SEM, EDS	(Padgurskas et al., 2013)
Al	Liquid paraffin	FM, AW	Tribofilm	SEM, EDS	(Peng, Kang, et al., 2010)
CuO	SAE30	FM, AW	Ball bearing, mending	SEM, EDS	(Y. Y. Wu et al., 2007)
	Mineral oil	FM, AW	Deposition, polishing	SEM, EDS	(V. S. Jatti & Singh, 2015)
	Liquid paraffin	FM, AW	Ball bearing	-	(Asrul et al., 2013)
BN, MoS ₂	PAO10	FM, AW	Tribofilm	Raman spectroscopy	(N. G. Demas et al., 2012)

‘Table 2.8: continued’

NPs	Oil	Additives Function	Mechanism	Surface Tool	Author
MoS ₂	SAE 20W-40	FM, AW, EP	Mending	SEM, EDS	(Thakur et al., 2016)
	PAO	FM, AW, EP	Tribofilm	SEM, EDS	(P. Nallasamy, Saravanakumar, Nagendran, Suriya, & Yashwant, 2014)
	Liquid paraffin	FM, AW, EP	Tribofilm	SEM, EDS	(Verma, Jiang, Abu Safe, Brown, & Malshe, 2008)
MoS ₂ , TiO ₂ , MoS ₂ /TiO ₂	Liquid paraffin	FM, AW	Mending, tribofilm	XPS	(K. H. Hu et al., 2011)
ZnO	60SN base oil	FM, AW	Mending	SEM	(Ran et al., 2016)
hBN	SAE 15W40	FM, AW	Ball bearing, polishing	SEM	(M. I. H. C. Abdullah, Abdollah, Amiruddin, Tamaldin, & Nuri, 2014)
Al ₂ O ₃	SAE 15W40	FM, AW	Ploughing effect	SEM	(M. I. H. C. Abdullah et al., 2014)
ZnO, CuO	Mineral oil	FM, AW	Deposition, tribofilm	SEM, EDS	(Alves et al., 2013)
	PAO	FM, AW	Deposition, tribofilm	SEM, EDS	(Alves et al., 2013)
	Sunflower oil	FM, AW	Tribofilm	SEM, EDS	(Alves et al., 2013)
	Soybean oil	FM, AW	Tribofilm	SEM, EDS	(Alves et al., 2013)
TiO ₂	10W-30	FM, AW	Ball bearing, deposition	-	(M. Laad & Jatti, 2016)
ZnAl ₂ O ₄	-	FM, AW	Mending	SEM, EDS	(X. Song et al., 2012)

2.4.1.11 The Tribological Performance

The fatty acids in naturally lubricants are useful in boundary lubrication due to their capacity to stick to metal bodies. This performance is owing to the acquired polar carboxyl group that stay constantly gathered, and create a single-layered film that is capable of decreasing friction and wear by reducing the metallic surfaces contacting (Grushcow, 2005). The structure of protecting groups of the fatty acid molecules on the metal areas as presented in Figure 2.15 (Chia-Jui Hsu, 2017). The polar heads of the fatty acid chains connected to metallic areas by a chemical method that provides a single-layered film to generate with the non-polar end of fatty acids adhering apart from the metal-to-metal contact leading in lowering in COF (Jayadas, 2007; H. Masjuki, & Maleque, M., 1997; H. Masjuki, Maleque, M., Kubo, A., & Nonaka, T., 1999; N. W. M. Zulkifli, Azman, S., Kalam, M., Masjuki, H., Yunus, R., & Gulzar, M., 2016). But this trend of protecting film structure has unfavorably influenced the environment of high oxidation. For example, before-mentioned research, the boundary lubricating characteristics have been reviewed for oxidized sunflower lubricant (Fox, 2003). After a duration of 28 days or more of aging, the boundary lubricating properties of sunflower lubricant was deteriorated substantially. Owing to the same purpose, the immediate application of vegetable lubricants is inappropriate for lengthy periods in IC engines and other uses that need suitable thermal and oxidative durability (Rudnick, 2006) which is a fundamental drawback for bio-base lubricant.

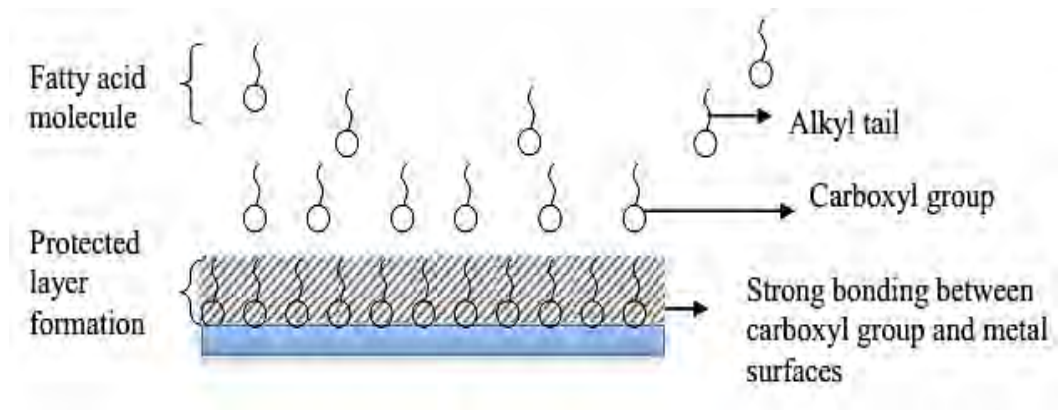


Figure 2.15: Protecting film structure on metal-to-metal contact by Bio-lubricant

Source: Nurin Wahidah Mohd Zulkifli (2014)

2.5 Conclusion

The literature survey drew attention to the researches revealing the ability of formulated lubricants for many goals generally and particularly the performance of nano-mixtures lubrication. Oils perform an essential part in the operation of machine. Lubricants also improve engine life, decreasing wear and damage, reduce friction and impeding components from fatigue. However, if the performance of lubrication is inadequate that can affect notable losses in material and energy. Nevertheless, it became clear that additive-free lubricants and bio-based oils individually could not provide the necessary lubrication efficiency nor energy or cost reduction. From these perspectives, the notable friction and wear reduction performance of dual nanoparticles make them appropriate chosen as additives to enhance the lubrication performance and therefore, energy and cost savings.

While reviewing tribology researches, several types of research presented upgraded tribological performance by using synthetic lubricants or bio-based lubricants and adequately formulated these oils when blended with nanoscale particles. However, nano lubricating generated by these lubricants with nanoscale particles contributed an answer to several difficulties accompanied by additive-free oils that can be made by substituting

the individual nanoparticle lubricants by dual synergetic nano-mixtures for lubricity enhancement.

As already reviewed earlier (TiO_2 (A) + Graphene) and (ZnO + Graphene) nanoparticles have most notably properties to be blended with base stock oil to formulate dual nanoparticles lubricant. In this respect, the dispersion stability, tribological performance, and surface characterization of different types of nanoscale particles as additives to a pure base oil Group II are supposed to be examined. Figure 2.16 presents the research gap of formulating excellent nanolubricant to obtain great lubrication performance as well as an adequate surface roughness improvement with low energy consumption and less cost.

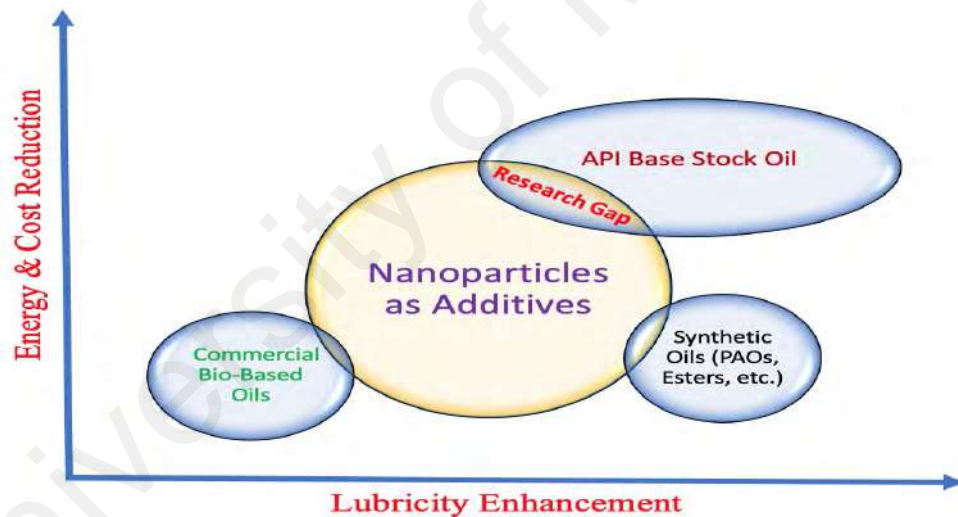


Figure 2.16: Potential research gap/ research problem of adding nanoscale particles to formulate effective nanolubricant

CHAPTER 3: MATERIALS AND METHODS

3.1 Introduction

This chapter will discuss three nanoparticles that have selected for this study TiO_2 , ZnO, and graphene. The first part of the research started with TiO_2 (anatase) and graphene, (single type of nanoparticles and dual types), with different concentrations to find out the best lubricant additive. The second part of the research started with ZnO and graphene, (single type of nanoparticles and dual types) with different concentrations to find out the best lubricant additive.

The materials were purchased from different sources as explained then characterized by TEM after that, nanolubricants were formulated with different concentrations for twelve types of lubricants as tabulated Table 3.1 and Table 3.2. Later, experimental set-up will be conducted sonication treatment and dispersion stability analysis. Tribology rigs will be discussed thoroughly. Furthermore, describing the surface characterization tools to understand the tribology behavior, lubrication mechanism, nano-additives role of each lubricant and scar wear analyses as well.

The research path of the study has illustrated in Figure 3.1. Also, nanolubricants research areas and methodologies used in the current study were graphically represented in Figure 3.2.

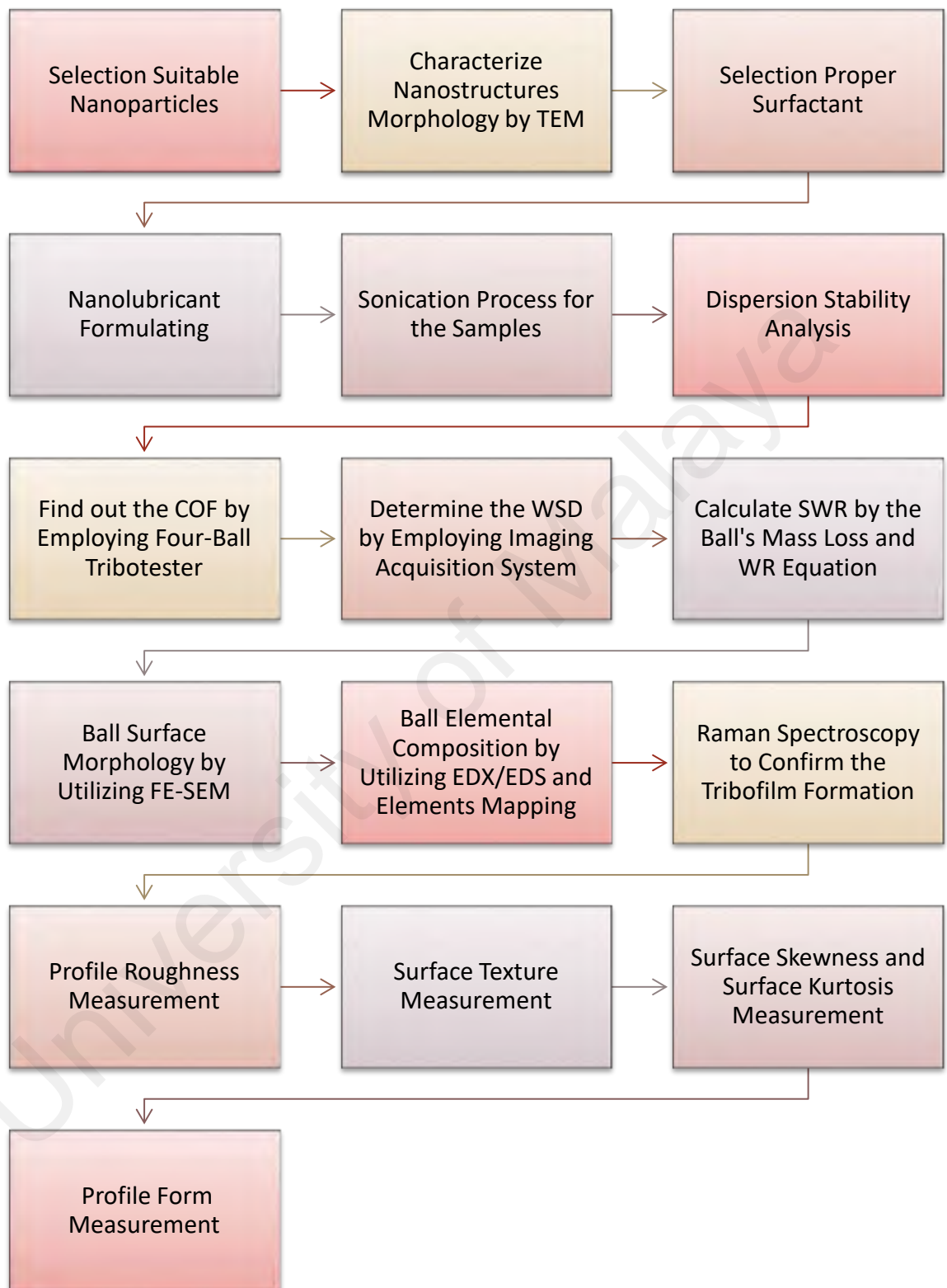


Figure 3.1: Research path of the study

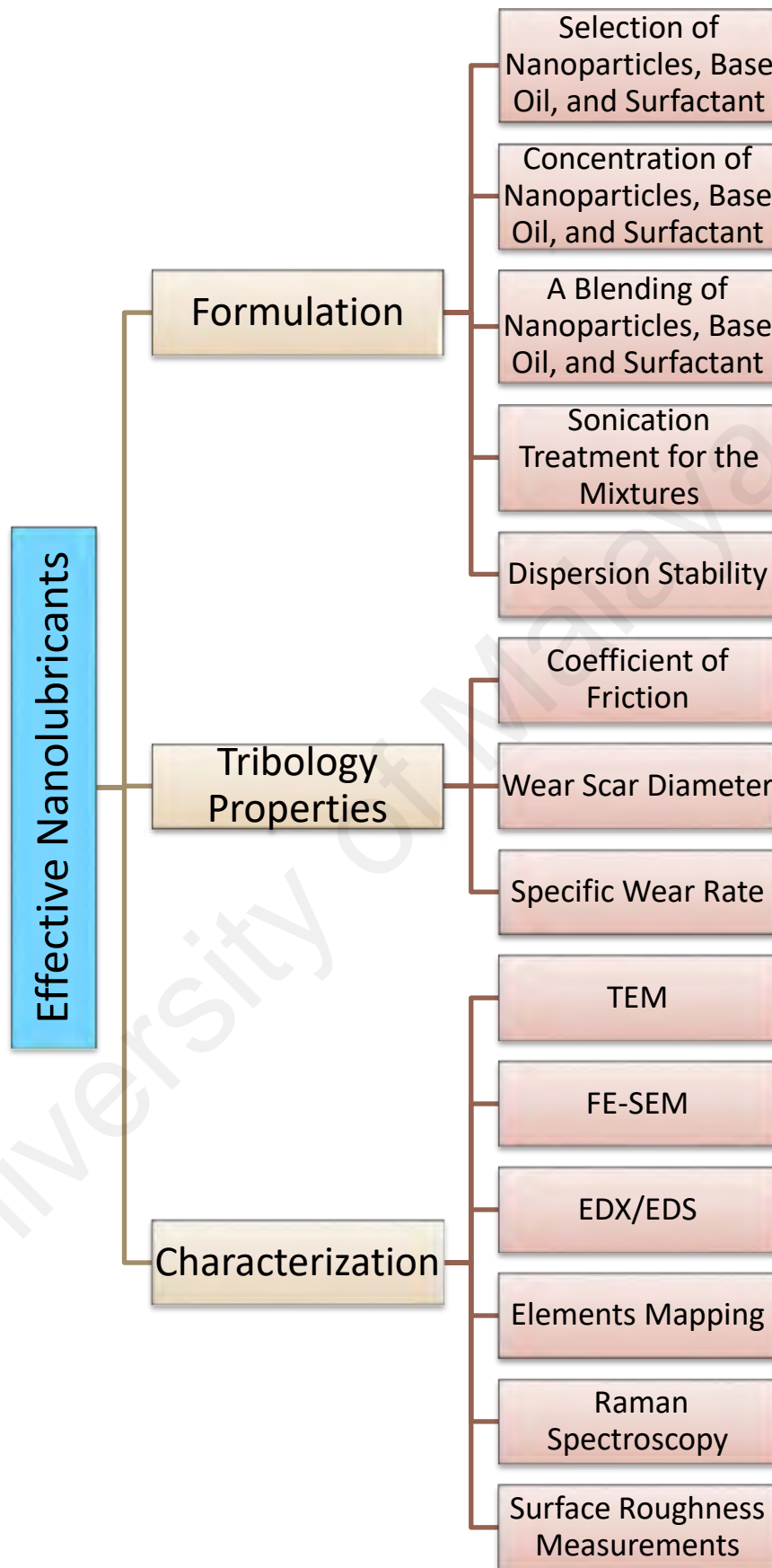


Figure 3.2: Nanolubricants research areas and methodologies

3.2 Source of Materials

Commercially available nanoparticles (TiO_2 , ZnO , and Graphene) were purchased from Sigma-Aldrich (Malaysia). Nano-titanium (IV) oxide, (<25 nm particle size anatase, and 99.7% trace metals), Zinc Oxide (ZnO) nanopowder (<100 nm particle size), and graphene nano-platelets of (~5 nm thickness and a surface area of $120 \text{ m}^2/\text{g}$). Oleic acid (OA) surfactant ($\text{C}_{18}\text{H}_{34}\text{O}_2$ extra pure M.Wt 282 (46 g/mol)) was purchased from Friedemann Schmidt chemical (Malaysia). Reagent n-Heptane $\text{CH}_3(\text{CH}_2)_5\text{CH}_3$ was purchased from Ajax Finechem Pty Ltd (Malaysia). API Group II base oil (PBO-GII) was purchased from GS Caltex Corporation (Korea). Moreover, steel balls were bought from Taat Bestari Sdn Bhd (Malaysia).

3.3 Characterization of Nanoparticles

The main type of electron microscopes is transmission electron microscopes (TEM) from Carl Zeiss Microscopy, as shown in Figure 3.3. TEM uses an electron beam to illuminate a specimen and can produce a magnified image 500,000 times its normal size.



Figure 3.3: Transmission electron microscopy (TEM) device by Carl Zeiss microscopy

Sample preparation of TEM viewing is blending 0.004 mg TiO_2 (A) with three droplets of water in small vial bottle very well. Next, pour it on the copper grid has a formvar film and let it dry for 3-minutes. After that, put it in a petri dish and sealed the sample with parafilm tape, as shown in Figure 3.4. Then, let it dry in desiccator cabinet at least three days before TEM viewing, as per Figure 3.5. The desiccator cabinet has silica gel granulates to absorb wets. Subsequent, same process repeated for 0.004 mg ZnO, and 0.002 mg graphene nanoparticles samples.

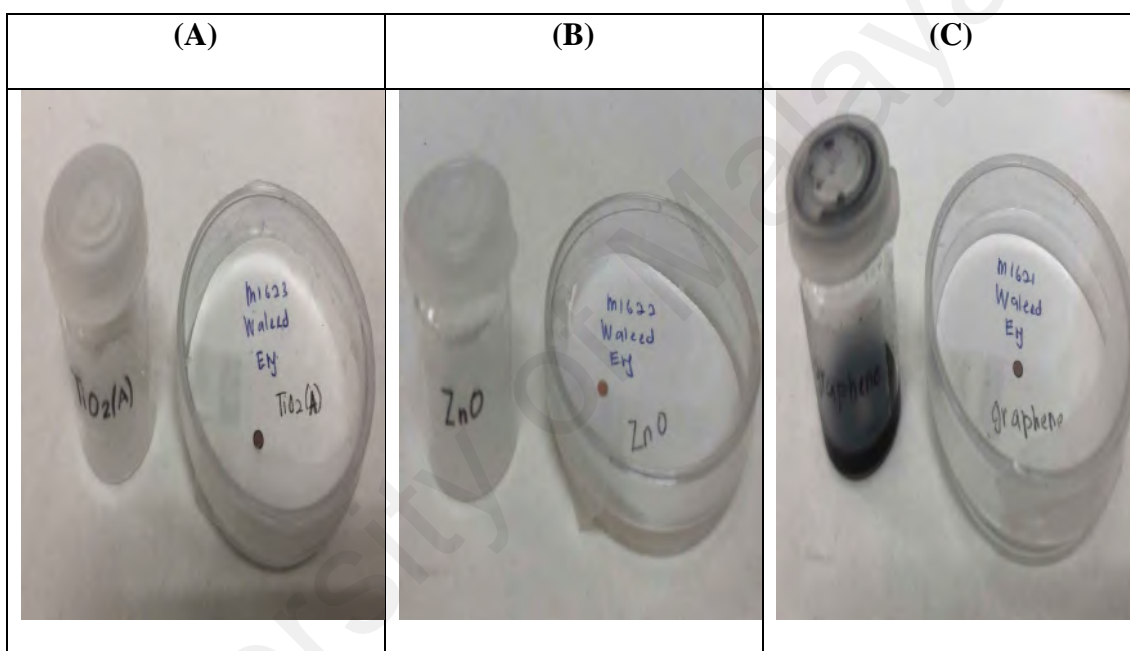


Figure 3.4: Nanoparticles (A) TiO_2 Anatase, (B) ZnO and (C) Graphene samples



Figure 3.5: Desiccator cabinet for drying the samples

3.4 Formulation of Nanoparticles

Firstly, TiO_2 anatase nanoscale particle was mixed with graphene nano-platelets to prepare dual nanoparticles (NPs) combination. Secondly, Zinc Oxide (ZnO) nanopowder was mixed with graphene nanoplatelets to prepare significantly synergetic nanoparticles combination. Afterward, PBO-GII added to both dual NPs combinations (TiO_2 A + Graphene) and (ZnO + Graphene). Finally, oleic acid added to these two mixtures to produce effective nanolubricants, as illustrated in Figure 3.6.



Figure 3.6: Addition stages of nanolubricant formulation

Oleic acid (OA) is an unsaturated fatty acid that helps improve nanoparticle dispersion into the base oil. Moreover, the addition of OA to nanolubricant will result in a considerable improvement in the tribological properties (Zhengfeng Jia 2014) and (Tiedan Chen, 2014). The composition of each lubricant for two types of nanoparticle combinations (TiO_2 (A) + Graphene) and (ZnO + Graphene) is presented in Table 3.1. and Table 3.2.

Table 3.1: Formulation of nanoparticles (TiO_2 (A) + Graphene), base stock, and surfactant for six types of samples

Sample No.	TiO_2 (A) wt% mg/ml	Graphene wt% mg/ml	Pure Base Oil Group II, ml	Oleic Acid ml
1.	0.0	0.0	10	0
2.	0.2	0.0	8	2
3.	0.0	0.2	8	2
4.	0.2	0.2	8	2
5.	0.2	0.4	8	2
6.	0.4	0.2	8	2

Table 3.2: Formulation of nanoparticles (ZnO + Graphene), base stock, and surface-agent for six types of samples

Sample No.	ZnO wt% mg/ml	Graphene wt% mg/ml	Pure Base Oil Group II, ml	Oleic Acid ml
1.	0.0	0.2	8	2
2.	0.2	0.0	8	2
3.	0.2	0.2	8	2
4.	0.2	0.4	8	2
5.	0.4	0.2	8	2
6.	0.0	0.0	10	0

The pure base oil Group II is a petroleum-based oil, light-yellow additive-free, and following the API groups classification. The specifications of this base oil are listed in Table 3.3.

Table 3.3: Specifications of pure Group II base oil

TEST	METHOD	VALUE	UNIT
Density	ASTM D 4052	0.8649	g/cm ³
Viscosity @ 40° C	ASTM D 445-06	92.9	cSt
Viscosity @ 100° C	ASTM D 445-06	10.32	cSt
Water by KF	ASTM D 6304-07	48.32	ppm
TAN	ASTM D 664-04	0.06	mg of KOH/g
Particle Size Distribution	ASTM D 7596	72.62	Size (d.nm)
Zeta Potential	ASTM D 4187-82	0.195	mV
Surface Tension	ASTM D 1331-11	31.678	mN/m

3.5 Experimental Set-up:

3.5.1 Sonication Treatment

Twelve samples were prepared, as in above tables (Table 3.1 and Table 3.2), 5 of which (excluding the base oil) were sonicated for (TiO₂ + Graphene) and (ZnO + Graphene) combinations, for 2 hours duration at 80 °C, as per Figure 3.7. The sonication helps assure the dispersion of the nanoparticles into the base oil forms a stable suspension (B. S. B. S.M. Alves, M.F. Trajano, K.S.B. Ribeiro, E. Moura., 2013). Nanographene commonly dispersed evenly in the base oil with no need to add a precursor/surfactant to the lubricant and can remain stable with a little sedimentation for a duration about one month (Varrla Eswaraiah, 2011). However, OA surfactant blended with mixtures and sonication treatment has been done for more stability and constancy of nanoparticles in the pure lubricant for uniform suspension and extreme dispersion with no sedimentation rate of nanoparticles in the plain oil.

A. TiO₂ (A) + graphene samples



B. ZnO + graphene samples



Figure 3.7: Stability and constancy of nanoparticles for two types of lubricant samples using a sonication device

3.5.2 Dispersion Stability Analysis

For studying dispersion stability purposes, many methods used. These investigations include sedimentation, zeta potential, spectral absorbency, and metallographic depiction stability analysis. Table 2.3 shows frequently used techniques in previous studies.

Dispersion stability investigations were carried out instantly after sonication treatments of nano mixtures. In the current study, sedimentation experiments were performed on (TiO₂ (A) + Graphene) and (ZnO + Graphene) samples for one month as shown in Figure 3.8.

A. TiO₂ (A) + graphene samples



B. ZnO + graphene samples



Figure 3.8: Dispersion stability analysis after 1-month of sedimentation for (A) (TiO₂ (A) + Graphene) samples and (B) (ZnO + Graphene) samples

In conclusion, it can be seen that the settling process of nanoparticles was very minimal after one month of sedimentation time owing to the nanoparticles used (TiO₂ (A), ZnO, and Graphene), surfactant addition (OA), and sonication treatment (L. Joly-Pottuz, Vacher, B., Ohmae, N., Martin, J. M., & Epicier, T., 2008; M. Laad, & Jatti, V. K. S., 2016; H. M. M. Gulzar, M Varman, MA Kalam, R.A. Mufti, NWM Zulkifli, R. Yunus, Rehan Zahid, 2015; D. X. Peng, Kang, Y., Chen, S., Shu, F., & Chang, Y., 2010; Siti Safiyah Nor Azman, 2016; Waleed Alghani, 2019; Xu Ran, 2016).

3.5.3 Tribology Tribo-testers

A four-ball rig was employed to examine the frictional torque value of all lubricants and then, to calculate the coefficient of friction (COF). In this study, DUCOM's four-ball tribometer model TR-30H was utilized as configured in Figure 3.9 and Figure 3.10. The four balls are situated in the tribotester, where three are in the pot, while the fourth is in the ball holder (spindle). Sample 1 was poured into the pot to submerge the three balls. This process was later repeated for the rest of the samples. Moreover, AISI standard steel balls were used in this study and were described in Table 3.4.

Table 3.4: Steel ball mechanical properties of the Four-ball tester

Property	Feature/Value
Ball material	Carbon-chrome alloy steel, made from AISI standard steel No. E-52100
Ball Grade	25 EP (Extra Polish)
Ball diameter	12.7 mm (0.5 in.)
Ball hardness	64–66 HRC
Ball density	7.79 g/cm ³
Ball surface roughness	0.022 μm

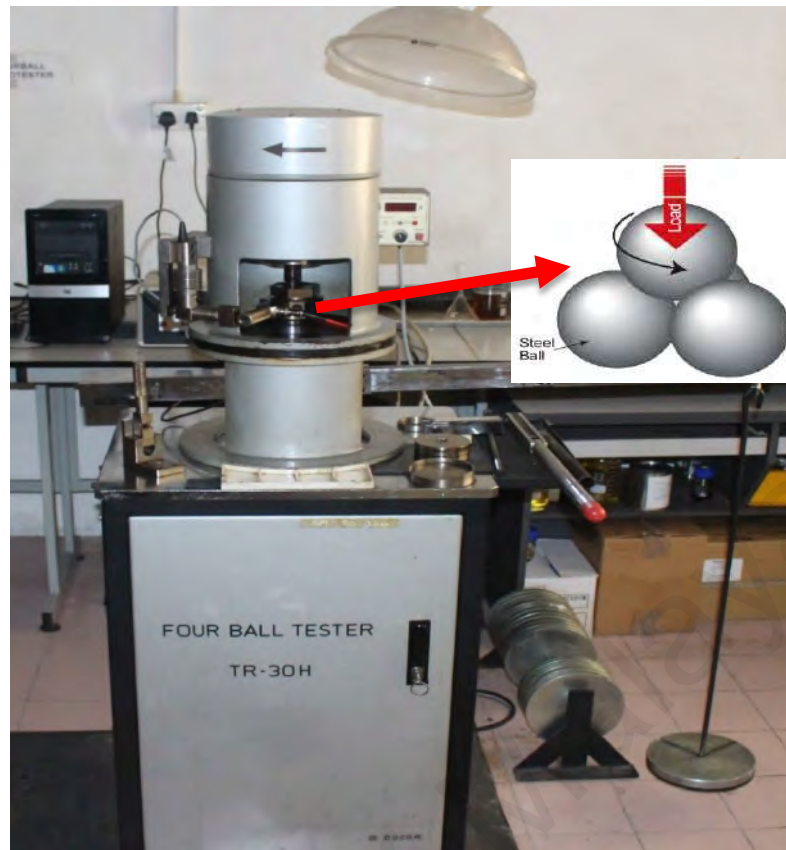


Figure 3.9: Lubricants tribo-examining utilizing DUCOM Four-Ball tribometer TR-30H

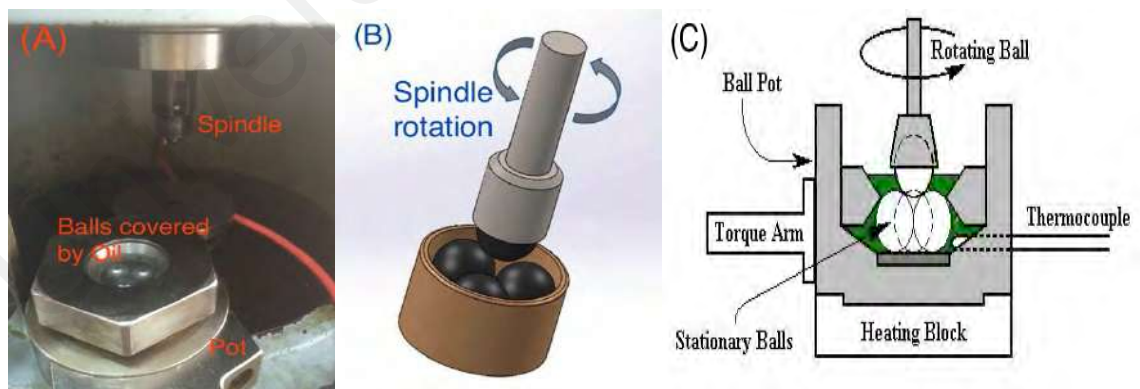


Figure 3.10: (A) Photograph of pot and spindle of the Four-ball machine. (B) 2D drawing of spindle fastened to one ball and pot clamped the three other balls. (C) Schematic diagram of the Four-ball tribotester arrangement

Source for (C): (Amit Suhane, 2014)

During series of experiments, lubricants were examined by applying the ASTM standard D4172: Test Specifications for Wear Preventive Characteristics of Lubricating Fluid (Four-ball Method) (J. E. F. R. A. Hernandez Battez, A. Navas Arias, J.L. Viesca Rodriguez, R. Chou Rodriguez, J.M. Diaz Fernandez, 2006). The principal experimental conditions are summarized in Table 3.5.

Table 3.5: ASTM Standard D4172 of the four-ball method

Condition	Operating Value
Test temperature	$75 \pm 2 \text{ }^\circ\text{C}$ ($167 \pm 4 \text{ }^\circ\text{F}$)
Test duration	$3600 \pm 60 \text{ s}$ ($60 \pm 1 \text{ min}$)
Spindle speed	$1200 \pm 60 \text{ rpm}$ ($20 \pm 1 \text{ cps}$)
Load	$40 \pm 0.2 \text{ kgf}$ ($392 \pm 2 \text{ N}$)

The balls and the pot were carefully cleaned with n-Heptane $\text{CH}_3(\text{CH}_2)_5\text{CH}_3 = 100.21$ and dried with industrial lint paper after each test to set up the stationary balls for image acquisition measurement and the pot for the subsequent run. Wear scar diameter (WSD) mean was measured for each sample by using a scar imaging microscope as shown in Figure 3.11.



Figure 3.11: Scar wear acquisition microscope

Afterward, finding the mass loss for each ball by using a weighing electronic scale with accuracy up to 100 μg to find out the specific wear diameter mean for each sample. Each experiment was conducted triple times to ensure result precision and stability. The standard deviation was measured too as outlined in later COF, WSD and SWR figures to show the differences in the finding's values.

3.6 Surface Characterization

To understand the tribology behavior, lubrication mechanism, nano-additives role for each lubricant, scar wear analyses must be done. For these reasons, different types of characterization and surface tools employed to describe and examine the tested AISI balls, such as FE-SEM, EDX/EDS, elements mapping, Raman spectroscopy, and 3-D surface roughness analysis.

3.6.1 Field Emission-Scanning Electron Microscope (FE-SEM)

An FE-SEM is a microscope that operates with electrons (particulates with a negatively charged) rather than light. These electrons are separated by a field emission power source. So, the object is examined by electrons in accordance with a zig-zag model. In this study, the equipment used for the FE-SEM analysis was from Carl Zeiss Group, Auriga series. This field emission scanning electron microscope device equipped with multi-balls specimen mount, as shown in Figure 3.12.

An FE-SEM is utilized to imagine tiny topographic features on the ball surface. It is a resourceful device for the study of surfaces at a wide spectrum of magnifications and high resolution. FE-SEM offers qualitative data about surface geometry, morphology, and general appearance of inspected surfaces. FE-SEM has been employed to study the morphology of worn surfaces in this research which assisted in understanding the lubrication performance for each lubricant. Researchers in tribology, apply this procedure to inspect morphologies that may be as tiny as 1 nanometer (= billion of a millimeter).

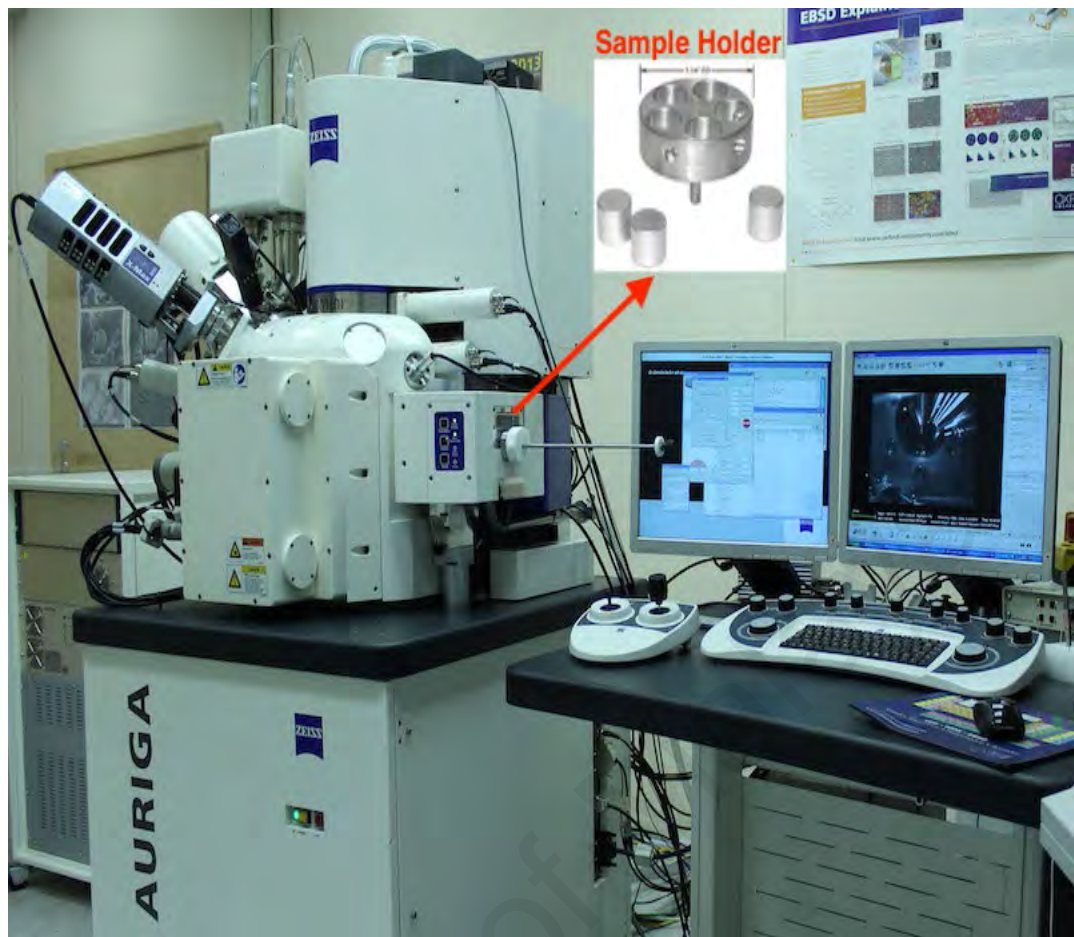


Figure 3.12: Field Emission-Scanning Electron Microscope (FE-SEM) apparatus equipped with multi units' specimen holder

3.6.2 Energy-Dispersive X-ray Spectroscopy and Elements Mapping

Energy-dispersive X-ray spectroscopy (EDS, EDX, EDXS or XEDS), in some cases, described energy dispersive X-ray analysis (EDXA) or energy dispersive X-ray microanalysis (EDXMA), is an analytic procedure employed for the elemental investigation or composition characterization of a specimen. It depends on the interaction of some source of X-ray excitation and a specimen. Its characterization abilities are owing in an important role to the significant principle that each element has an individual atomic composition providing an uncommon band of peaks on its electromagnetic emission range (Joseph Goldstein, 2003) (which is the principal law of spectroscopy). Energy-Dispersive X-ray Spectroscopy EDX/EDS and elemental mapping device equipped with

sample holder mounted inside the Phenom device chamber, as shown in Figure 3.13. The chemical structure of elements placed/penetrated on/in worn areas was examined utilizing Carl Zeiss ultra plus scanning electron microscope (SEM), model AG ULTRA55. This Oxford tool, energy dispersive x-ray (EDX) system combined with SEM configuration. By analyzing the energy spectrum of X-rays emitted from the sample, it is feasible to identify its elemental profile. The elemental data by EDX originate from around the first 1 μm below the surface of the examined sample. In this research, EDX assisted in analyzing the lubricants mechanisms and the deposited particles over the scar surface by comparing the chemical composition of the elements on the worn surfaces with the known composition of the ball before tribo-testing. It gives the proof of mending/repairing by deposited of nanoscale particles on tribologically examined balls.



Figure 3.13: Energy-Dispersive X-ray Spectroscopy EDX/EDS and elemental mapping device with sample holder

3.6.3 Raman Spectroscopy

Raman spectra is an optical spectroscopic technique in which the examined sample is lighted with a monochromatic laser beam, and the light scattered from the inspected surface is investigated. A major part of these spread light waves has an equal wavelength as that of the incidental light, but there is slight scattering with various wavelength. This difference or shifting of wavelength is a consequence of the application of vibrational modes in the specimen material. So, vibrations are an effect of either molecules or mixed motion of atoms. The energy variation between the vibrational elements gives the wavelength change. Raman analysis was selected in this research owing to its benefit of contributing information about aggregates on the ball surface and to further confirm the existence of the generated tribofilm over the ball scar wear rather depending solely on an elemental structure by EDX/EDS and elements mapping. RENISHAW inVia confocal Raman microscope (Figure 3.14) was employed to conduct inVia Raman analysis utilizing argon-ion laser possessing excitation wavelength of 532 nm edge, 10 mW laser power, and the spectrum field of 100 cm^{-1} to 3200 cm^{-1} .



Figure 3.14: Raman microscope employed to investigate worn of scar balls

3.6.4 Surface Roughness Measurements

The scars morphology after tribological tests were examined employing optical 3D surface analysis. For this objective, Alicona Infinite Focus 3D surface analyzer was employed as shown in Figure 3.15.

The analysis rule depends on focus-change with non-contact, optical, and 3D features. This instrument links the minor depth of focus of an optical pattern with vertical scan to produce topographical and color data. Original and innovative algorithms build this into a single 3D information collection with distinct topographical data. Surface depth resolution can be as low as (10 nm) enabling the apparatus perfect for the surface investigation of both uniform and mixture materials. For surface roughness characterization, targeted magnification of (20 x) with a perpendicular interpretation of

(50 nm) was applied. Regarding height, level accuracy was (0.05 %) with a maximum calculable area of (10000 mm²). The position of a ball specimen as presented in Figure 3.15.

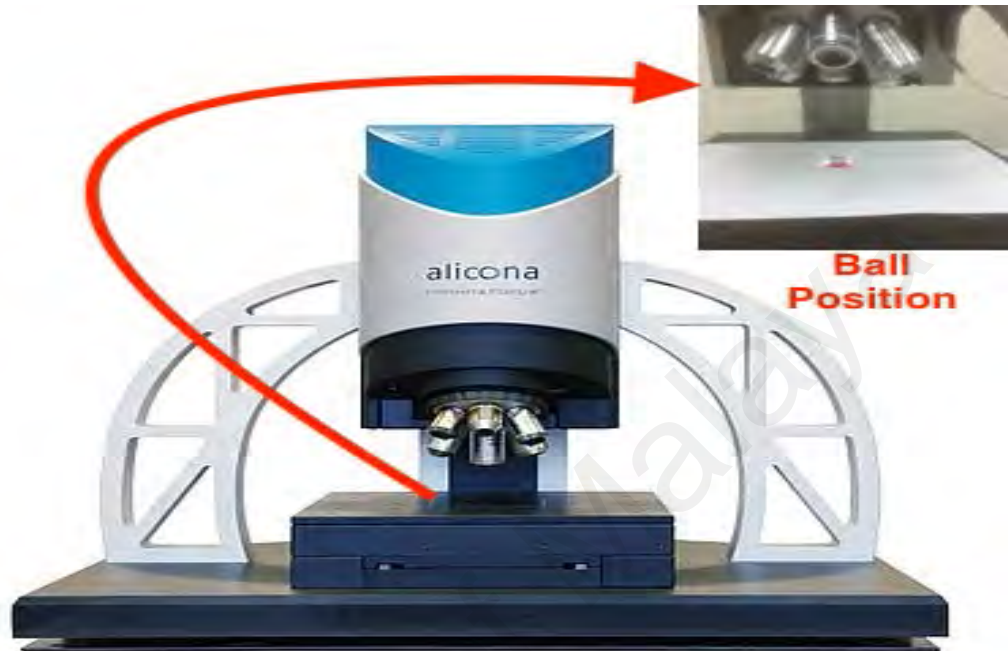


Figure 3.15: Alicona Infinite Focus 3-Dimensional surface, contact-free, surface finish analysis device

3.7 Conclusion

In this chapter sources of materials and suppliers have aforementioned. Transmission electron microscopes (TEM) from Carl Zeiss Microscopy device have been explained. Also, three nanostructured TiO₂ (Anatase), ZnO, and graphene have prepared for characterization via (TEM). Formulation of nanoparticles have made with a different range of concentrations (0.0 wt%, 0.2 wt%, 0.4 wt%, and 0.6 wt% mg/ml) of two groups of dual nanoparticles which include (TiO₂ Anatase + Graphene) and (ZnO + Graphene) were blended with PBO-GII individually to identify the minimum friction and wear losses that occur during sliding contact. Sonication treatment has conducted for ten samples for (TiO₂ Anatase + Graphene) and (ZnO + Graphene) groups, for 2 hours duration at 80 °C.

For studying dispersion stability purposes, sedimentation experiments were performed on (TiO₂ Anatase + Graphene) and (ZnO + Graphene) samples for one month. A four-ball rig was employed to examine the frictional torque value of all lubricants and then, to calculate the coefficient of friction (COF). In this study, DUCOM's four-ball tribometer model TR-30H was utilized. AISI standard steel balls were used in this study. The steel ball mechanical properties of the four-ball tester were described initially. Lubricants were examined by applying the ASTM standard D4172: Test Specifications for Wear Preventive Characteristics of Lubricating Fluid (Four-ball Method). Wear scar diameter (WSD) mean was measured for each sample by using a scar imaging microscope. Afterward, finding the mass loss for each ball by using a weighing electronic scale with accuracy up to 100 µg to find out the specific wear diameter mean for each sample. Different types of characterization and surface tools employed to describe and examine the tested AISI balls, such as FE-SEM, EDX/EDS, and elements mapping, Raman spectroscopy, and 3-D surface roughness analysis.

CHAPTER 4: RESULTS AND DISCUSSION

4.1 Introduction

This chapter will explain about three types of nanoparticles have chosen in this research TiO₂ anatase, ZnO, and graphene. The morphological characterization for these three nanostructures done by utilizing TEM spectroscopic. This study can be divided into two sections:

First section: TiO₂ anatase and graphene, (an individual type of nanoparticles and dual types), with various concentrations to figure out the superior oil additive.

Second section: ZnO and graphene, (an individual type of nanoparticles and dual types) with various concentrations to figure out the superior oil additive.

The synergetic lubrication effect of nano TiO₂ (A) and graphene showed the excellent coefficient of friction (COF, μ), wear scar diameter (WSD, mm) and specific wear rate (SWR, m³/Nm). Where improvements of COF, WSD, and SWR for 1-hour duration were 38.83 %, 36.78 %, and 15.78 %, respectively, for (0.4 wt% TiO₂ (A) + 0.2 wt% Graphene) nanolubricant compared to the PBO-GII. The synergetic lubrication outcome of nano ZnO and graphene nanoparticles exhibited wear and friction enhancing properties as an excellent lubricant additive. The average reductions in COF, WSD, and SWR were 43.81%, 36.78%, and 39.47% respectively, for (0.4 wt% ZnO + 0.2 wt% Graphene) nanolubricant compared to pure base oil group two. Furthermore, topographical characterization (FE-SEM), elemental composition analyses (EDX/EDS and elements mapping), Raman spectroscopy, and surface roughness analyses were discussed for all types of lubricants.

4.2 TEM Characterization for Nanoparticles

The morphology of these three nanostructures of TiO₂ (A), ZnO, and graphene was magnified for 200 nm and 500 nm respectively by transmission electron microscopy (TEM), as revealed in Figure 4.1. TiO₂ anatase has a tetragonal crystalline structure (dipyramidal habit) (S. K. H. M. Vijayaraj, A. K. Harinarain, and S. S. V. Ramakumar, 2016) resembles a semi-spheres geometry as shown in Figure 4.1 (A) that roller bearing impact could be one of the principal lubricating mechanism led to a reduction in friction and wear. ZnO nanoparticles have a polycrystalline geometry that similar to a seed-like structure (Manjula G. Nair, 2011) or nearly spherical morphology (J. E. F. R. A. Hernandez Battez, A. Navas Arias, J.L. Viesca Rodriguez, R. Chou Rodriguez, J.M. Diaz Fernandez, 2006), as per Figure 4.1 (B). It packs up the micro- and nanoholes of the sliding balls thus it prevents immediate rubbing of the steel balls and reduces the friction and wear as will be further analyzed next chapter. The graphene's geometry is planar as shown in Figure 4.1 (C), so it simply slips during sliding of surfaces in the lubricant. It could be delivered most beneficial outcomes for the excellent mixture of nanoparticles in the pure base oil. Furthermore, the thickness of graphene nanoplatelets in the current research is (~5 nm), this can develop a nano bearing mechanism between sliding balls. This case would cause smooth sliding when applying the load. Consequently, blended nano additive to the plain lubricant can perform as a mechanical reinforcing compound throughout friction and hence, increase the load-carrying capacity of the nano-oils (Varrla Eswaraiah, 2011).

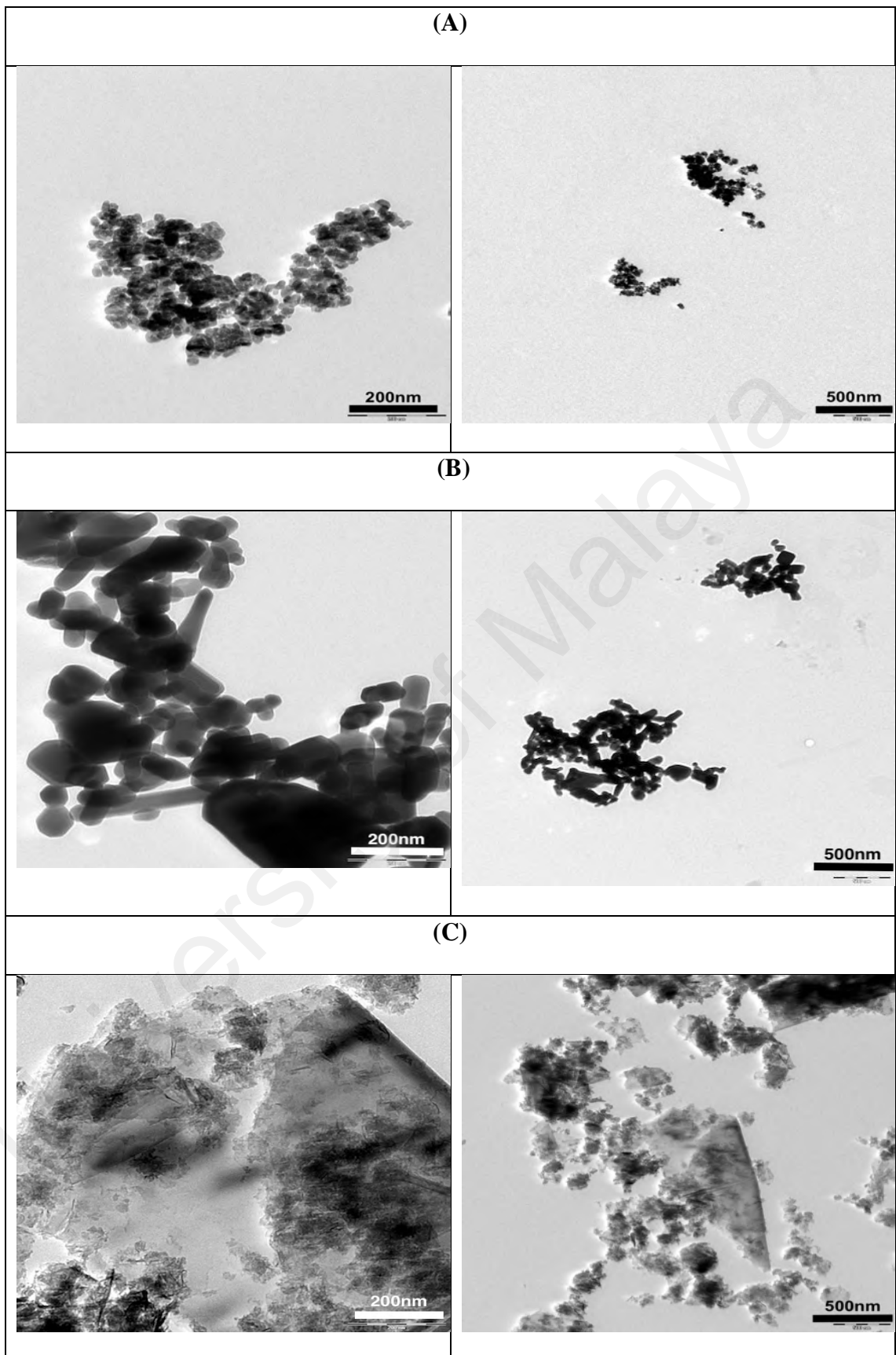


Figure 4.1: The morphology of nanoparticles by TEM (A) TiO₂ (Anatase), (B) ZnO, and (C) graphene

4.3 Coefficient of Friction (COF) Behavior

4.3.1 TiO₂ (A) + Graphene COF

Six types of lubricants were formulated to find out an appropriate concentration that may drive to high-grade lubrication qualities. After collecting the frictional torque from a 4-ball tribometer data was applied to compute the coefficient of friction (COF) using Equation 4.1 (F. Sundus, 2017).

$$\mu = \frac{T \sqrt{6}}{3 W r} \dots\dots\dots \text{Equation 4.1}$$

Where T is the frictional torque (kg/mm), W is the applied load (kgf), and r is the distance from the center of the mating surfaces on the bottom balls to the axis of rotation (3.67 mm). Friction and wear analyses were conducted at stable parameters as tabulated in Table 3.5. Each analysis was replicated three times with the same test conditions and the COF described here is the average of these three experiments. The standard deviation was computed which is integrated with diagrams to reveal the variation in the finding's values.

Particularly, a single type of nanoparticles (0.2 wt% TiO₂ (A)) and (0.2 wt% Graphene) were not able to escalate the tribo-features than synergic dual nanoparticles. Likewise, the minimal TiO₂ (A) concentration in samples (0.2 wt% TiO₂ (A) + 0.2 wt% Graphene) and (0.2 wt% TiO₂ (A) + 0.4 wt% Graphene) produced inadequate COF in comparison with the superior mixture (0.4 wt% TiO₂ (A) + 0.2 wt% Graphene) owing to the shortage of a lubricative nano-scale tribofilm to counter friction (Siti Safiyah Nor Azman, 2016). The nanolubricant (0.4 wt% TiO₂ (A) + 0.2 wt% Graphene) presented a more favorable COF in comparison with PBO-GII as plotted in Figure 4.2. Higher COF was a consequence of intense shear force on the surface which notched the surface by abrasion action (Sudeep Ingole, 2013). The nano-formulation was slightly adjusted to produce a

continuous transfer film during the mating action, which decreased the friction coefficient and wear rate. Pertinently, the tribofilm was ineffectual of carrying the load against the steel ball, however, it contributed to hinder the immediate contact among metallic surfaces. The anti-wear capability enhanced, while the friction coefficient diminished prominently (Tiedan Chen, 2014). Consequently, five nanolubricants presented reduced COF through experiments with respect to the COF of base oil individually.

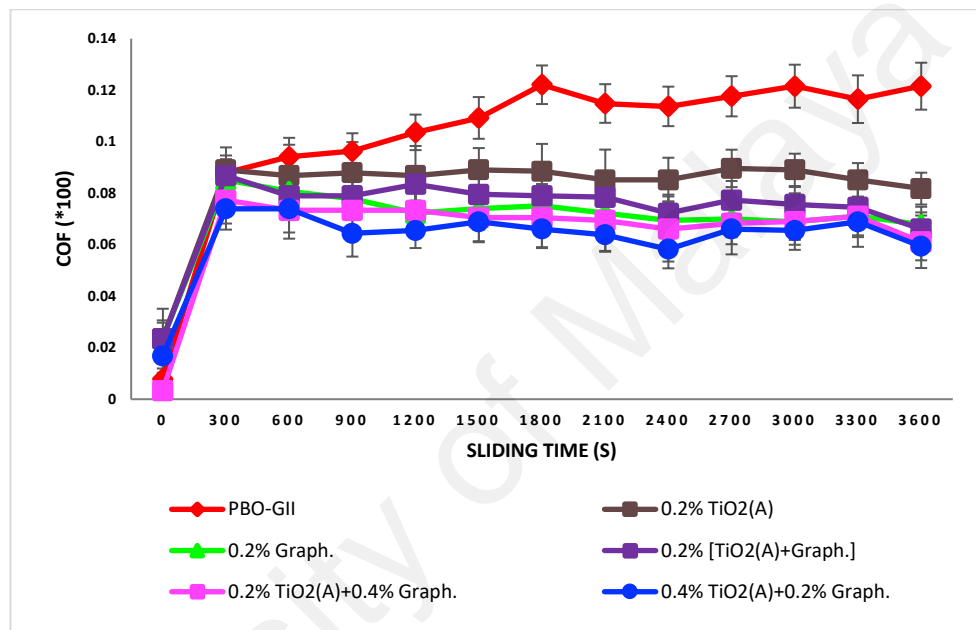


Figure 4.2: Differences in coefficient of friction among six different types of lubricants

4.3.2 ZnO + Graphene COF

Six lubricants were mixed to acquire the appropriate amount that is capable to lead to high-quality lubrication properties. Frictional torque obtained was applied to calculate the coefficient of friction (COF) using Equation 4.1.

Friction and wear experiments were carried out at constant test circumstances as tabulated in Table 3.5.

Each run was tested three times with the identical testing parameters and the COF discussed in this study is the mean of these three tests. The standard deviation implemented for COF analysis to reveal the differences in the obtained results, as demonstrated in Figure 4.3.

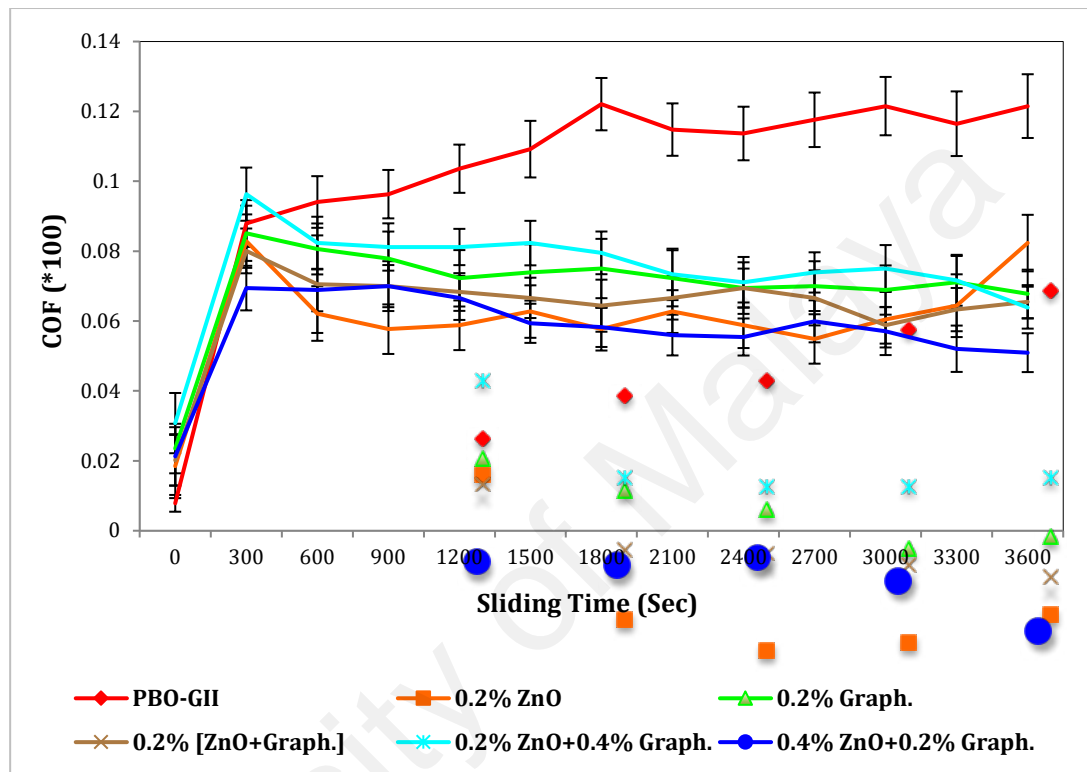


Figure 4.3: Coefficient of friction measurement (dimensionless) for six lubricants

The coefficient of friction (COF) in the tribopairs was calculated based on sliding time, load, torque, temperature and speed. In addition, researches on oiled textures exhibit that surfaces with plateau-like contour and unevenly separated thin grooving can provide adequate lubrication, which reduces friction under mixed lubrication method (B. P. Marko Sedlaček, Jože Vižintin, 2012) as presented in Figure 4.3.

The current research findings verify that the mean enhancement in COF was 43.81% in favor of 0.4 wt% ZnO + 0.2 wt% Graphene nano-oil. This is ascribed to the superior

mixture in this nano-oil (Hao-Jie Song, 2010), and (Shanhong Wan, 2016). The nano-mixture was entirely adapted to deliver a uniform transfer layer throughout the sliding action, which decreased the coefficient of friction and wear rate. Furthermore, 0.2 wt% ZnO showed satisfactory anti-friction, but this behavior did not last long due to the absence function of graphene nanoscale particles (Emad Sadeghinezhad, 2016) and a smaller amount of ZnO nanoscale particles (Shibo Wang, 2009).

The high/poorer COF was noted for the PBO-GII sample. High COF was owing to the additive-free oil. Consequently, the high shear force on the ball area removed a level from the texture zone by abrasive effect (Sudeep Ingole, 2013). The left nano-oils (0.2 wt% Graphene, 0.2 wt% ZnO + 0.2 wt% Graphene, and 0.2 wt% ZnO + 0.4 wt% Graphene) presented more moderate COF than PBO-GII sample and reasonable enhancement in COF due to the deficiency of ZnO (Shibo Wang, 2009) and (Heba Isawi, 2016), as exhibited in Figure 4.3. Relatedly, the tribo-layer was ineffectual of bearing the load upon the metal contacts, yet, help prevent tribocontacts from severe damage in steel ball textures. Consequently, the anti-wear characteristic improved, and friction coefficient reduced considerably (K. S. Novoselov, 2004). Correspondingly, five nano-oils offered more inferior COF throughout four-ball runs in comparison with COF of additive-free oil.

4.4 Wear Scar Diameter (WSD) Behavior

4.4.1 TiO₂ (A) + Graphene WSD

The wear scar diameter (WSD) analysis was selected as one of the most relevant considerations to identify the wear action for lubricants. The wear scars have occurred owing to the sliding movement of the spindle (Mikel Aingeru Urchegui, 2008). A digital image acquisition system was employed to analyze and scale the wear scar diameter of the three fixed balls via Equation 4.2.

$$\text{WSD Mean (mm)} = \frac{\text{scar (1) diameter} + \text{scar (2) diameter} + \text{scar (3) diameter}}{3}$$

.....Equation 4.2

The lowest WSD was measured for the nanolubricant (0.4 wt% TiO₂ (A) + 0.2 wt% Graphene), as shown in Figure 4.3. The minor wear scar diameter was due to the creation of a wear-protecting tribolayer on the mating surfaces, and that was generated by the result of the coupled nanoparticles (TiO₂ (A) + Graphene) in the scar zone as evidenced via FE-SEM and EDX in Figure 4.13. Besides, metal oxide (TiO₂ Anatase) has a high specific area and better dispersion of the formulation (D. P. Macwan, 2011) which grants the TiO₂ nanoparticles to perform superior anti-friction and anti-wear characteristics (S. K. H. M. Vijayaraj, A. K. Harinarain & S. S. V. Ramakumar, 2016). Balls with a less wear scar were found to maintain greater lubricity and anti-wear qualities in respect of other oils experimented under similar machining conditions (Yitian Peng, 2007).

The nanolubricants (0.2 wt% TiO₂ (A) + 0.2 wt% Graphene) and (0.2 wt% TiO₂ (A) + 0.4 wt% Graphene) exhibited average WSD characteristics as a result of TiO₂ (A) nanoparticles insufficiency in the blend, which hindered the double nanoparticles from forming an appropriate tribofilm. Single nanolubricants (0.2 wt% TiO₂ (A)) and (0.2 wt% Graphene) incapacitated to contribute adequate reduction in metal-to-metal WSD and produced dents and furrows in the sliding direction as presented in Figure 4.11 (B) and (C).

Furthermore, the bigger WSD was identified for additive-free lubricant owing to PBO-GII lubricant failed to produce a tribofilm. The missing tribo-layer forms metal-to-metal contact. This adhesive sliding delivered abrasion of micro asperities and plastic deformation of the material. A high force of friction developed the temperature and caused severe wear (N. W. M. Zulkifli, 2014). Additionally, for PBO-GII lubricant, on

the edge of the scar, it is an apparent piece of the ball was notched when abrasion happened as exhibited in presented in Figure 4.11 (A).

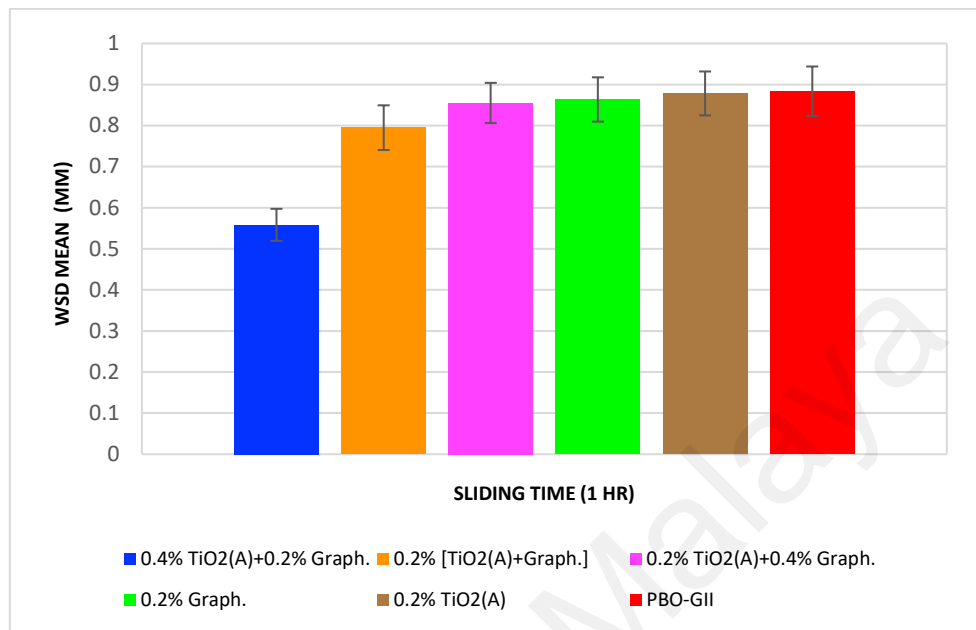


Figure 4.4: Differences in wear scar diameter mean (mm) for six sorts of lubricants

4.4.2 ZnO + Graphene WSD

The wear scar diameter (WSD) analysis is considered one of the most suitable methods of identifying the wear performance of oils (R. Sarin, 1993). In this research, wear scars developed owing to the sliding action of the spindle, as presented in Figure 4.5.

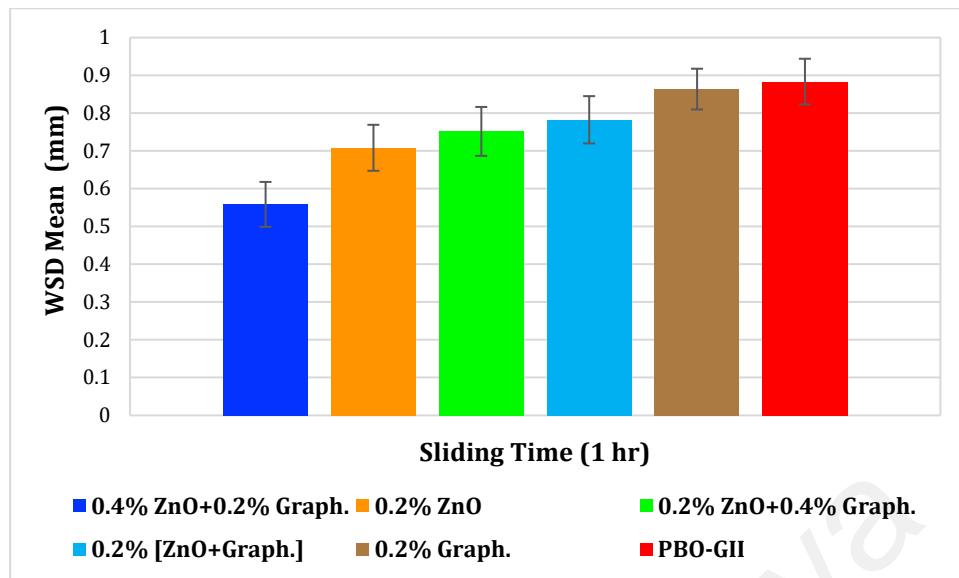


Figure 4.5: Wear scar diameter mean measurement (mm) for six different lubricants

An image retrieval device utilized to scrutinize and measure the average wear scar diameter of the constant balls applying Equation 4.2.

Under the same parameters of wear analysis such as applied load, sliding speed, time, and temperature, the most diminutive wear rates were calculated for the (0.4 wt% ZnO + 0.2 wt% Graphene) nano-oil, while the maximum values took place for PBO-GII lubricant, as displayed in Figure 4.5.

The slight wear scar diameter was induced by the generation of a wear-protective tribofilm on the sliding areas, and that was created by the impact of the nano-mixture particulates (ZnO + Graphene) in the machined surface as validated via FE-SEM Figure 4.16 (F) and EDX/EDS and elements mapping Figure 4.18.

Balls with a smaller wear defect were deemed to maintain more prominent lubrication and anti-wear qualities compared to other lubrication oils tested under equivalent criteria (Yitian Peng, 2007).

The mean WSD decrement of 36.78 % was obtained for 0.4 wt% ZnO + 0.2 wt% Graphene nano-oil. Accordingly, using 0.4 wt% ZnO + 0.2 wt% Graphene nano-oil exhibited better action by decreasing the WSD due to the metal oxide (ZnO) could notably decrease friction and wear (Xu Ran, 2016). Besides, ZnO exhibits outstanding behavior in friction reduction, wear protection, and a better film formation (B. S. B. S.M. Alves, M.F. Trajano, K.S.B. Ribeiro, E. Moura., 2013). Likewise, ZnO nanoscale particles can reduce the coefficient of friction and improve the wear lifecycle to different degrees (Hao-Jie Song, 2010).

Comparatively, 0.2 wt% ZnO nano-oil exhibited satisfying WSD. whereas the rest three nano-oils (0.2 wt% Graphene, 0.2 wt% ZnO + 0.2 wt% Graphene, and 0.2 wt% ZnO + 0.4 wt% Graphene) exhibited moderate WSD as a consequence of the lack of ZnO particulates in the above nano-oils, which hindered the blend of producing enough tribo-layer.

Nevertheless, the highest/worst WSD was remarked for the pure oil assigned to the PBO-GII sample which fails to formulate a tribofilm. The absence of a tribo-layer presents a severe sliding contact. This rigid sliding produced abrasion of micro sharpened edges and plastic deformity in the contacting areas. A prominent consequence of friction raised the temperature and made substantial wear (N. W. M. Zulkifli, 2014). Besides, on the scar right side, apparently, there is a portion of the ball was removed by scraping as displayed in Figure 4.16 (A) and Figure 4.17.

4.5 Specific Wear Rate (SWR) Behavior

4.5.1 TiO₂ (A) + Graphene SWR

The purpose behind this analysis (SWR) was to calculate wear loss along with a number of repetitions and for various mass loss to investigate the impact of the formed

nano-oils via specific wear rate on an AISI steel ball employed in four-ball tribotester (Irena Nowotyńska, 2014). Mass loss of balls was calibrated utilizing an electronic scale device precise up to 100 µg.

$$\text{Mass loss (g)} = \text{standard ball mass} - \text{scarred ball mass} \dots\dots\dots \text{Equation 4.3}$$

While the standard ball mass = 8.3369 g.

The sliding distance (L) and SWR were measured with the subsequent equations:

$$L = 2\pi \times 3.67 \times \text{RPM} \times 60/1000 \dots\dots\dots \text{Equation 4.4}$$

$$\text{SWR (m}^3\text{/N.m)} = \text{mass loss } (\Delta m) / \text{density } (\rho) / \text{load (F)} / \text{sliding distance (L)} \dots\dots\dots \text{Equation 4.5}$$

Each run was conducted three times and an average of the values was graphed. The PBO-GII lubricant delivered the largest SWR in comparison with other nano-oils. Pertinently, standard base oil caused immediate interface among AISI steel balls which performs acute abrasion and severe plastic deformation of surface as presented in Figure 4.11 (A) and Figure 4.14 (A). The right increment of nanoscale particles generated a prominent diminishing in the specific wear rate, particularly for the dual mixture of (0.4 wt% TiO₂ (A) + 0.2 wt% Graphene), as represented in Figure 4.6.

The nano-oils (0.2 wt% TiO₂ (A) + 0.4 wt% Graphene) and (0.2 wt% Graphene) revealed satisfactory SWR properties are ascribed to the existence of graphene nanoscale particles of 6.27 wt% and 04.22 wt% consecutively, on the worn path are validated by

EDS/EDX microanalysis and Raman's spectra as displayed in Table 4.1 and Figure 4.19 consecutively.

(0.2 wt% TiO₂ (A) + 0.2 wt% Graphene) and (0.2 wt% TiO₂ (A)) showed typical SWR attributed to the existence of a nano-additive in the lubricants provides a separation between mating surfaces that perform antiwear among the sliding metals surfaces (Wani, 2018). As a result, it would seem sensible presumed that nano-mixtures particulates participated in contact during the ball's sliding generated a slight tribo-layer on the mating surfaces. The tiny physical tribo-layer exhibited wear protection and friction reduction characteristics (Tiedan Chen, 2014) and (Wani, 2018) as verified by FE-SEM and EDS/EDX analyses, and Raman spectroscopy presented in Figure 4.13 and Figure 4.19 consecutively.

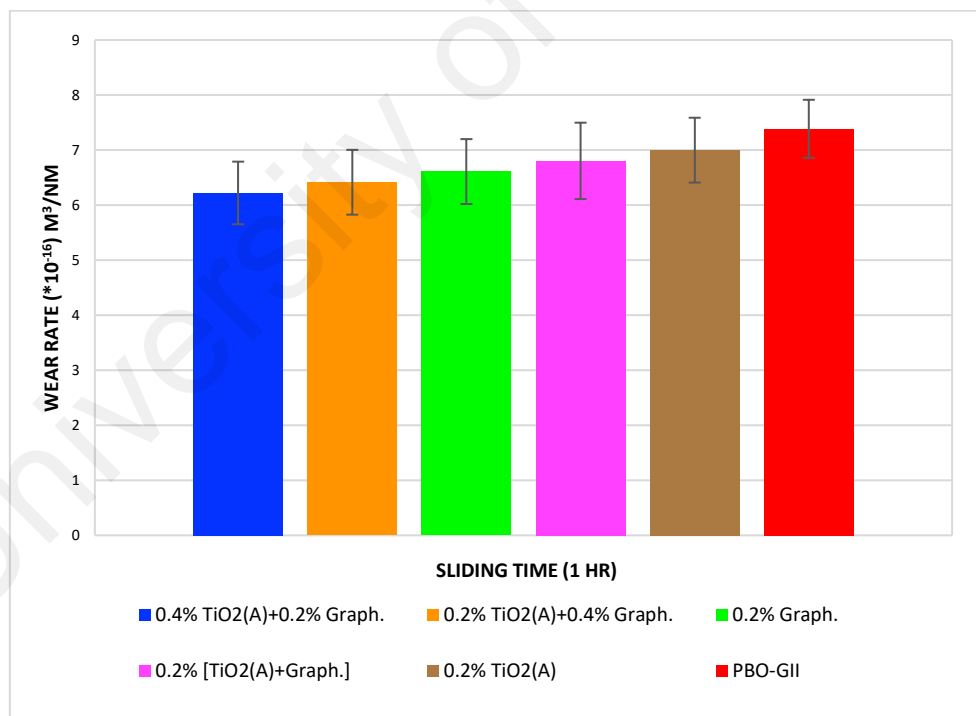


Figure 4.6: Differences in specific wear rate (*10⁻¹⁶) m³/Nm for 1-hour duration for six sorts of lubricants

4.5.2 ZnO + Graphene SWR

The purpose behind such analysis (SWR) was to find wear damage with a series of cycles and for different measurement losses to analyze the influence of the formulated lubricants through a specific wear rate on AISI balls used in four-ball equipment (Irena Nowotyńska, 2014). Balls' mass losses were weighed applying an electronic balance with precision up to 100 μg , as per Equation 4.3. At the same time, the steel ball mass is 8.3369 g.

The sliding distance (L) and SWR were calculated via Equation 4.4 and Equation 4.5. Each test was carried three times and an average of the rates was acknowledged as outlined in Figure 4.7.

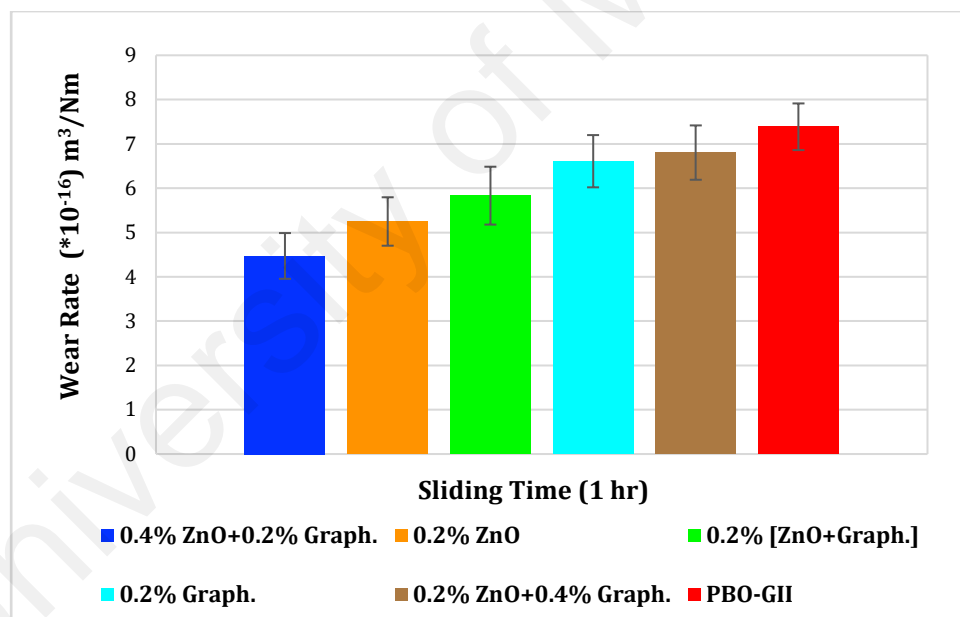


Figure 4.7: Specific wear rate ($\times 10^{-16}$) m^3/Nm measurement for six lubricants

The experiment parameters (load, temperature, time and speed) were run constantly for all tests. Furthermore, the diminished wear is essentially as a result of the formation of a wear-resistant surface coating, which creates by blended nanoscale particles on the

worn regions, therefore, lowering ball-to-ball coaction and acting as load-carrying capacities (R. G. A. Hernandez Battez, J.L. Viesca, J.E. Fernandez, J.M. D'iaz Fernandez, A. Machado, R. Chou, J. Riba., 2008).

The worst/highest SWR amongst these six samples was identified for PBO-GII. Relevantly, pure oil driven AISI balls for instantaneous metallic connection which expose acute notch and harsh plastic distortion on the ball surface is displayed in Figure 4.16 (A) and Figure 4.17. Although the best/tiniest SWR was for 0.4 wt% ZnO + 0.2 wt% Graphene nano-oil. Consequently, it can be deemed that the synergetic effect of the blend supplementing the mating steel balls formed a coated tribofilm helped in preventing the applied load at high temperature from causing wear and tear in the AISI steel ball surface.

The thinned substance tribofilm operated as abrasion-resistant and rubbing diminution characteristics (Tiedan Chen, 2014) and (Wani, 2018) as validated by EDX/EDS and elements mapping, and Raman spectra illustrated in Figure 4.18 and Figure 4.20 respectively. Besides, 0.2 wt% ZnO nano-oil acted well practically and reported reduced SWR accredited to the employment of ZnO nanoscale material of 1.13 wt% on the adhering region is recognized by FE-SEM and EDX/EDS presented in Figure 4.16 (B) and Table 4.2 consecutively.

In a similar way, the left nano-oils (0.2 wt% Graphene), (0.2 wt% ZnO + 0.2 wt% Graphene), and (0.2 wt% ZnO + 0.4 wt% Graphene) showed more favorable SWR than PBO-GII ascribed to the presence of nanoscale particles in the formulated oils offer protection in the AISI ball texture through given wear resistance of the mating metals (Wani, 2018), as illustrated in Figure 4.7.

The average enhancement in SWR was 39.47% for 0.4 wt% ZnO + 0.2 wt% Graphene nano-oil in comparison to PBO-GII sample owing to the abrasion protection

mechanism of nanoscale (ZnO and Graphene) particulates (R. G. A. Hernandez Battez, J.L. Viesca, J.E. Fernandez, J.M. D'iaz Fernandez, A. Machado, R. Chou, J. Riba., 2008) and (A.K. Rasheed, 2016).

4.6 Lubrication Mechanism

The combined lubrication impact of nano-TiO₂ anatase and graphene presented novel tribology properties (COF, μ), (WSD, mm) and (SWR, m³/Nm). The enhancements in COF, WSD, and SWR after 1-hour duration were 38.83%, 36.78%, and 15.78%, consecutively, for (0.4 wt% TiO₂ (A) + 0.2 wt% Graphene) nanolubricant as compared to PBO-GII.

Likewise, the dual lubrication influence of nano-ZnO and graphene nanoparticles showed wear and friction improving characteristics as an outstanding lubricant additive. The average reduction in COF, WSD, and SWR were 43.81%, 36.78%, and 39.47% consecutively, for (0.4 wt% ZnO + 0.2 wt% Graphene) nanolubricant in respect to pure base oil Group II.

The lubrication mechanism of (TiO₂ Anatase and Graphene) and (ZnO and Graphene) nanomaterials involves particle flow pattern effect as per Figure 4.8 and Figure 4.9. The driving force for nanomaterials in base oil entering the contacting surfaces throughout three mechanisms:

- A. The micro rolling bearing procedure,
- B. depositing film method, and
- C. mending effect technique (Hongxing Wu, 2017) and see Table 2.8.

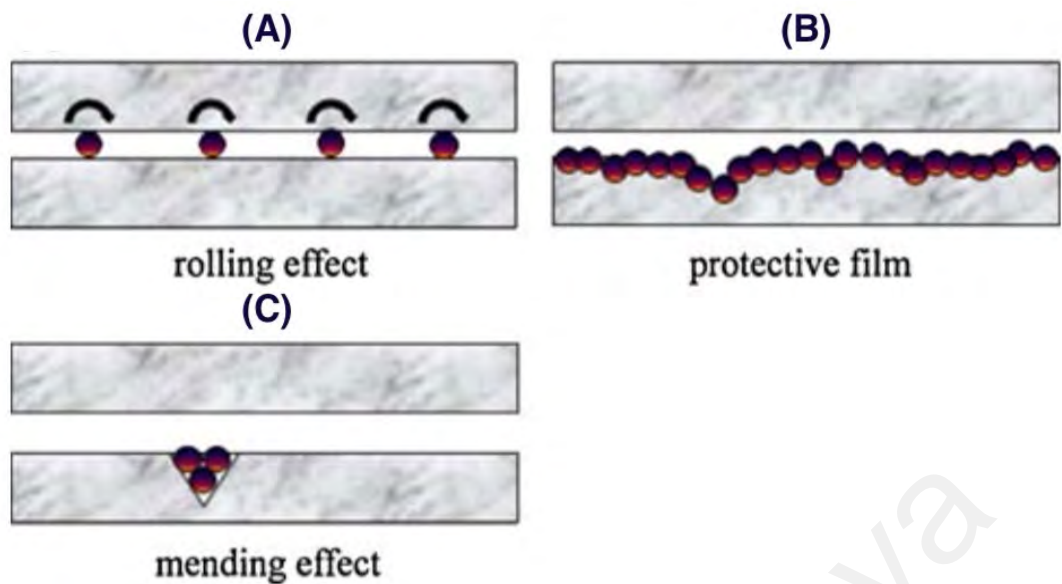


Figure 4.8: Mechanism and role of dual nanoparticles during nano-lubrication

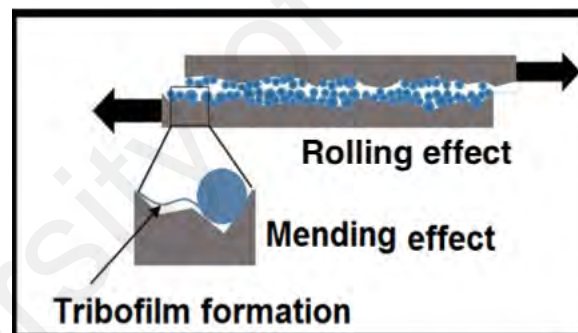


Figure 4.9: Schematic diagram of lubrication mechanisms for synergetic nanoparticles

Aggregation of nanoparticles happened in several samples specifically (0.4 wt% TiO_2 (A) and 0.2 wt% graphene), it entered the contact area and formed well-distributed (TiO_2 (A) + Graphene) tribofilm (Figure 4.10) reduces friction and wear (M. Laad, & Jatti, V. K. S., 2016; Varrla Eswaraiah, 2011).

Similarly, deposition of nanoparticles took place in many cases particularly (0.2 wt% ZnO + 0.4 wt% Graphene) and (0.4 wt% ZnO + 0.2 wt% Graphene), it is going in the mating region and created homogenized (ZnO + Graphene) tribofilm (Figure 4.10) diminishes friction and wear (R. G. A. Hernandez Battez, J.L. Viesca, J.E. Fernandez, J.M. D'iaz Fernandez, A. Machado, R. Chou, J. Riba, 2008; Varrla Eswaraiah, 2011).

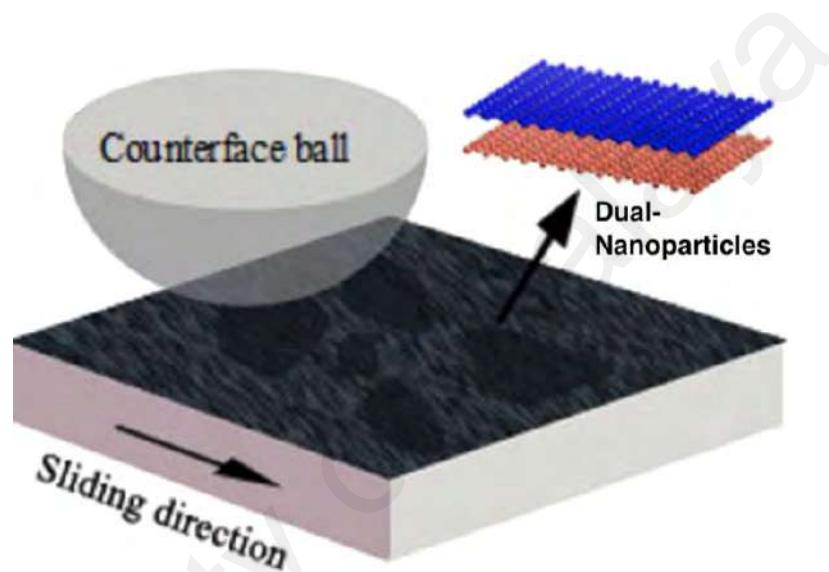


Figure 4.10: Nanoparticles entered the interacting surfaces and formed well-distributed tribofilm overcomes friction and wear

The formulation of dual nanoparticles (TiO₂ A + Graphene) and (ZnO + Graphene) and base oil with oleic acid surfactant and the sonication treatment led to the creation of the tribofilm. So, it is not pure solid lubrication. It is a mixture of solid lubrication and fluid lubrication under boundary conditions.

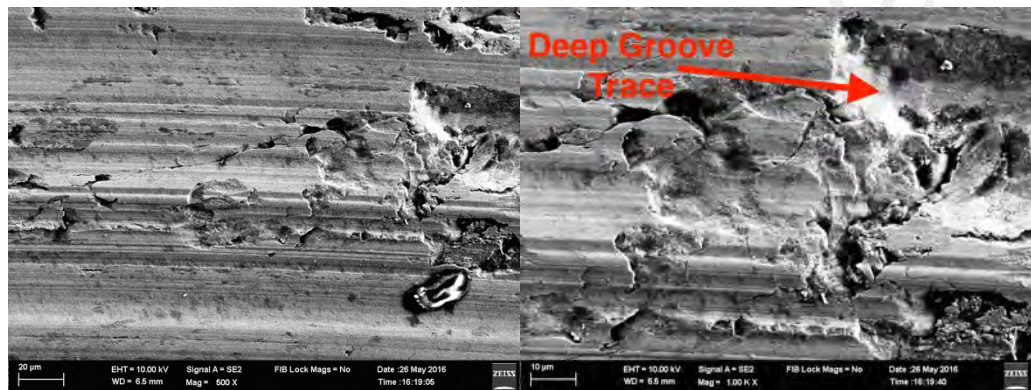
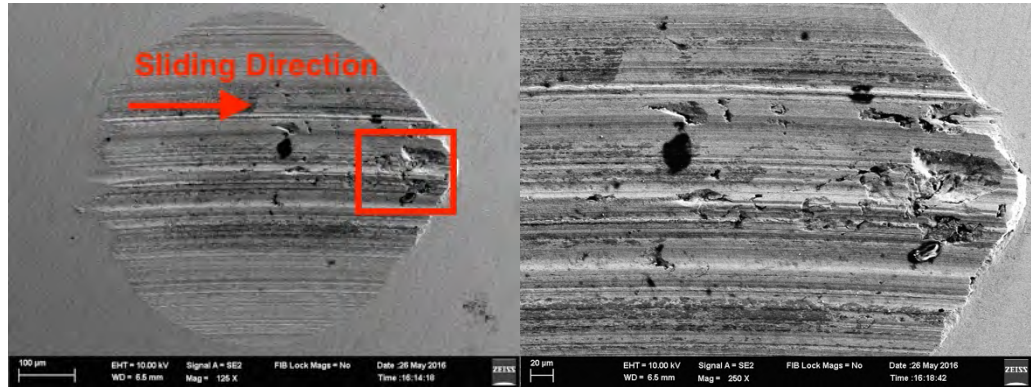
4.7 Metallographic Characterization

4.7.1 FE-SEM Characterization for TiO₂ (A) + Graphene

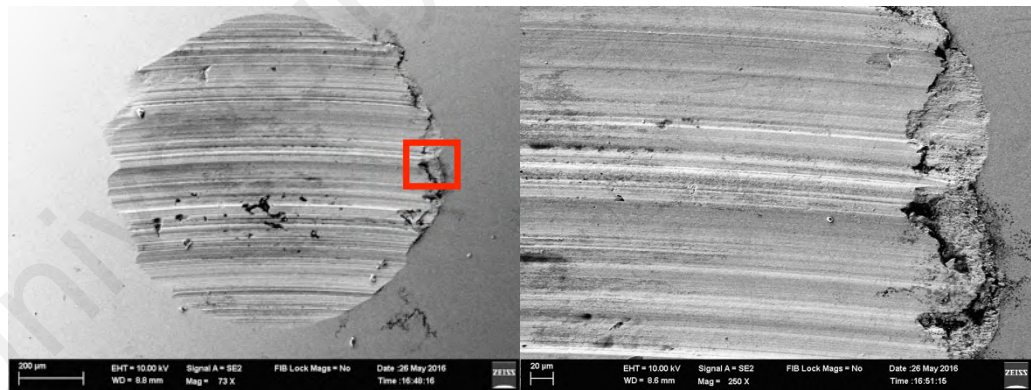
The balls immersed in PBO-GII exhibited an extremely fluted portion separated from the exterior surface as a result of friction action and adhering wear (N.K. Myshkin, 2005). Furthermore, the removed edge was sharply notched and experienced periodical of layers detaching that produced wide fragments (Jien-Min Wu, 2006), as presented in Figure 4.11 (A). Concurrently, the AISI balls submerged in the nano-blend showed smallest scuff signs, shallow mark lines, white trace stripes, and seldom notch or scratch at the worn region boundaries, as represented in Figure 4.11 (B), (C), (D) and (E). These shapes were seen on the scratched areas of the AISI balls after intense stress and fast speed frictional contact. Some scarred regions were scratched and experienced periodic abrasion which produced lots of debris (Jien-Min Wu, 2006), as shown in Figure 4.11.

Moreover, the steel balls immersed with (0.4 wt% TiO₂ (A) + 0.2 wt% Graphene) demonstrated lowest adhering wear and no surface damaging as a consequence of the outstanding nano-oil (A. E. Jiménez, 2010). It generated a tribo-layer (Figure 4.13) among the rubbing balls (C. Zhao, 2014) and triggered nanoscale particles to settle on the abraded sliding balls (Chuanli Zhao, 2013), which diminished the intense rubbing and decreased the severe abrasion apart from individual PBO-GII oil. Delicate agglomerations also developed throughout the aggregation procedure by nanoscale particles centrifugation (B. S. B. S.M. Alves, M.F. Trajano, K.S.B. Ribeiro, E. Moura., 2013). The FE-SEM illustrations exhibit the existence of miniature pieces resembled rhomboids on the worn region, as per Figure 4.11 (D). Identifying texture morphology is necessary for characterizing and explaining the tribological attitude of solids in contacts. As a result, FE-SEM utilized to analyze the steel balls with six sorts of blending oils.

A. PBO-GII

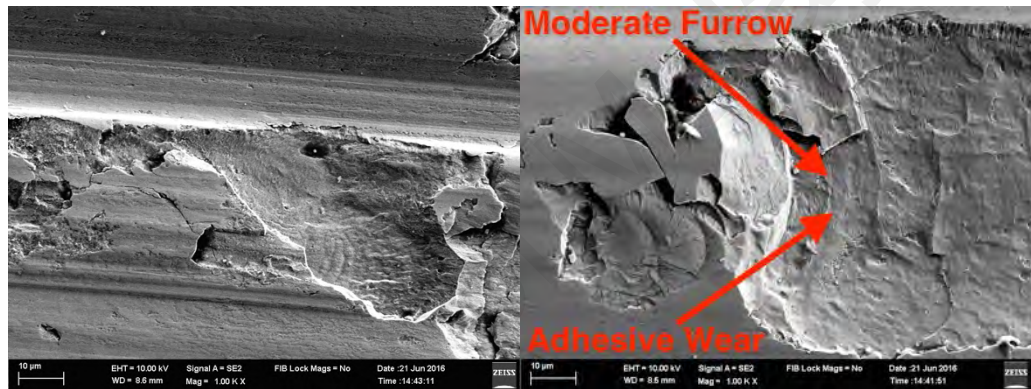
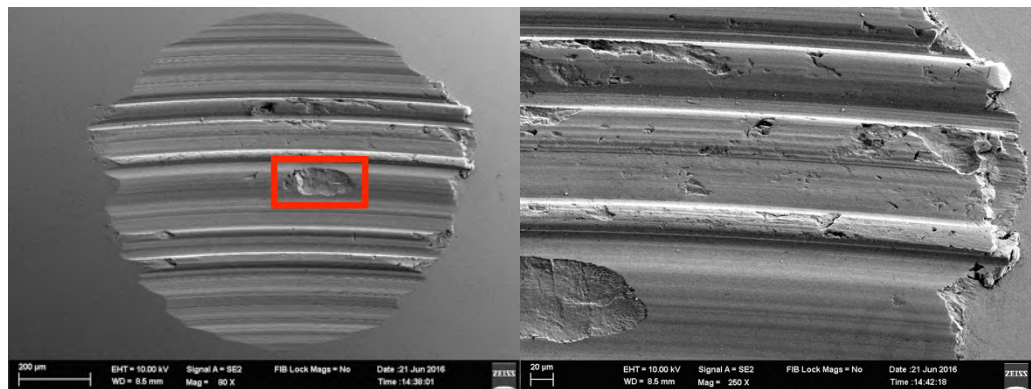


B. 0.2 wt% TiO₂ (A)

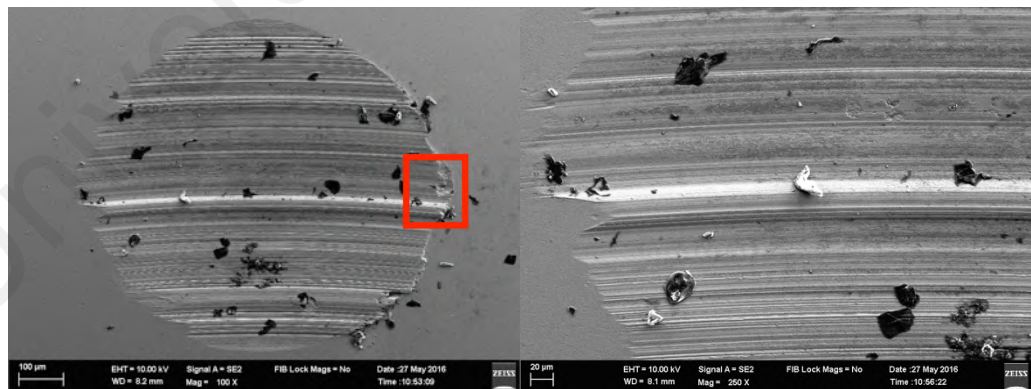


'Figure 4.11: continued'

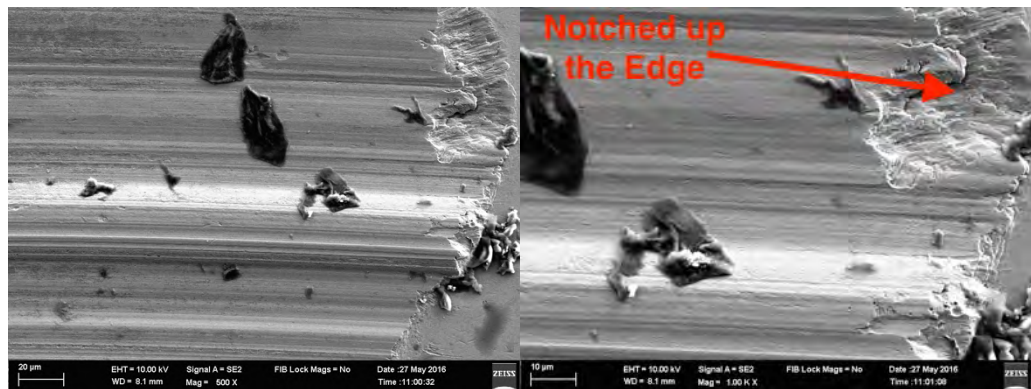
C. 0.2 wt% Graphene



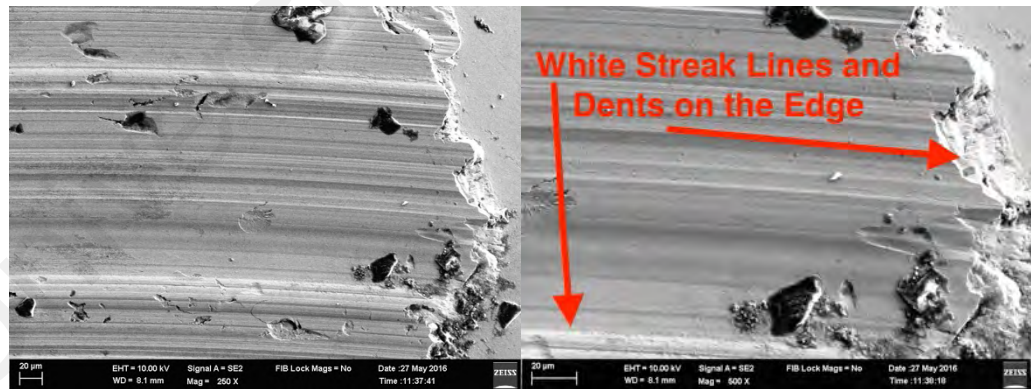
D. 0.2 wt% TiO₂ (A) + 0.2 wt% Graphene



'Figure 4.11: continued'



E. 0.2 wt% TiO₂ (A) + 0.4 wt% Graphene



'Figure 4.11: continued'

F. 0.4 wt% TiO₂ (A) + 0.2 wt% Graphene

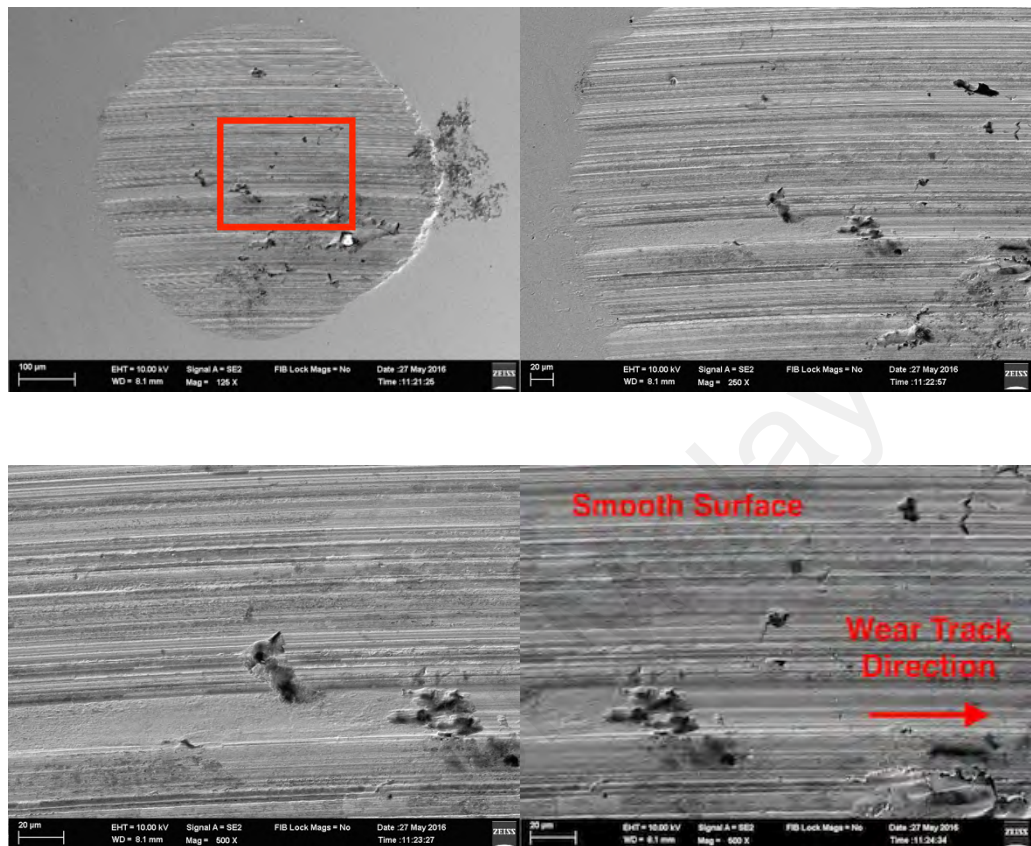


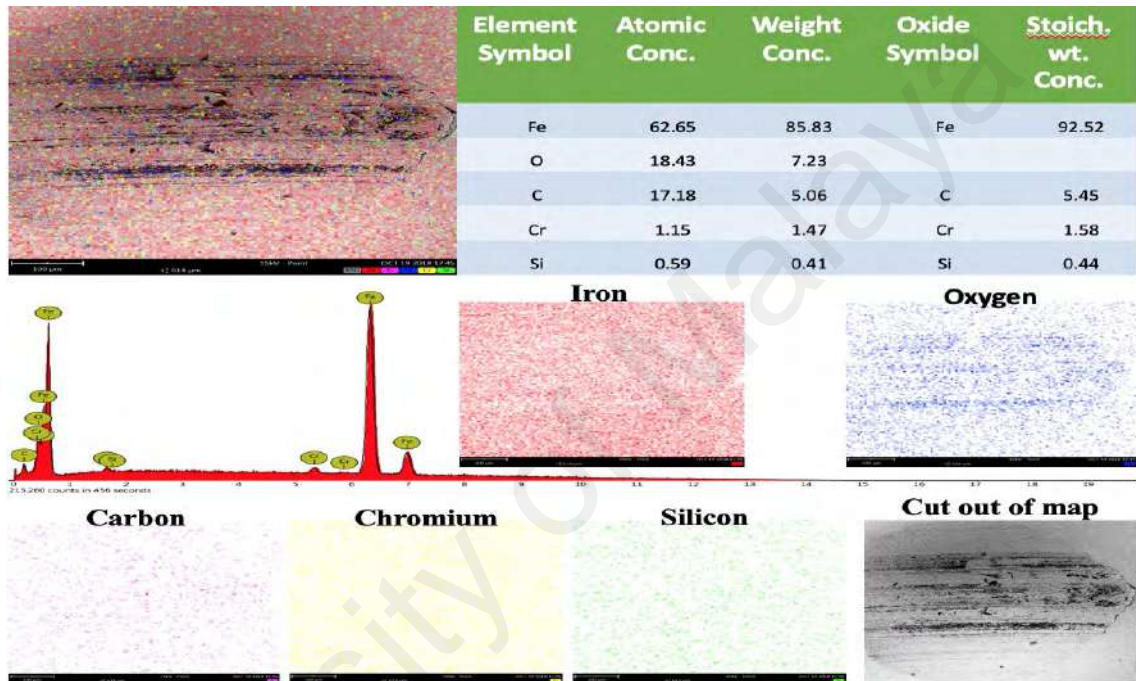
Figure 4.11: FE-SEM micrographs of the surface morphology of AISI balls treated with six sorts of lubricants

4.7.2 EDX/EDS and Elements Mapping for TiO₂ (A) + Graphene

EDX/EDS spectroscopy exhibited fundamental substances at the engaging surfaces and the ball surface remaining when simple lubricant or formulated lubricant was operated. An element map is an illustration displaying the spatial dispersion of particles in a specimen. Since it is obtained from a scarred section, it is a 2D image within the specimen. Constituent images are greatly beneficial for presenting element concentrations in textural form, especially for proving formulation presence. It was remarked that many

chemical particles settled on the zone of application for each sample, as analyzed in Figure 4.12 and Table 4.1.

A. Element Symbols, Atomic Concentrations, Weight Concentrations, Stoich Weight Concentrations, Spectrum, and Elements Mapping for the ball treated with PBO-GII Lubricant



B. Element Symbols, Atomic Concentrations, Weight Concentrations, Stoich Weight Concentrations, Spectrum, and Elements Mapping for the ball treated with (0.4 wt% TiO₂ (A) + 0.2 wt% Graphene) Nanolubricant

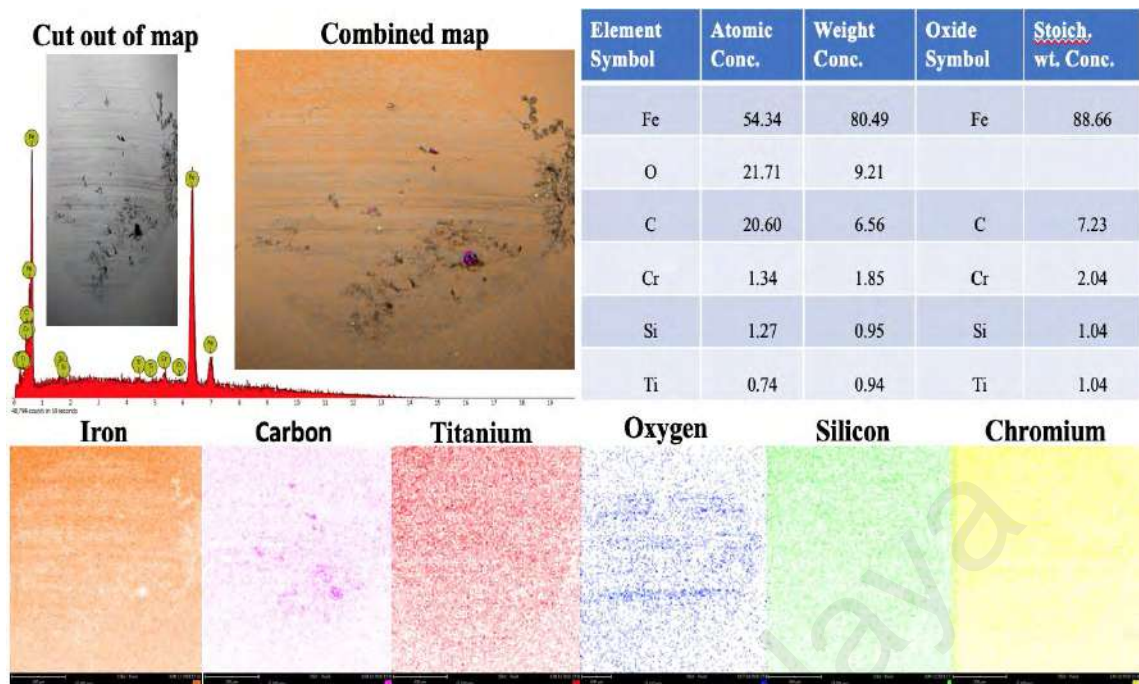


Figure 4.12: EDX/EDS, elements mappings, and spectrums of steel balls treated with (A) plain lubricant and (B) dual nanoparticles lubricant

Table 4.1: Observed element weight percentages via EDX/EDS analysis for six different lubricants

Sample No.	Lubricant Type	Fe wt%	C wt%	Ti wt%	O wt%	Si wt%	Cr wt%
5.	PBO-GII	85.83	5.06	0.0	7.23	0.41	1.47
6.	0.2 wt% TiO ₂ (A)	77.57	8.71	0.79	11.18	0.0	1.74
7.	0.2 wt% Graphene	92.96	04.22	0.0	02.82	0.0	0.0
8.	0.2 wt% [TiO ₂ (A) + Graphene]	84.42	05.94	02.59	04.02	0.0	03.02

9.	0.2 wt% TiO ₂ (A) + 0.4 wt% Graphene	81.09	6.27	1.41	8.87	0.0	2.35
10.	0.4 wt% TiO ₂ (A) + 0.2 wt% Graphene	80.49	6.56	0.94	9.21	0.95	1.85

The chemical state of the initial and machined balls stated no direct variations (Hongxuan Li, 2006). EDX/EDS chemical spectroscopic affirmed the disposition of tribo-coating consists of nanoscale particles (Juozas Padgurskas, 2013), as presented at Figure 4.12 (B) and Figure 4.13.

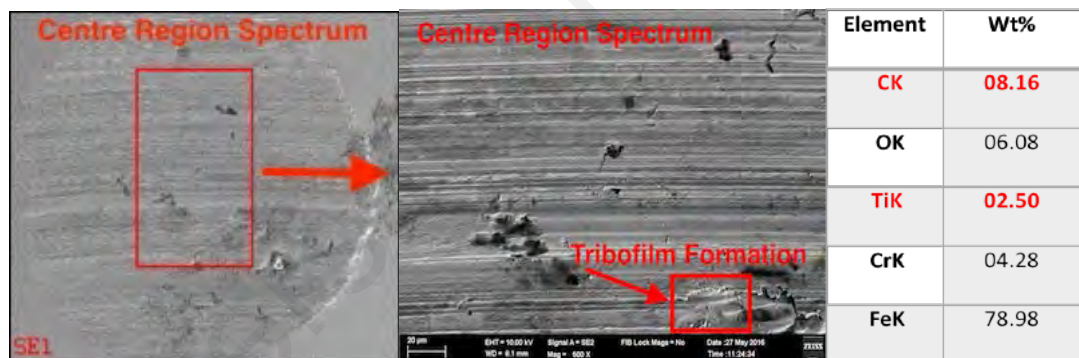
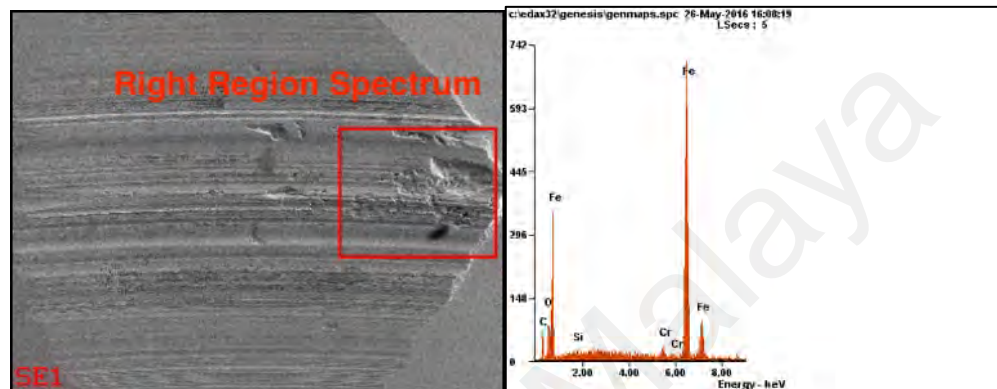


Figure 4.13: FE-SEM and EDX demonstrate the formation of a protective film on the scar region of ball treated with (0.4 wt% TiO₂ (A) + 0.2 wt% Graphene) nanolubricant

This fact indicates the result of uniform nanoscale particle spreading on enhanced wear-resistant surface (H. M. M. Gulzar, M Varman, MA Kalam, R.A. Mufti, NWM Zulkifli, R. Yunus, Rehan Zahid, 2015). Subsequently, there were no existing for titanium nanoscale particles on the machined regions of AISI balls engulfed in PBO-GII. Therefore, it was clear enough that the mating surfaces gained acute grooving, as a result,

of the lack of nano-additives, as illustrated in Figure 4.14 (A). Nevertheless, the AISI balls employed with nano-oil (0.4 wt% TiO₂ (A) + 0.2 wt% Graphene) revealed minimum wear trace owing to the role of titanium and carbon/graphene nanoscale particulates that were distinguished in EDX/EDS spectrum as depicted in Figure 4.14 (B).

A. Additive-Free Lubricant (PBO-GII)



B. Synergetic Lubricant (0.4 wt% TiO₂ (A) + 0.2 wt% Graphene)

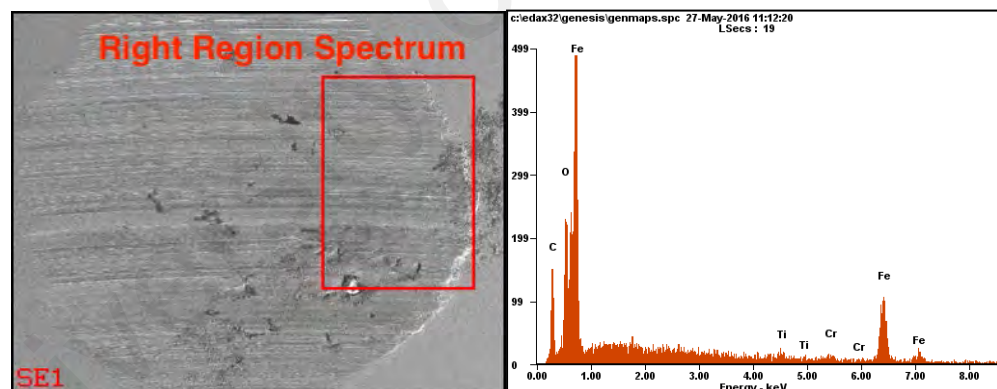


Figure 4.14: EDX of the surface morphology of AISI balls treated with (A) pure base oil Group II and (B) dual nanoparticles lubricant

Furthermore, the components' topography (elements mapping spectroscopy) revealed the atomic, weight, and stoich weight concentrations of titanium and carbon/graphene particles on the worn path, as per Figure 4.15. The structure of these agglomerated particles confirms the smooth sides and sphere shapes of the machined balls.

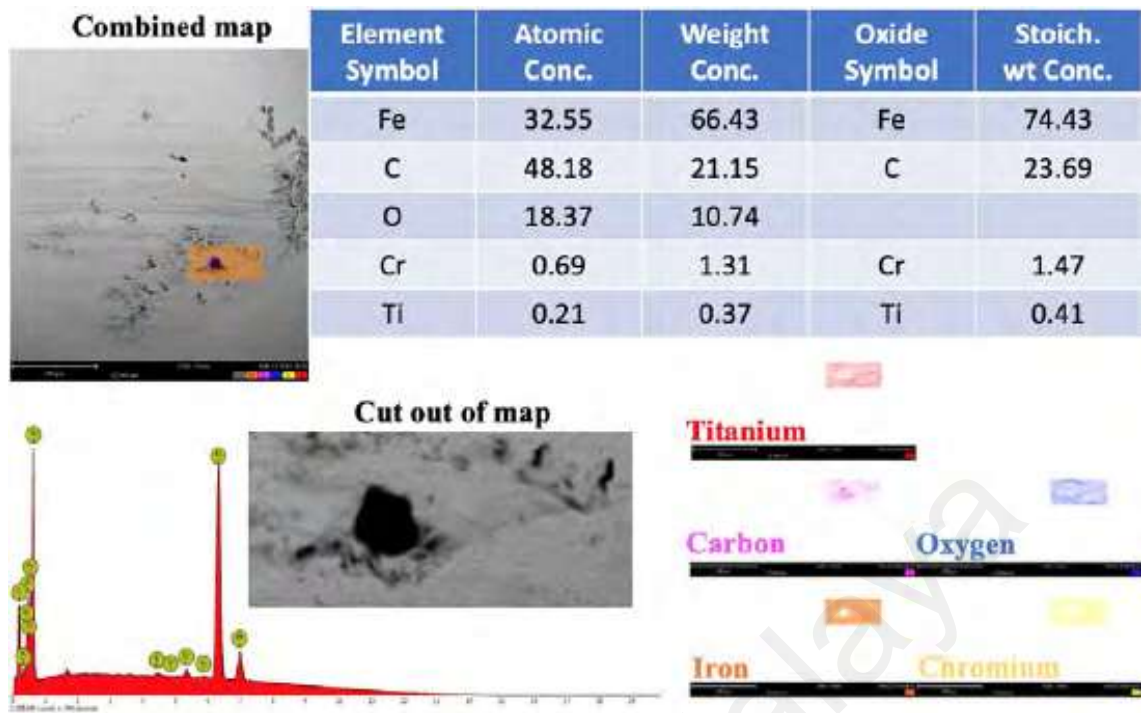
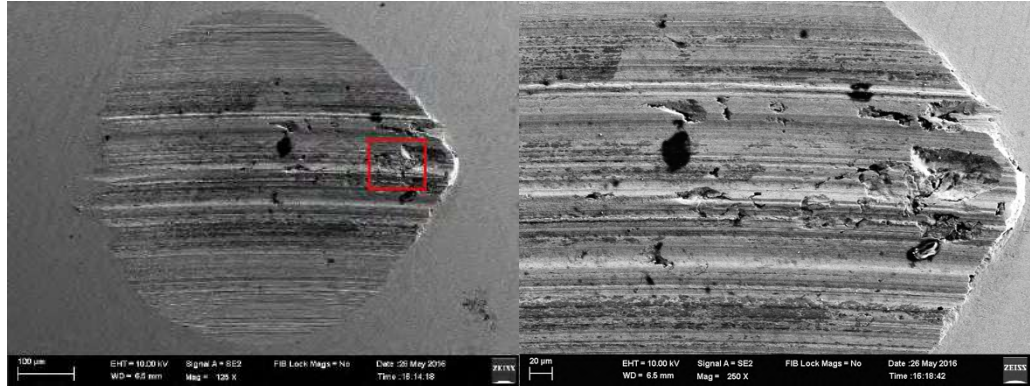


Figure 4.15: Elements mapping confirm the deposition of titanium and graphene on the sliding surface of synergetic lubricant (0.4 wt% TiO₂ (A) + 0.2 wt% Graphene)

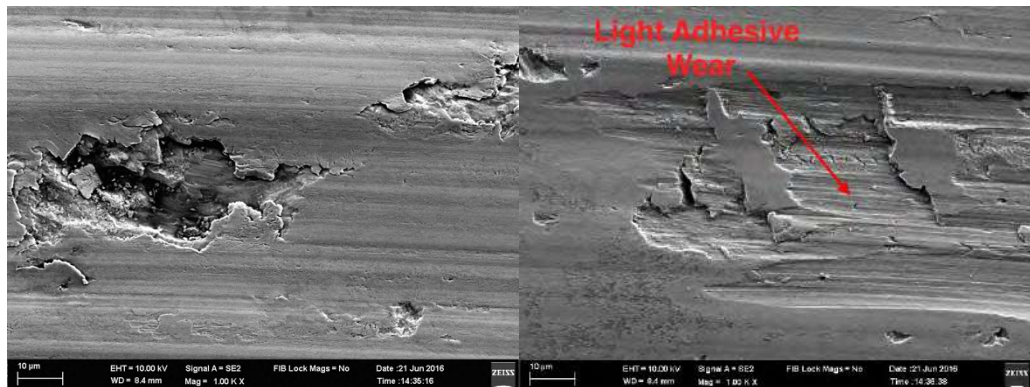
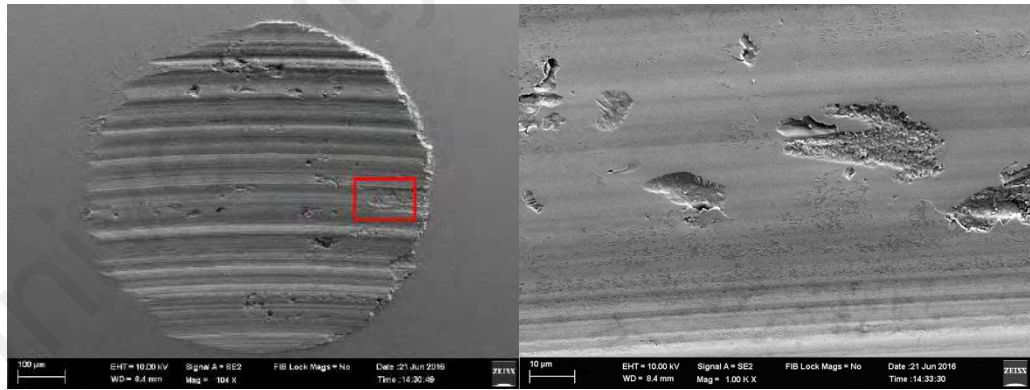
4.7.3 FE-SEM Characterization for ZnO + Graphene

Characterizing the scar texture is essential for understanding and distinguishing the protection and abrasion behavior of metals in contact. Whereby, FE-SEM was employed to examine the steel balls with six samples of prepared lubricants. The wear defects were enlarged multiple times to investigate the texture damage that occurred on those marked scars for different structures that may be observed. FE-SEM spectroscopic carried out after tribological experiments as illustrated in Figure 4.16.

A. PBO-GII

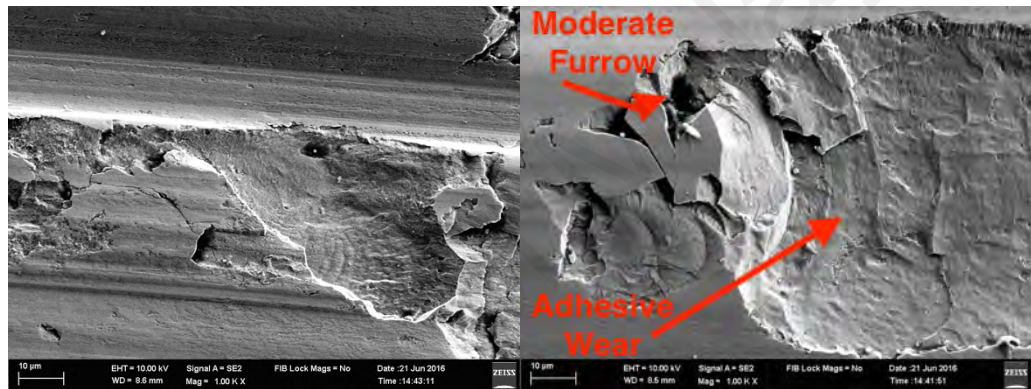
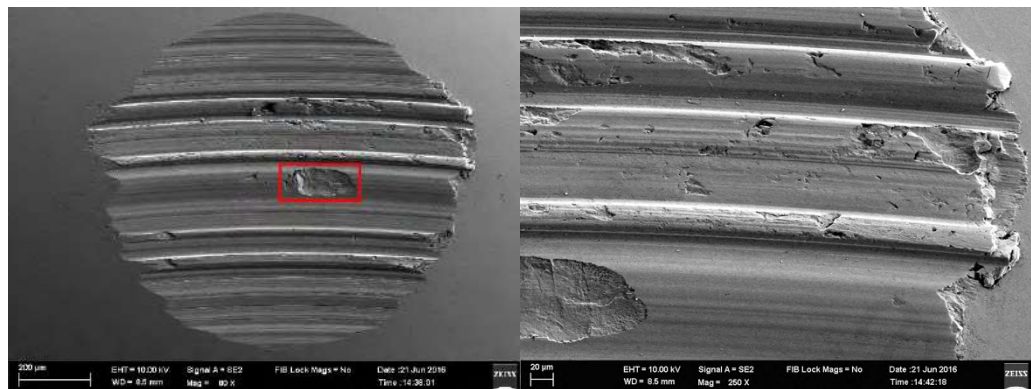


B. 0.2 wt% ZnO

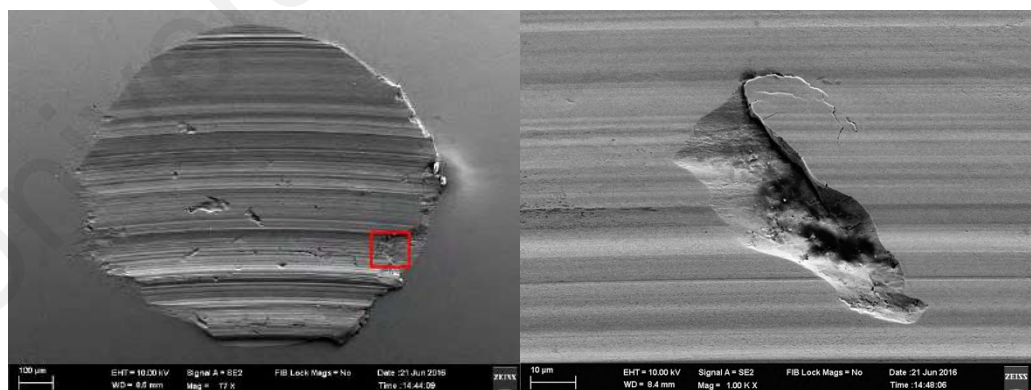


'Figure 4.16: continued'

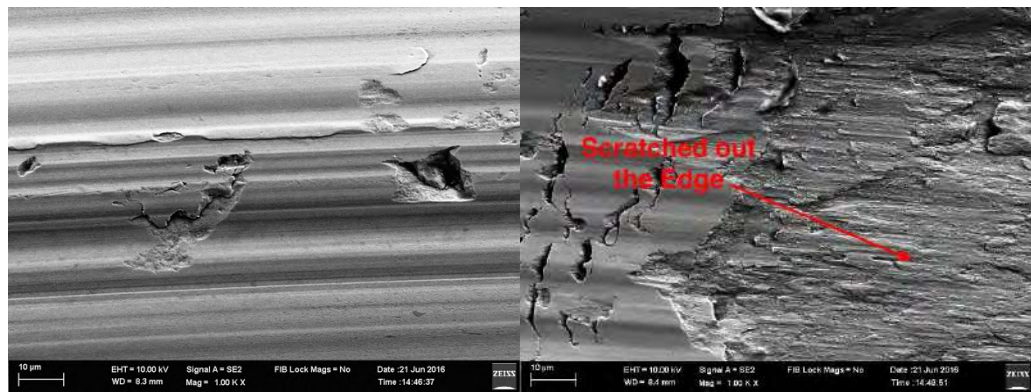
C. 0.2 wt% Graphene



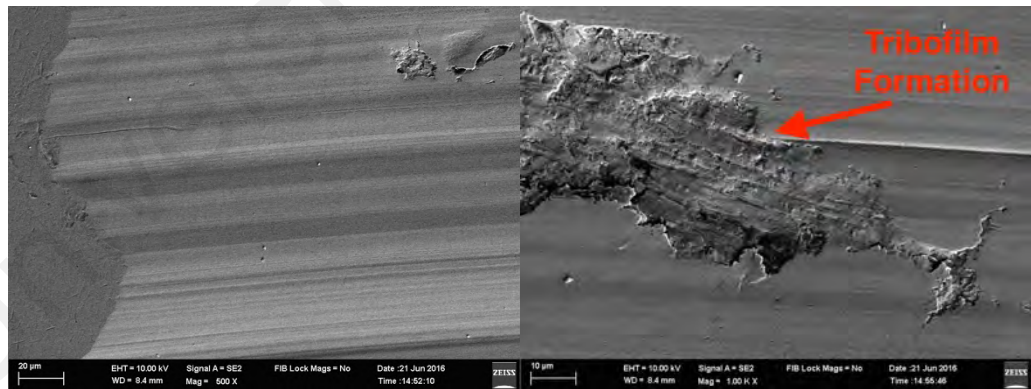
D. 0.2 wt% ZnO + 0.2 wt% Graphene



'Figure 4.16: continued'



E. 0.2 wt% ZnO + 0.4 wt% Graphene



'Figure 4.16: continued'

F. 0.4 wt% ZnO + 0.2 wt% Graphene

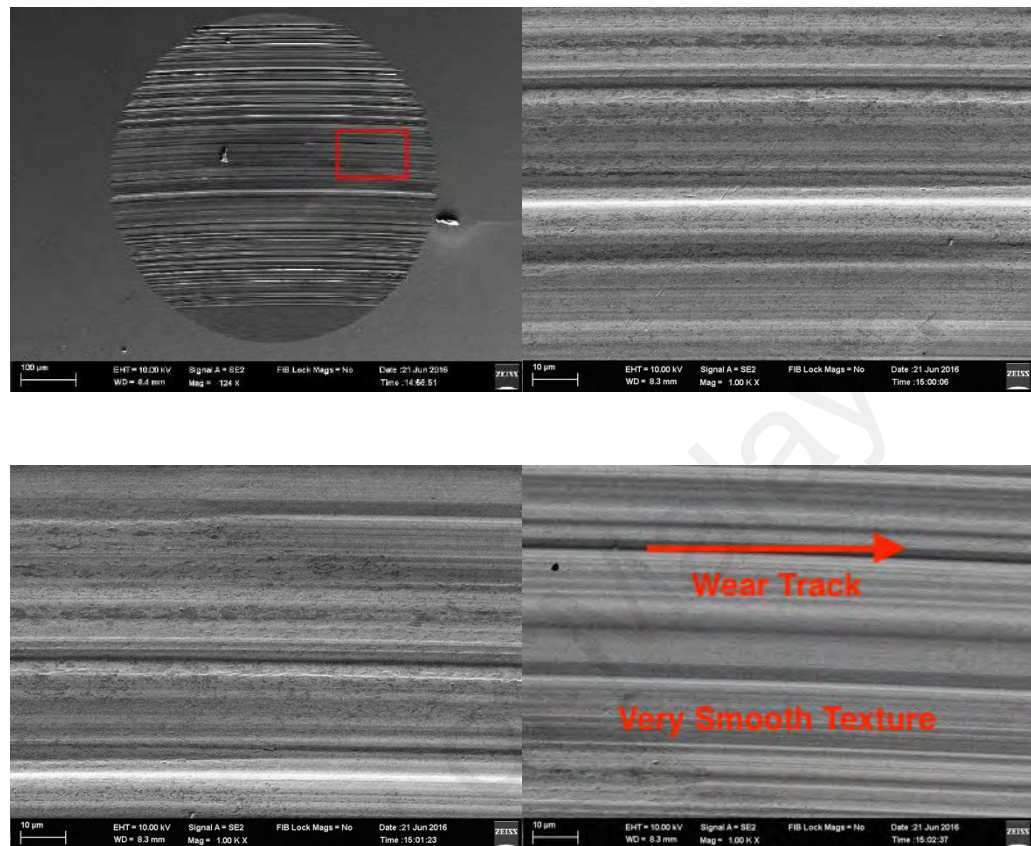


Figure 4.16: Field Emission Scanning Electron Microscopy (FE-SEM) of surface topography of AISI balls employed with six types of oils (A) PBO-GII, (B) 0.2 wt% ZnO, (C) 0.2 wt% Graphene, (D) 0.2 wt% ZnO + 0.2 wt% Graphene, (E) 0.2 wt% ZnO + 0.4 wt% Graphene, and (F) 0.4 wt% ZnO + 0.2 wt% Graphene

An intense crack mark appeared on the scar generated from severe metal-to-metal rubbing and micro-abrasion defect when PBO-GII oil was employed (N.K. Myshkin, 2005). Additionally, the scarred region was intensely indented and undergone cyclic abrasion which delivered plenty of debris (Jien-Min Wu, 2006), as illustrated in Figure 4.16 (A). Besides, slight to mild adhesive wear, such as dents and marks are displayed in Figure 4.16 (B), (C), and (D). Therefore, the shortage of (ZnO and Graphene) nano particulates in the three nano-oils, that restricted the nanometer-sized suspensions of

forming mixture enriched layer. On the other hand, (0.2 wt% ZnO + 0.4 wt% Graphene) nano-oil performed flat texture topography by reason of the coalescence layer of nanoparticle through Figure 4.16 (E). Consequently, nanometer-sized will separate metals in contact by generating a tribo-boundary layer and thus enhance the wear-resistance ability (Siti Safiyah Nor Azman, 2016). Likewise, a smooth texture was demonstrated when (0.4 wt% ZnO + 0.2 wt% Graphene) nano-oil suspension was employed, as outlined in Figure 4.15 (F). Rolling, nano bearing, and deposition mechanisms (R. G. A. Hernandez Battez, J.L. Viesca, J.E. Fernandez, J.M. D'iaz Fernandez, A. Machado, R. Chou, J. Riba, 2008; F. A. Essa, 2017; B. S. B. S.M. Alves, M.F. Trajano, K.S.B. Ribeiro, E. Moura., 2013; Siti Safiyah Nor Azman, 2016; Varrla Eswaraiah, 2011) of nanoscale particles transpired in the case of (0.4 wt% ZnO + 0.2 wt% graphene), nano-suspended engaged with mating metals and produced well-organized (ZnO + Graphene) slim coating as through Figure 4.18, diminishes rubbing action and adhesive wear as presented in Figure 4.2, Figure 4.4, and Figure 4.6.

4.7.4 EDX/EDS and Elements Mapping for ZnO + Graphene

To study the elemental components and mapping of six samples, microanalyses of chemical compounds using EDX/EDS and elements mapping were employed. The element symbol, atomic concentration, weight concentration, stoich weight concentration, spectrums, and elements mapping for the ball treated with PBO-GII lubricant as per Figure 4.17, and for the ball treated with (0.4 wt% ZnO + 0.2 wt% Graphene) nanolubricant as per Figure 4.18. The element weight concentrations for the described scars are listed in Table 4.2 for the balls treated with six types of lubricants.

Table 4.2: Element weight percentages deducted via EDX analysis for six different lubricants.

Sample Type	<i>Fe</i> Wt%	<i>C</i> Wt%	<i>Zn</i> Wt%	<i>O</i> Wt%	<i>Si</i> Wt%	<i>Cr</i> Wt%	<i>Mn</i> Wt%	<i>Ni</i> Wt%	<i>S</i> Wt%	<i>P</i> Wt%
PBO-GII	85.83	5.06	0.0	7.23	0.41	1.47	0.0	0.0	0.0	0.0
0.2 wt% ZnO	87.23	7.56	1.13	0.0	0.39	1.81	0.77	0.88	0.13	0.10
0.2 wt% Graphene	92.96	04.22	0.0	02.82	0.0	0.0	0.0	0.0	0.0	0.0
0.2 wt% ZnO + 0.2 wt% Graphene	86.85	7.33	3.29	02.50	0.39	1.49	0.54	0.0	0.11	0.0
0.2 wt% ZnO + 0.4 wt% Graphene	94.09	1.19	2.65	02.32	0.28	1.81	0.0	0.0	0.0	0.0
0.4 wt% ZnO + 0.2 wt% Graphene	87.74	8.37	1.62	01.90	0.47	1.81	0.0	0.0	0.0	0.0

The texture defect was more prominent owing to additive-free oil as presented in Figure 4.17, where intense micro-abrasion crack is can be noticed at the right side of the scar region, while delaminating wear occurred at scar's center area (Siti Safiyah Nor Azman, 2016). It is apparent that ZnO nanoscale particles do not exist in the damaged

region when simple base oil employed. Consequently, the sliding balls got broad scratches due to the lack of nano-additives. It can be seen manganese and sulfur elements detected in the 0.2 wt% ZnO + 0.2 wt% graphene sample, which belongs to the constituents of the chrome steel ball.

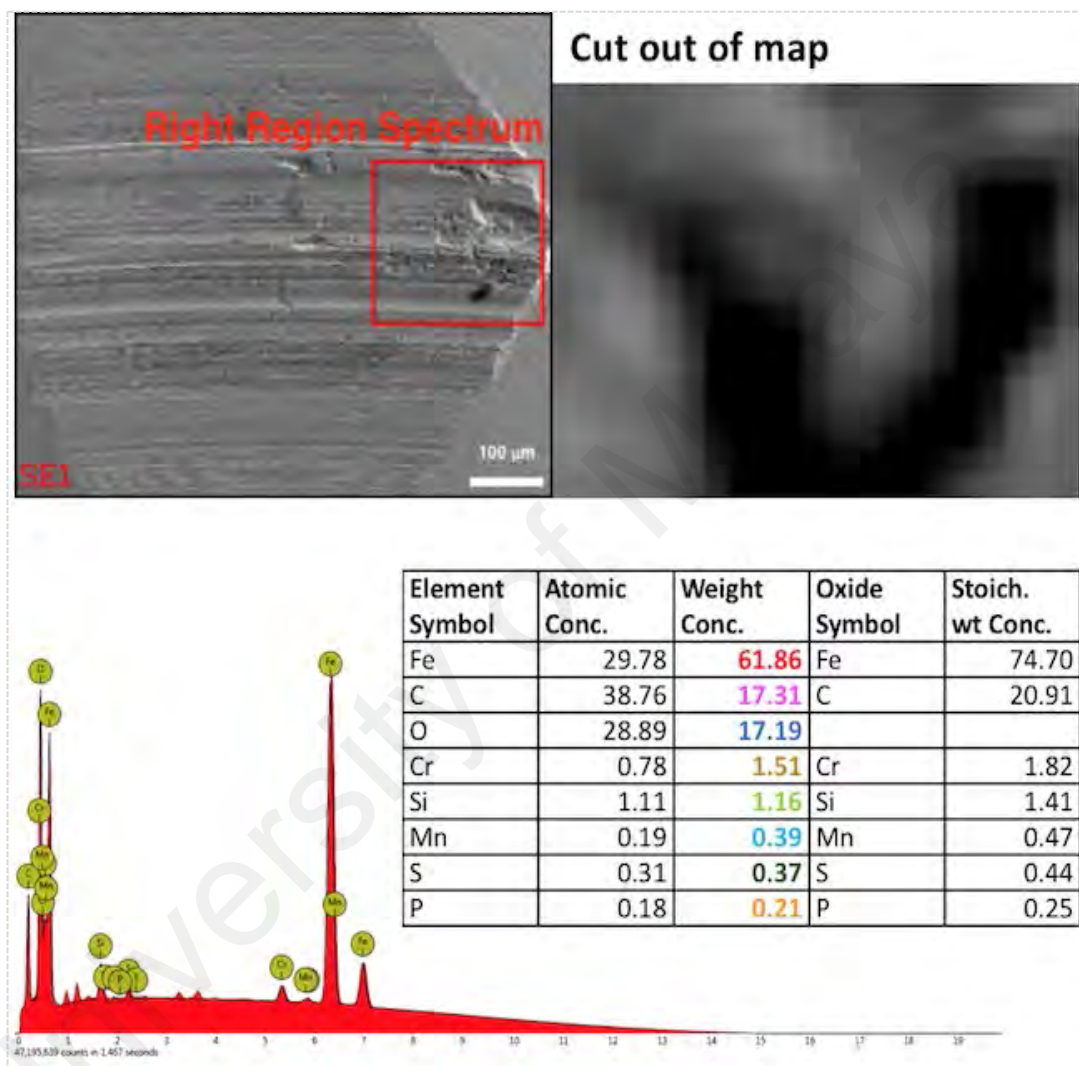


Figure 4.17: Energy Dispersive X-Ray Spectroscopy (EDX/EDS) for PBO-GII oil presenting the ball combinations without nanoscale particles detection

On the other hand, steel balls engulfed with (0.4 wt% ZnO + 0.2 wt% Graphene) nano-oil reported smooth and even texture by reason of the presence of ZnO and graphene nanoscale particles which detected via EDX/EDS and spatial distribution of elements Figure 4.18.

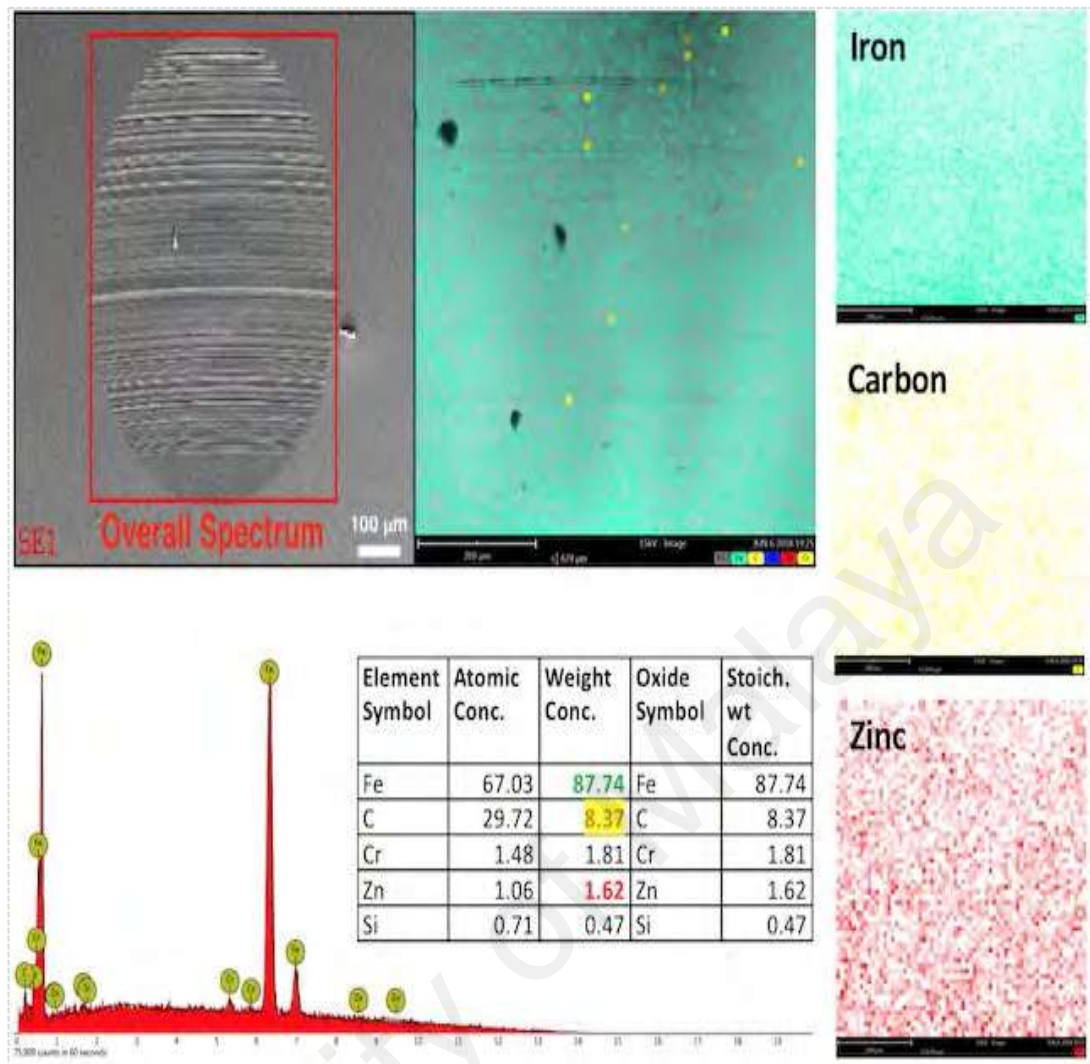


Figure 4.18: EDX/EDS and elements mapping identifying Zinc and Carbon (Graphene) elements on the steel ball's scar employed with (0.4 wt% ZnO + 0.2 wt% Graphene) nano-oil

EDX/EDS chemical identification and element map validated the formulation of a tribo-boundary film compounded of very fine particles (Juožas Padgurskas, 2013). This feature points out the consequence of consistent nanoparticle distribution on enhancing the micro-abrasion protection (H. M. M. Gulzar, M Varman, MA Kalam, R.A. Mufti, NWM Zulkifli, R. Yunus, Rehan Zahid, 2015). The investigations demonstrated the perfect combination of ZnO and graphene particles on the zone of application, as per Figure 4.18. The mentioned results are in compliance with Raman spectra which presented an obvious ZnO and graphene peaks. In addition, the defected regions were

little for ZnO nano-oils, and there were no micro-cracks marks on the ball surface, as displayed in Figure 4.16 (B), (D), (E), and (F). The nanometer-sized particles, consequently, enabled the AISI balls to possess protection against adhesive wear (R. G. A. Hernandez Battez, J.L. Viesca, J.E. Fernandez, J.M. D'iaz Fernandez, A. Machado, R. Chou, J. Riba., 2008).

4.8 Raman Spectra

4.8.1 Raman Spectroscopy for TiO₂ (A) + Graphene

Raman analysis is an essential spectroscopic device was applied to further examine the existence of the TiO₂ anatase, and graphene in five nano-oils (except the additive-free lubricant), as presented in Figure 4.19. Raman spectroscopy was implemented for the spectrum scale of 100 cm⁻¹ to 3200 cm⁻¹ and subjected to argon-ion laser application at (532 nm). The peaks displayed TiO₂ anatase vibrational groups at 144, 383-397, and 511-512 cm⁻¹ matching with Raman modes of E_g, B_{1g}, and A_{1g} or B_{1g} consecutively, (Sudeep Ingole, 2013), (Venkata Ramana Posa, 2016), and (Dae-Hyun Cho, 2015). The spectrum revealed three signals for powerful groups resembling the G, D, and 2D in the spectra field approximately 1600 cm⁻¹ (G band) and 1350 cm⁻¹ (D band), and 2700 cm⁻¹ (2D band), which are a standard feature of graphene (Venkata Ramana Posa, 2016), (Zengshi Xu, 2015) and (Wani, 2018). The collected Raman shifts and equivalent modes are noted in Table 4.3.

Table 4.3: Raman shifts of the TiO₂ Anatase groups associated with Raman modes

Raman Shift (cm ⁻¹)	Mode
144	E _g
383, 387, 395, 397	B _{1g} (1)
511, 512	A _{1g} / B _{1g} (2)

Micro-Raman spectroscopic analysis was conducted to further examine the tribo-boundary film formation over the scar surfaces. Mixture enriched layers and adjacent-surface particles direct the tribological performances of the interaction surfaces. The TiO₂ anatase- and graphene-enhanced nano-oils generated coalescence layer, thus helping in reducing wear of sliding balls (H. M. M. Gulzar, M Varman, MA Kalam, R.A. Mufti, NWM Zulkifli, R. Yunus, Rehan Zahid, 2015).

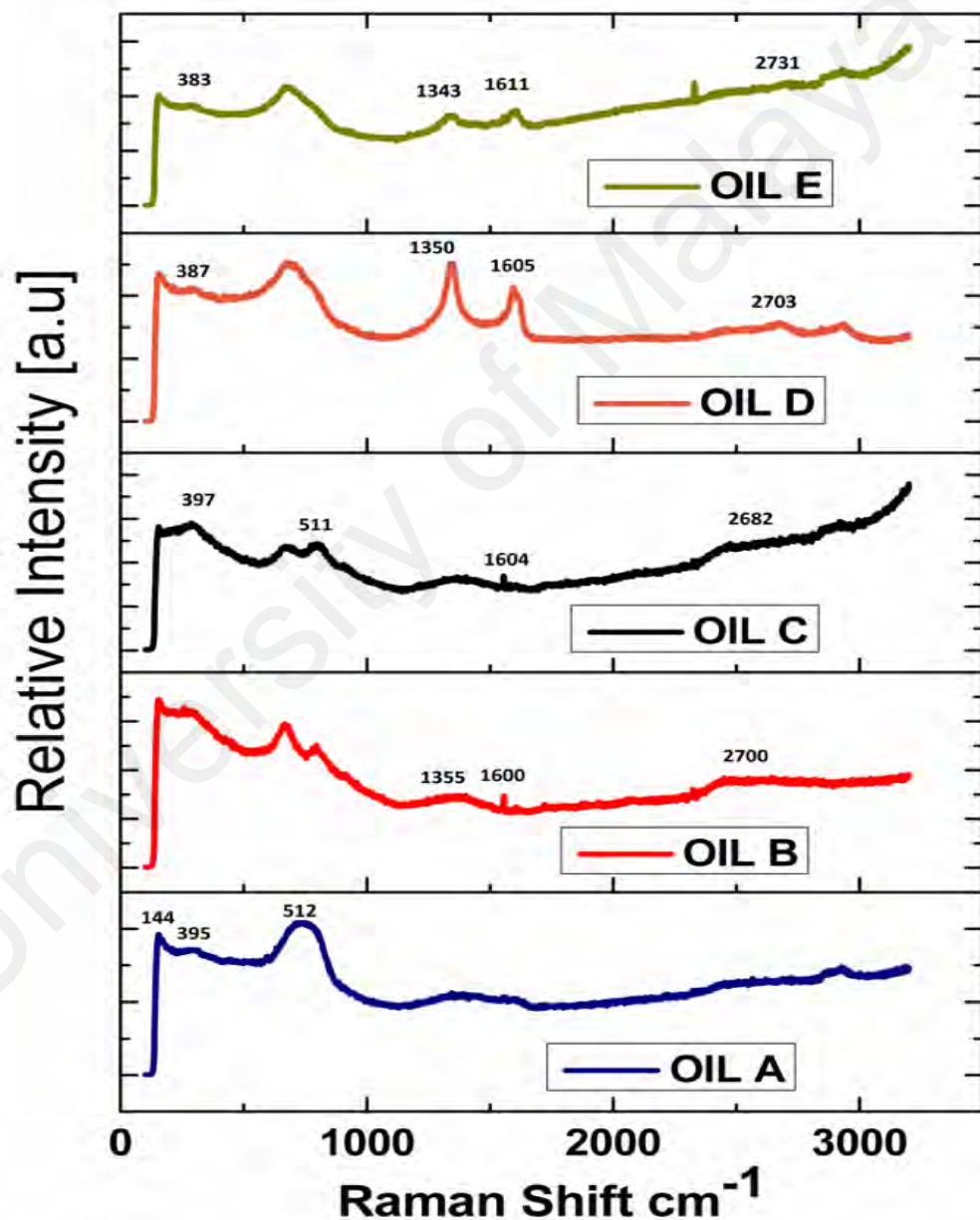


Figure 4.19: Raman spectra of five nano-oils: Oil (A) 0.2 wt% TiO₂ anatase, Oil (B) 0.2 wt% Graphene, Oil (C) 0.2 wt% TiO₂ anatase + 0.2 wt% Graphene, Oil (D) 0.2 wt% TiO₂ anatase + 0.4 wt% Graphene, Oil (E) 0.4 wt% TiO₂ anatase + 0.2 wt% Graphene

It signifies that the small-sized island-structure layer in Figure 4.13 are TiO₂ (A)/graphene-packing particulates, which simply shear and are conformal anti-wear protecting coating and thereby significantly diminish the friction coefficient and wear values concerning (0.4 wt% TiO₂ (A) + 0.2 wt% Graphene) nanolubricant (Zengshi Xu, 2015).

4.8.2 Raman Spectroscopy for ZnO + Graphene

Raman peaks analysis was carried out to continue analyzing the coalescence layer compounds on a region of interaction of ZnO and graphene specimens. Raman spectra are a primary approach to represent the nanometer-sized particles of five nanolubricants. Raman peaks of the ZnO and graphene nanoparticles deposition illustrated in Figure 4.20 originated from five different nano-oils employing an argon ion laser excitation of (532 nm) edge and the band domain from 100 cm⁻¹ to 3200 cm⁻¹ (Mallika Dasari, 2018).

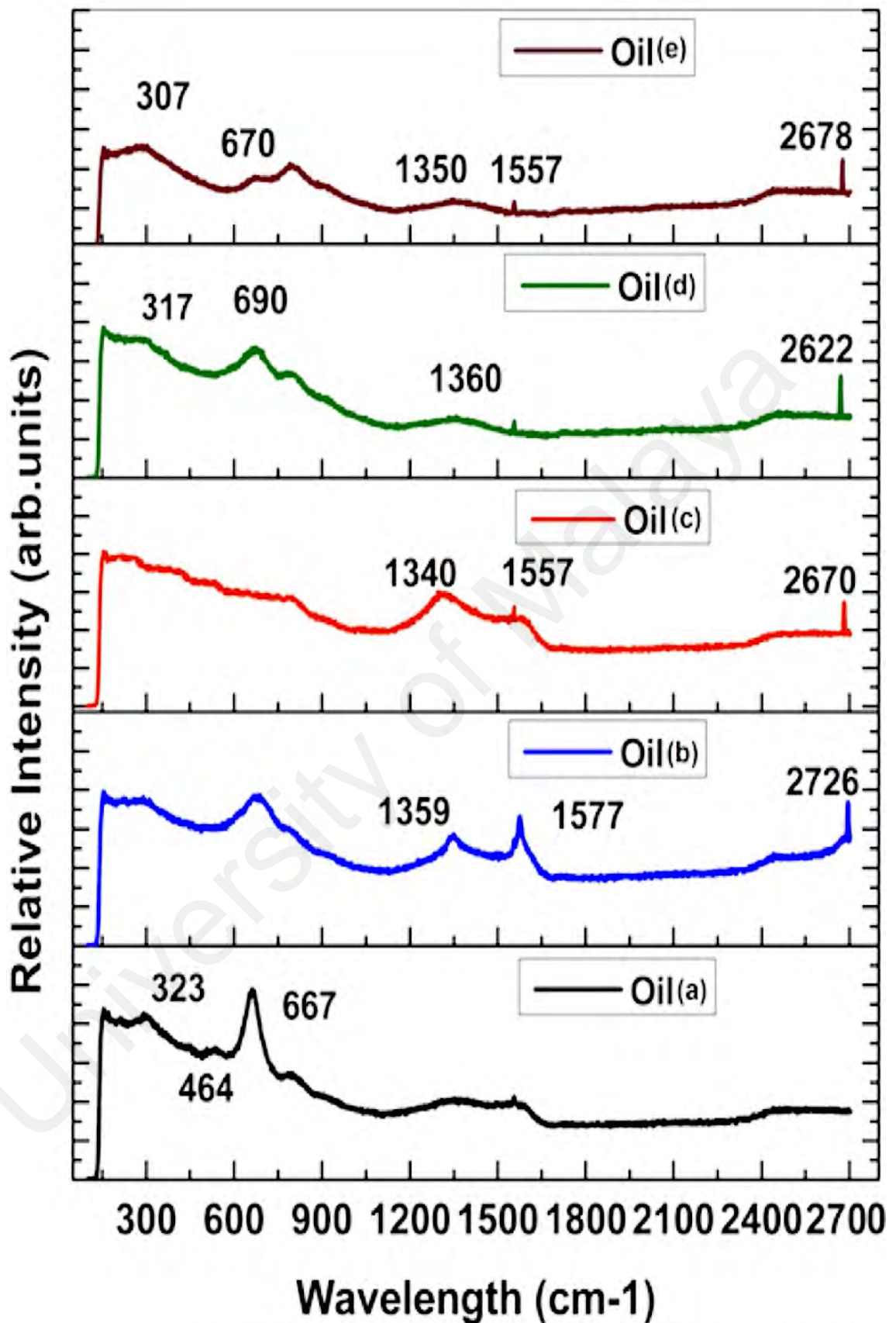


Figure 4.20: Raman spectra of five nanolubricants Oil (a) 0.2 wt% ZnO, Oil (b) 0.2 wt% Graphene, Oil (c) 0.2 wt% ZnO + 0.2 wt% Graphene, Oil (d) 0.2 wt% ZnO + 0.4 wt% Graphene, Oil (e) 0.4 wt% ZnO + 0.2 wt% Graphene

The spectrum presented ZnO vibrating collections about 307 – 323 cm^{-1} which are ascribed to the second-order various phonon $2E_1$ (Longitudinal Optic (LO)), and 464 cm^{-1} agrees with E_2^{high} (D N Montenegro, 2013) and (M. Salem, 2018). On the other hand, the peaks 667-690 cm^{-1} do not correspond with ZnO regular bands. These peaks are special vibrating modes correlating texture flaws (D N Montenegro, 2013). Overall, the stokes-phonon energy shifting produced by laser application of the graphene nano particulates developed of three primary peaks around 1350, 1557, and 2670 cm^{-1} .

These peaks correspond to D, G, and 2D groups sequentially. These three notable bands D, G, and 2D in the spectrum which is a regular feature of graphene nano particulates (Venkata Ramana Posa, 2016), (Zengshi Xu, 2015) and (Wani, 2018). The G-band resemble as expanding waves of sp^2 carbon atoms in graphene, the D-band conform with the breathing form of sp^2 carbon atoms in groups possessing defects (non-graphitic carbon). The 2D group is correlated with dual phonon spread like electron-electron or electron-hole or hole-hole band. Besides, it noted as a consequence of D peak, but it does not necessarily represent defects in the lattice structure (Mallika Dasari, 2018) and (Wani, 2018).

Tribolayers and close to-surface elements control the interacting surfaces in the relative motion of tribological behavior. The ZnO- and graphene-enhanced nano-oils created tribofilm, through maintaining the elimination of contacting damage (H. M. M. Gulzar, M Varman, MA Kalam, R.A. Mufti, NWM Zulkifli, R. Yunus, Rehan Zahid, 2015). It indicates that the formed layers on the mating surfaces are ZnO/graphene-protective thin layers, that simply shear and are conformal scarring protection coatings and hence significantly diminish the friction coefficient and abrasion scales (Zengshi Xu, 2015).

4.9 Surface Characterization

4.9.1 Surface Roughness Characterization for TiO₂ (A) + Graphene

The surface roughness for each AISI ball was investigated by a 3D visual (contactless) surface texture analyzing device after tribological experimentations (H. X. Mohamed Kamal Ahmed Ali, Liqiang Mai, Cai Qingping, Richard Fiifi Turkson, Chen Bicheng, 2016). The surface roughness of interacted balls is among the major testing in characterizing texture finish and abrasion and adhesion operation for each ball. The optical detection of a machined ball treated with (0.4 wt% TiO₂ (A) + 0.2 wt% Graphene) nano-oil verifies that it was more even than the defected ball when treated with PBO-GII oil Figure 4.21.

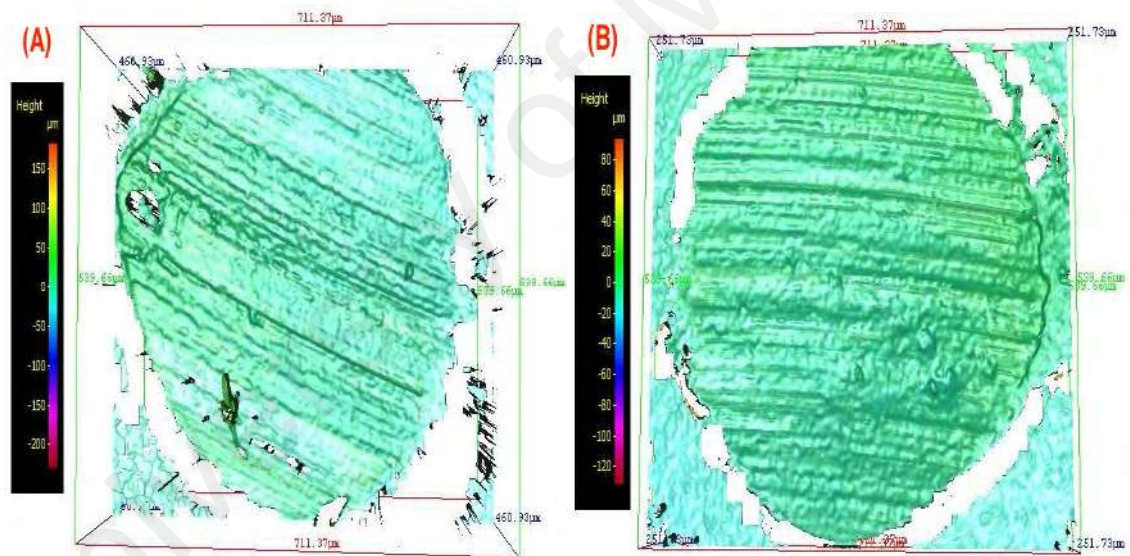
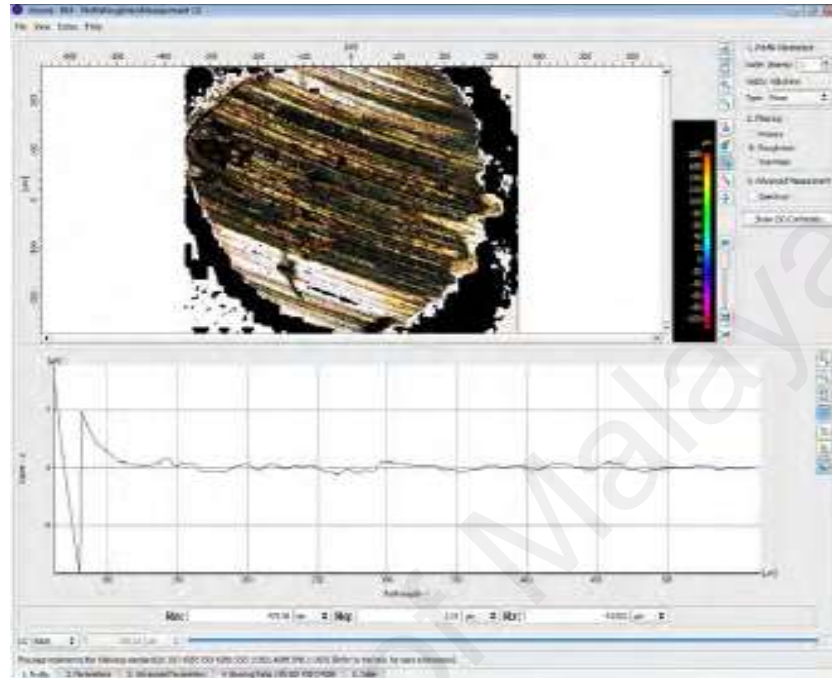


Figure 4.21: (A) Worn surface of a ball when applying PBO-GII lubricant and (B) sliding region of a ball when applying (0.4 wt% TiO₂ (A) + 0.2 wt% Graphene) nanolubricant

The minimum profile roughness parameters were reported for the AISI ball surface testing with the (0.4 wt% TiO₂ (A) + 0.2 wt% Graphene) nano-oil, with arithmetic mean roughness (Ra) of 103.25 nm, root mean square (RMS) or (Rq) of 130.72 nm, and mean roughness depth (Rz) of 550.93 nm, while the highest-profile roughness parameters (Ra),

(Rq), and (Rz) were reported for PBO-GII 475.56 nm, 1190 nm, and 4032.1 nm respectively as presented in Figure 4.22 and Figure 4.23.

(A) PBO-GII Oil



(B) 0.4 wt% TiO₂ (A) + 0.2 wt% Graphene Nano-oil

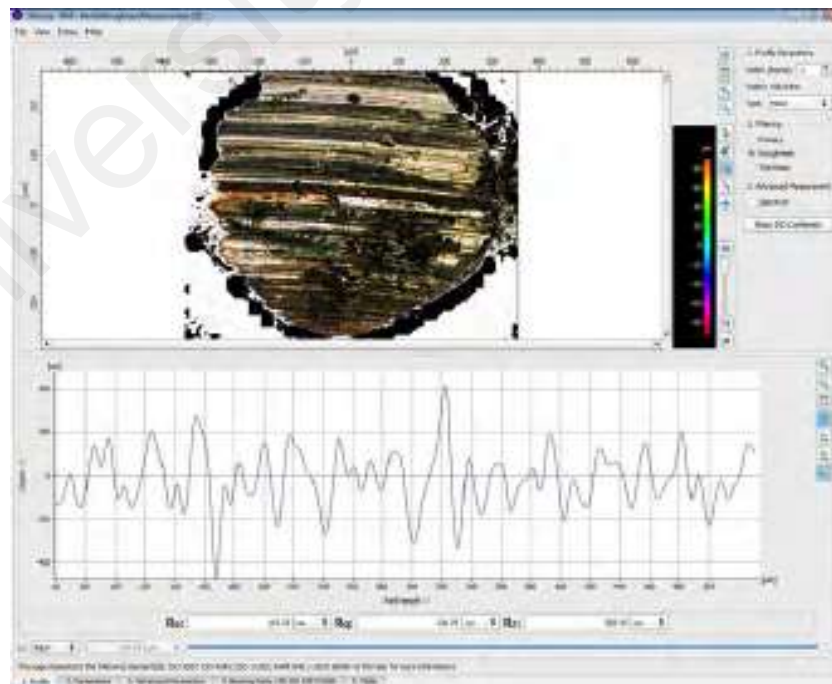


Figure 4.22: Profile roughness measurement (Ra), (RMS) or (Rq), and (Rz) for (A) PBO-GII oil and (B) (0.4 wt% TiO₂ (A) + 0.2 wt% Graphene) nano-oil

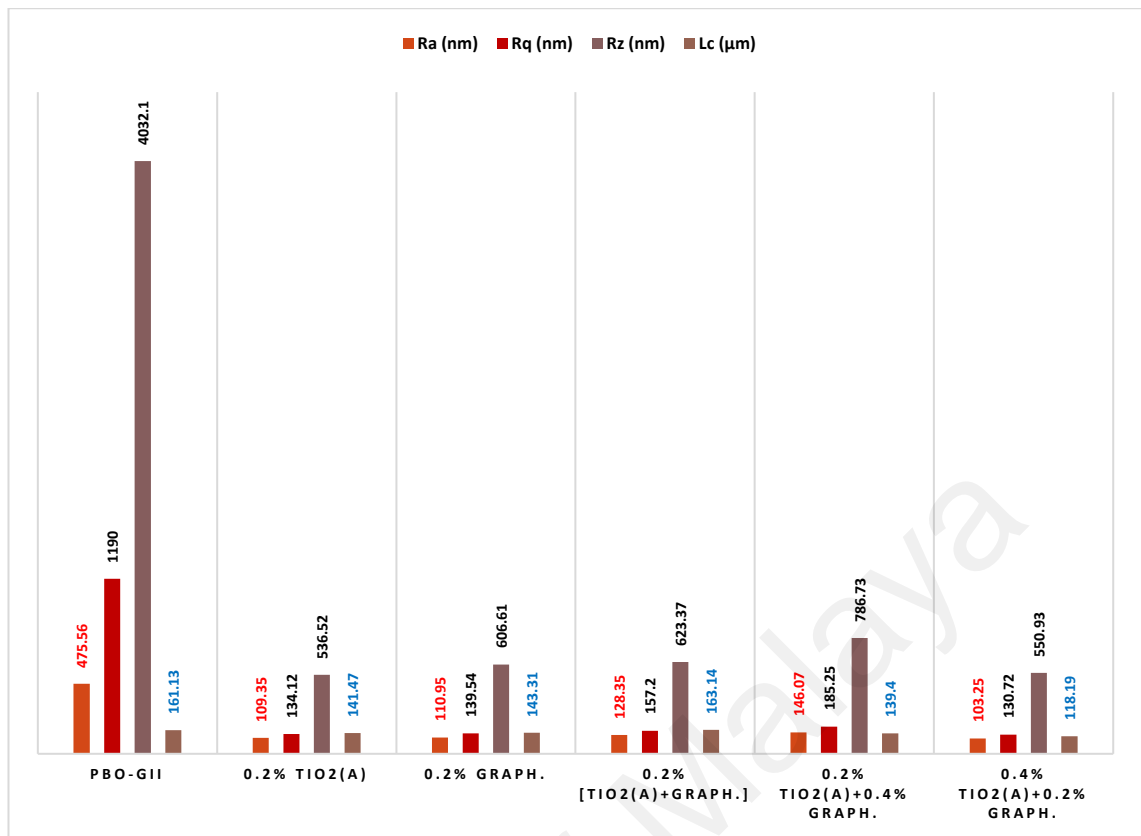
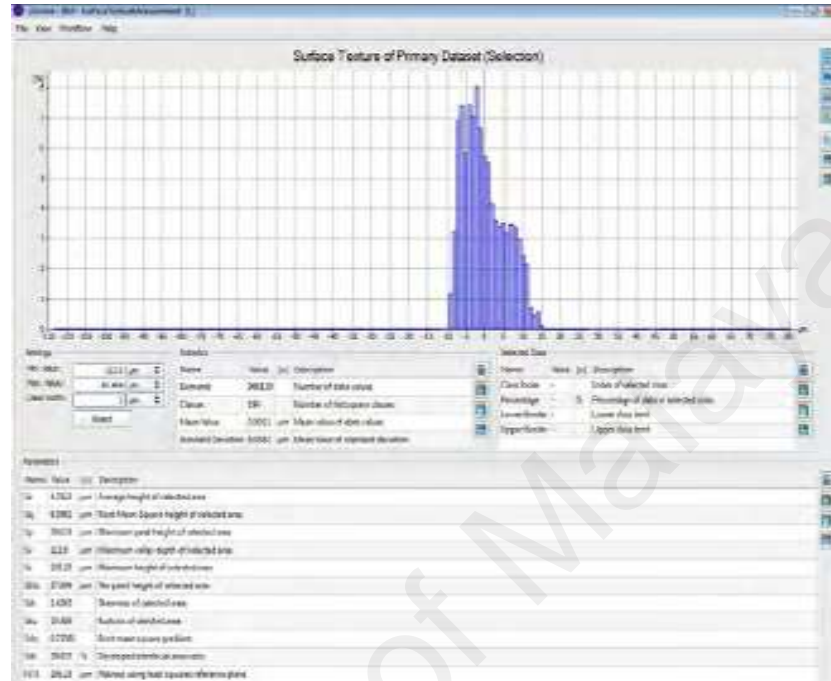


Figure 4.23: Profile roughness investigation of surface morphology of AISI balls employed with six various sorts of lubricants

In accordance with ISO 25178 (Anna Góral, 2017) the surface height parameters were computed on the basis of all measured values from the visually investigated 3-dimensional boundaries. The mean surface height (S_a), which presents a well-known overall representation of the height differences, was the maximum ($4.7822 \mu\text{m}$) for the additive-free lubricant and the minimum ($2.1792 \mu\text{m}$) for (0.4 wt% TiO_2 (A) + 0.2 wt% Graphene) nano-oil, as shown in Figure 4.24. The variations in S_a and root-mean-square height (S_q) data for the scanned balls were considerably graphed in Figure 4.25. The enhancement was noticed for the variables of the average surface height (S_a), the root-mean-square height (S_q), maximum valley height S_v , which was the minimum for the (0.4 wt% TiO_2 (A) + 0.2 wt% Graphene) nano-oil. A variation was merely noticed for the factors of the maximum peak height (S_p) and the maximum height (S_z), which was the

maximum for (0.4 wt% TiO₂ (A) + 0.2 wt% Graphene) nano-oil in comparison with (0.2 wt% Graphene) and (0.2 wt% TiO₂ + 0.2 wt% Graphene).

(A) Additive-free Oil



(B) Effective Nano-oil

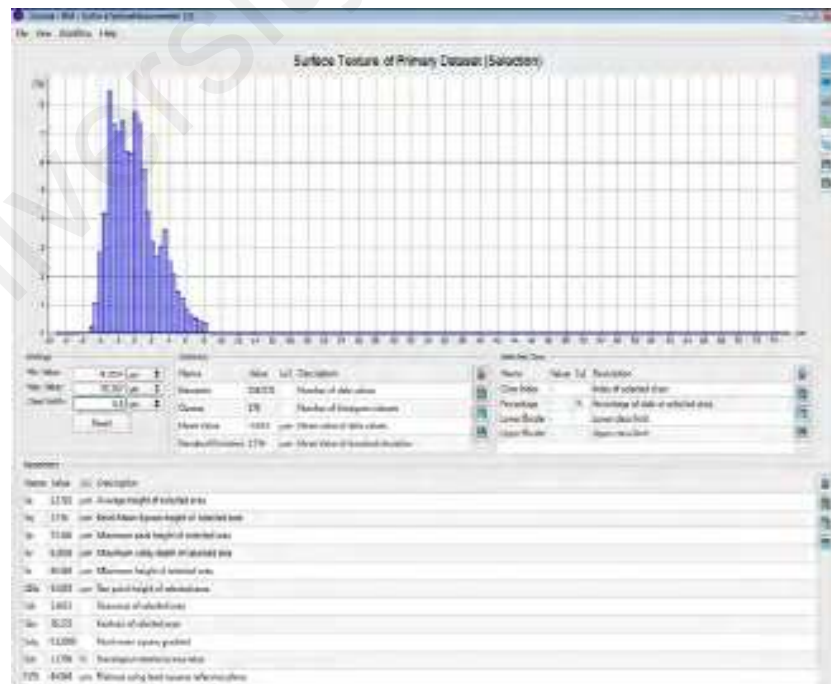


Figure 4.24: Surface texture measurement (Sa), (Sq), (Sp), (Sv), (Sz), (Ssk), and (Sku) for (A) additive-free oil, and (B) effective nano-oil

Sp, Sv, and Sz parameters/variables depend on single surface characteristics, such as heights or cavities. These parameters/variables are defined by the low repeatability while consecutive analyses. For this reason, the measurement of the three parameters/variables should be preceded by enough filtration so that it is possible to acquire a statistically substantial consequence. The filtration is carried out on the extracting of inexact pits or cavities originating from measuring errors. The Sz parameter/variable is the total of Sp and Sv variables values; it is the difference between the largest peak and the deepest valley, for this reason, the amount of Sz variable increases correspondingly to the addition of Sp and Sv. When enough value of lube provided to the zone of application produces tribological influence, which results in the roughness of the interacted surface become flattened. This is especially noticeable for arithmetical variables, such as Sa and Sq (G.M. Krolczyk, 2018).

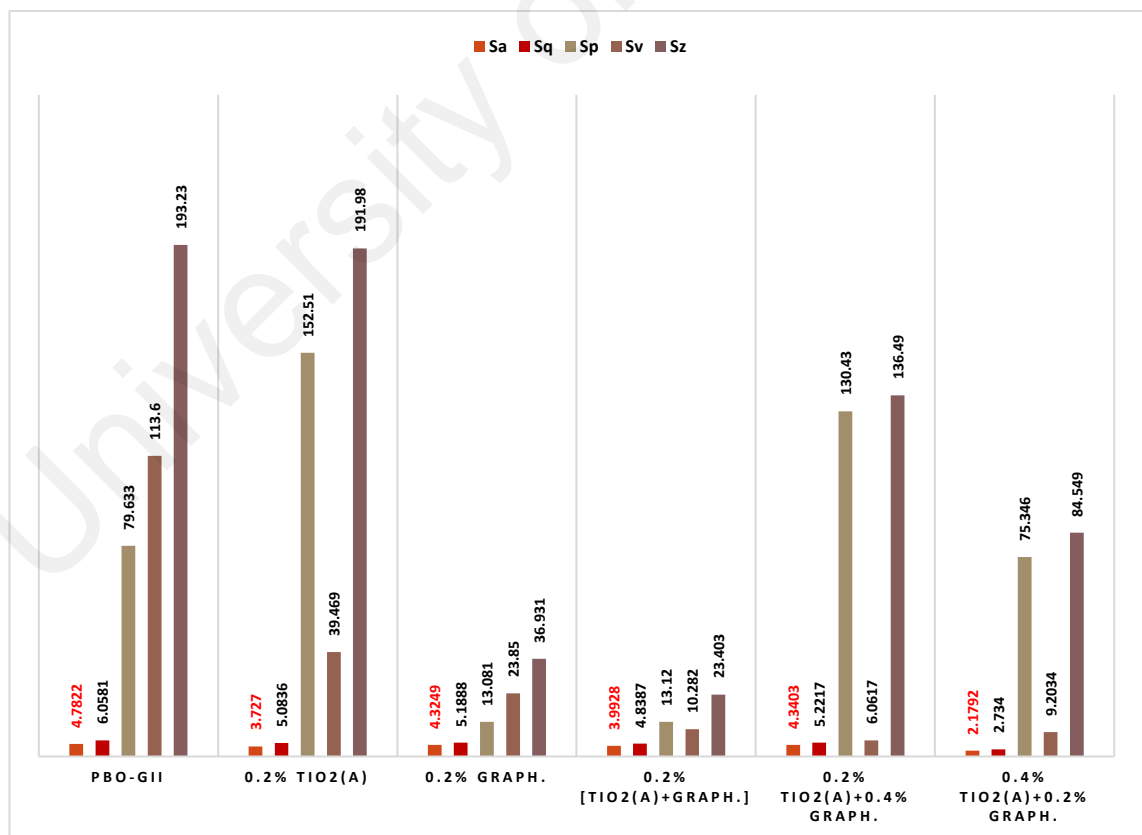


Figure 4.25: Surface texture investigation (μm) of the surface morphology of AISI balls used with six various sorts of lubricants

The arithmetical variables of surface roughness S_a and S_q are insufficient to characterize the tribological performance of interaction balls. Therefore, surface skewness (S_{sk}) and surface kurtosis (S_{ku}) were evaluated (Figure 4.24), which are two fundamental parameters specifying the asymmetry and the flatness of the surface configuration. The most essential variable is S_{sk} . The smaller S_{sk} is, the more moderate the friction we can presume, even at larger mean surface height S_a . Besides, friction diminishes when variable S_{ku} rises. Surface roughness variables S_{ku} and S_{sk} can be employed to address surfaces for appropriate tribological performance. Consequently, roughness variables S_{ku} and S_{sk} were analyzed to confirm the potential relationship with tribological characteristics as illustrated in Figure 4.26. The obtained value of surface kurtosis S_{ku} for (0.4 wt% TiO_2 (A) + 0.2 wt% Graphene) nano-oil has better tribological characteristics than PBO-GII lubricant. The test findings confirm that S_{sk} and S_{ku} can be applied to identify surface texture, with a bigger surface kurtosis S_{ku} value and more negative value of surface skewness S_{sk} resulting in smaller friction among interaction AISI balls (P. G. B. P. Marko Sedlaček, 2017). The analyses prove that (0.4 wt% TiO_2 (A) + 0.2 wt% Graphene) nano-oil is more reliable than PBO-GII oil, as illustrated in Figure 4.26.

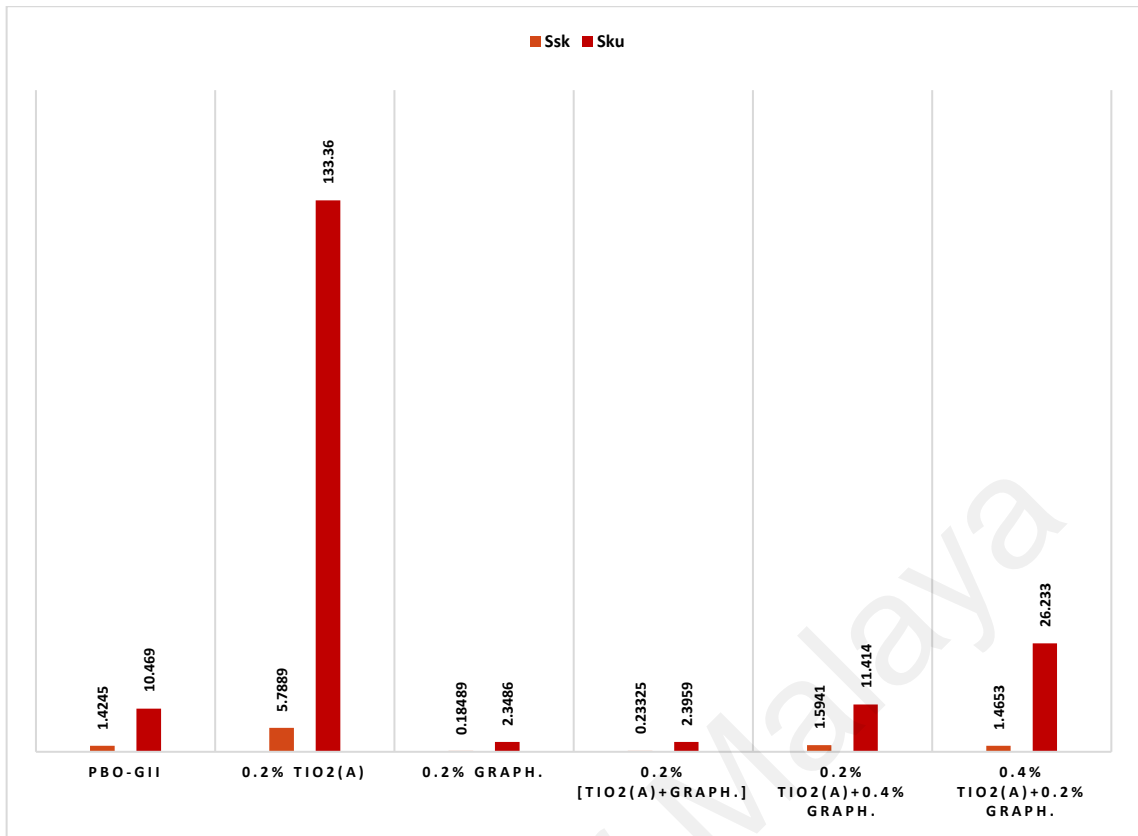


Figure 4.26: Surface skewness and surface kurtosis measurement (dimensionless) of the surface morphology of AISI balls employed with six various sorts of lubricants

On top of that, profile form measurement was implemented to confirm that employing (0.4 wt% TiO₂ (A) + 0.2 wt% Graphene) nano-oil is more advanced than PBO-GII oil. As reported by this analysis, the surface depth (Z1) for the PBO-GII oil was larger than for the (0.4 wt% TiO₂ (A) + 0.2 wt% Graphene) nano-oil. Furthermore, the surface depth (Z2) for the PBO-GII oil was larger than for the (0.4 wt% TiO₂ (A) + 0.2 wt% Graphene) nano-oil, as shown in Figure 4.27.

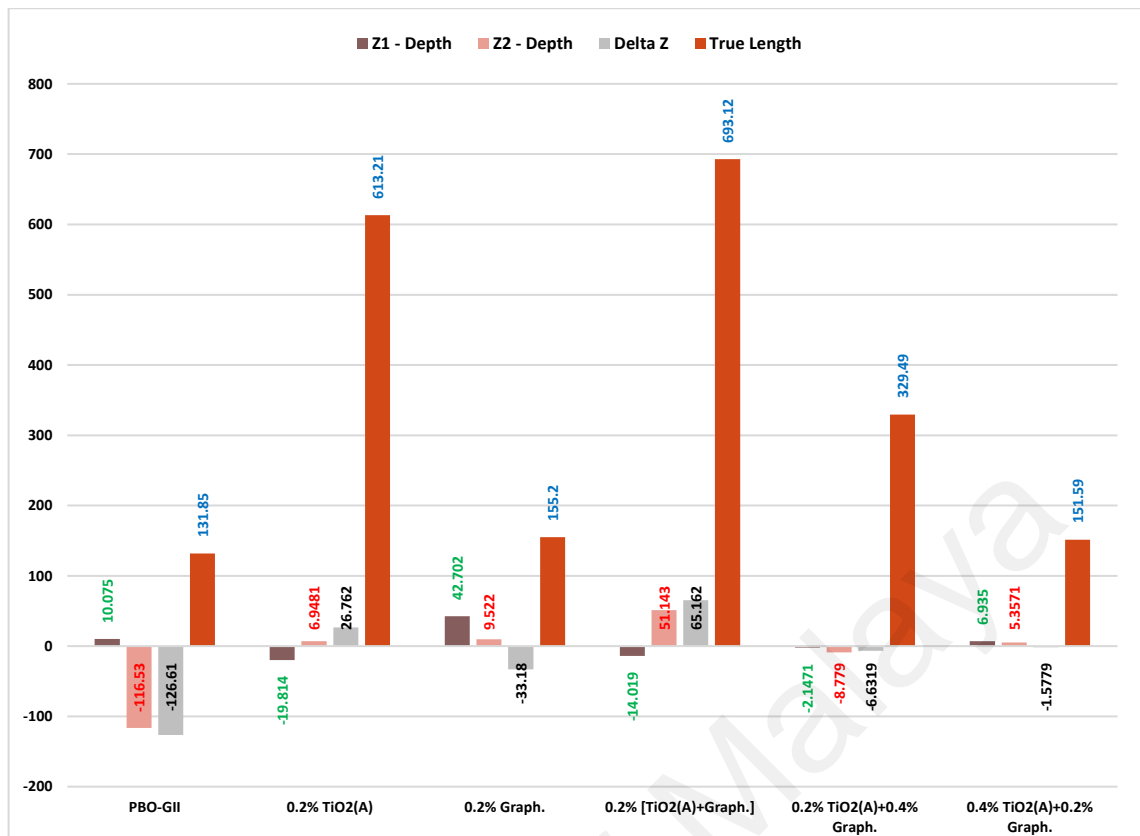


Figure 4.27: Profile form investigation (μm) of the surface morphology of AISI balls employed with six various sorts of lubricants

4.9.2 Surface Roughness Characterization for ZnO + Graphene

Surface roughness analyses were appropriated to describe the scarred topographies and to distinguish surface finish and adhesion and abrasion performance of all samples/lubricants. The texture morphology of each AISI ball was measured with a 3-dimensions high-end visual (contact-free) surface roughness equipment after tribology analyses (H. X. Mohamed Kamal Ahmed Ali, Liqiang Mai, Cai Qingping, Richard Fiifi Turkson, Chen Bicheng, 2016). It was noted while (0.4 wt% ZnO + 0.2 wt% Graphene) nano-oil implemented the interaction surfaces of the balls was flatter than the notched area on the ball when PBO-GII oil employed Figure 4.28.

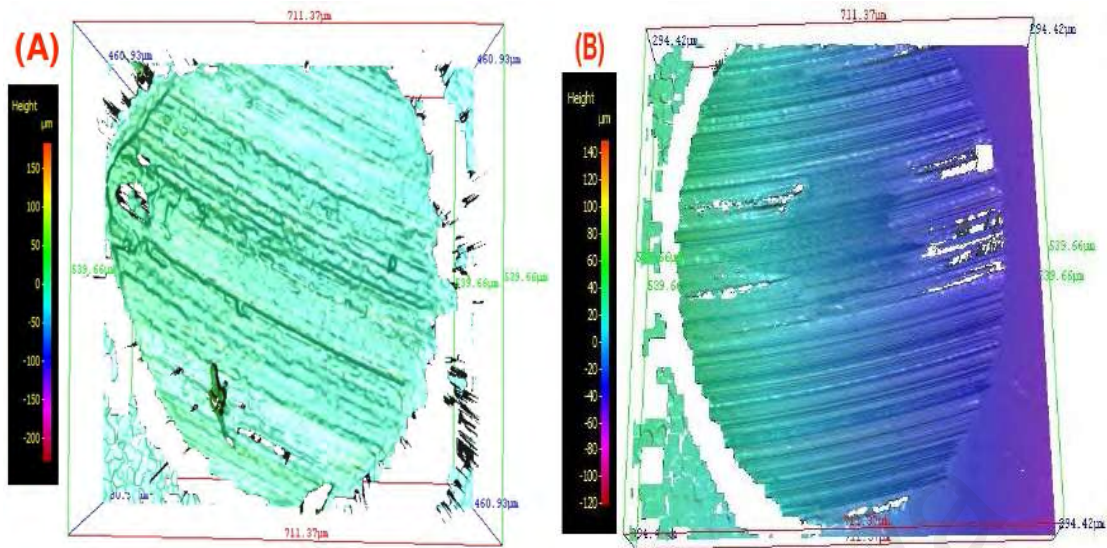
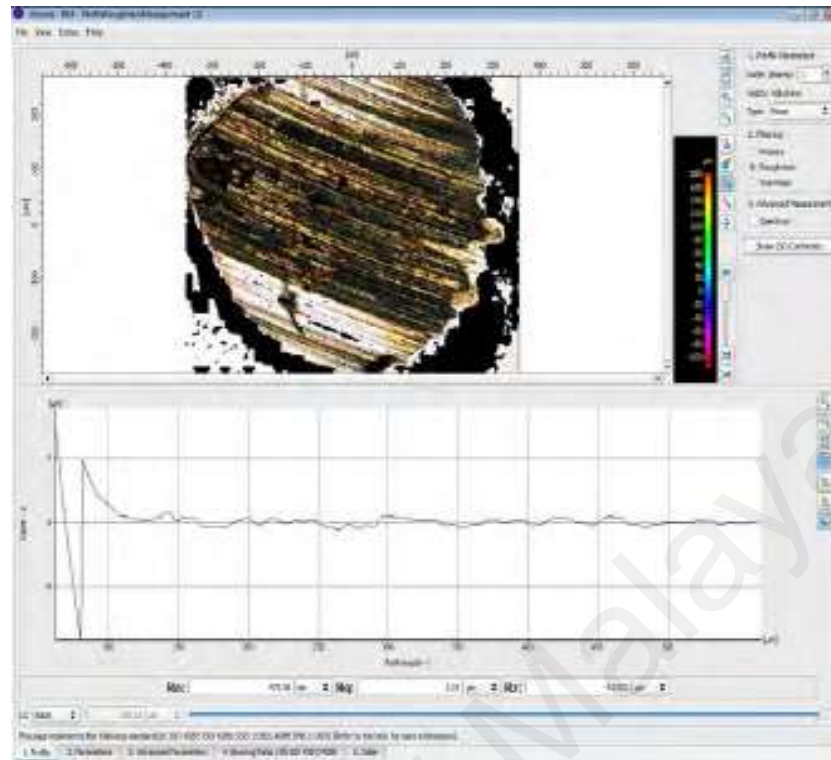


Figure 4.28: (A) Worn ball region after using PBO-GII lubricant and (B) Scar ball surface after using (0.4 wt% ZnO + 0.2 wt% Graphene) nanolubricant

The addressed values of profile roughness were $R_a=475.56$ nm and $R_a=59.558$ nm for PBO-GII oil and (0.4 wt% ZnO + 0.2 wt% Graphene) nanolubricant, consecutively (Figure 4.29).

The profile roughness variables (arithmetic mean roughness R_a , root mean square RMS or R_q , and mean roughness depth R_z) were measured for all experimented AISI balls as illustrated in Figure 4.30. Consequently, the most diminutive surface profile roughness parameters (R_a , R_q , and R_z) were stated for the steel ball employed with (0.4 wt% ZnO + 0.2 wt% Graphene) nanolubricant as demonstrated in Figure 4.30.

(A) Additive-free oil



(B) (0.4 wt% ZnO + 0.2 wt% Graphene) nano-oil

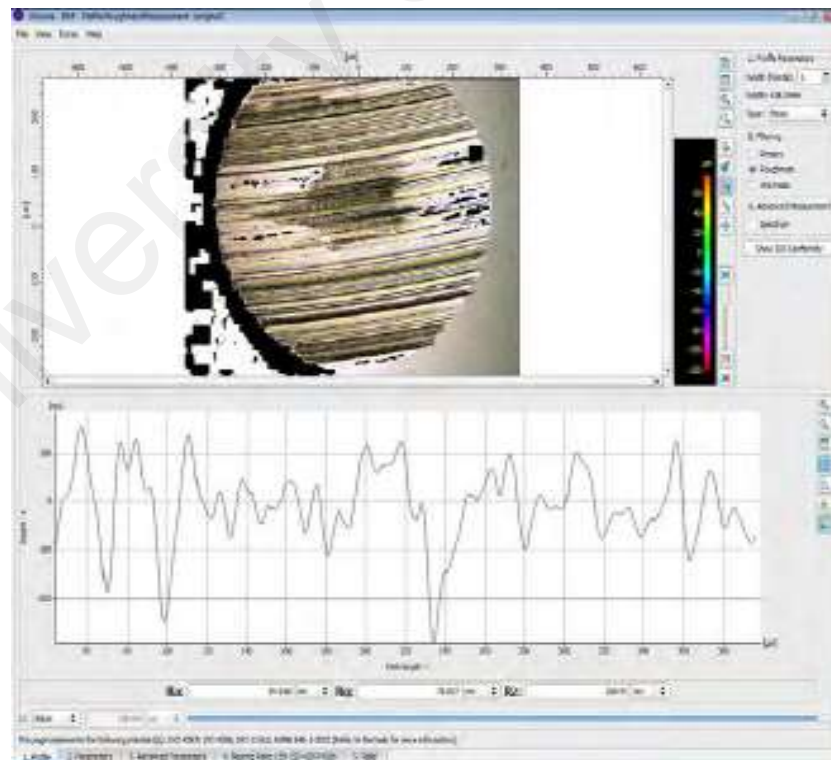


Figure 4.29: Profile roughness measurement (Ra), (RMS) or (Rq), and (Rz) for (A) Additive-free oil and (B) (0.4 wt% ZnO + 0.2 wt% Graphene) nano-oil

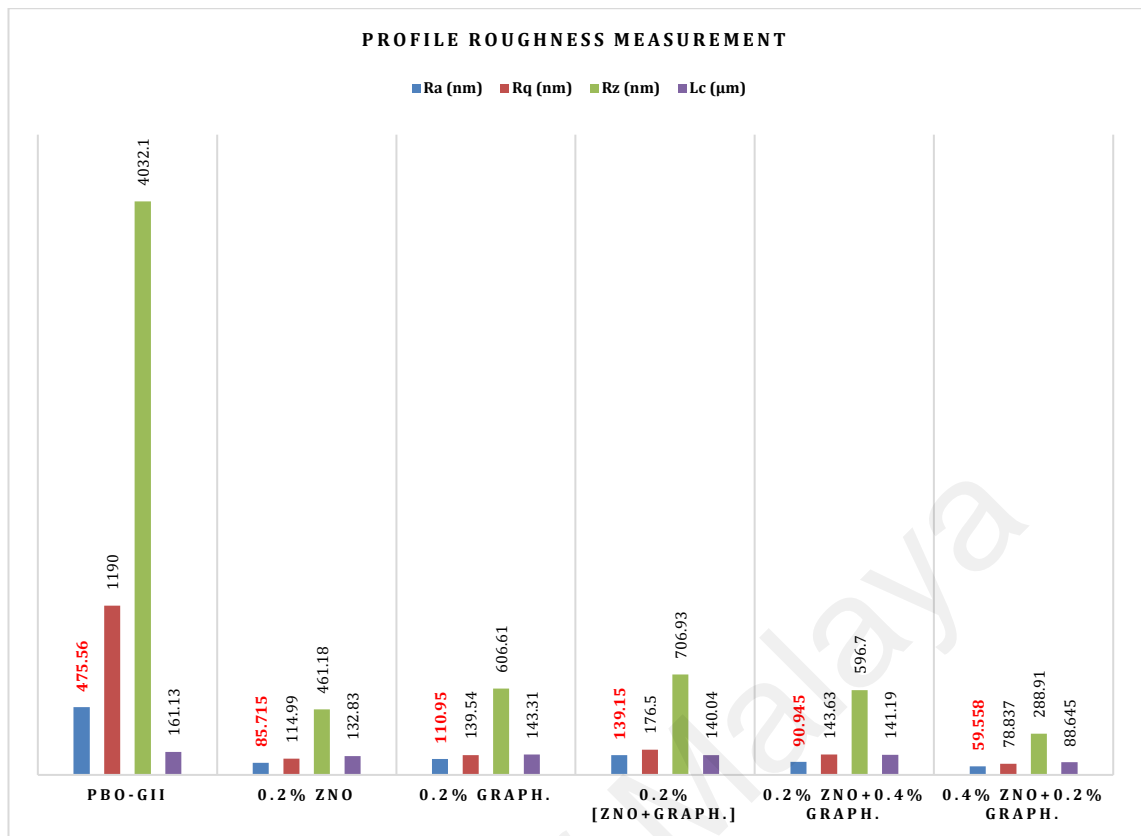
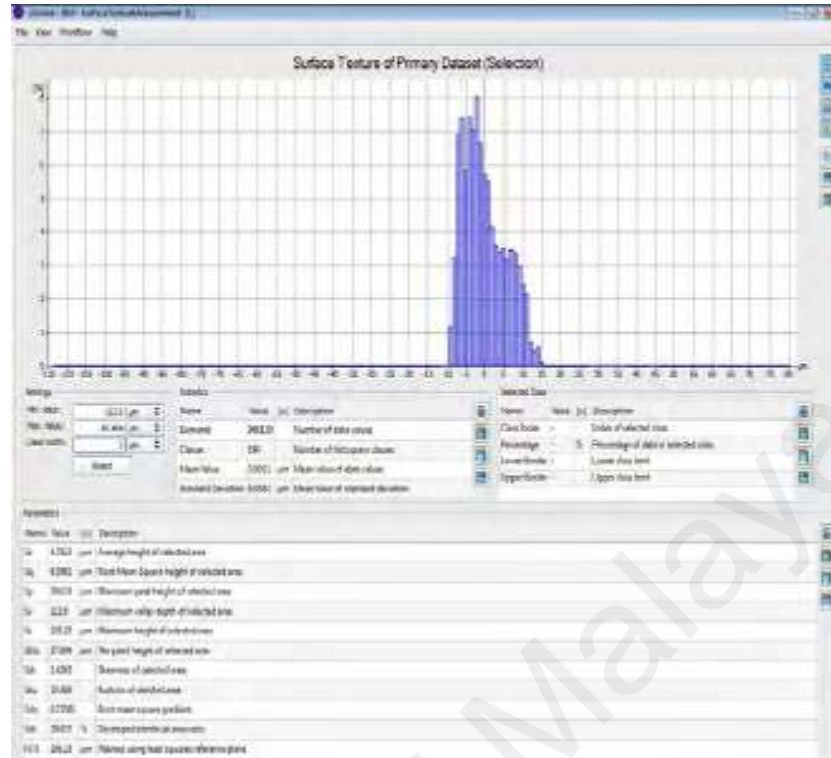


Figure 4.30: Profile roughness investigation of the surface morphology of AISI balls employed with six various sorts of lubricants

Of all sorts of samples, the tiniest value of roughness variable Sa was for the (0.4 wt% ZnO + 0.2 wt% Graphene) nanolubricant, which implies excellent hydrodynamic characteristics and subsequently reduced friction (B. P. Marko Sedlaček, Jože Vižintin, 2012). In accordance with ISO 25178 (Anna Góral, 2017), the texture roughness parameters/variables were specified based on entire study statistics from comprehensive texture finish equipment of measured scarred areas. The Sa offers an excellent value of the height variations were the maximum (4.7822 µm) for the PBO-GII oil and the lowest (2.8802 µm) for (0.4 wt% ZnO + 0.2 wt% Graphene) nanolubricant (Figure 4.31).

(A) PBO-GII Oil



(B) (0.4 wt% ZnO + 0.2 wt% Graphene) Nanolubricant

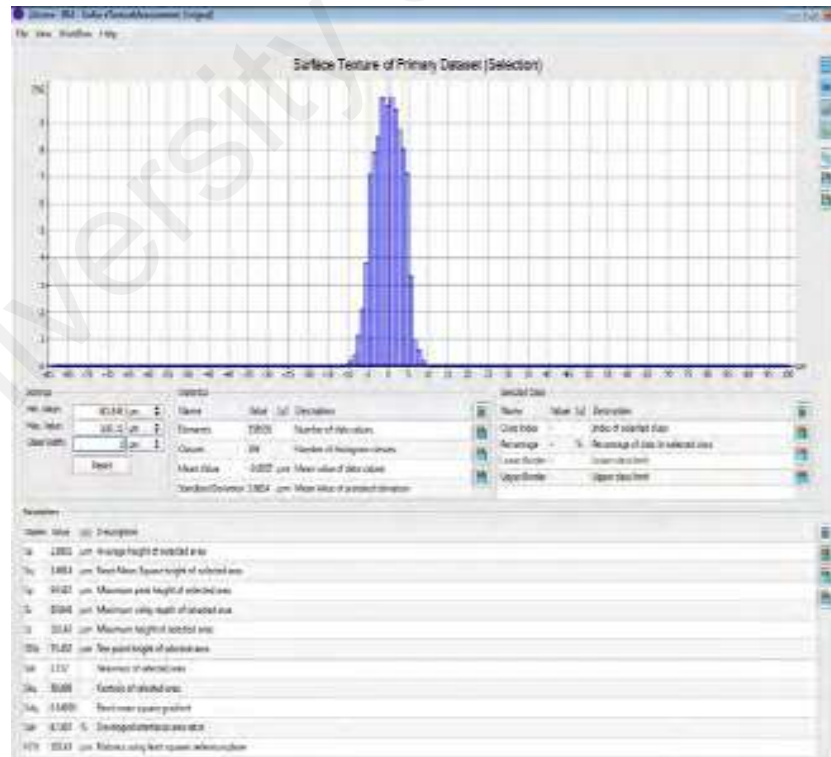


Figure 4.31: Surface texture measurement (Sa), (Sq), (Sp), (Sv), (Sz), (Ssk), and (Sku) for (A) PBO-GII oil, and (B) (0.4 wt% ZnO + 0.2 wt% Graphene) nanolubricant

The average surface height (Sa), root-mean-square height (Sq), maximum peak height (Sp), maximum valley depth (Sv), and maximum height (Sz) for all AISI balls scars involved in this measurement are described Figure 4.32.

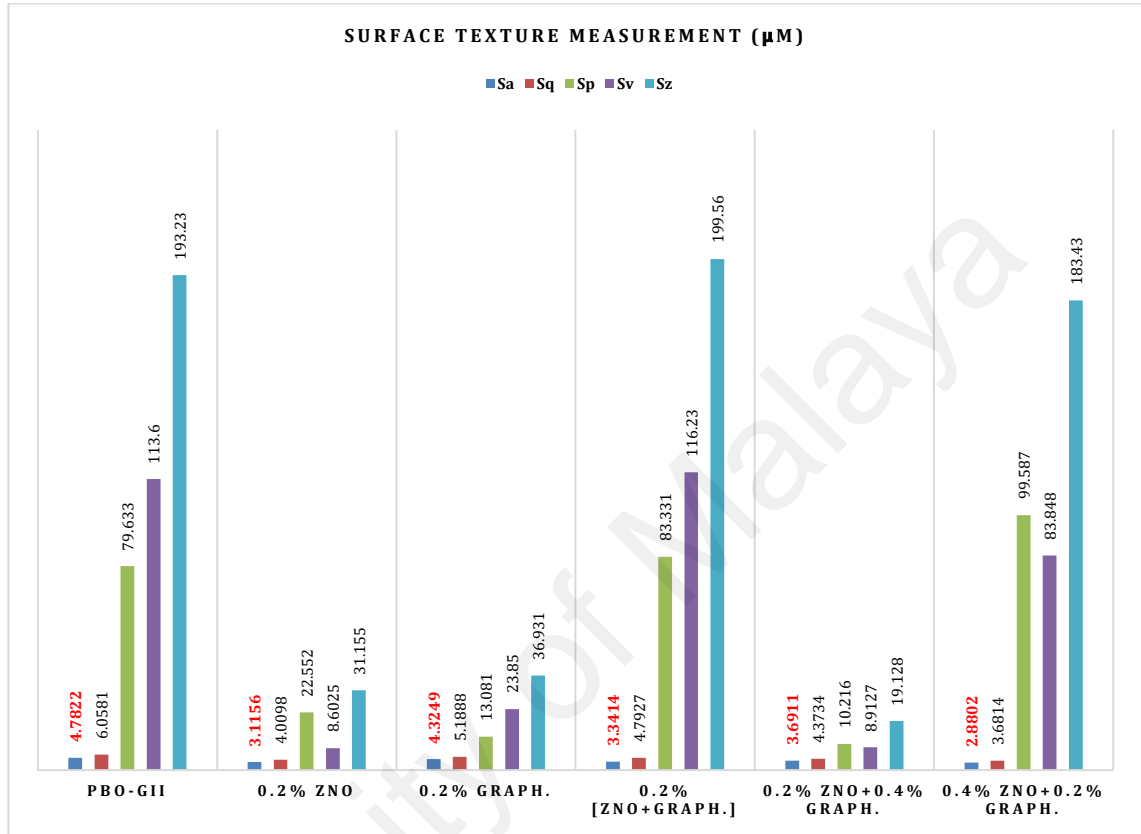


Figure 4.32: Surface texture investigation (μm) for the surface morphology of AISI balls employed with six various sorts of lubricants

The variations in mean surface heights Sa and root-mean-square height Sq results for six tested lubricants were impressive (Figure 4.32). The improvement was remarked for the parameters of Sa and Sq which was the smallest for (0.4 wt% ZnO + 0.2 wt% Graphene) nanolubricant. The differences in average surface height amounts for the six tested oils were reasonable. A contrast was especially remarked for the variables of Sp, Sv, and Sz, thus the highest was for (0.4 wt% ZnO + 0.2 wt% Graphene) nano-oil in comparison with nano-oils (0.2 wt% Graphene), and (0.2 wt% ZnO + 0.4 wt% Graphene). Sp, Sv and Sz variables rely on specific position properties, such as peaks or pits. These

parameters are described by inadequate repetition through sequential investigations. Subsequently, the analysis of three parameters needs to be submitted to appropriate filtration to achieve numerically relevant findings. The filtration is based on the exclusion of wrong pits resulting from calculation imprecision. The Sz parameter is the sum of Sp and Sv amounts; it is the variation between maximum peak and deepest valley, thus, the value of Sz rises appropriately to the increment of Sp and Sv. When the least amount of lubrication supplied to the zone of application, the unevenness of the scarred surface becomes smoother. This is prominently obvious for analytical parameters, such as Sa and Sq (G.M. Krolczyk, 2018). This detailed examination of surface texture takes into consideration the relationship between the surface finish variables (skewness and kurtosis) and the tribology behavior.

The fundamental surface texture variables Sa and Sq are incapable to identify the tribological characteristics of AISI interacted balls. Accordingly, surface skewness (Ssk) and surface kurtosis (Sku) were considered to confirm the potential correlation with tribological properties as presented in Figure 4.33. The additional essential parameter is Ssk. The tiny Ssk is, the tiny friction we can expect, even at the higher average surface texture. In the same way, friction reduces if Sku increases. Texture finish parameters Ssk and Sku could be carried out to control surfaces to preferable tribological operation (B. P. Marko Sedlaček, Jože Vižintin, 2012). To achieve this objective, texture finish parameters Ssk and Sku were investigated to describe the potential relations with tribological operation in this study. The most prominent roughness parameter Sku value was obtained for (0.4 wt% ZnO + 0.2 wt% Graphene) nano-oil which implies superb tribological characteristics as compared with PBO-GII oil.

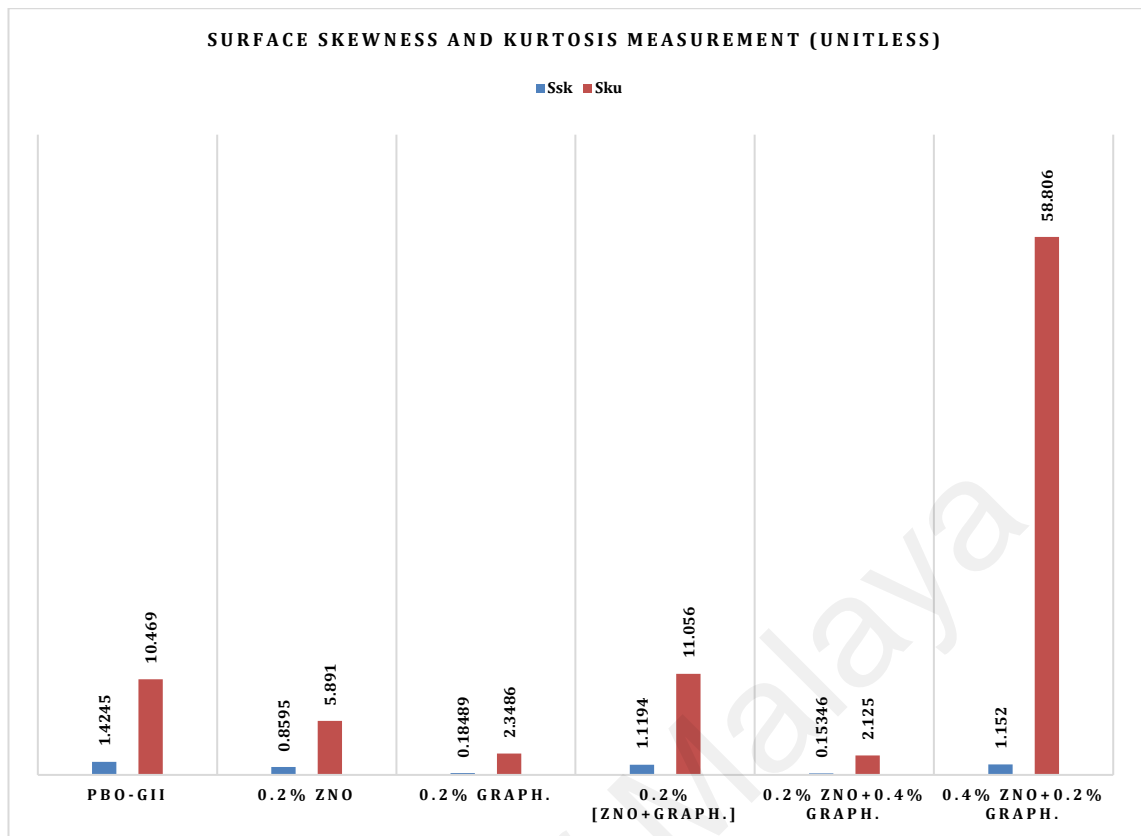
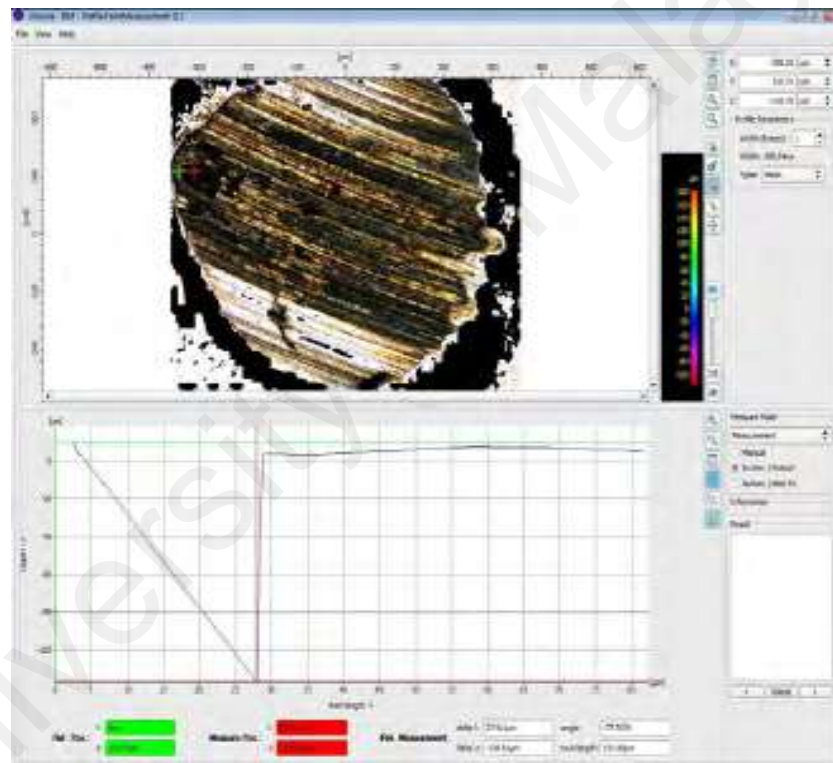


Figure 4.33: Surface skewness and kurtosis measurement (dimensionless parameters) of the surface morphology of AISI balls employed with six various sorts of lubricants

The experimental statistics prove that Ssk and Sku can be implemented to distinguish texture finishing, with a higher Sku value and more negative Ssk leading to reduce friction among lubricated interaction surfaces (P. G. B. P. Marko Sedlaček, 2017). The measurement prove that (0.4 wt% ZnO + 0.2 wt% Graphene) nano-oil is optimal compared with PBO-GII oil, as demonstrated in Figure 4.31 and Figure 4.33. The lowest roughness parameter Ssk value was obtained for the (0.2 wt% ZnO), (0.2 wt% ZnO + 0.4 wt% Graphene), (0.2 wt% Graphene), and (0.2 wt% ZnO + 0.2 wt% Graphene). However, the highest Sku rate was taken for the (0.4 wt% ZnO + 0.2 wt% Graphene) nano-oil, which indicates excellent tribological features than all lubricants.

A new description of a surface is profiled form analysis, which supported (0.4 wt% ZnO + 0.2 wt% Graphene) blended nano-oil over the PBO-GII as well. Furthermore, it was stated that surface depth $Z_2 = -116.53 \mu\text{m}$ for PBO-GII additive-free lubricant has the deepest valley (pit) compared with $Z_2 = 2.1306 \mu\text{m}$ for (0.4 wt% ZnO + 0.2 wt% Graphene) formulated nano-oil, as demonstrated in Figure 4.34. Additionally, a surface depth $Z_2 = 2.1306 \mu\text{m}$ for (0.4 wt% ZnO + 0.2 wt% Graphene) nanolubricant was the lowest value compared with all lubricants (surfaces depth) as illustrated in Figure 4.35

(A) Additive-free Lubricant



(B) Formulated Dual Nanoparticles Lubricant

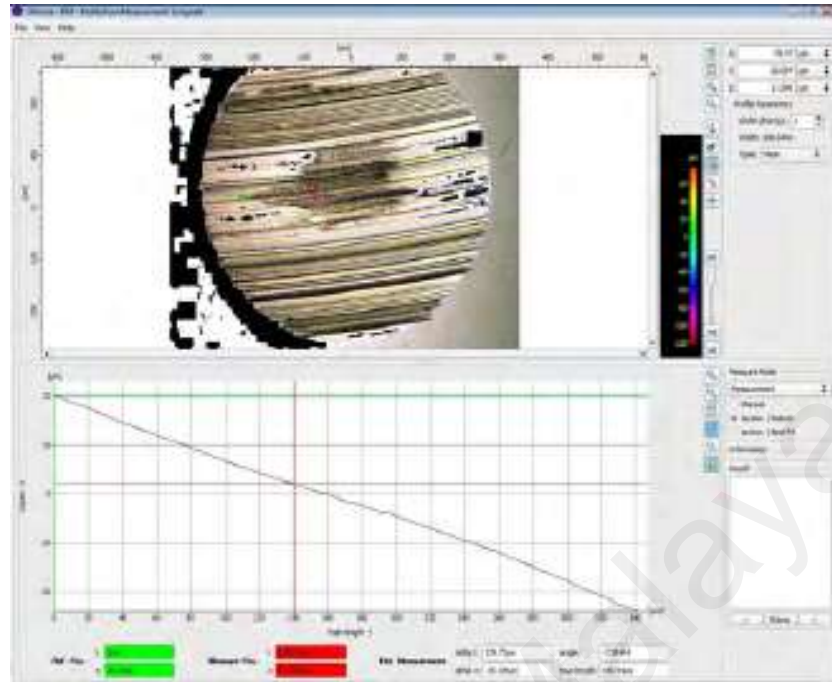


Figure 4.34: Profile form measurement for (A) additive-free lubricant and (B) formulated dual nanoparticles lubricant

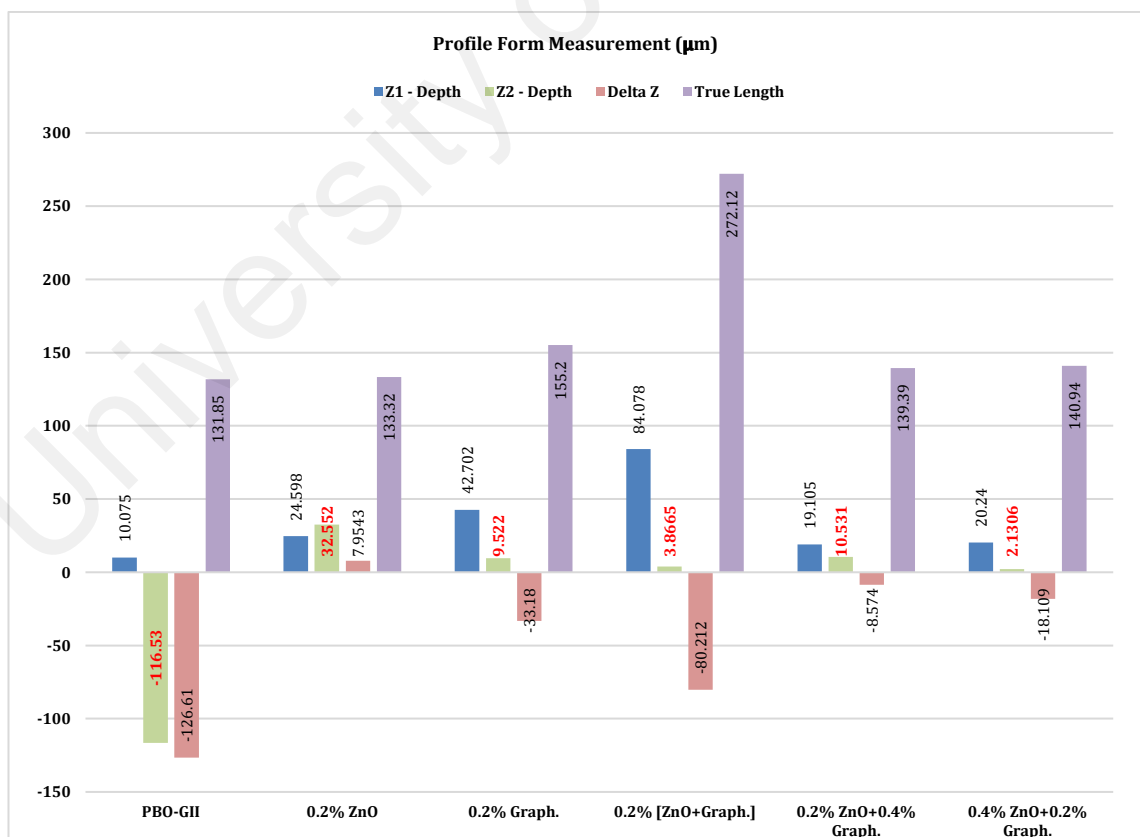


Figure 4.35: Profile form measurement (µm) of the surface morphology of AISI balls employed with six various sorts of lubricants

4.10 Conclusion

Morphological analyses have been done for three nanostructures to reveal the geometrical shape of each nanoparticles to predict the mechanism of these nanoscale particles during sliding interaction. Tribological experiments have been conducted for two groups of nanoparticles (TiO_2 A + Graphene) and (ZnO + Graphene). (0.4 wt% TiO_2 (A) + 0.2 wt% Graphene) nanolubricant presented superior COF in comparison with PBO-GII. The current research findings verify that the mean enhancement in COF was 43.81% in favor of 0.4 wt% ZnO + 0.2 wt% Graphene nano-oil. The nano-mixture was entirely adapted to deliver a uniform transfer layer throughout the sliding action, which decreased the coefficient of friction and wear rate. The lowest WSD was measured for the nanolubricant (0.4 wt% TiO_2 (A) + 0.2 wt% Graphene) compared with PBO-GII. The most diminutive scar wear diameter was 36.78% calculated for the (0.4 wt% ZnO + 0.2 wt% Graphene) nano-oil. The prominent diminishing in the specific wear rate was particularly for the dual mixture of (0.4 wt% TiO_2 (A) + 0.2 wt% Graphene). While the average enhancement in SWR was 39.47% for 0.4 wt% ZnO + 0.2 wt% Graphene nano-oil owing to the dispersion of the nanoscale (ZnO and Graphene) particulates on the mating surfaces. The standard deviation was computed for COF, WSD, and SWR which is integrated with diagrams to reveal the variation in the finding's values.

Metallographic characterization have been conducted after the tribological experiments. FE-SEM characterization revealed the morphological structures of each ball treated with different lubricants. The balls immersed in PBO-GII exhibited an extremely fluted portion separated from the exterior surface as a result of friction action and adhering wear. While the steel balls immersed with (0.4 wt% TiO_2 (A) + 0.2 wt% Graphene) demonstrated lowest adhering wear and no surface damaging as a consequence of the outstanding nano-oil. Likewise, a smooth texture was demonstrated when (0.4 wt% ZnO + 0.2 wt% Graphene) nano-oil suspension was employed. EDX/EDS spectroscopy exhibited

fundamental substances at the engaging surfaces and the ball surface remaining when simple lubricant or formulated lubricant was operated. An element map is an illustration displaying the spatial dispersion of particles in a specimen. EDX/EDS chemical spectroscopic and elements mapping affirmed the disposition of tribo-coating consists of nanoscale particles. Raman analysis was applied to further examine the existence of the TiO₂ anatase, ZnO, and graphene in different samples. The surface roughness for each AISI ball was investigated by a 3D visual (contactless) surface texture analyzing device.

The surface roughness of interacted balls is among the major testing in characterizing texture finish and abrasion and adhesion operation for each ball. The optical detection of a machined ball treated with (0.4 wt% TiO₂ (A) + 0.2 wt% Graphene) nano-oil and (0.4 wt% ZnO + 0.2 wt% Graphene) nanolubricant verifies that it was more even than the defected ball when treated with PBO-GII oil. The lowest profile roughness parameters Ra of 103.25 nm, Rq of 130.72 nm, and Rz of 550.93 nm were reported for the AISI ball surface treating with the (0.4 wt% TiO₂ (A) + 0.2 wt% Graphene) nano-oil, while the highest profile roughness parameters Ra, Rq, and Rz were reported for PBO-GII 475.56 nm, 1190 nm, and 4032.1 nm respectively. The minimum addressed values of profile roughness parameters were Ra=59.558 nm, Rq=78.837, and Rz=288.91 for (0.4 wt% ZnO + 0.2 wt% Graphene) nanolubricant, consecutively. The mean surface height Sa, which presents a well-known overall representation of the height differences, was the maximum 4.7822 μm for the additive-free lubricant and the minimum 2.1792 μm for (0.4 wt% TiO₂ (A) + 0.2 wt% Graphene) nano-oil. While roughness parameter Sa value was 2.8802 μm for the (0.4 wt% ZnO + 0.2 wt% Graphene) nanolubricant. Surface skewness (Ssk) and surface kurtosis (Sku) are two fundamental parameters specifying the asymmetry and the flatness of the surface configuration. The smaller Ssk is, the more moderate the friction we can presume, even at larger mean surface height Sa. Besides, friction diminishes when variable Sku rises. Surface roughness parameters Sku and Ssk can be employed to address

surfaces for appropriate tribological performance. Consequently, roughness variables S_{ku} and S_{sk} were analyzed to confirm the potential relationship with tribological characteristics. The obtained value of $S_{ku}=26.233$ for (0.4 wt% TiO_2 (A) + 0.2 wt% Graphene) nano-oil has better $S_{ku}=10.469$ than PBO-GII lubricant. While the optimal $S_{ku}=58.806$ was for (0.4 wt% ZnO + 0.2 wt% Graphene) nano-oil. On top of that, profile form measurement was implemented to confirm that employing dual nanolubricant is more advanced than additive-free lubricant. Thus, the surface depth $Z_2= -116.53$ for the PBO-GII oil was higher than $Z_2=5.3571$ for the (0.4 wt% TiO_2 (A) + 0.2 wt% Graphene) nano-oil. However, the lowest surface depth $Z_2 = 2.1306 \mu m$ was for (0.4 wt% ZnO + 0.2 wt% Graphene) formulated nano-oil.

CHAPTER 5: CONCLUSIONS AND RECOMMENDATIONS

5.1 Introduction

This work was dedicated to studying the lubrication performance of different nanoparticle mixtures as additives to API base oil Group II by utilizing several tribological and surface characterization devices.

The aim of the study was on lubrication performance improvement by employing a synergetic dual nanoparticles additive to reduce the friction of interaction, wear defects, and surface roughness among AISI balls.

The important contribution of this research was formulating a tribologically improved nano-oil while revealing the scarred morphologies, elements mapping, Raman spectra, and to distinguish the surface finish of AISI interacted balls by utilizing sophisticated surface roughness tool.

This research has illustrated the potential of synergetic nanoparticles lubricant in hopes that in future the microscale industry will upgrade the level of lubrication criteria towards efficient and economic lubrication solutions.

5.2 Conclusions

Much work has been made to explore and develop new sorts of lubricating oil nano-additive to diminish wear and friction in tribological configurations and to enhance surface morphology. It has been noted that the use of dual nano-additives should be examined for the lubricating capacity and durability of lubricant.

Transmission electron microscopy (TEM) was conducted for TiO₂ anatase, ZnO, and graphene to characterize the morphology of these nanostructures. Sonication treatment,

and dispersion stability analysis were performed after the formulation of nanoparticles with surfactant and API group II base oil (PBO-GII) for certain concentrations. A range of concentrations (0.0 wt%, 0.2 wt%, 0.4 wt%, and 0.6 wt% mg/ml) of two groups of dual nanoparticles which include (TiO₂ Anatase + Graphene) and (ZnO + Graphene) were blended with PBO-GII individually to identify the minimum friction and wear losses that occur during sliding contact. Moreover, tribological experiments were conducted to find out (coefficient of friction, wear scar diameter, and specific wear rate) for each sample/lubricant. The investigations were further aided by surface characterization tools FE-SEM, EDX/EDS, and elements mapping microanalyses to examine the worn area on each ball. What is more, Raman scattering utilized for additional investigation of the existence/behavior of (TiO₂ (A) + Graphene) and (ZnO + Graphene) on the AISI balls. In addition, a 3-dimensional optical (contact-free) surface texture analyzer utilized to scan the defected area on each ball. Furthermore, surface roughness measurements (profile roughness measurement, surface texture measurement, surface skewness and surface kurtosis measurement, and profile form measurement) carried out for describing surface finish, friction, and wear behavior of all samples.

This study demonstrated the crucial role of dual nanoparticles (TiO₂ (A) + Graphene) and (ZnO + Graphene) in improving the tribological properties via surface activity of the additives (confirmed by the COF, WSD, SWR, FE-SEM, EDX/EDS, elements mapping, Raman spectra, and surface roughness measurements). The exact synergy effect of the superior blended nanolubricants structure remarkably diminished the COF, WSD, and SWR values.

Based on the results obtained by experiments work, the following main conclusions can be listed:

1. The investigation of dual nanoscale particles (TiO_2 (A) + Graphene) reported that the nanolubricant (0.4 wt% TiO_2 (A) + 0.2 wt% Graphene) revealed significant values for the performance parameters considered.
2. The average reduction in COF, WSD, and SWR after an hour was 38.83%, 36.78%, and 15.78% respectively for (0.4 wt% TiO_2 (A) + 0.2 wt% Graphene) nanolubricant compared to PBO-GII.
3. The formation of a tribofilm of nanoparticles (TiO_2 (A) + Graphene) on the worn contacts protected the surfaces of the balls from severe friction and adhesion wear was approved via FE-SEM, EDX/EDS, elements mapping, Raman spectra, and surface roughness measurements.
4. This phenomenon proved the significance of uniform nanoparticle dispersion for enhanced wear protection.
5. Another investigation was for dual nanoscale particles (ZnO + Graphene) while, three types of analyses (coefficient of friction, wear scar diameter, and specific wear rate) was conducted to calculate and evaluate the tribological performance of lubricants.
6. The ZnO and graphene nanoparticles exhibited wear and friction improving characteristics as a standard oil additive. The average reduction in COF, WSD, and SWR was 43.81%, 36.78%, and 39.47% respectively, for (0.4 wt% ZnO + 0.2 wt% Graphene) nano-oil in comparison with PBO-GII lubricant.
7. The mix of ZnO and graphene nanoparticles formed a flexible tribolayer on the scar surface during sliding activity and led to significant tribological properties.
8. The superb lubrication performance was due to the tribofilm as a result of the nanoparticle mixture deposition on the mating metal surfaces during sliding motion. The tribofilm had relatively low hardness and stuck on the balls during sliding movement.

9. The driving force for nanomaterials (TiO_2 (A) + Graphene) and (ZnO + Graphene) in base stock entering the contacting surfaces throughout three mechanisms:
- micro rolling bearing effect,
 - depositing film effect, and
 - mending effect.
10. It can be seen obviously selecting a combination of nanoparticles has shown better results than API base oil Group II.
11. (0.4 wt% ZnO + 0.2 wt% Graphene) nanolubricant has exhibited superior tribological properties compared with all-types of lubricants.
12. The synergetic effect of nanoparticles has created a tribofilm that protects the ball surface from the friction and extreme damage of wear.
13. The three types of calculations (coefficient of friction, wear scar diameter, and specific wear rate) was clearly demonstrated and evaluated the tribological performance of all lubricants.
14. The surface characterization tools TEM, FE-SEM, EDX/EDS, elements mapping, Raman spectra, and surface roughness measurements have certainly described the nanostructure role and lubrication mechanisms.

5.3 Recommendations for Future Work

Nowadays, nanomaterials become a skeleton bone in advance technology. These nano-smart materials have broad applications in several industries. Moreover, there are many companies worldwide that would like to improve and upgrade the lube oil and enhance its performance. For this purpose, there is a big concern for improving the lube oil by using nanotechnology and more precisely with using nanomaterials. Therefore, several forthcoming study areas can be done, such as:

1. Examining different metal oxides such as CuO, ZrO₂, Fe₃O₄, and Al₂O₃ with graphene and figure out the excellent nano-oil for better tribological behavior.
2. Using Group III base stock instead of Group II base oil and find out the potential tribological properties with certain nano-additives.
3. It would be interesting to examine Zinc Dialkyl Dithiophosphates (ZDDPs) (probably C4-C8) with group two base stock for cost-saving and considerable tribological performance. Moreover, ZDDPs are very effective antiwear agents that are used as machine lubricants with (greases, hydraulic oils, or motor oils), including applications in the automotive industry.
4. Bio-based or synthetic oils (Group IV – PAOs) or (Group V – esters) instead of Group II base stock and figure out the hypothetical tribological performance.
5. Determining other desirable qualities such as oxidation stability, high viscosity index, low pour point, low volatility, high flash point, antifoaming, and excellent demulsibility by formulating the same or different base oil with same or various nanoparticles to achieve these qualities.
6. Understanding and discovering the steady dispersions by utilizing a proper type and concentrations of a nanoscale particle together with surfactant or surface modification. The dispersion stability findings reveal that for similar base oil and surface agents, the stability of the suspensions varies by changing the nanoparticle concentrations. The dispersion balance is directly connected to the tribological behavior of nanoparticles mixed with oil. From this perspective, future researches can explore several mixtures among a diversity of base stocks, surface agents, nanoscale particles in terms of (types, size, concentrations, morphology, structure), surface modification techniques and dispersion techniques.

7. Exploring the nano-oils tribological behavior by blending with ionic liquids (ILs) - Current advancements in the application of ionic liquids as hypothetical competitors for lubricants and lubricant additives could be beneficial to tackle the environmental matters. In this area, multiple combinations of nanoparticles, ionic liquids, and bio-based stocks can be studied.
8. For specific applications, exploring the performance of the lubricants by setting genuine lubricating oil conditions. A notable variation in the concentrations and effects of frictional torque and wear volumes will be reported in order to explain the adaptability of oils for specific applications.

University of Malaya

REFERENCES

- A. E. Jiménez, M. D. B. (2010). Ionic Liquids as Lubricants of Titanium–Steel Contact. Part 2: Friction, Wear and Surface Interactions at High Temperature. *Tribology Letters*, 37(2), 431-443. doi:10.1007/s11249-009-9539-y
- A. Hernandez Battez, R. G., D. Felgueroso, J.E. Fernandez, Ma. del Rocío Fernandez, M.A. Garcia, I. Penueles. (2007). Wear prevention behaviour of nanoparticle suspension under extreme pressure conditions. *Wear*, 263(7–12), 1568–1574. Retrieved from http://ac.els-cdn.com/S004316480700405X/1-s2.0-S004316480700405X-main.pdf?_tid=da30d642-6057-11e6-84c6-00000aacb35e&acdnat=1470984292_889dc05811e5780cf586ab1e252df2b0
- A.K. Rasheed, M. K., W. Rashmi, T.C.S.M. Gupta, A. Chan. (2016). Graphene based nanofluids and nanolubricants – Review of recent developments. *Renewable and Sustainable Energy Reviews*, 63, 346–362. Retrieved from http://ac.els-cdn.com/S1364032116301058/1-s2.0-S1364032116301058-main.pdf?_tid=1ba8dbd4-6147-11e6-8187-00000aacb35e&acdnat=1471087051_8f587523b133ad54a2d714d9c7171644
- Abdullah, M. I. H. C., Abdollah, M. F., Amiruddin, H., Tamaldin, N., & Nuri, N. R. M. (2014). Effect of hBN/Al₂O₃ nanoparticle additives on the tribological performance of engine oil. *Jurnal Teknologi*, 66(3).
- Abdullah, M. I. H. C., Abdollah, M. F. B., Tamaldin, N., Amiruddin, H., Mat Nuri, N. R., Gachot, C., & Kaleli, H. (2016). Effect of hexagonal boron nitride nanoparticles as an additive on the extreme pressure properties of engine oil. *Industrial Lubrication and Tribology*, 4(68), 441-445.
- Adli Bahari, R. L. T. S. (2017). Friction and Wear Phenomena of Vegetable Oil–Based Lubricants with Additives at Severe Sliding Wear Conditions. *Tribology Transactions*, 1-13.
- Akbulut, M. (2012). Nanoparticle-based lubrication systems. *Journal of Powder Metallurgy & Mining* 1(1). doi:10.4172/2168-9806.1000e101
- Alves, S. M., Barros, B. S., Trajano, M. F., Ribeiro, K. S. B., & Moura, E. (2013). Tribological behavior of vegetable oil-based lubricants with nanoparticles of oxides in boundary lubrication conditions. *Tribology International*, 65(0), 28-36. Retrieved from <http://www.sciencedirect.com/science/article/pii/S0301679X13001734>
- Amiruddin, H., Abdollah, M., Idris, A., Abdullah, M., & Tamaldin, N. (2015). *Stability of nano-oil by pH control in stationary conditions*. Paper presented at the Mechanical Engineering Research Day MERD'15.
- Amit Suhane, R. M. S., A.Rehman and H.K.Khaira. (2014). Experimental Study of Castor Oil Based Lubricant for Automotive Applications. *Journal of Engineering*

Research and Applications www.ijera.com, 4(1), 104-107. Retrieved from http://www.ijera.com/papers/Vol4_issue1/Version%201/P4101104107.pdf

- Anna Góral, L. L.-D., and Marcin Kot. (2017). Effect of Surface Roughness and Structure Features on Tribological Properties of Electrodeposited Nanocrystalline Ni and Ni/Al₂O₃ Coatings. *Journal of Materials Engineering and Performance*, 26(5), 2118–2128.
- Arumugam, S., & Sriram, G. (2014). Synthesis and characterization of rapeseed oil bio-lubricant dispersed with nano copper oxide: Its effect on wear and frictional behavior of piston ring–cylinder liner combination. *Proceedings of the Institution of Mechanical Engineers, Part J: Journal of Engineering Tribology*, 228(11), 1308-1318.
- Asrul, M., Zulkifli, N. W. M., Masjuki, H. H., & Kalam, M. A. (2013). Tribological properties and lubricant mechanism of nanoparticle in engine oil. *Procedia Engineering*, 68, 320-325.
- Batista, C. A. S. L., Ronald G.; Kotov, Nicholas A. . (2015). Nonadditivity of nanoparticle interactions. *Science*, 350(6257), 1242477. doi:10.1126/science.1242477
- Battez, H. A., Fernandez Rico, J. E., Navas Arias, A., Viesca Rodriguez, J. L., Chou Rodriguez, R., & Diaz Fernandez, J. M. (2006). The tribological behaviour of ZnO nanoparticles as an additive to PAO6. *Wear*, 261(3–4), 256-263. Retrieved from <http://www.sciencedirect.com/science/article/pii/S0043164805004886>
- Battez, H. A., González, R., Viesca, J. L., Fernández, J. E., Fernández, D. J. M., Machado, A., . . . Riba, J. (2008). CuO, ZrO₂ and ZnO nanoparticles as antiwear additive in oil lubricants. *Wear*, 265(3), 422-428.
- C. Zhao, Y. K. C., Y. Jiao, A. Loya, G.G. Ren. (2014). The preparation and tribological properties of surface modified zinc borate ultrafine powder as a lubricant additive in liquid paraffin. *Tribology International*, 70, 155–164. doi:10.1016/j.triboint.2013.10.007
- Çelik, O. N., Ay, N., & Göncü, Y. (2013). Effect of nano hexagonal boron nitride lubricant additives on the friction and wear properties of AISI 4140 steel. *Particulate Science and Technology*, 31(5), 501-506. Retrieved from <http://dx.doi.org/10.1080/02726351.2013.779336>
- Chen, S., & Liu, W. (2006). Oleic acid capped PbS nanoparticles: Synthesis, characterization and tribological properties. *Materials Chemistry and Physics*, 98(1), 183-189. Retrieved from <http://www.sciencedirect.com/science/article/pii/S0254058405006255>
- Chia-Jui Hsu, A. S., Andreas Rosenkranz and Carsten Gachot. (2017). Enhanced Growth of ZDDP-Based Tribofilms on Laser-Interference Patterned Cylinder Roller Bearings. *Lubricants*, 5(4), 39. doi:doi:10.3390/lubricants5040039
- Chiñas-Castillo, F., & Spikes, H. . (2003). Mechanism of action of colloidal solid dispersions. *Journal of Tribology*, 3(125), 552-557.

- Cho, Y., Park, J., Ku, B., Lee, J., Park, W.-G., Lee, J., & Kim, S. H. (2012). Synergistic effect of a coating and nano-oil lubricant on the tribological properties of friction surfaces. *INTERNATIONAL JOURNAL OF PRECISION ENGINEERING AND MANUFACTURING*, 1(13), 97-102.
- Chou, R., Battez, A. H., Cabello, J. J., Viesca, J. L., Osorio, A., & Sagastume, A. (2010). Tribological behavior of polyalphaolefin with the addition of nickel nanoparticles. *Tribology International*, 43(12), 2327-2332. Retrieved from <http://www.sciencedirect.com/science/article/pii/S0301679X1000201X>
- Chuanli Zhaoa, Y. K. C., G. Rena. (2013). A Study of Tribological Properties of Water-Based Ceria Nanofluids. *Tribology Transactions*, 56(2), 275-283. doi:10.1080/10402004.2012.748948
- D N Montenegro, V. H., O Mart'inez, M C Mart'inez-Tomas, V Sallet, V Munoz-Sanjose´ and J Jimenez. (2013). Non-radiative recombination centres in catalyst-free ZnO nanorods grown by atmospheric-metal organic chemical vapour deposition. *Journal of Physics D: Applied Physics*, 46(Number 23), 0022-3727.
- D. P. Macwan, P. N. D., Shalini Chaturvedi. (2011). A review on nano-TiO₂ sol-gel type syntheses and its applications. *Journal of Materials Science*, 46, 3669–3686. doi:10.1007/s10853-011-5378-y
- Dae-Hyun Cho, J. J. Y.-Z. L. (2015). Effects of Oxide Layer Formation during Lubricated Sliding on the Frictional Properties of Titanium-Coated Silicon. *Tribology Transactions*, 58(1), 44-50.
- Debrupa Lahiri, F. H., Mikael Thiesse, Andriy Durygin, Cheng Zhang, Arvind Agarwal. (2014). Nanotribological behavior of graphene nanoplatelet reinforced ultra high molecular weight polyethylene composites. *Tribology International*, 70, 165–169. doi:10.1016/j.triboint.2013.10.012
- Demas, N. G., Timofeeva, E. V., Routbort, J. L., & Fenske, G. R. (2012). Tribological effects of BN and MoS₂ nanoparticles added to polyalphaolefin oil in piston skirt/cylinder liner tests. *Tribology Letters*, 47(1), 91-102.
- Diana Berman, A. E., Anirudha V. Sumant. (2014). Graphene: a new emerging lubricant. *Materials Today*, 17(1).
- Einstein, A. (1905). On the movement of small particles suspended in a stationary liquid demanded by the molecular-kinetic theory of heart. *Annalen der physik*, 17, 549-560. .
- Emad Sadeghinezhad, M. M., R. Saidur, Mehdi Mehrali, Sara Tahan Latibari, Amir Reza Akhiani, Hendrik Simon Cornelis Metselaar. (2016). A comprehensive review on graphene nanofluids: Recent research, development and applications. *Energy Conversion and Management*, 111, 466–487. Retrieved from http://ac.els-cdn.com/S0196890416000200/1-s2.0-S0196890416000200-main.pdf?_tid=30852520-628d-11e6-9552-00000aacb35d&acdnat=1471227102_50dc6a58809b0afae8a31365ed1778c9

- Ettefaghi, E.-o.-l., Ahmadi, H., Rashidi, A., & Mohtasebi, S.-S. (2013). Investigation of the anti-wear properties of nano additives on sliding bearings of internal combustion engines. *International Journal of Precision Engineering and Manufacturing*, 14(5), 805-809.
- F. A. Essa, Q. Z., Xingjiu Huang, Mohamed Kamal Ahmed Ali, Ahmed Elagouz, Mohamed, A. A. Abdelkareem. (2017). Effects of ZnO and MoS₂ Solid Lubricants on Mechanical and Tribological Properties of M50-Steel-Based Composites at High Temperatures: Experimental and Simulation Study. *Tribology Letters*, 65(97).
- F. Sundus, H. H. M. M. A. F. (2017). Analysis of Tribological Properties of Palm Biodiesel and Oxidized Biodiesel Blends. *Tribology Transactions*, 60(3), 530-536
- F.A. Essa, Q. Z., Xingjiu Huang. (2017). Investigation of the effects of mixtures of WS₂ and ZnO solid lubricants on the sliding friction and wear of M50 steel against silicon nitride at elevated temperatures. *Wear*, 374–375, 128-141. doi:10.1016/j.wear.2017.01.098
- Falvo, M. R., & Superfine, R. (2000). Mechanics and Friction at the Nanometer Scale. *Journal of Nanoparticle Research*, 3, 237-248.
- Fenske G, E. R., Ajayi O, Masoner A, Comfort A. (2009). *Impact of friction reduction technologies on fuel economy for ground vehicles*. Paper presented at the DIAs Ground Vehicle Systems Engineering and Technology Symposium (GVSETS) Troy, Michigan, USA.
- Fernandez, J. E., Viesca, J. L., & Battez, H. A. (2008). *Tribological behaviour of copper oxide nanoparticle suspension*. Paper presented at the Lubrication Management and Technology Conference & Exhibition, San Sebastian, Spain.
- Fox, N., & Stachowiak, G. (2003). Boundary lubrication properties of oxidized sunflower oil. *Tribology & Lubrication Technology*, , 2(59), 15.
- G.M. Krolczyk, R. W. M., J.B. Krolczyk, P. Nieslony, S. Wojciechowski, S. Legutko. (2018). Parametric and nonparametric description of the surface topography in the dry and MQCL cutting conditions. *Measurement* 121, 225–239.
- Gao, C., Wang, Y., Hu, D., Pan, Z., & Xiang, L. (2013). Tribological properties of magnetite nanoparticles with various morphologies as lubricating additives. *Journal of Nanoparticle Research*, 15(3), 1-10. Retrieved from <http://dx.doi.org/10.1007/s11051-013-1502-z>
- Ghaednia, H. (2014). *An Analytical and Experimental Investigation of Nanoparticle Lubricants*. Auburn University,
- Ginzburg, B., Shibaev, L., Kireenko, O., Shepelevskii, A., Baidakova, M., & Sitnikova, A. (2002). Antiwear Effect of Fullerene C₆₀ Additives to Lubricating Oils. *Russian journal of applied chemistry*, 8 (75), 1330-1335.

- Granqvist, C. G., Buhrman, R. A., Wyns, J., & Sievers, A. J. (1976). Far-Infrared Absorption in Ultrafine Al Particles. *Physical Review Letters*, 37(10), 625-629. doi:10.1103/PhysRevLett.37.625
- Grushcow, J., & Smith, M. (2005). *Next generation feedstocks from new frontiers in oilseed engineering*. Paper presented at the Paper presented at the World Tribology Congress III.
- Gullac, B., & Akalin, O. (2010). Frictional characteristics of IF-WS₂ nanoparticles in simulated engine conditions. *Tribology Transactions*, 53(6), 939-947.
- H. Kato, K. K. (2007). Tribofilm formation and mild wear by tribo-sintering of nanometer-sized oxide particles on rubbing steel surfaces. *Wear*, 262(1–2), 36–41. doi:10.1016/j.wear.2006.03.046
- Hakimizad, A. B. K. R. A. (2015). An investigation of the characteristics of Al₂O₃/TiO₂ PEO nanocomposite coating. *Applied Surface Science*, 351(1), 13-26.
- Hao-Jie Song, Z.-Z. Z., Xue-Hu Men, Zhuang-Zhu Luo. (2010). A study of the tribological behavior of nano-ZnO-filled polyurethane composite coatings. *Wear*, 269(1–2), 79–85. Retrieved from http://ac.els-cdn.com/S0043164810001146/1-s2.0-S0043164810001146-main.pdf?_tid=8629b140-610b-11e6-8187-00000aacb35e&acdnat=1471061460_e8bbebf7d0f23b08ff9499fe8a05e225
- Hayrettin Düzcükoğlua, Ş. E., Ömer Sinan Şahinb, Ahmet Avcıc, Mürsel Ekremc & Mahmut Ünalda. (2015). Enhancement of Wear and Friction Characteristics of Epoxy Resin by Multiwall Carbon Nano Tube and Boron Nitride Nano Particles. *Tribology Transactions*, 58(4), 635-642
- Heba Isawi, M. H. E.-S., Xianshe Feng, Hosam Shawkya, Mohamed S. Abdel Mottaleb. (2016). Surface nanostructuring of thin film composite membranes via grafting polymerization and incorporation of ZnO nanoparticles. *Applied Surface Science*, 385, 268–281. Retrieved from http://ac.els-cdn.com/S0169433216311710/1-s2.0-S0169433216311710-main.pdf?_tid=e26461b6-606c-11e6-8781-00000aacb35d&acdnat=1470993325_77ab5a226ea9a6d7528c452246b9dac7
- Hendrik Heinz, C. P., Ozge Heinz, Yifu Ding, Ratan K. Mishra, Delphine Marchon, Robert J. Flatt, Irina Estrela-Lopis, Jordi Llop, Sergio Moya, Ronald F. Ziolo. (2017). Nanoparticle decoration with surfactants: Molecular interactions, assembly, and applications. *Surface Science Reports*, 72(1), 1-58. doi:<https://doi.org/10.1016/j.surfrep.2017.02.001>
- Holmberg K, A. P., Erdemir A. . (2012). Global energy consumption due to friction in passenger cars. *Tribology International*, 47, 221-234. doi:10.1016/j.triboint.2011.11.022
- Hongxing Wu, L. Q., Guangneng Dong, Meng Hua, Shuncheng Yang, Junfeng Zhang. (2017). An investigation on the lubrication mechanism of MoS₂ nano sheet in point contact: The manner of particle entering the contact area. *Tribology International*, 107, 48-55.

- Hongxuan Li, T. X., Chengbing Wang, Jianmin Chen, Huidi Zhou, Huiwen Liu. (2006). Friction-induced physical and chemical interactions among diamond-like carbon film, steel ball and water and/or oxygen molecules. *Diamond and Related Materials*, 15(9), 1228–1234. doi:10.1016/j.diamond.2005.09.038
- Horst Czichos, M. W. (2017). Introduction to Tribology and Tribological Parameters. In G. E. Totten (Ed.), *Friction, Lubrication, and Wear Technology* (Vol. 18, pp. 3 - 15): ASM Handbook.
- Hu, K. H., Huang, F., Hu, X. G., Xu, Y. F., & Zhou, Y. Q. (2011). Synergistic effect of Nano-MoS₂ and anatase Nano-TiO₂ on the lubrication properties of MoS₂/TiO₂ Nano-Clusters. *Tribology Letters*, 43(1), 77-87.
- Hu, Z. S., Lai, R., Lou, F., Wang, L. G., Chen, Z. L., Chen, G. X., & Dong, J. X. (2002). Preparation and tribological properties of nanometer magnesium borate as lubricating oil additive. *Wear*, 5–6(252), 370-374.
- Hui Wu, J. Z., Liang Luo, Shuiquan Huang, Lianzhou Wang, Suoquan Zhang, Sihai Jiao, Han Huang, and Zhengyi Jiang. (2018). Performance evaluation and lubrication mechanism of water-based nanolubricants containing nano-TiO₂ in hot steel rolling. *Lubricants*, 6(57). doi:10.3390/lubricants6030057
- I. Tzanakis, M. H., B. Thomas, S.M. Noya, I. Henshaw, S. Austen. (2012). Future perspectives on sustainable tribology. *Renewable and Sustainable Energy Reviews*, 16(6), 4126-4140. doi:<https://doi.org/10.1016/j.rser.2012.02.064>
- Irena Nowotyńska, S. K. (2014). Examining the Effect of the Die Angle on Tool Load and Wear in the Extrusion Process. *Journal of Materials Engineering and Performance*, 23(4), 1307–1312. Retrieved from http://download.springer.com/static/pdf/567/art%253A10.1007%252Fs11665-014-0872-4.pdf?originUrl=http%3A%2F%2Flink.springer.com%2Farticle%2F10.1007%2Fs11665-014-0872-4&token2=exp=1471794646~acl=%2Fstatic%2Fpdf%2F567%2Fart%25253A10.1007%25252Fs11665-014-0872-4.pdf%3ForiginUrl%3Dhttp%253A%252F%252Flink.springer.com%252Farticle%252F10.1007%252Fs11665-014-0872-4*~hmac=349c14d55da7e58ce397346af6c554eb44a002793d6772a1445b36be8ad6c0d1
- Jatti, V. S., & Singh, T. P. (2015). Copper oxide nano-particles as friction-reduction and anti-wear additives in lubricating oil. *Journal of Mechanical Science and Technology*, 29(2), 793-798. Retrieved from <http://dx.doi.org/10.1007/s12206-015-0141-y>
- Jayadas, N., & Prabhakaran Nair, K. (2007). Tribological evaluation of coconut oil as an environment-friendly lubricant. *Tribology International*, 2(40), 350-354.
- Jeffrey M. Guevremont, G. H. G., Dewey Szemenyei, Mark T. Devlin and Tze-Chi Jao (2008). Enhancement of Engine Oil Wear and Friction Control Performance through Titanium Additive Chemistry. *Tribology Transactions*, 51(3), 324-331.

- Jiao, D., Zheng, S., Wang, Y., Guan, R., & Cao, B. (2011). The tribology properties of alumina/silica composite nanoparticles as lubricant additives. *Applied Surface Science*, 257(13), 5720-5725. Retrieved from <http://www.sciencedirect.com/science/article/pii/S0169433211001206>
- Jien-Min Wu, S.-J. L., Jien-Wei Yeh, Swe-Kai Chen, Yuan-Sheng Huang, Hung-Cheng Chen. (2006). Adhesive wear behavior of Al_xCoCrCuFeNi high-entropy alloys as a function of aluminum content. *Wear*, 261(5–6), 513–519. doi:10.1016/j.wear.2005.12.008
- Joly-Pottuz, L., Vacher, B., Ohmae, N., Martin, J. M., & Epicier, T. (2008). Anti-wear and friction reducing mechanisms of carbon nano-onions as lubricant additives. *Tribology Letters*, 30(1), 69-80. Retrieved from <http://dx.doi.org/10.1007/s11249-008-9316-3>
- Joseph Goldstein, D. E. N., David C. Joy, Charles E. Lyman, Patrick Echlin, Eric Lifshin, Linda Sawyer, J.R. Michael. (2003). *Scanning Electron Microscopy and X-Ray Microanalysis* (Third ed.): Springer.
- Jost, H. P., Great Britain. Department of, E., Science, Jost, H. P., Great Britain. Department of, E., Science, . . . Science. (1966). *Lubrication (tribology) : education and research : a report on the present position and industry's needs*. London: H.M.S.O.
- Juozas Padgurskas, R. R., Igoris Prosyčevs, Raimondas Kreivaitis. (2013). Tribological properties of lubricant additives of Fe, Cu and Co nanoparticles. *Tribology International*, 60, 224–232.
- K. S. Novoselov, A. K. G., S. V. Morozov, D. Jiang, Y. Zhang, S. V. Dubonos, I. V. Grigorieva, A. A. Firsov. (2004). Electric Field Effect in Atomically Thin Carbon Films. *Science*, 306(5696), 666-669. Retrieved from <http://science.sciencemag.org/content/sci/306/5696/666.full.pdf>
- Kolodziejczyk, L., Martinez-Martinez, D., Rojas, T., Fernandez, A., & Sanchez-Lopez, J. (2007). Surface-modified Pd nanoparticles as a superior additive for lubrication. *Journal of Nanoparticle Research*, 9(4), 639-645.
- Kong, L., Sun, J., & Bao, Y. (2017). Preparation, characterization and tribological mechanism of nanofluids. *RSC Advances*, 7(21), 12599-12609. doi:10.1039/C6RA28243A
- Koshy, C. P., Rajendrakumar, P. K., & Thottackkad, M. V. (2015). Evaluation of the tribological and thermo-physical properties of coconut oil added with MoS₂ nanoparticles at elevated temperatures. *Wear*, 330–331, 288-308. Retrieved from <http://www.sciencedirect.com/science/article/pii/S0043164814004244>
- Kwangho Lee, Y. H., Seongir Cheong, Youngmin Choi, Laeun Kwon, Jaekeun Lee, Soo Hyung Kim. (2009). Understanding the Role of Nanoparticles in Nano-oil Lubrication. *Tribology Letters*, 35, 127–131. doi:10.1007/s11249-009-9441-7
- L. Rapoport, V. L., I.Lapskera, Yu. Volovik, O. Nepomnyashchy, M. Lvovsky, R. Popovitz-Biro, Y. Feldman R. Tenne. (2003). Tribological properties of WS₂

nanoparticles under mixed lubrication. *Wear*, 7-12(255), 785-793.
doi:[https://doi.org/10.1016/S0043-1648\(03\)00044-9](https://doi.org/10.1016/S0043-1648(03)00044-9)

- Laad, M., & Jatti, V. K. S. (2016). Titanium oxide nanoparticles as additives in engine oil. *Journal of King Saud University-Engineering Sciences*. doi:10.1016/j.jksues.2016.01.008
- Lee, C.-G., Hwang, Y.-J., Choi, Y.-M., Lee, J.-K., Choi, C., & Oh, J.-M. (2009). A study on the tribological characteristics of graphite nano lubricants. *International Journal of Precision Engineering and Manufacturing*, 10(1), 85-90.
- Lee, K., Hwang, Y., Cheong, S., Choi, Y., Kwon, L., Lee, J., & Kim, S. H. (2009). Understanding the role of nanoparticles in nano-oil lubrication. *Tribology Letters*, 2(35), 127-131.
- Li, W., Zheng, S., Cao, B., & Ma, S. (2011). Friction and wear properties of ZrO₂/SiO₂ composite nanoparticles. *Journal of Nanoparticle Research*, 13(5), 2129-2137. Retrieved from <http://dx.doi.org/10.1007/s11051-010-9970-x>
- Liu, G., Li, X., Lu, N., & Fan, R. (2005). Enhancing AW/EP property of lubricant oil by adding nano Al/Sn particles. *Tribology Letters*, 18(1), 85-90.
- Liu, G., Li, X., Qin, B., Xing, D., Guo, Y., & Fan, R. (2004). Investigation of the mending effect and mechanism of copper nano-particles on a tribologically stressed surface. *Tribology Letters*, 4(17), 961-966.
- Lubrication, M. (2019). Base Oil Groups Explained. Retrieved from <https://www.machinerylubrication.com/Read/29113/base-oil-groups>
- Lukas Bogunovic, S. Z., Katja Toensing and Dario Anselmetti. (2015). An Oil-Based Lubrication System Based on Nanoparticulate TiO₂ with Superior Friction and Wear Properties. *Tribology Letters*, 59(2). doi:DOI 10.1007/s11249-015-0557-7
- Luo, T., Wei, X., Huang, X., Huang, L., & Yang, F. (2014). Tribological properties of Al₂O₃ nanoparticles as lubricating oil additives. *Ceramics International*, 40(5), 7143-7149. Retrieved from <http://www.sciencedirect.com/science/article/pii/S0272884213016660>
- M. Gulzar, H. H. M., M. A. Kalam, M. Varman, N. W. M. Zulkifli, R. A. Mufti, Rehan Zahid. (2016). Tribological performance of nanoparticles as lubricating oil additives. *Journal of Nanoparticle Research*, 8(18), 223.
- M. Gulzar, H. M., M Varman, MA Kalam, R.A. Mufti, NWM Zulkifli, R. Yunus, Rehan Zahid. (2015). Improving the AW/EP ability of chemically modified palm oil by adding CuO and MoS₂ nanoparticles. *Tribology International*, 88, 271-279.
- M. Salem, S. A., I. Massoudi, Y. Litaïem, M. Gaidi, K. Khirouni. (2018). Photoelectrochemical and optical properties tuning of graphene-ZnO nanocomposites. *Journal of Alloys and Compounds*, 767, 982-987. doi:10.1016/j.jallcom.2018.07.202

- M. Vijayaraj, S. K. H., A. K. Harinarain & S. S. V. Ramakumar. (2016). Tribochemical Transformation of Nano TiO₂ to Ilmenite on the Surface of Wearing Steel Parts: Antiwear Action of Nano TiO₂ as an Additive in Engine Oil. *Tribology Transactions*, 59(3), 435-440.
- Ma, S., Zheng, S., Cao, D., & Guo, H. (2010). Anti-wear and friction performance of ZrO₂ nanoparticles as lubricant additive. *Particuology*, 5(8), 468-472.
- Mallika Dasari, M. P. H., Haiyan Fan-Hagenstein, Brice Adam Russell, Aldo D. Migone and Punit Kohli. (2018). Large area ultra-thin graphene films for functional photovoltaic devices. *Journal of Materials Research*, 33(16), 2306-2317.
- Manjula G. Nair, M. N., K. Rekha, A. Anukaliani. (2011). Structural, optical, photo catalytic and antibacterial activity of ZnO and Co doped ZnO nanoparticles. *Materials Letters*, 65(12), 1797–1800. Retrieved from http://ac.els-cdn.com/S0167577X1100334X/1-s2.0-S0167577X1100334X-main.pdf?_tid=3d7d6e0a-6070-11e6-af36-00000aab0f27&acdnat=1470994766_73fe7eb987fdea11db8bab8d34bc2028
- Mark Winter, T. U. o. S. a. W. L., UK. (2019). Zinc oxide. Retrieved from https://www.webelements.com/compounds/zinc/zinc_oxide.html
- Marko Sedlaček, B. P., Jože Vižintin. (2012). Correlation between standard roughness parameters skewness and kurtosis and tribological behaviour of contact surfaces. *Tribology International*, 48, 102-112. doi:<https://doi.org/10.1016/j.triboint.2011.11.008>
- Marko Sedlaček, P. G. B. P. (2017). Use of the Roughness Parameters Ssk and Sku to Control Friction—A Method for Designing Surface Texturing. *Tribology Transactions*, 60(2), 260-266.
- Masjuki, H., & Maleque, M. (1997). Investigation of the anti-wear characteristics of palm oil methyl ester using a four-ball tribometer test. *Wear*, 1(206), 179-186.
- Masjuki, H., Maleque, M., Kubo, A., & Nonaka, T. (1999). Palm oil and mineral oil based lubricants—their tribological and emission performance. *Tribology International*, 6(32), 305-314.
- Mikel Aingeru Urchegui, W. T., Xabier Gómez. (2008). Wear Evolution in a Stranded Rope Subjected to Cyclic Bending. *Journal of Materials Engineering and Performance*, 17(4), 550–560. Retrieved from http://download.springer.com/static/pdf/264/art%253A10.1007%252Fs11665-007-9165-5.pdf?originUrl=http%3A%2F%2Flink.springer.com%2Farticle%2F10.1007%252Fs11665-007-9165-5&token2=exp=1471423625~acl=%2Fstatic%2Fpdf%2F264%2Fart%25253A10.1007%25252Fs11665-007-9165-5.pdf%3ForiginUrl%3Dhttp%253A%252F%252Flink.springer.com%252Farticle%252F10.1007%252Fs11665-007-9165-5*~hmac=f459274cf558575172173ba70840bd1eef1f9753f58c3cca02f4f75f918fd2b5

- Min, Y., Akbulut, M., Kristiansen, K., Golan, Y., & Israelachvili, J. (2008). The role of interparticle and external forces in nanoparticle assembly. *Nature materials*, 7(7), 527-538.
- Mohamed Kamal Ahmed Ali, H. X., Liqiang Mai, Cai Qingping, Richard Fiifi Turkson, Chen Bicheng. (2016). Improving the tribological characteristics of piston ring assembly in automotive engines using Al₂O₃ and TiO₂ nanomaterials as nano-lubricant additives. *Tribology International*, 103, 540–554.
- Mohammad Mehrali, S. T. L., Mehdi Mehrali, Teuku Meurah Indra Mahlia, Hendrik Simon Cornelis Metselaar. (2013). Preparation and properties of highly conductive palmitic acid/graphene oxide composites as thermal energy storage materials. *Energy*, 58, 628–634. Retrieved from http://ac.els-cdn.com/S0360544213004696/1-s2.0-S0360544213004696-main.pdf?_tid=e34992ae-6292-11e6-80c0-00000aab0f26&acdnat=1471229550_e378774b4dd50c73155a2e95cd721f4c
- Mohammad Mehrali, S. T. L., Mehdi Mehrali, Teuku Meurah Indra Mahlia, Hendrik Simon Cornelis Metselaar, Mohammad Sajad Naghavi, Emad Sadeghinezhad, Amir Reza Akhiani. (2013). Preparation and characterization of palmitic acid/graphene nanoplatelets composite with remarkable thermal conductivity as a novel shape-stabilized phase change material. *Applied Thermal Engineering*, 61(2), 633–640. Retrieved from http://ac.els-cdn.com/S1359431113006212/1-s2.0-S1359431113006212-main.pdf?_tid=92180ae4-6294-11e6-9fd0-00000aab0f27&acdnat=1471230272_28b56b16a515e2490cde28ae8369edc0
- Moly, L. (2019). Base Oil Types and Variations. Retrieved from <https://liquimolymalaysia.my/blogs/news/base-oil-types-and-variations>
- Monireh B. Moghaddam, E. K. G., Mohammad H. Entezari, Paul Nancarrow. (2013). Preparation, characterization, and rheological properties of graphene–glycerol nanofluids. *Chemical Engineering Journal*, 231, 365–372. Retrieved from http://ac.els-cdn.com/S1385894713009133/1-s2.0-S1385894713009133-main.pdf?_tid=3e485b34-6290-11e6-98f8-00000aacb361&acdnat=1471228414_ac8c1ebc16f21f928e32780eb31b5a80
- Mukesh, K. D., Jayashree, B., & SSV, R. (2013). PTFE based nano-lubricants. *Wear*, 306(1), 80-88.
- N. W. M. Zulkifli, M. A. K., H. H. Masjuki, K. A. H. Al Mahmud & R. Yunus. (2014). The Effect of Temperature on Tribological Properties of Chemically Modified Bio-Based Lubricant. *Tribology Transactions*, 57(3), 408-415.
- N.K. Myshkin, M. I. P., A.V. Kovalev. (2005). Tribology of polymers: Adhesion, friction, wear, and mass-transfer. *Tribology International*, 38(11-12), 910–921. doi:10.1016/j.triboint.2005.07.016
- Nallasamy, P., Saravanakumar, N., Nagendran, S., Suriya, E., & Yashwant, D. (2014). Tribological investigations on MoS₂-based nanolubricant for machine tool slideways. *Proceedings of the Institution of Mechanical Engineers, Part J: Journal of Engineering Tribology*, 229(5), 559-567.

- Padgurskas, J., Rukuiza, R., Prosyčevs, I., & Kreivaitis, R. (2013). Tribological properties of lubricant additives of Fe, Cu and Co nanoparticles. *Tribology International*, 60(0), 224-232. Retrieved from <http://www.sciencedirect.com/science/article/pii/S0301679X12003490>
- Peña-Parás, L., Taha-Tijerina, J., Garza, L., Maldonado-Cortés, D., Michalczewski, R., & Lapray, C. (2015). Effect of CuO and Al₂O₃ nanoparticle additives on the tribological behavior of fully formulated oils. *Wear*, 332–333, 1256-1261. Retrieved from <http://www.sciencedirect.com/science/article/pii/S0043164815001477>
- Peng, D. X., Chen, C. H., Kang, Y., Chang, Y. P., & Chang, S. Y. (2010). Size effects of SiO₂ nanoparticles as oil additives on tribology of lubricant. *Industrial Lubrication and Tribology*, 62(2), 111-120. Retrieved from <http://www.emeraldinsight.com/doi/abs/10.1108/00368791011025656>
- Peng, D. X., Kang, Y., Chen, S., Shu, F., & Chang, Y. (2010). Dispersion and tribological properties of liquid paraffin with added aluminum nanoparticles. *Industrial Lubrication and Tribology*, 62(6), 341-348. Retrieved from <http://www.emeraldinsight.com/doi/abs/10.1108/00368791011076236>
- Pullela K Sarma, V. S., Vedula Dharma Rao, Ayyagari Kiran Kumar. (2011). Experimental study and analysis of lubricants dispersed with nano Cu and TiO₂ in a four-stroke two wheeler. *Nanoscale Research Letters*, 6, 233. doi:<https://doi.org/10.1186/1556-276X-6-233>
- R. Sarin, A. K. G., A. V. Sureshbabu, V. Martin, A. K. Misra and A. K. Bhatnagar. (1993). Soluble molybdenum compound and sulphur ep additive combinations: Synergistic and adverse effects on antifriction and antiwear characteristics. *Lubrication Science*, 5(3), 213–239.
- Rabaso, P. (2014). *Nanoparticle-doped lubricants: potential of Inorganic Fullerene-like (IF-) molybdenum disulfide for automotive applications*. INSA de Lyon
- Rabaso, P., Ville, F., Dassenoy, F., Diaby, M., Afanasiev, P., Cavoret, J., . . . Le Mogne, T. (2014). Boundary lubrication: Influence of the size and structure of inorganic fullerene-like MoS₂ nanoparticles on friction and wear reduction. *Wear*, 320(1–2), 161-178. Retrieved from <http://www.sciencedirect.com/science/article/pii/S0043164814002786>
- Ran, X., Yu, X., & Zou, Q. (2016). Effect of Particle Concentration on Tribological Properties of ZnO Nanofluids. *Tribology Transactions*, 1-17. Retrieved from <http://dx.doi.org/10.1080/10402004.2016.1154233>
- Rapoport, L., Leshchinsky, V., Lapsker, I., Volovik, Y., Nepomnyashchy, O., Lvovsky, M., . . . Tenne, R. (2003). Tribological properties of WS₂ nanoparticles under mixed lubrication. *Wear*, 255(7-12), 785-793.
- Rapoport, L., Leshchinsky, V., Lvovsky, M., Nepomnyashchy, O., Volovik, Y., & Tenne, R. (2002). Mechanism of friction of fullerenes. *Industrial Lubrication and Tribology*, 4(54), 171-176.

- Rudnick, L. R. (2006). *Synthetics, mineral oils, and bio-based lubricants: chemistry and technology*. Boca Raton: CRC Press Taylor & Francis Group.
- S.A. Angayarkanni, J. P. (2015). Review on thermal properties of nanofluids: Recent developments. *Advances in Colloid and Interface Science*, 225, 146–176.
- S.M. Alves, B. S. B., M.F. Trajano, K.S.B. Ribeiro, E. Moura. (2013). Tribological behavior of vegetable oil-based lubricants with nanoparticles of oxides in boundary lubrication conditions. *Tribology International*, 65, 28–36. Retrieved from http://ac.els-cdn.com/S0301679X13001734/1-s2.0-S0301679X13001734-main.pdf?_tid=74e50690-0c39-11e6-874d-00000aacb360&acdnat=1461735339_db72b4e4b0ba91ad0181b417270ea60a
- Schiøtz, J., & Jacobsen, K. W. (2003). A maximum in the strength of nanocrystalline copper. *Science*, 5638(301), 1357-1359.
- Shailesh K. Dhoke, A. S. K., T. Jai Mangal Sinha. (2009). Effect of nano-ZnO particles on the corrosion behavior of alkyd-based waterborne coatings. *Progress in Organic Coatings*, 64(4), 371–382. Retrieved from http://ac.els-cdn.com/S0300944008001811/1-s2.0-S0300944008001811-main.pdf?_tid=34ae44d0-6079-11e6-803a-00000aacb35d&acdnat=1470998617_3315a7e4e16aadf2ec3d3becad248d98
- Shanhong Wan, A. K. T., Yana Xia, Hongtao Zhu, Bach H. Tran, Shaogang Cui. (2016). An overview of inorganic polymer as potential lubricant additive for high temperature tribology. *Tribology International*, 102, 620–635. Retrieved from http://ac.els-cdn.com/S0301679X16301815/1-s2.0-S0301679X16301815-main.pdf?_tid=ac9ebf5e-6143-11e6-af69-00000aab0f6b&acdnat=1471085576_a5a9edf80a550075815c27ce41cab05e
- Shibo Wang, S. G., Dekun Zhang. (2009). Comparison of tribological behavior of nylon composites filled with zinc oxide particles and whiskers. *Wear*, 266(1–2), 248–254. Retrieved from http://ac.els-cdn.com/S0043164808003414/1-s2.0-S0043164808003414-main.pdf?_tid=1a61709c-6449-11e6-b596-00000aab0f01&acdnat=1471417762_c80ed3363802681f57c604c46005c790
- Siti Safiyah Nor Azman, N. W. M. Z., Hassan Masjuki, Mubashir Gulzar and Rehan Zahid. (2016). Study of tribological properties of lubricating oil blend added with graphene nanoplatelets. *Journal of Materials Research*, 31(13), 1-7. doi:10.1557/jmr.2016.24.
- Song, X., Zheng, S., Zhang, J., Li, W., Chen, Q., & Cao, B. (2012). Synthesis of monodispersed ZnAl₂O₄ nanoparticles and their tribology properties as lubricant additives. *Materials Research Bulletin*, 47(12), 4305-4310.
- Song, X., Zheng, S., Zhang, J., Li, W., Chen, Q., & Cao, B. (2012). Synthesis of monodispersed ZnAl₂O₄ nanoparticles and their tribology properties as lubricant additives. *Materials Research Bulletin*, 12(47), 4305-4310.
- Spikes, H. (2015). Friction Modifier Additives. *Tribology Letters*, 1(60), 1-26.
- Spikes, H. (2015). Friction Modifier Additives. *Tribology Letters*, 60(1), 1-26.

- Su, Y., Gong, L., & Chen, D. (2015). An investigation on tribological properties and lubrication mechanism of graphite nanoparticles as vegetable based oil additive. *Journal of Nanomaterials*, 16(1). Retrieved from <http://dx.doi.org/10.1155/2015/276753>
- Sudeep Ingole, A. C., Amol Kakade, S.S.Umare, D.V. Bhatt, Jyoti Menghani. (2013). Tribological behavior of nano TiO₂ as an additive in base oil. *Wear*, 301(1–2), 776-785.
- Sui, T., Song, B., Zhang, F., & Yang, Q. (2015). Effect of particle size and ligand on the tribological properties of amino functionalized hairy silica nanoparticles as an additive to polyalphaolefin. *Journal of Nanomaterials*, 2015, 1-9. Retrieved from <http://dx.doi.org/10.1155/2015/492401>
- Sui, T., Song, B., Zhang, F., & Yang, Q. (2015). Effect of particle size and ligand on the tribological properties of amino functionalized hairy silica nanoparticles as an additive to polyalphaolefin. *Journal of Nanomaterials*, 2015, 1-9.
- Tao, X., Jiazheng, Z., & Kang, X. (1996). The ball-bearing effect of diamond nanoparticles as an oil additive. *Journal of Physics D: Applied Physics*, 11(29), 2932.
- Thakur, M. R. N., Srinivas, D. V., & Jain, D. A. K. (2016). Anti-wear, anti-friction and extreme pressure properties of motor bike engine oil dispersed with molybdenum disulphide nano-particles. *Tribology Transactions*. doi:10.1080/10402004.2016.1142034
- Thomas, A. (2002). Fats and Fatty Oils. In Wiley-VCH (Ed.), *Ullmann's Encyclopedia of Industrial Chemistry*. Weinheim, Germany.
- Thottackkad, M. V., Perikinalil, R. K., & Kumarapillai, P. N. (2012). Experimental evaluation on the tribological properties of coconut oil by the addition of CuO nanoparticles. *International Journal of Precision Engineering and Manufacturing*, 13(1), 111-116.
- Tianyi Sui, B. S., Yu-ho Wen & Feng Zhang. (2016). Bifunctional hairy silica nanoparticles as high-performance additives for lubricant. *Scientific Reports*, 6(22696). doi:10.1038/srep22696
- Tiedan Chen, Y. X., Zhengfeng Jia, Zhilu Liu, and Haobo Zhang. (2014). Synthesis, Characterization, and Tribological Behavior of Oleic Acid Capped Graphene Oxide. *Journal of Nanomaterials*, 2014(Article ID 654145), 8 pages. doi:<http://dx.doi.org/10.1155/2014/654145>
- Tribology, t. G. C. o. (2019). Friction, Lubrication, and Wear. Retrieved from <https://www.gft-ev.de/en/german-tribology-conference-2019/>
- U.S. Naval Research Lab, D. o. t. N. O. o. N. R., Materials Science and Technology Division. (2019). The Anatase (TiO₂, C5) Structure. Retrieved from <http://aflowlib.duke.edu/users/egossett/lattice/struk/c5.html>

- V. Srinivas, R. N. T. A. K. J. (2016). Anti-wear, anti-friction and extreme pressure properties of motor bike engine oil dispersed with molybdenum disulphide nanoparticles. *Tribology Transactions*, 60(1), 12-19. doi:doi:10.1080/10402004.2016.1142034
- V.N. Bakunin, A. Y. S., G.N. Kuzmina and O.P. Parenago,. (2004). Synthesis and application of inorganic nanoparticles as lubricant components – a review. *Journal of Nanoparticle Research*, 6, 273–284.
- Varrla Eswaraiyah, V. S. a. S. R. (2011). Graphene-Based Engine Oil Nanofluids for Tribological Applications. *ACS Appl. Mater. Interfaces*, 3(11), 4221–4227. Retrieved from www.acsami.org
- Venkata Ramana Posa, V. A., Janardhan Reddy Koduru, Prathima Bobbala, Madhavi V & Adinarayana Reddy Somala. (2016). Preparation of graphene–TiO₂ nanocomposite and photocatalytic degradation of Rhodamine-B under solar light irradiation. *Journal of Experimental Nanoscience*, 11(9), 722-736.
- Verma, A., Jiang, W., Abu Safe, H. H., Brown, W. D., & Malshe, A. P. (2008). Tribological behavior of deagglomerated active inorganic nanoparticles for advanced lubrication. *Tribology Transactions*, 51(5), 673-678. Retrieved from <http://dx.doi.org/10.1080/10402000801947691>
- Viesca, J. L., Battez, A. H., González, R., Chou, R., & Cabello, J. J. (2011). Antiwear properties of carbon-coated copper nanoparticles used as an additive to a polyalphaolefin. *Tribology International*, 44(7–8), 829-833. Retrieved from <http://www.sciencedirect.com/science/article/pii/S0301679X11000284>
- Vikas Kumar, A. K. T., Subrata Kumar Ghosh. (2015). Application of nanofluids in plate heat exchanger: A review. *Energy Conversion and Management*, 105, 1017–1036. Retrieved from http://ac.els-cdn.com/S0196890415008079/1-s2.0-S0196890415008079-main.pdf?tid=1ca9c86a-62a8-11e6-b06f-00000aab0f26&acdnat=1471238665_97618894ea4ac2711b35452afbf05419
- Waleed Alghani, M. S. A. K., Samira Bagheri, Nor Amirah M. Amran & M. Gulzar. (2019). Enhancing the Tribological Behavior of Lubricating Oil by Adding TiO₂, Graphene, and TiO₂/Graphene Nanoparticles, . *Tribology Transactions*, 3(62), 452-463. doi:10.1080/10402004.2019.1573282
- Wan, Q., Jin, Y., Sun, P., & Ding, Y. (2014). Rheological and tribological behaviour of lubricating oils containing platelet MoS₂ nanoparticles. *Journal of Nanoparticle Research*, 16(5), 1-9.
- Wang, Z. L. (2008). Splendid One-Dimensional Nanostructures of Zinc Oxide: A New Nanomaterial Family for Nanotechnology. *ACS Nano*, 2(10), 1987–1992. Retrieved from <http://pubs.acs.org/doi/abs/10.1021/nm800631r>
- Wani, P. K. M. F. (2018). Tribological Characterisation of Graphene Oxide as Lubricant Additive on Hypereutectic Al-25Si/Steel Tribopair. *Tribology Transactions*, 61(2), 335-346.

- Watson, S. A. (2010). *Lubricant-derived ash: in-engine sources and opportunities for reduction*. (PhD). Massachusetts Institute of Technology,
- Weertman, J. (1993). Hall-Petch strengthening in nanocrystalline metals. *Materials Science and Engineering: A*, 1-2(166), 161-167.
- Wei Dai, B. K., Hong Gao, Hong Liang. (2016). Roles of nanoparticles in oil lubrication. *Tribology International*, 102, 88–98. Retrieved from http://ac.els-cdn.com/S0301679X16301116/1-s2.0-S0301679X16301116-main.pdf?_tid=0634fa28-6136-11e6-b6b2-00000aab0f6c&acdnat=1471079714_9b7e508da345b8e70e393c0a54f2e730
- Wei Li, Z. L. C., Zan Liu. (2017). Synthesis and tribological behaviour of oleic acid-capped lanthanum borate/graphene oxide nanocomposites. *Lubrication Science*, 29(1), 59–70.
- Wenzhen Xia, J. Z., Hui Wu, Xianming Zhao, Xiaoming Zhang, Jianzhong Xu, Ay Ching Hee & Zhengyi Jian. (2017). Effects of Nano-TiO₂ Additive in Oil-in-Water Lubricant on Contact Angle and Anti-scratch Behavior. *Tribology Transactions* 60(2), 362-372.
- Wu, Y. Y., Tsui, W. C., & Liu, T. C. (2007). Experimental analysis of tribological properties of lubricating oils with nanoparticle additives. *Wear*, 262(7-8), 819-825.
- Xiaodong, Z., Xun, F., Huaqiang, S., & Zhengshui, H. (2007). Lubricating properties of Cyanex 302-modified MoS₂ microspheres in base oil 500SN. *Lubrication Science*, 1(19), 71-79.
- Xie, H., Jiang, B., He, J., Xia, X., & Pan, F. (2015). Lubrication performance of MoS₂ and SiO₂ nanoparticles as lubricant additives in magnesium alloy-steel contacts. *Tribology International*, 93(A), 63-70. Retrieved from <http://www.sciencedirect.com/science/article/pii/S0301679X15003515>
- Xin Quan, M. H., Xiaoming Gao, Yanlong Fu, Lijun Weng, Desheng Wang, Dong Jiang, Jiayi Sun. (2016). Friction and wear performance of dual lubrication systems combining WS₂-MoS₂ composite film and low volatility oils under vacuum condition. *Tribology International*, 99, 57–66. Retrieved from http://ac.els-cdn.com/S0301679X16300032/1-s2.0-S0301679X16300032-main.pdf?_tid=16191baa-b6a3-11e6-9c09-00000aab0f26&acdnat=1480472404_5383b72c16e710723193d73770997a9b
- Xu Ran, X. Y., and Qian Zou. (2016). Effect of Particle Concentration on Tribological Properties of ZnO Nanofluids. *Tribology Transactions*, 60(1), 154-158.
- Y.Y. Wu, W. C. T., T.C. Liu. (2007). Experimental analysis of tribological properties of lubricating oils with nanoparticle additives. *Wear*, 262(7–8), 819–825. Retrieved from http://ac.els-cdn.com/S0043164806003292/1-s2.0-S0043164806003292-main.pdf?_tid=ded225ca-605c-11e6-84c6-00000aacb35e&acdnat=1470986447_9f72697daf7dbedea64d1d7b9660b3e6

- Yadgarov, L., Petrone, V., Rosentsveig, R., Feldman, Y., Tenne, R., & Senatore, A. (2013). Tribological studies of rhenium doped fullerene-like MoS₂ nanoparticles in boundary, mixed and elasto-hydrodynamic lubrication conditions. *Wear*, 297(1-2), 1103-1110. Retrieved from <http://www.sciencedirect.com/science/article/pii/S0043164812004280>
- Ye, W., Cheng, T., Ye, Q., Guo, X., Zhang, Z., & Dang, H. (2003). Preparation and tribological properties of tetrafluorobenzoic acid-modified TiO₂ nanoparticles as lubricant additives. *Materials Science and Engineering: A*, 1(359), 82-85.
- Yitian Peng, Y. H., and Hui Wang. (2007). Tribological behaviors of surfactant-functionalized carbon nanotubes as lubricant additive in water. *Tribology Letters*, 25(3), 247-253. doi:10.1007/s11249-006-9176-7
- Yu, W., & Xie, H. (2012). A review on nanofluids: preparation, stability mechanisms, and applications. *Journal of Nanomaterials*, 2012(1).
- Zainal, N., Zulkifli, N., Yusoff, M., Masjuki, H., & Yunus, R. (2015). *The feasibility study of CaCO₃ derived from cockleshell as nanoparticle in chemically modified lubricant*. Paper presented at the Proceedings of Malaysian International Tribology Conference 2015.
- Zengshi Xu, Q. Z., Xiaoliang Shi, Wenzheng Zhai & Kang Yang. (2015). Tribological Properties of TiAl Matrix Self-Lubricating Composites Containing Multilayer Graphene and Ti₃SiC₂ at High Temperatures. *Tribology Transactions*, 58(6), 1131-1141.
- Zhang, Y., Xu, Y., Yang, Y., Zhang, S., Zhang, P., & Zhang, Z. (2015). Synthesis and tribological properties of oil-soluble copper nanoparticles as environmentally friendly lubricating oil additives. *Industrial Lubrication and Tribology*, 67(3), 227-232. Retrieved from <http://www.emeraldinsight.com/doi/abs/10.1108/ILT-10-2012-0098>
- Zhao, Y., Zhang, Z., & Dang, H. (2004). Fabrication and tribological properties of Pb nanoparticles. *Journal of Nanoparticle Research*, 6(1), 47-51. Retrieved from <http://dx.doi.org/10.1023/B:NANO.0000023223.79545.af>
- Zhengfeng Jia , Y.-q. X., Xin Shao , San-ming Du. (2014). Synthesis, characterization and tribological behavior of oleic acid-capped core-shell lanthanum borate-SiO₂ composites. *Industrial Lubrication and Tribology*, 66(1), 1 - 8. doi:<http://dx.doi.org/10.1108/ILT-06-2011-0041>
- Zin, V., Agresti, F., Barison, S., Colla, L., & Fabrizio, M. (2015). Influence of Cu, TiO₂ nanoparticles and carbon nano-horns on tribological properties of engine oil. *Journal of Nanoscience and Nanotechnology*, 15(5), 3590-3598. Retrieved from <http://dx.doi.org/10.1166/jnn.2015.9839>
- Zou, L. G. a. Q. (2013). Friction and Wear Characteristics of Oil-Based ZnO Nanofluids. *Tribology Transactions*, 56(2), 236-244. doi:10.1080/10402004.2012.740148

Zulkifli, N. W. M. (2014). *Lubricity and anti-wear characteristic of trimethylolpropane ester derived from edible and non-edible resources*. (PhD). University of Malaya, Malaysia. (TJ7 UMP 2014 Nurwmz)

Zulkifli, N. W. M., Azman, S., Kalam, M., Masjuki, H., Yunus, R., & Gulzar, M. (2016). Lubricity of bio-based lubricant derived from different chemically modified fatty acid methyl ester. *Tribology International*, 93, 555-562.

Zulkifli, N. W. M., Kalam, M. A., Masjuki, H. H., & Yunus, R. (2013). Experimental analysis of tribological properties of biolubricant with nanoparticle additive. *Procedia Engineering*, 68, 152-157. Retrieved from <http://www.sciencedirect.com/science/article/pii/S1877705813020158>

University of Malaya

LIST OF PUBLICATIONS AND PAPERS PRESENTED

Doctoral Research Seminar on Renewable and Green Energy at the Cube 2, Engineering Summit on March 10, 2016.

Higher Degree Seminar, Faculty of Engineering, University of Malaya, at Alumni Meeting Room, Level 4, Faculty of Engineering on March 13, 2016.

The ISI-Indexed proceedings paper (Adding Nano Titanium Dioxide Anatase and Graphene to Base Oil Group II for Lubrication Optimization) was presented at International Conference on Advanced Processes and Systems in Manufacturing (APSIM 2016) at Putrajaya, Malaysia on August 30, 2016.

The ISI-indexed proceedings paper (Tribological Effects Toward Material Characteristic in HSS Hacksaw Blade) was presented at International Conference on Advanced Processes and Systems in Manufacturing (APSIM 2016) at Putrajaya, Malaysia on August 30, 2016.

The ISI-indexed research paper (Material characterization of tribological effects in HSS hacksaw blade) was published in Industrial Lubrication and Tribology on May 08, 2017.

The ISI-indexed research paper (Enhancing the Tribological Behavior of Lubricating Oil by Adding TiO₂, Graphene, and TiO₂/Graphene Nanoparticles) was published in Tribology Transactions Journal on February 1, 2019.

The AIP Conference Proceedings (Scopus-Indexed) paper (Characterization Investigation of ZnO, Graphene, and ZnO/Graphene Nanoparticles as Nanoscale Lubricants Additives) was presented at 4th International Conference on The Science and Engineering of Materials (ICoSEM 2019) at Kuala Lumpur, Malaysia on August 27, 2019.

The ISI-indexed research paper (Investigation of ZnO, Graphene, and ZnO/Graphene Nanoparticles as Nanoscale Lubricants Additives) was accepted for publication in a special volume of Materials Science and Engineering Technology Journal (Materialwissenschaft und Werkstofftechnik) on August 02, 2020.